

PEROXIREDOXINS

Novel mediators of cellular timekeeping

Vom Fachbereich Biologie
der Technischen Universität Kaiserslautern
zur Erlangung des akademischen Grades
„Doktor der Naturwissenschaften“ (Dr. rer. nat.)
genehmigte Dissertation

vorgelegt von

M. Sc. Prince Saforo Amponsah

Datum der wissenschaftlichen Aussprache:

15. Januar 2020

Prüfungskommission

- 1. Gutachter: Prof. Dr. Bruce Morgan
- 2. Gutachter: Prof. Dr. Zuzana Storchová
- Vorsitzender: Prof. Dr. Johannes M. Herrmann

Kaiserslautern, 2020

D386

...To my family

TABLE OF CONTENTS

LIST OF PUBLICATIONS.....	iv
SUMMARY	v
ZUSAMMENFASSUNG.....	vii
1 INTRODUCTION.....	1
1.1 Historical perspectives of cellular timekeeping.....	1
1.2 Circadian clocks: Molecular players and mechanisms	3
1.2.1 Transcriptional clocks.....	4
1.2.2 Non-transcriptional clocks.....	6
1.3 The Yeast Metabolic Cycle as a model metabolic clock.....	8
1.4 Hydrogen peroxide in redox signaling.....	9
1.4.1 Direct oxidation or ‘floodgate’ hypothesis.....	10
1.4.2 Facilitated oxidation or ‘ <i>relay</i> ’ hypothesis.....	10
1.5 Peroxiredoxins: structure, catalytic mechanism and function	12
1.6 Genetically encoded thiol peroxidase-based biosensors.....	13
1.7 Crosstalk between the cellular redox state, metabolism, cell cycle and circadian/ultradian clocks ..	15
1.7.1 Reciprocal regulation of clock mechanism by redox homeostasis.....	15
1.7.2 Redox/metabolic state versus cell division cycle	16
1.8 Aims of this thesis.....	17
2 RESULTS.....	18
2.1 Establishment of YMC-synchronized cultures.....	18
2.1.1 The YMC consists of synchronized respiratory oscillations	18
2.1.2 Chemical inhibition of gene translation perturbs the YMC.....	19
2.2 The YMC is responsive to and modulated by chemical redox changes	21
2.3 Cyclical changes in cellular H ₂ O ₂ occur during the YMC.....	23
2.3.1 Integration of roGFP2-Tsa2ΔC _R biosensor into yeast genome.....	23
2.3.2 Cyclical H ₂ O ₂ changes are synchronized to YMC phase	25
2.3.3 H ₂ O ₂ is not important for population synchrony	26
2.4 A signaling role for H ₂ O ₂ and peroxiredoxins during the YMC.....	27
2.4.1 High exogenous H ₂ O ₂ induces metabolic switch to HOC	27
2.4.2 High peroxide-induced switch to HOC during YMC is phase-independent	27
2.4.3 Peroxiredoxin inactivation upon high peroxide mediates metabolic switch to HOC	30

2.5 Cytosolic peroxiredoxins are essential for YMC regulation.....	34
2.5.1 Loss of cytosolic 2-Cys peroxiredoxins is associated with decreased YMC period	34
2.5.2 Multiple peroxiredoxins function to mediate peroxide-induced metabolic switch to HOC	35
2.5.3 Combined loss of <i>TSA1</i> and <i>AHP1</i> in prototrophic yeast leads to non-viability	38
2.5.4 An auxin-inducible degron system reveals toxicity of Ahp1 degradation in a <i>Δtsa1</i> background	40
2.5.5 Repression of Ahp1 in a <i>Δtsa1Δtsa2</i> background perturbs the YMC	42
2.6 Peroxiredoxin-mediated YMC regulation is thioredoxin dependent	42
2.7 Peroxiredoxins couple metabolic oscillations in yeast to the cell division cycle (CDC).....	45
2.7.1 Oscillatory metabolism is coordinated with cell division.....	46
2.7.2 Temporary inactivation or loss of peroxiredoxins leads to decoupling of CDC from YMC.....	47
2.8 Chemical redox perturbations of the YMC modulate entry into and exit from the cell division cycle.....	49
2.8.1 Induction of HOC upon thiol disulfide reduction promotes cell cycle entry.....	49
2.8.2 Prolongation of LOC upon thiol disulfide oxidation delays cell cycle entry	50
3 DISCUSSION	52
3.1 The YMC is a redox clock that is regulated by thiol switch(es).....	52
3.2 Peroxiredoxins and thioredoxins are crucial for stable metabolic clock function	59
3.3 The cellular redox/metabolic state regulates the cell division cycle.....	64
3.4 Peroxiredoxins couple changes in cell metabolism to cell division.....	66
4 OUTLOOK.....	69
5 MATERIALS AND METHODS	71
5.1 Molecular Biology Methods	71
5.1.1 Plasmid DNA isolation from <i>Escherichia coli</i> (<i>E. coli</i>)	71
5.1.2 Determination of DNA concentration.....	71
5.1.3 Polymerase chain reaction for DNA amplification.....	71
5.1.4 Restriction digestion of DNA	72
5.1.5 Ligation of DNA fragments with vectors	72
5.1.6 Agarose gel electrophoresis.....	72
5.1.7 Chemical transformation of <i>E. coli</i> cells	73
5.1.8 One-step transformation of <i>S. cerevisiae</i> cells.....	73
5.1.9 Plasmids and primers.....	73
5.2 Cell Biology Methods.....	74
5.2.1 Yeast strains.....	74
5.2.2 Construction of a genomically integrated roGFP2-Tsa2ΔC _R expressing yeast strain	74

5.2.3 Construction of yeast strains capable of conditional genomic Ahp1 depletion via an auxin-inducible degron (AID) system	74
5.2.4 Yeast mating, sporulation and tetrad dissection	75
5.2.5 Media for <i>E. coli</i> cultivation	75
5.2.6 Media for <i>S. cerevisiae</i> cultivation	75
5.2.7 Establishment of continuous culture	76
5.2.8 Online monitoring of roGFP2-Tsa2 Δ C _R	76
5.2.9 NEM-based alkylation for degree of oxidation of roGFP2-Tsa2 Δ C _R determination	76
5.2.10 Flow cytometry analysis of DNA content	77
5.2.11 Budding index determination and DNA visualization by DAPI staining and microscopy	77
5.2.12 Fluorescence Microscopy	78
5.3 Protein biochemistry methods	78
5.3.1 Protein extraction	78
5.3.2 SDS-polyacrylamide gel electrophoresis (SDS-PAGE)	78
5.3.3 Western blot transfer and detection	79
5.3.4 Autoradiography	79
REFERENCES	85
ABBREVIATIONS	94
ACKNOWLEDGEMENTS	97
CURRICULUM VITAE	99
DECLARATION	101
APPENDIX	102

LIST OF PUBLICATIONS

Amponsah PS, Metwally G, Mergel S, Storchova Z and Morgan B (2019). Peroxiredoxins couple metabolism and cell division in an ultradian clock. *Nat Chem Biol* (under revision)

Calabrese G, Peker E, **Amponsah PS**, Hoehne MN, Riemer T, Mai M, Deponte M, Morgan B, Riemer J (2019). Hyperoxidation of mitochondrial peroxiredoxin limits H₂O₂-induced cell death in yeast. *EMBO J* 38(18):e101552

Amponsah PS (2016). Cellular redox – living chemistry. *Science in School* 36: 15-17

Morgan B, Van Laer K, Owusu TN, Ezeriņa D, Pastor-Flores D, **Amponsah PS**, Tursch A, Dick TP (2016). Real-time monitoring of basal H₂O₂ levels with peroxiredoxin-based probes. *Nat Chem Biol* 12(6): 437-43

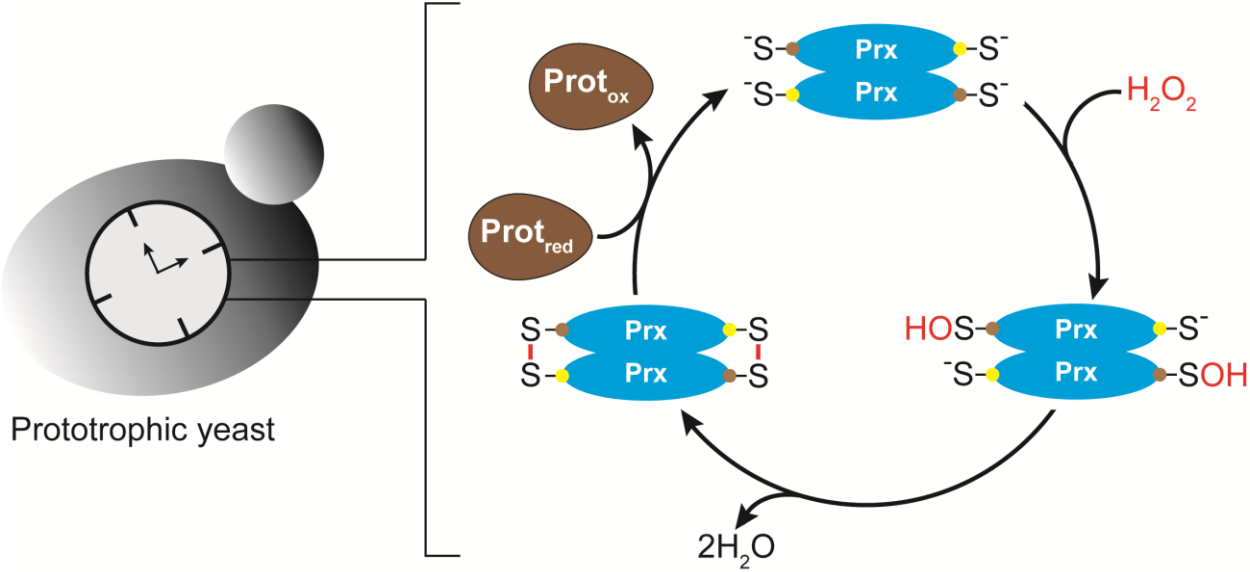
SUMMARY

Biological clocks exist across all life forms and serve to coordinate organismal physiology with periodic environmental changes. The underlying mechanism of these clocks is predominantly based on cellular transcription-translation feedback loops in which clock proteins mediate the periodic expression of numerous genes. However, recent studies point to the existence of a conserved timekeeping mechanism independent of cellular transcription and translation, but based on cellular metabolism. These metabolic clocks were concluded based upon the observation of circadian and ultradian oscillations in the level of hyperoxidized peroxiredoxin proteins. Peroxiredoxins are enzymes found almost ubiquitously throughout life. Originally identified as H_2O_2 scavengers, recent studies show that peroxiredoxins can transfer oxidation to, and thereby regulate, a wide range of cellular proteins. Thus, it is conceivable that peroxiredoxins, using H_2O_2 as the primary signaling molecule, have the potential to integrate and coordinate much of cellular physiology and behavior with metabolic changes. Nonetheless, it remained unclear if peroxiredoxins are passive reporters of metabolic clock activity or active determinants of cellular timekeeping. Budding yeast possess an ultradian metabolic clock termed the Yeast Metabolic Cycle (YMC). The most obvious feature of the YMC is a high amplitude oscillation in oxygen consumption. Like circadian clocks, the YMC temporally compartmentalizes cellular processes (e.g. metabolism) and coordinates cellular programs such as gene expression and cell division. The YMC also exhibits oscillations in the level of hyperoxidized peroxiredoxin proteins.

In this study, I used the YMC clock model to investigate the role of peroxiredoxins in cellular timekeeping, as well as the coordination of cell division with the metabolic clock. I observed that cytosolic 2-Cys peroxiredoxins are essential for robust metabolic clock function. I provide direct evidence for oscillations in cytosolic H_2O_2 levels, as well as cyclical changes in oxidation state of a peroxiredoxin and a model peroxiredoxin target protein during the YMC. I noted two distinct metabolic states during the YMC: low oxygen consumption (LOC) and high oxygen consumption (HOC). I demonstrate that thiol-disulfide oxidation and reduction are necessary for switching between LOC and HOC. Specifically, a thiol reductant promotes switching to HOC, whilst a thiol oxidant prevents switching to HOC, forcing cells to remain in LOC. Transient peroxiredoxin inactivation triggered rapid and premature switching from LOC to HOC. Furthermore, I show that cell division is normally synchronized with the YMC and that deletion of typical 2-Cys peroxiredoxins leads to complete uncoupling of cell division from metabolic cycling. Moreover, metabolic oscillations are crucial for regulating cell cycle entry and exit. Intriguingly, switching to HOC is crucial for initiating cell cycle entry whilst switching to LOC is crucial for cell cycle completion and exit. Consequently, forcing cells to remain in HOC by application of a thiol reductant leads to multiple rounds of cell cycle entry despite failure to complete the preceding cell cycle. On the other hand, forcing cells to remain in LOC by treating with a thiol oxidant prevents initiation of cell cycle entry.

In conclusion, I propose that peroxiredoxins – by controlling metabolic cycles, which are in turn crucial for regulating the progression through cell cycle – play a central role in the coordination of cellular

metabolism with cell division. This proposition, thus, positions peroxiredoxins as active players in the cellular timekeeping mechanism.



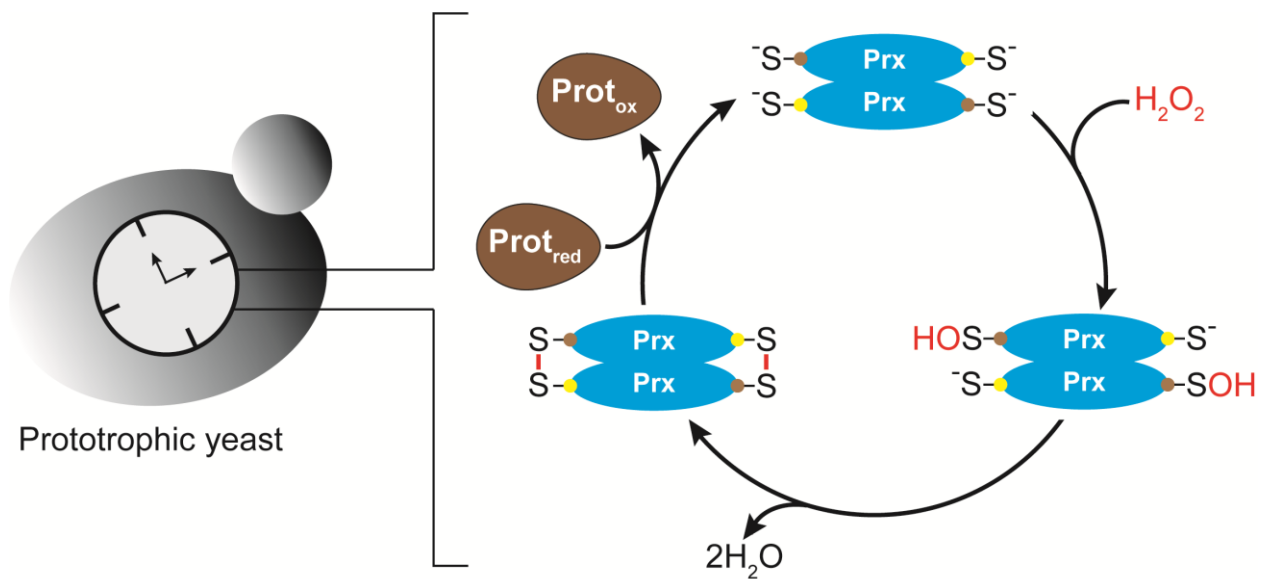
ZUSAMMENFASSUNG

In sämtlichen Lebensformen gibt es biologische Uhren, die die Physiologie des jeweiligen Organismus mit sich periodisch verändernden Umweltbedingungen koordinieren. Der molekulare Mechanismus dieser Uhren besteht zumeist aus zellulären Transkriptions-Translations-Feedback-Loops, in denen Zeitgeber-Proteine die periodische Expression zahlreicher Gene steuern. Jüngere Studien legen jedoch nahe, dass eine weitere konservierte Zeitgeberfunktion existiert, die unabhängig von Transkription und Translation ist, sondern auf dem zellulären Metabolismus beruht. Die Existenz solcher metabolischen Uhren wurde postuliert basierend auf der Beobachtung, dass die Level von hyperoxidierten Peroxiredoxin-Proteinen circadianen und ultradianen Schwankungen unterliegen. Peroxiredoxine sind Enzyme, die es fast in sämtlichen lebenden Zellen gibt. Ursprünglich als Radikalfänger zur Entgiftung von Wasserstoffperoxid identifiziert, ist heute bekannt, dass Peroxiredoxine die Oxidation – und damit Regulation – einer großen Bandbreite von Proteinen bewerkstelligen. Es liegt daher nahe, dass Peroxiredoxine Wasserstoffperoxid als primäres Signalmolekül nutzen können, um einen Großteil der zellulären Physiologie und Verhalten mit metabolischen Veränderungen zu integrieren und koordinieren. Unklar blieb jedoch bislang, ob Peroxiredoxine lediglich passive Reporter für die Aktivität metabolischer Uhren sind, oder vielmehr aktive Zeitgeber darstellen. Auch die Bäckerhefe besitzt eine ultradiane metabolische Uhr, den Yeast Metabolic Cycle (YMC). Dessen offensichtlichste Eigenschaft ist die starke periodische Schwankung im zellulären Sauerstoff-Bedarf. Ähnlich den circadianen Uhren trennt der YMC zelluläre Prozesse (z.B. metabolische) zeitlich voneinander und koordiniert zelluläre Programme wie etwa Genexpression und Zellteilung. Auch im YMC zeigen sich Oszillationen in der Menge an hyperoxidierten Peroxiredoxinen.

In der vorliegenden Arbeit habe ich den YMC als Modell genutzt, um die Rolle der Peroxiredoxine in der zellulären Zeitgebung und der Koordination der Zellteilung mit der metabolischen Uhr zu untersuchen. Ich habe cytosolische 2-Cys Peroxiredoxine als essentiell für eine robuste Funktion der metabolischen Uhr identifiziert. Auch konnte ich zyklische Schwankungen sowohl in der zellulären H_2O_2 -Menge als auch im oxidativen Status eines Peroxiredoxins und eines Modellsubstrates während des YMC messen. Dieser besitzt zwei verschiedene metabolische Phasen, eine mit geringem Sauerstoffverbrauch (LOC, low oxygen consumption) und eine mit hohem Sauerstoffverbrauch (HOX, high oxygen consumption). Ich konnte zeigen, dass Thiol-Disulfid-Oxidation und -Reduktion notwendig für das Umschalten zwischen LOC und HOC sind. Insbesondere triggert ein Thiol-Oxidans das Umschalten in die HOC-Phase, während umgekehrt Thiol-Reduktion dieses Umschalten verhindert und Zellen in der LOC-Phase hält. Eine vorübergehende Inaktivierung von Peroxiredoxinen führte zu einem schnellen und vorzeitigen Switch von der LOC- in die HOC-Phase. Darüber hinaus zeigte ich, dass Zellteilung normalerweise mit dem YMC synchronisiert ist und die Deletion eines typischen 2-Cys Peroxiredoxins zu einer kompletten Entkopplung von Zellzyklus und metabolischer Uhr führt. Metabolische Oszillationen sind wichtig für die Regulation von Eintritt und Ende des Zellzyklus. Dabei ist das Umschalten in die HOC-Phase entscheidend für die Initiation der Zellteilung, während Eintritt in die LOC-Phase wichtig ist für die

Vervollständigung und den Austritt aus dem Zellzyklus ist. Folgerichtig führt das Verweilen von Zellen in der HOC-Phase, erzwungen durch Zugabe von Thiol-Reduktantien, zu mehreren Runden von Zellzyklus-Eintritt, obwohl der vorangegangene Zellzyklus nicht vollendet werden konnte. Umgekehrt verhindert das Arretieren von Zellen in der LOC-Phase den Eintritt in die Zellteilung.

Basierend auf diesen Beobachtungen schlage ich vor, dass Peroxiredoxine eine zentrale Rolle in der Koordination von zellulärem Metabolismus und Zellzyklus spielen, indem sie metabolische Zyklen kontrollieren, die wiederum ausschlaggebend für die Progression durch den Zellzyklus sind. Peroxiredoxine spielen somit eine aktive Rolle in der zellulären Zeitgebung..



1 INTRODUCTION

All living species order their biological processes - at the molecular, cellular, tissue or organ levels. The timing of these biological processes is intrinsic and essential for coordination of periodic physiological and behavioral responses. This intrinsic timekeeping mechanism is called the biological clock, which enables living species to anticipate oscillatory environmental changes – day/night cycles, temperature rhythms, time of feeding etc. Underlying biological clocks are biological rhythms with periods of approximately 24 hours (termed Circadian) or less (termed Ultradian) or periods ranging from weeks to months and years (Fig. 1.0). Essential features of circadian clocks include:

- Free-running or self-sustained in nature – this means that the rhythms continue to exist even under constant conditions, such as constant darkness, without the influence of external signals. This distinguishes circadian rhythms from diurnal rhythms, which are influenced by external cues such as light.
- Rhythms are entrainable - this means that the rhythm is reset or synchronized by external time cues called *Zeitgebers* (German word meaning ‘time giver’).
- Rhythms are temperature-compensated – this means that the circadian period is not dictated by the prevailing environmental temperature [1].

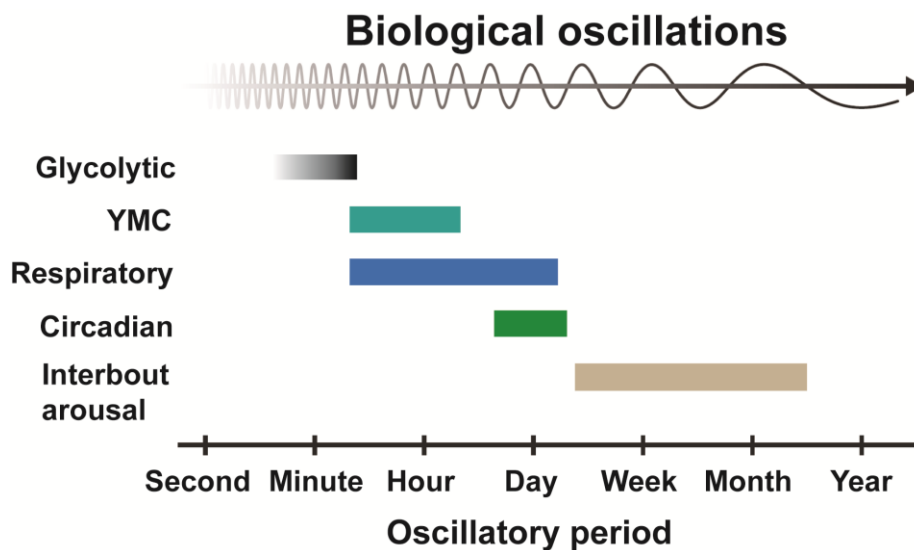


Figure 1.0: Biological oscillations in living systems. Diverse species exhibit biological rhythms that span periods ranging from several seconds to hours and months. These oscillations optimize the species' adaptability to its environment. Image modified from [2].

1.1 Historical perspectives of cellular timekeeping

The term Circadian originates from the Latin words, *circa* – meaning ‘around’ and *dies* – meaning ‘day’, coined by Franz Halberg (a Romanian chronobiologist) in 1959 [3]. This implied that physiological rhythms occur within periods of about 24 hours. The first documented description of an intrinsic circadian rhythm was the observation that leaves of *Mimosa pudica* plant opened and closed with a 24-hour period

when kept under constant darkness conditions (Fig. 1.1). This experiment was performed by the French Geophysicist Jean-Jacques d'Ortous de Mairan in 1729, and showed for the first time that circadian clocks were self-sustaining or free-running in nature, without the influence of external stimuli [4].

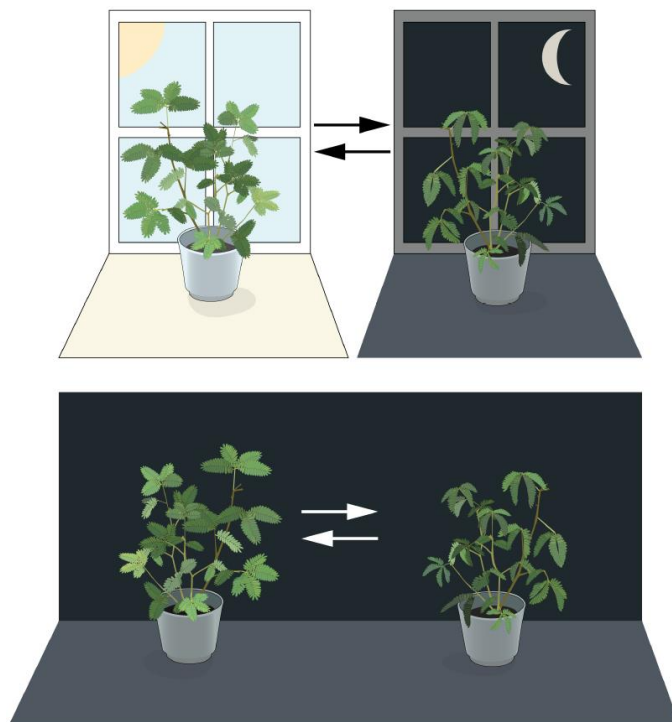


Figure 1.1: The plant, *M. pudica*, possesses an internal biological clock. Leaves of mimosa plants open towards the sun during daytime and close at dusk. Jean Jacques d'Ortous de Mairan placed a mimosa plant in constant dark and found that the leaves continued to follow their daily rhythm for several days. This suggested that mimosa plants have a cell autonomous clock that can maintain the biological rhythm even under constant conditions. Image and legend adapted from [@nobelprize.org](https://www.nobelprize.org).

Michel Siffre, the French cave explorer, lived isolated in a cave in the French Alps for two months to investigate the body's clock. His initial plan was to undertake a geological expedition to study underground glaciers for about fifteen days. However, he extended his stay in the cave to two months, with the idea to investigate how the natural rhythms of human life would be affected by living "beyond time". To achieve this, he lived in the cave without access to clock, calendar or sun and slept and ate only when his body told him to. Additionally, he had a team at the entrance of the cave who took notice of his sleep-wake activity without him personally knowing what time it was on the outside. He called them only when he woke up, when he ate, and just before he went to sleep. During his wake times, he performed a psychological test by counting from 1 to 120, at the rate of one digit per second. He also took record of his pulse and measured his body temperature, which got as low as 34 °C. After the experiment, Siffre noted that he had completely lost conscious perception of the passing of time. It took him five minutes to count to 120. He went into the cave on July 16 and planned to finish the experiment on September 14. When he was notified that the date was due, he thought it was August 20, believing he still had another month to spend in the cave. Thus, his psychological time had compressed by a factor of two. Siffre's experiment showed that humans, like lower mammals such as rat, possess an internal biological clock [5, 6]. In line with Siffre's reports, the German physician, Jürgen Aschoff, observed in laboratory settings that the circadian clock controlled daily physiological and psychological parameters such as blood pressure, body temperature, plasma hormone levels and cognitive performance [7] (Fig. 1.2).

These descriptions of biological timekeeping ignited interests in previously observed, but unexplained, rhythmic behavior. For instance, Antle and Silver described in their article, circadian rhythms in feeding times of bees as observed by Hugo Berthold von Buttel-Reepen and Auguste Forel in the early 20th Century [8]. Observations by Hugo Berthold von ButtelReepen, a German zoologist, indicated that

bees exhibited a time-sense for feeding, thus, visited a buckwheat field only in the morning while the flowers were open and secreting nectar. On the other hand, Auguste Forel, during his vacation in the Swiss Alps observed that bees came to feed on his marmalade while he ate breakfast outdoor. As the days went by, the number of bees which visited him increased until he was unable to eat outdoors anymore. He noted that the bees persistently arrived during breakfast time, although he and his marmalade were safely indoors, suggesting these insects appeared to have a time-memory for when breakfast was served [8]. Although these observations did not necessarily constitute evidence of clocks, they demonstrate how organismal behavior is timed with environmental changes.

Subsequent studies have demonstrated that insects such as *Drosophila sp.* possessed an endogenous circadian clock [9, 10]. The discovery and functional annotation of the *period* (“*per*”) gene as a key determinant of *Drosophila sp.* circadian rhythmicity, birthed the transcription-translation feedback loop (TTFL) model of circadian timekeeping, for which the Noble Prize in Physiology and Medicine was awarded to Jeffrey Hall, Michael Rosbash and Michael Young in 2017.

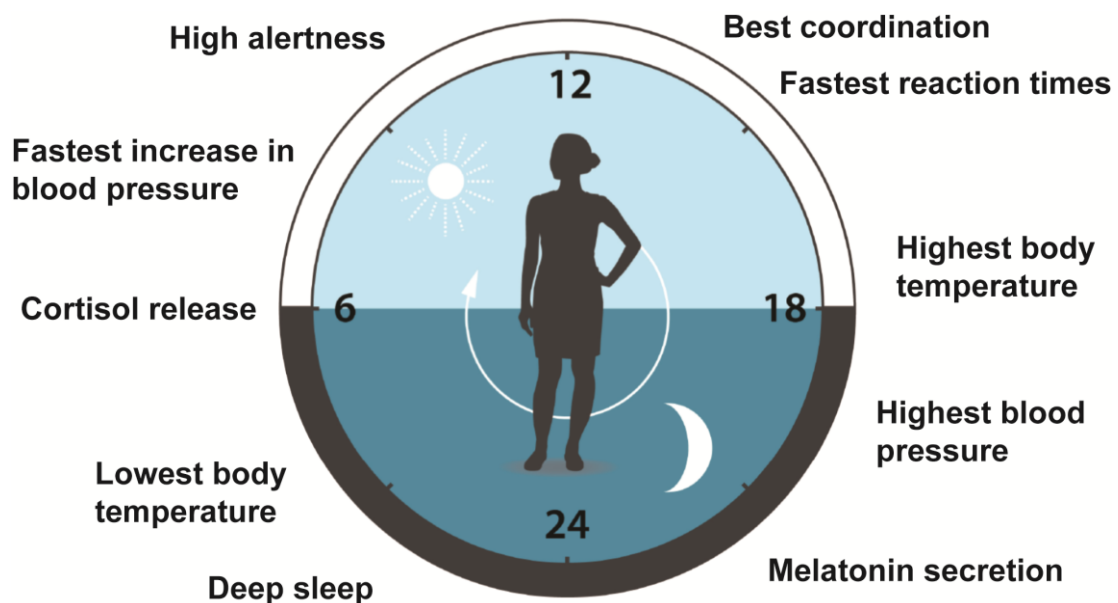


Figure 1.2: The circadian clock has an impact on many aspects of human physiology. This clock helps to regulate sleep patterns, feeding behavior, hormone release, blood pressure and body temperature. Image modified and legend adapted from [@nobelprize.org](https://www.nobelprize.org).

1.2 Circadian clocks: Molecular players and mechanisms

Until the late 20th century, the prevailing evidence for biological timekeeping were based on organismal behavioral rhythmicity, such as ‘time-sense’ feeding of bees and closure and opening of plant leaves in response to day-night cycles. However, the basic mechanistic underpinnings for these rhythms were largely not understood. Subsequent discovery and characterization of several ‘clock genes’ in diverse organisms led to the hypothesis that the cellular clockwork must consist of a feedback system that is able to generate approximately 24-hour cycles in various cellular parameters (i.e. TTFL) [11].

Although the TTFL model of the clockwork is the prominent mechanistic basis for circadian behavior, ‘clock genes’ are not conserved across different species. Moreover, some ‘clock genes’ are non-essential, without which circadian rhythms persist [12, 13]. These apparent ‘anomalies’ to the TTFL-based model therefore ignited interests in the search for alternative cellular timekeeping models that function independent of cellular transcription (ie. non-transcriptional clocks). I summarize below some key findings that contributed to postulations on transcription and non-transcription based clock models.

1.2.1 Transcriptional clocks

As recounted earlier, the identification of the *per* gene as a genetic determinant of circadian rhythmicity in *Drosophila* made way for the postulation of the TTFL-model as the underlying mechanism of circadian clocks [14]. To arrive at this hypothesis, Konopka and Benzer performed a genetic screen for abnormal eclosion rhythms in *Drosophila* flies. Eclosion is the process of transition from pupa into adult *Drosophila*. Before the genetic screen by Konopka and Benzer, Colin Pittendrigh had earlier observed that the eclosion process exhibited a circadian behavior and showed that temperature played an essential role in determining the period of eclosion rhythm, but not its rhythmicity [15]. Konopka and Benzer’s genetic screen revealed three mutations that traced to the same genomic locus. Of the three mutant alleles, one was arrhythmic; another had short-period rhythms of 19 hours, and the third had long-period rhythms of 28 hours [14]. They called this genomic locus *period* (“*per*”). Subsequently, the labs of Ronald Konopka, Jeffrey Hall, Michael Roshbash and Michael Young isolated and characterized *per* and showed that both *per* mRNA and its protein were expressed in a circadian manner [11, 14, 16-18]. They further demonstrated that the *per* locus was the center of the circadian rhythm and that loss of *per* terminates circadian activity. They therefore proposed a model where PER protein, in cooperation with another protein called TIMELESS (TIM), auto-regulated its own expression [11, 19, 20] (Fig. 1.3A). Further studies led to the discovery of two transcriptional factors, CLOCK (CLK) and CYCLE (CYC), which were proposed to control the expression of *tim* and *per* to provide a closure to the feedback loop [21-23]. The expression of *clock* (“*clk*”) and *cycle* (“*cyc*”) were also shown to be auto-regulated by their own protein products (Fig. 1.3B).

The basic mechanism of the TTFL-model is dependent on a transcriptional activator that induce the transcription of a repressor. The repressor accumulate over time until it reaches levels enough to inhibit its own activation [2] (Fig. 1.4). This clock model has been described in a number of species that demonstrate circadian activity. The core clock components are not conserved across species, although the mechanisms remain similar [24].

In mammals, CLOCK (NPAS2) and BMAL1 are the central transcriptional machinery that activate expression of *per* and *cryptochrome* (“*cry*”) gene families. PER and CRY protein products accumulate over time in the cytoplasm and form complexes that repress CLOCK and BMAL1 transactivation upon translocation into the nucleus [25]. A second feedback loop also involves upregulation of REV-ERB α and

REV-ERB β transcription by CLOCK and BMAL1, which in turn accumulate to repress *Bmal1* transcription [26] (Fig. 1.4).

In *Drosophila*, the central clock proteins, CLK and CYC, form the positive elements of the transcriptional loop whilst PER and TIM mediate the negative feedback. CLK and CYC form heterodimers that positively regulate transcription of *per* and *tim* by binding directly to E-box elements found in the *per* and *tim* promoters. PER and TIM self-antagonize their own expression by binding to the CLK/CYC complex to prevent binding to DNA. A second transcriptional feedback loop consists of the transcription factor VRILLE (VRI) whose repression alters *tim* expression as well as the rhythm [24, 27] (Fig. 1.4).

In *Neurospora crassa*, the protein product of *frequency* (“*frq*”), FRQ, represses its own transcription. Protein products of the core clock oscillator, *white collar* (“*wc*”), WC1 and WC2, form heterodimers to activate expression of *frq*. FRQ accumulates and translocate into the nucleus to repress its own mRNA levels by binding to and interfering with WC1 and WC2 activity [28, 29] (Fig 1.4).

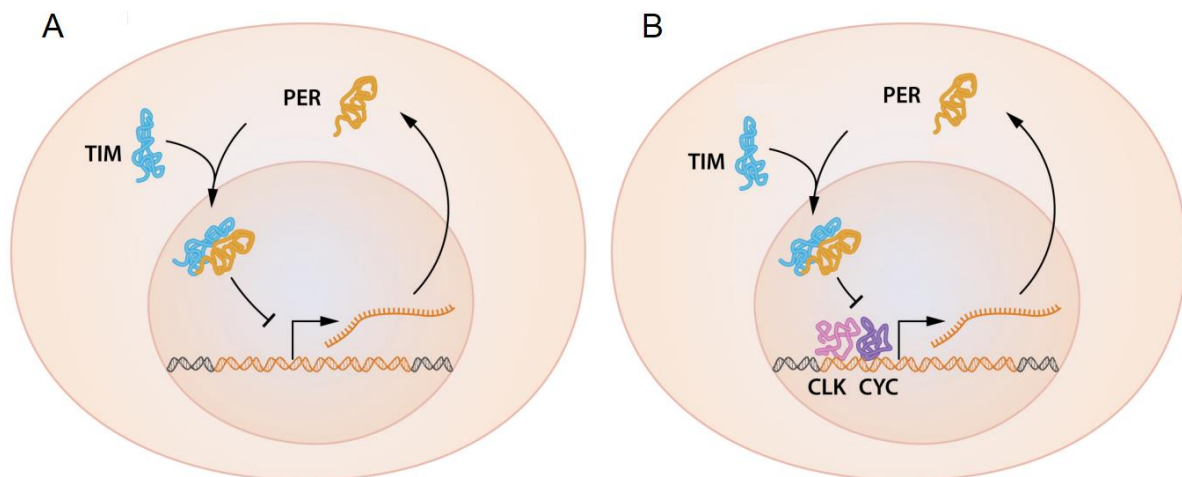


Figure 1.3: A simplified illustration of the feedback regulation of the *period* gene. (A) Both *period* mRNA and PER protein oscillate, with PER protein accumulating several hours after the peak in *period* mRNA. PER protein localizes in the nucleus, and the *period* gene activity oscillates because of PER protein feedback inhibition of its own gene. TIM protein, encoded by the *timeless* gene also oscillates and interacts with PER protein. This interaction is critical for PER protein nuclear accumulation and repression of the *period* gene. (B) CLK and CYC, encoded by the clock and cycle genes, are two transcription factors that activate the *period* gene. Image and legend modified from [@nobelprize.org](http://nobelprize.org).

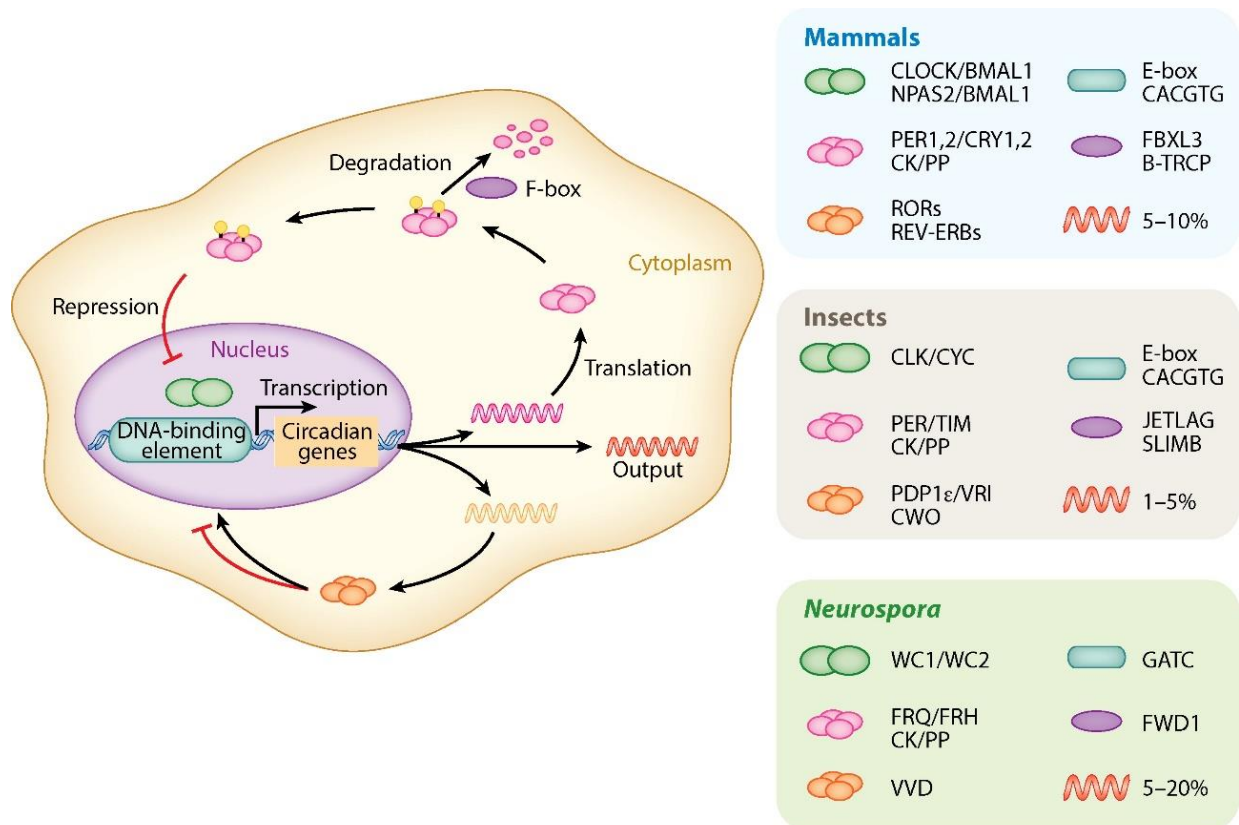


Figure 1.4: The TTFL model of cellular timekeeping. The architecture and basic principle (left) of transcription-based clocks seems to be conserved among species, although the core clock components differ. The core clock components for three different model organisms are shown (right). Image adapted from [2].

1.2.2 Non-transcriptional clocks

The notion that non-transcriptional processes might drive circadian clocks dates back to the year 1960. Observations in the single nucleus unicellular alga *Acetabularia sp.* showed that the enucleated plant cell could retain viability over several weeks and exhibited intrinsic rhythms in photosynthesis and chloroplast shape in constant conditions [30, 31]. Furthermore, pharmacologically inhibiting cellular transcription in this plant did not affect the observed rhythms in the first fortnight of treatment, suggesting that transcription is dispensable for generating rhythmicity. Nonetheless, transcription was required to maintain the levels of key oscillator components [32].

The first intriguing evidence for an autonomous non-transcriptional oscillator came from studies in *S. elongates* by Kondo and colleagues. The core oscillator in this organism consists of three genes – *kaiA*, *kaiB* and *kaiC* – which, together with their protein products control the periodic transcription of other genes [33-35]. In this system, KaiC is the main oscillator with both auto-kinase and -phosphatase activities; KaiA activates the kinase and inhibits the phosphatase activities of KaiC, whilst KaiB antagonizes the activity of KaiA. The interactions between these proteins lead to 24-hour oscillations in KaiC phosphorylation state, which successively drives rhythmic changes in transcription of genes, including that of the *kaiBC* operon (Fig. 1.5). Subsequent experiments showed that the oscillations in KaiC phosphorylation state was not dictated by the rhythmic transcription of the *kaiBC* operon. A simple biochemical experiment reconstituting

the three Kai proteins in a test tube, supplemented with ATP as a source of phosphates showed that the 24-hour rhythms in phosphorylation and de-phosphorylation of the KaiC protein could persist. This observation demonstrated the existence of an oscillator that functioned independent of transcription. Nonetheless, transcription was required to maintain the levels of *Kai* proteins *in vivo*.

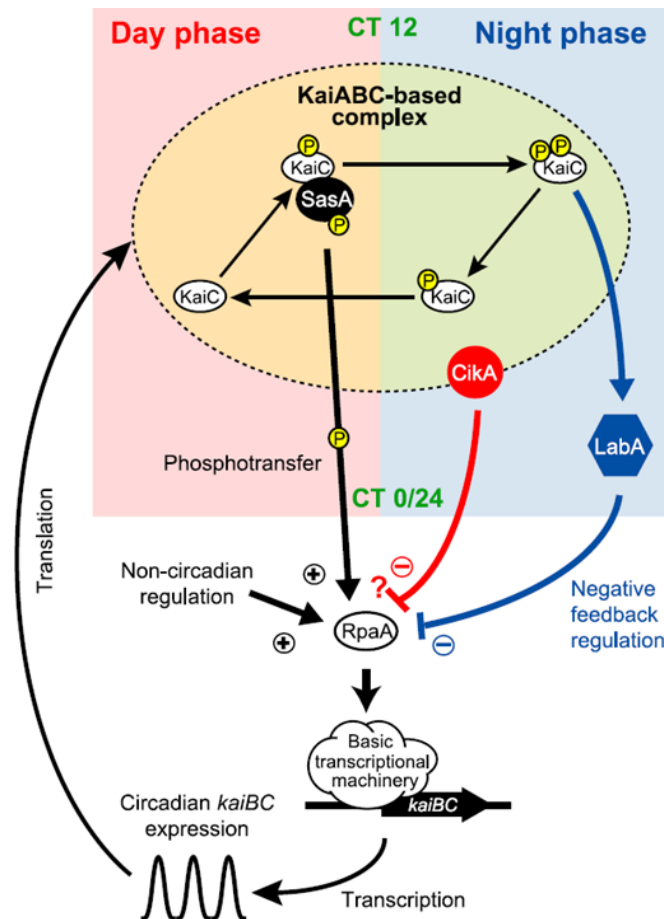


Figure 1.5: The cyanobacterial circadian clock. The cyanobacterial clock demonstrated that phosphorylation of a substrate can exhibit 24-hour rhythms *in vivo* (even upon inhibition of transcription) and *in vitro*, providing the first mechanistic explanation for non-transcriptional rhythms. The core oscillator consists of three proteins (KaiA, KaiB, and KaiC), which via a feedback loop, regulate the expression of numerous genes including the *kaiBC* promoter. Image adapted from [36].

John O’Neil and colleagues showed evidence for the existence of a non-transcription based clock mechanism that functions together with the TTFL model in *Ostreococcus tauri* [37]. They demonstrated that after complete termination of transcription in constant darkness, *O. tauri* cultures could restore transcriptional rhythms once transferred to constant light. They concluded that a non-transcriptional mechanism ran in parallel to preserve the phase of the clock, since the transfer to light did not alter the phase of the oscillations [37]. The subsequent

discovery of redox oscillations in the levels of hyperoxidized (or sulfynylated) peroxiredoxin proteins in human RBCs (which lack nucleus) and *O. tauri* (even during transcriptional arrest) showed that non-transcriptional oscillators might not only be restricted to small organisms like cyanobacteria [37, 38]. Later on, peroxiredoxin hyperoxidation rhythms have been shown to be conserved across all domains of life [39]. These peroxiredoxin hyperoxidation rhythms, together with oscillations in cellular metabolites such as NAD^+/NADH , $\text{NADP}^+/\text{NADH}$ and ADP/ATP underlie cellular metabolic clocks [37, 38, 40]. Metabolic clocks can function independent of cellular transcription.

Furthermore, oscillations in cellular biochemical parameters were described and proposed to complement the TTFL to explain circadian behavior. For instance, Cornelius and Rensing reported that Mg^{2+} -dependent ATPase activity in the membranes of RBCs cultured *in vitro* was rhythmic [41]. Radha *et al.* showed that *in vitro* cultures of human platelets exhibited oscillations in the levels of glutathione [42]. Edmunds and colleagues described a non-transcriptional feedback loop model for observed rhythms in nicotine adenine dinucleotides, NAD^+ and NADP^+ , in *Euglena sp.* [43]. More recently, circadian oscillations in magnesium (Mg^{2+}) and potassium (K^+) levels were also observed in cultured human cells and *O. tauri* (even during transcriptional arrest) under constant conditions [44].

1.3 The Yeast Metabolic Cycle as a model metabolic clock

In budding yeast, *Saccharomyces cerevisiae*, long period oscillations in oxygen consumption – termed Yeast Metabolic Cycle (YMC) – occur over several hours during continuous, glucose-limited growth [45-48]. *S. cerevisiae*, is a unicellular eukaryote that shares many protein homologs with other multicellular organisms.

The most obvious feature of the YMC is high amplitude changes in oxygen consumption in a continuous culture system (Fig. 1.6). There exists two main phases of the YMC: a high oxygen consumption (HOC) phase where cells rapidly consume oxygen and a low oxygen consumption (LOC) phase where there is highest dissolved oxygen levels during the continuous culture (Fig. 1.7). Cyclical changes in the levels of more than 50 % of cellular genes also occur during the YMC. Additionally, the YMC appears to regulate entry into and exit from the cell division cycle. Strikingly, DNA replication and cell division are precisely gated to temporal windows when oxygen consumption decreases, in ways reminiscent of the circadian gating of cell division observed in cyanobacteria, mouse liver, and cultured fibroblasts [46, 49-55]. Moreover, genetic or chemical perturbation of cellular redox processes with H₂O₂ can strongly disrupt the YMC [47, 49, 56].

It is not entirely clear how the oscillations in the YMC are generated and sustained. However, it has been proposed that cells build and accumulate storage carbohydrates, such as trehalose and glycogen during LOC [51]. Upon accumulating enough of these carbohydrates, a proportion of the yeast population are thought to commit to HOC and liquidate their storage carbohydrates in the process, to generate energy for cellular biosynthetic processes via aerobic metabolism [57]. Through a mechanism termed, YMC-to-YMC coupling, it is believed that this metabolically committed yeast sub-population produce and secrete metabolites such as ethanol, acetaldehyde and dihydrogen sulfide that serve to shift the YMC phase of other cells in order to achieve synchronous oxygen consumption [58-60]. It has also been shown that during the YMC, cyclical changes in cell metabolism is coordinated with cellular processes such as gene expression, respiration, mitochondria biogenesis, ribosome biogenesis, DNA replication, cell division, fatty acid oxidation, glycolysis and vacuole-mediated catabolism [47, 49, 50].



BIOSTAT A Bioreactor

Figure 1.6: The Chemostat system for generation of the YMC. The bioreactor consists of a culture vessel connected via tubes to a system unit. The system unit is equipped with probes to measure pH and dissolved oxygen in the culture vessel. Peristaltic pumps are affixed to control media in-flow and out-flow. An additional unit serves as a cooling chamber to control the operating temperature. Image sourced from @Satorious GmbH.

The YMC represents the yeast metabolic clock and shares several features that are conserved with circadian clocks in other organisms [40, 61]. These include (1) generation of temperature-compensated rhythms, (2) exhibition of oscillations that are coupled with the cell division cycle, (3) oscillatory period that is determined by post-translational mechanisms, such as phosphorylation of clock proteins by casein kinase

1 (CK1) and glycogen synthase kinase β (GSK β), and (4) rhythmic oscillations in the cellular redox state (eg. hyperoxidation of peroxiredoxin proteins) [40, 47]. On this basis, the YMC serves as a convenient model to investigate metabolic clock activity.

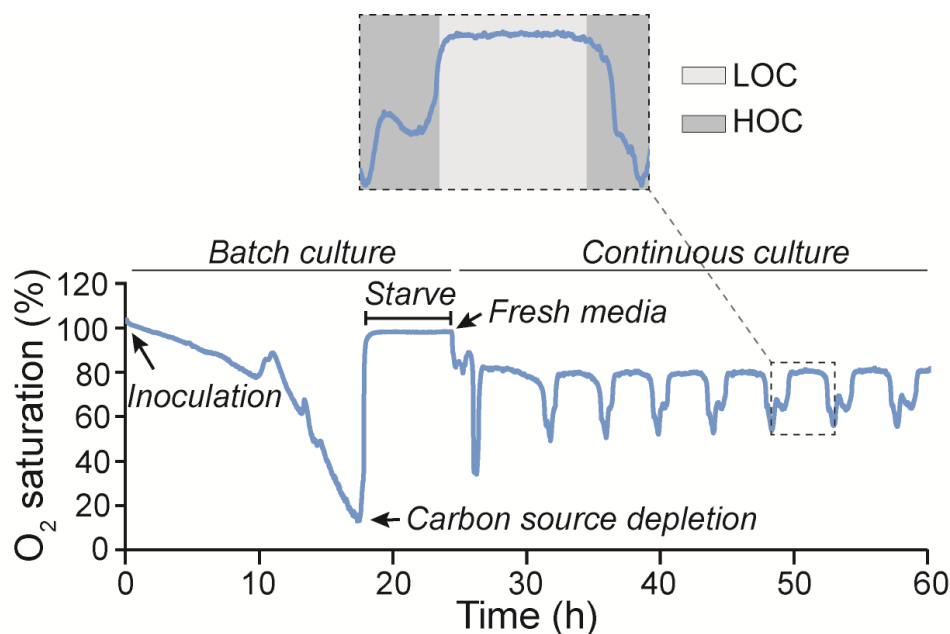


Figure 1.7: The Yeast Metabolic Cycle. Representative oxygen trace showing the procedure for establishing YMC-synchronized continuous cultures. Cells inoculated into the fermenter are allowed to grow in a batch phase to maximum density until dissolved oxygen is almost depleted. Following starvation for nearly 6 hours, fresh media is pumped into the culture vessel at a constant dilution rate of 0.05 h^{-1} , which results in the generation of synchronized self-sustained oscillations between fermentative and respiratory metabolism with a period of nearly 5 hours. **LOC** – low oxygen consumption, **HOC** – high oxygen consumption.

1.4 Hydrogen peroxide in redox signaling

Hydrogen peroxide (H_2O_2) is a redox metabolite that functions as a secondary messenger in a variety of cell signaling events [62]. These include, but not limited to, antimicrobial defense, inflammation, cell migration, cell proliferation, angiogenesis and regulation of gene expression [63]. Within the cell, H_2O_2 production is regulated, and mediated by enzymes such as superoxide dismutases (SODs), NADPH oxidases, as well as the mitochondrial electron transport chain (ETC). Under physiological conditions, steady-state cellular H_2O_2 concentration ranges between approximately 1 - 10 nM, and can rise to approximately 0.5 - 0.7 μM during oxidative events such as aerobic respiration and fatty acid β -oxidation [64, 65].

It is not entirely clear how H_2O_2 oxidizes protein thiols within cells. This is because most redox-regulated proteins exist in low abundance within cells. Moreover, most thiol-containing redox-regulated proteins generally exhibit poor direct reactivity towards H_2O_2 , with $k \approx 10^0\text{--}10^2 \text{ M}^{-1}\text{s}^{-1}$ [66]. Furthermore, peroxiredoxins – the most prominent group of thiol peroxidases – exhibit the highest intrinsic reactivity of any protein towards H_2O_2 , and are predicted to capture nearly all of the H_2O_2 generated inside cells [67]. In addition, peroxiredoxins are highly expressed proteins with overall cytosolic concentration 2 - 3 orders of magnitude higher than that of most redox-regulated proteins. Owing to their high abundance and high

reactivity, peroxiredoxins are effective competitors for H_2O_2 compared to all other protein thiols [68]. Glutathione peroxidases are also a group of thiol peroxidases that exhibit high reactivity towards H_2O_2 .

Although the mechanisms that ensure target specificity of H_2O_2 -induced thiol oxidation events are not fully resolved, two contrasting but mutually non-exclusive schools of thought explain H_2O_2 signaling within cells: direct oxidation or ‘*floodgate*’ and facilitated oxidation or ‘*relay*’ hypotheses.

1.4.1 Direct oxidation or ‘*floodgate*’ hypothesis

The ‘*floodgate*’ hypothesis suggests that at sources of generation, H_2O_2 accumulates to high levels and directly mediates oxidation of protein thiols. Here, peroxiredoxins and other thiol peroxidases are viewed as competitors or scavengers of H_2O_2 , thereby thwarting direct H_2O_2 -mediated oxidation of protein thiols [63]. Therefore for direct thiol oxidation to occur, peroxiredoxins must be temporarily rendered inactive by posttranslational modifications such as hyperoxidation or phosphorylation. Under such conditions, H_2O_2 locally accumulates to levels that allow for selective and direct oxidation of protein thiols with modest intrinsic H_2O_2 reactivity (Fig. 1.8). This hypothesis makes two predictions: (1) upon H_2O_2 , cysteine sulfenic acid (Cys-SOH) should form directly on target protein thiols, and (2) upon deletion of peroxiredoxins, H_2O_2 -induced protein thiol oxidation should increase. Evidence for direct H_2O_2 -mediated thiol oxidation was described in A431 human epidermoid carcinoma cells. The Rhee lab showed that transient increase in the intracellular concentration of H_2O_2 either by exogenous addition or via epidermal growth factor (EGF) signaling caused inactivation of recombinant protein-tyrosine phosphatase 1B (PTP1B) *in vitro* by oxidizing its catalytic site cysteine, most likely to sulfenic acid [69]. Although the thiol state of peroxiredoxins was not analyzed in their study, it is plausible that peroxiredoxins were hyperoxidized by the amounts of H_2O_2 used. In a related study, they also showed that localized inactivation of membrane-associated PrxI by phosphorylation in response to EGF leads to local accumulation of H_2O_2 for cell signaling [70].

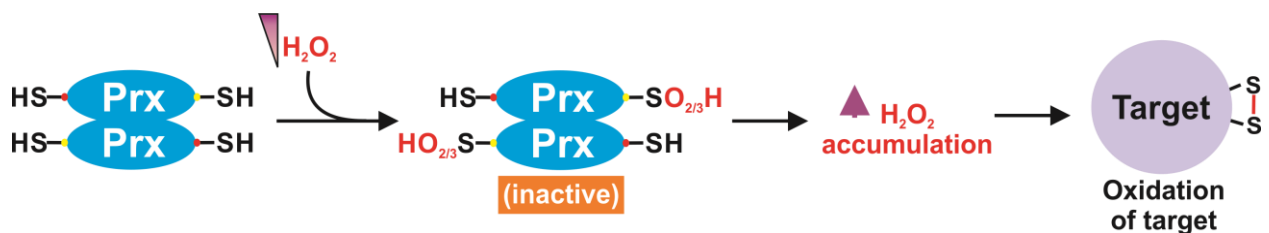


Figure 1.8: Floodgate hypothesis of H_2O_2 signaling. This model of signaling positions peroxiredoxins as scavengers of H_2O_2 , which frustrate thiol protein oxidation within cells.

1.4.2 Facilitated oxidation or ‘*relay*’ hypothesis

The ‘*relay*’ hypothesis suggests that the levels and exceptional intrinsic reactivity of thiol peroxidases to H_2O_2 position them as effective recipients and competitors for H_2O_2 , above all other potential protein thiols [71]. These proteins must therefore receive oxidizing equivalents from H_2O_2 via the action of thiol peroxidases – which act as transmitters –, in order to become oxidized. Here, thiol peroxidases are

viewed as enablers of protein thiol oxidation, not as competitors. As such, inactivation by hyperoxidation or phosphorylation inhibits this ‘relay’ function and renders target protein thiols reduced (Fig. 1.9). In contrast to the ‘floodgate’ model, this hypothesis predicts that: (1) upon H_2O_2 , Cys-SOH should not form directly on target protein thiols, as only thiol peroxidases are prone to react directly with H_2O_2 , and (2) upon deletion of thiol peroxidases, H_2O_2 -induced protein thiol oxidation should decrease.

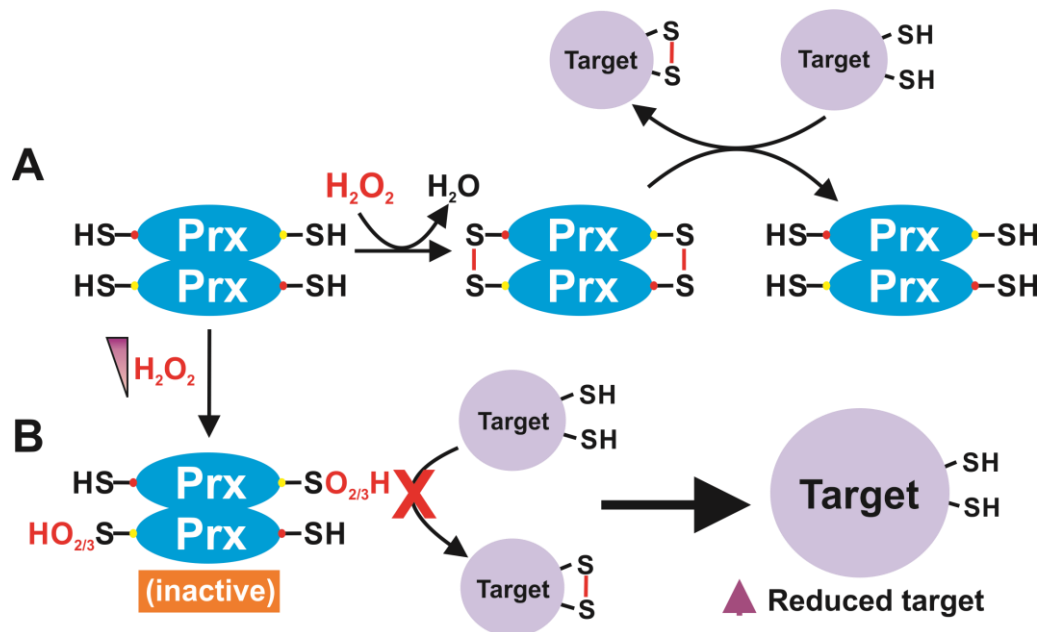


Figure 1.9: Relay hypothesis of H_2O_2 signaling. This model of signaling positions peroxiredoxins as facilitators or enablers of protein thiol oxidations, without which thiol protein oxidations barely occur within cells. (A) Peroxiredoxin-mediated oxidation of protein thiol. (B) Protein thiol oxidation is inhibited upon peroxiredoxin hyperoxidation.

Evidence for the ‘relay’ hypothesis has been demonstrated in yeast and mammalian cells. Recent studies by Stöcker and colleagues suggest that mammalian proteins such as ANXA2, ASK1 and CBS mostly depend on the relay function of PRDX1 and PRDX2 in order to facilitate their thiol oxidation [72]. It has also been shown that PRDX2 transfers oxidizing equivalents to the STAT3 transcription factor via a redox relay [73] (Fig 1.10). In *S. cerevisiae*, the thiol peroxidase Orp1 forms mixed disulfides with the Yap1 transcription factor, leading to the activation of Yap1 via an intramolecular disulfide [74]. In *S. pombe*, the 2-Cys peroxiredoxin, Tpx1, activates the p38/JNK homolog, Sty1, upon H_2O_2 [75].

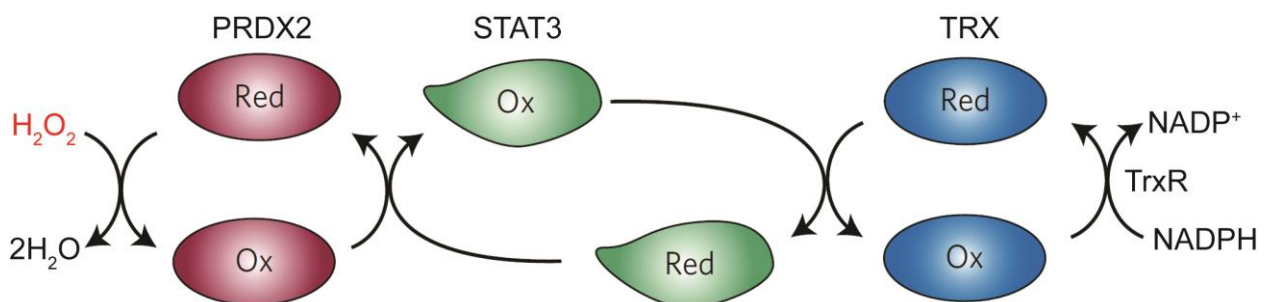


Figure 1.10: Example of endogenous peroxiredoxin redox relay. Redox-regulated protein, STAT3, receive oxidizing equivalents from a peroxiredoxin, PRDX2. The oxidized STAT3 translocate into the nucleus to mediate transcription of genes involved in cell growth and apoptosis. The oxidized STAT3 can be reduced by thioredoxin. Image modified from [73]

1.5 Peroxiredoxins: structure, catalytic mechanism and function

Budding yeast possesses eight thiol peroxidases, consisting of three cysteine-dependent glutathione peroxidases (Gpx1, Gpx2, Gpx3/Orp1) and five peroxiredoxins. Peroxiredoxins (Prxs) are a very large and highly conserved family of thiol peroxidases that are distributed across cellular compartments: three cytosolic (i.e. Tsa1, Tsa2 and Ahp1) one nuclear (i.e. Dot5) and one mitochondrial (i.e. Prx1). Of all thiol peroxidases, peroxiredoxins are the most reactive towards H_2O_2 with rate constants, $k \approx 10^7\text{--}10^9 \text{ M}^{-1} \text{ s}^{-1}$ [76-79].

A highly conserved cysteine (Cys) residue called the ‘peroxidatic’ cysteine (C_P) acts as the site of oxidation by peroxides and mediates catalytic activity of peroxiredoxins [80, 81]. During catalysis, the C_P performs a nucleophilic attack on one of the oxygens in H_2O_2 , which leads to the oxidation of the C_P sulfhydryl ($\text{C}_\text{P}\text{-SH}$) to a sulfenic acid ($\text{C}_\text{P}\text{-SOH}$) intermediate. Depending on the number of Cys residues involved in the catalysis, peroxiredoxins can be classified into either 1-Cys or 2-Cys. In 2-Cys peroxiredoxins, the $\text{C}_\text{P}\text{-SOH}$ reacts with another Cys residue, called the ‘resolving’ cysteine (C_R) to form a disulfide that is subsequently reduced by an appropriate electron donor such as thioredoxins (Trxs) to complete the catalytic cycle. One-Cys peroxiredoxins (e.g. Prx1) lack a C_R and therefore the $\text{C}_\text{P}\text{-SOH}$ is reduced by small molecule antioxidants such as glutathione [82].

The location of the C_R residue in 2-Cys peroxiredoxins further results in two subclasses: typical 2-Cys and atypical 2-Cys peroxiredoxins [83, 84]. Typical 2-Cys peroxiredoxins (e.g. Tsa1, Tsa2) are catalytically active as homodimers with a C_P and C_R per monomer. The $\text{C}_\text{P}\text{-SOH}$ intermediate on one monomer is resolved by the C_R from the other monomer to form an intermolecular disulfide (S-S) bond. In atypical 2-Cys Prxs (e.g. Ahp1), a C_R from the same subunit resolves the $\text{C}_\text{P}\text{-SOH}$ intermediate to form an intramolecular disulfide bond.

The $\text{C}_\text{P}\text{-SOH}$ intermediate of 2-Cys peroxiredoxins can undergo further oxidation to generate reversible sulfinic ($\text{C}_\text{P}\text{-SO}_2\text{H}$) and irreversible sulfonic ($\text{C}_\text{P}\text{-SO}_3\text{H}$) acid forms [85-87]. This phenomenon results in catalytic peroxiredoxin inactivation and is termed hyperoxidation. The $\text{C}_\text{P}\text{-SO}_2\text{H}$ form can be reactivated by sulfiredoxin (Srx) through an ATP-dependent reduction reaction [88] (Fig. 1.11).

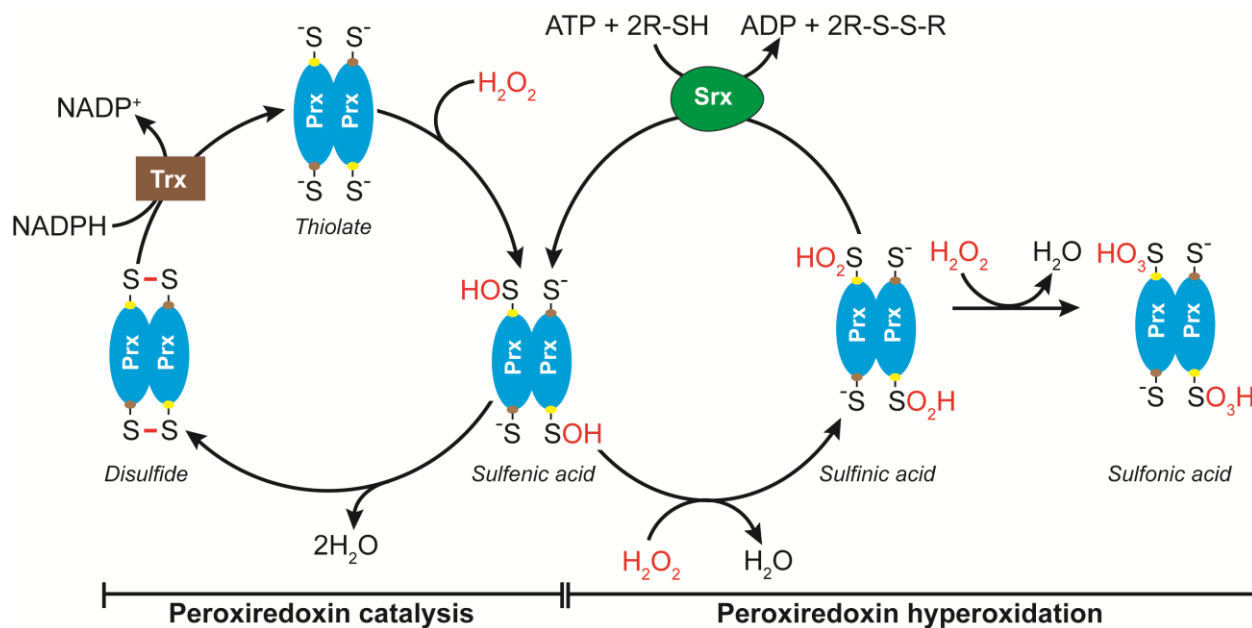


Figure 1.11: Catalytic mechanism of typical 2-Cys Peroxiredoxins. Upon encountering H_2O_2 , the peroxidatic cysteine of peroxiredoxins undergo peroxidation to form sulfenic acid ($\text{C}_\text{P}\text{-SOH}$), followed by disulfide bond (S-S) formation mediated by the resolving cysteine (C_R). The peroxiredoxin is recycled via a step catalyzed by thioredoxin (Trx). However, upon further exposure to H_2O_2 , the sulfenic acid intermediate can be oxidized to sulfinic and sulfonic acid forms ($\text{C}_\text{P}\text{-SO}_2\text{H}$). The overoxidized $\text{C}_\text{P}\text{-SO}_3\text{H}$ can be recycled through ATP-dependent reduction by sulfiredoxin (Srx). The hyperoxidized $\text{C}_\text{P}\text{-SO}_3\text{H}$ form is irreversible.

1.6 Genetically encoded thiol peroxidase-based biosensors

Taking advantage of naturally occurring redox relays and the extreme sensitivity of the $\text{C}_\text{P}\text{-SH}$ of thiol peroxidases towards H_2O_2 , genetically encoded H_2O_2 fluorescent sensors have been developed by fusing a thiol peroxidase to redox sensitive green fluorescent protein (e.g. roGFP2) [89-91]. Typical examples of such biosensors include the roGFP2-Orp1, roGFP2-Tsa1, roGFP2-Tsa2, roGFP2-PRDX2 [90-92]. RoGFP2 is based upon an enhanced GFP, modified to contain two cysteine residues capable of forming a disulfide bond. These biosensors work on the principle that upon encountering oxidizing equivalents, the thiol peroxidase gets oxidized and transfers its oxidation state via a multi-step process to the cysteine residues in roGFP2 (Fig. 1.12). RoGFP2 exhibits two excitation maxima at 405 nm and 488 nm when fluorescence emission is monitored at 510 nm [93]. The two excitation wavelengths permit ratiometric measurements, which renders the sensor readout independent of changes in sensor concentration.

Together with my colleagues, we developed and applied a more sensitive (approximately 20-fold) variant of the roGFP2-Tsa2 sensor, roGFP2-Tsa2 ΔC_R , in the measurement of ‘basal’ endogenous H_2O_2 levels in yeast [90]. We fused the thiol specific antioxidant Tsa2, a typical 2-Cys peroxiredoxin from *S. cerevisiae*, deleted for its resolving cysteine (i.e. Tsa2 ΔC_R), to roGFP2. We deleted the resolving cysteine of the Tsa2 moiety in order to limit the formation of Tsa2 disulfide and subsequent reduction by thioredoxins. This ensures direct transfer of oxidation from the peroxidatic cysteine of Tsa2 ΔC_R to roGFP2 and enhances the fluorescence signal (i.e. sensitivity). The roGFP2-Tsa2 ΔC_R biosensor specifically

measures H_2O_2 levels and does not significantly contribute to cellular H_2O_2 scavenging. RoGFP2 itself exhibits poor direct reactivity towards H_2O_2 ; hence, any H_2O_2 -driven oxidation of roGFP2 is mediated by the Tsa2 ΔC_R moiety. However, roGFP2 reduction is mediated by cellular glutaredoxins (Grx) using glutathione (GSH).

Functionally, roGFP2-thiol peroxidase fusion biosensors represent an artificial reconstitution of an entire thiol peroxidase redox relay. However, instead of a transcriptional response upon oxidation, as is the case with natural relays, a fluorescence response is elicited in the context of the biosensor. Excess or non-physiological levels of H_2O_2 can hyperoxidize Tsa2 ΔC_R . When the $\text{C}_P\text{-SH}$ of the Tsa2 ΔC_R becomes hyperoxidized to the sulfinic or sulfonic acid, transfer of oxidizing equivalents to roGFP2 is prevented and the sensor ceases to function as an H_2O_2 sensor. Upon Tsa2 ΔC_R inactivation, roGFP2 equilibrates with GSH/GSSG via the action of glutaredoxins. A reduced roGFP2 in this scenario does not represent an absence of, or low, H_2O_2 levels.

I have relied on the capacity of the roGFP2-Tsa2 ΔC_R sensor to make long-term, non-disruptive, real-time, fully dynamic H_2O_2 measurements in yeast, to answer the outstanding question of whether the peroxiredoxin hyperoxidation rhythms that underlie circadian and ultradian metabolic clocks have any functional relevance. I have re-engineered the sensor and expressed it from the genome of prototrophic yeast to measure cyclical H_2O_2 changes and evaluate peroxiredoxin activity during the YMC.

roGFP2-Tsa2 ΔC_R : a reconstituted thiol peroxidase redox relay

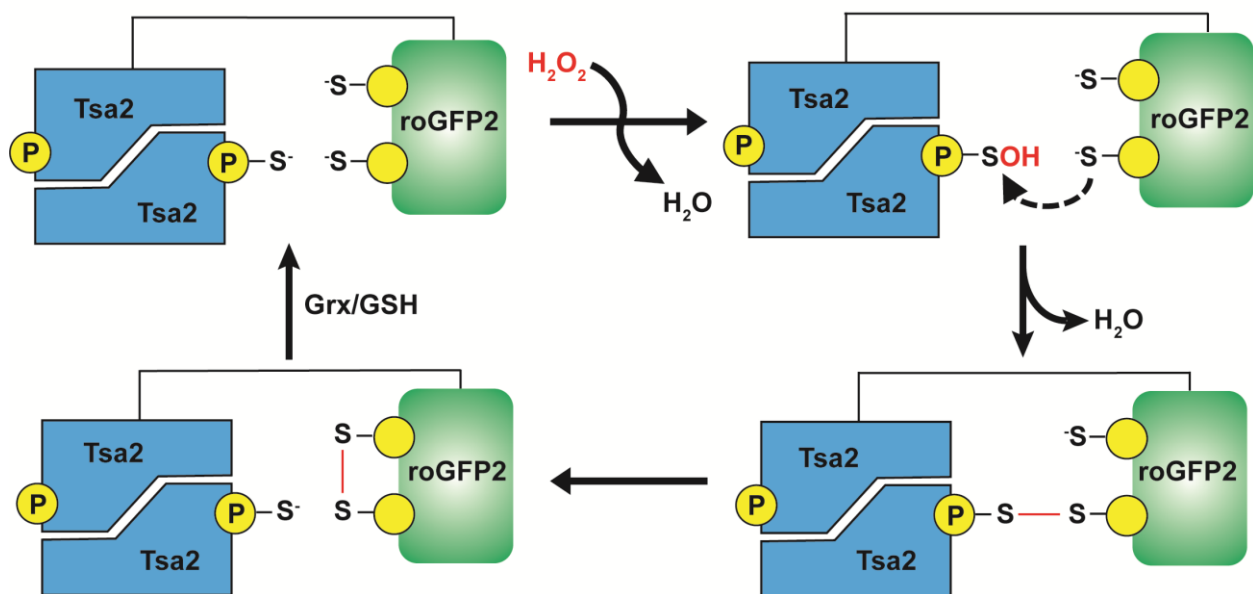


Figure 1.12: Mechanism of the roGFP2-Tsa2 ΔC_R sensor. Diagram to illustrate the mechanism of the roGFP2-Tsa2 ΔC_R sensor, which is based on the principle of a thiol peroxidase-based redox relay. All cysteine residues of the sensor remain in a reduced thiolate state in the absence of H_2O_2 . Upon encountering H_2O_2 , the peroxidatic cysteine ($\text{C}_P\text{-SH}$) of the Tsa2 ΔC_R performs a nucleophilic attack to extract oxidizing equivalents from H_2O_2 . The oxidizing equivalents are transferred via a two-step process resulting in the formation of an intramolecular roGFP2 disulfide bond. The oxidized roGFP2 can be reduced by glutaredoxins (Grx) using glutathione (GSH).

1.7 Crosstalk between the cellular redox state, metabolism, cell cycle and circadian/ultradian clocks

1.7.1 Reciprocal regulation of clock mechanism by redox homeostasis

Preliminary evidence for the existence of crosstalk between metabolism, redox homeostasis and circadian clocks was demonstrated using a non-physiological *in vitro* biochemical assay. In their studies, Rutter *et al.* showed that nuclear NAD⁺/NADH and NADP⁺/NADPH ratios influence the transcriptional activity of the CLOCK (NPAS2)/BMAL1 heterodimer [94]. It has also been shown that oscillations in NAD(P)⁺ and NAD(P)H cofactors accompany peroxiredoxin-sulfinylation rhythms that underlie metabolic clocks [37, 38].

Redox changes regulate expression of clock-related genes in multiple systems. In *S. cerevisiae*, the glutathione peroxidase, Orp1, relays signals from H₂O₂ to the Yap1 transcription factor to elevate antioxidant response systems [74]. Yap1 shuttles in and out of the nucleus during the YMC [47]. In zebrafish, H₂O₂ generated from light regulates the expression of clock genes, *cry1* and *per2*, via the action of catalase [95]. In *N. crassa* and cyanobacteria, H₂O₂ influences the daily expression pattern of clock and clock-controlled genes involved in coordinating photosynthesis [96-98]. Furthermore, the redox sensor, light-dependent period A (LdpA) modulates cyanobacterial circadian clock period length by controlling the levels of *CikA* and *KaiA*, in response to light [99, 100]. Oscillations in overexpressed mammalian PRDX2 nuclear levels dampen oscillations in BMAL1 in HaCaT keratinocytes [101, 102]. Hyperoxidation of mitochondrial PRDX3 has also been shown to be essential for circadian rhythms in adrenal steroidogenesis [103].

Alternatively, clock genes can regulate the expression of multiple redox systems. For instance, wildtype Canton S flies exhibit oscillations in glutamate-cysteine ligase and glutathione S transferase D1 transcript levels, which is abolished in mutants lacking the *per* and *cyc* clock genes [104]. *D. melanogaster* flies exhibit diurnal rhythms in susceptibility to H₂O₂, which are abolished in *per* gene mutants [105]. *A. thaliana* exhibits diurnal rhythms in the generation and scavenging of H₂O₂, which is perturbed in mutants of the core clock regulator, circadian clock-associated 1 (CCA1) [106]. Finally, it was shown that *Bmal1*^{-/-} mice accumulate higher ROS levels compared to their wildtype counterparts, which impinges on aging pathologies [107].

Although abundance of evidence for reciprocal crosstalk between cellular metabolism, redox homeostasis and circadian/ultradian systems exist, the underlying mechanisms by which redox changes may govern circadian/ultradian rhythms are not fully understood.

1.7.2 Redox/metabolic state versus cell division cycle

In order to grow, living organisms undergo cell division. During this highly ordered and regulated process, living cells give rise to either two (ie. somatic or mitotic division) or four (i.e. gametic or meiotic division) daughter cells. *S. cerevisiae* undergoes mitotic cell division, which is ordered in four phases: G₁ (Gap1), S (Synthesis), G₂ (Gap2) and M (Mitosis). In G₁ the cell increases in size until it reaches the checkpoint at which critical decisions to undergo division, or not, is taken. This ‘committed step’ is termed ‘restriction point’ in mammals and ‘Start’ in budding yeast [108-111]. During the S phase, cellular DNA is duplicated and cells proceed to segregate this DNA into two daughter cells during the M phase. In S phase, the fidelity of DNA replication is controlled by checkpoint mechanisms that become activated to repair damaged DNA if replication forks stall [112]. Between the transition from S to M phase is a G₂ that is less distinct in *S. cerevisiae* [113].

It has been suggested that the decision to undergo cell division is determined by the cellular metabolic state (or metabolic oscillator), and governed by the availability of macromolecules and energy to power cells through the process [114]. For instance, budding yeast cell cycle ‘Start’ is coordinated with the liquidation of storage carbohydrates and their daughter cells spend more time in G₁, accumulating biomass until they have reached a critical size before committing to cell division [57, 115].

Several reports indicate that the cellular redox state is a key regulator of the cell cycle, i.e. transient oxidative mechanisms control key cell cycle regulatory proteins possibly via thiol-disulfide exchanges at critical cysteine residues [116-119]. It is believed that low levels of cellular oxidation, possibly from superoxide (O₂⁻) and H₂O₂, are required for proper mitogenic signaling [117, 120, 121]. In mammalian cells, this oxidative mechanism is thought to control the activities of cyclin-dependent kinases (Cdks) and the retinoblastoma protein at G₁, to permit entry into S phase for DNA replication [122-124]. Thereafter, a more general reduction of the cellular environment is necessary to enable cells progress to the G₂ and M phases [125]. Moreover, it has been suggested that the G₁ phase is characterized by low cellular GSH, which levels must necessarily increase to facilitate cell cycle progression from G₁ to S [126].

Although redox metabolism cannot be divorced from cell cycle regulation, the identification of redox-regulated proteins or thiol peroxidase relays relevant to each cell cycle phase remains an enormous challenge.

1.8 Aims of this thesis

Circadian and ultradian peroxiredoxin hyperoxidation rhythms exist across the three domains of life, including during the yeast metabolic cycle (YMC), and have been proposed as the mechanistic basis for cellular metabolic clocks [37-40]. However, to date it has remained largely unclear if peroxiredoxins are involved in cellular timekeeping or are merely convenient reporters of metabolic oscillations. The aims of this thesis were to investigate (1) whether peroxiredoxins are active determinants of cellular timekeeping, using the yeast metabolic clock as a model, and (2) whether peroxiredoxins are important for the coordination between metabolic clocks and the cell division cycle. My specific objectives included the following:

- a) Establishment and characterization of YMC-synchronized cultures.
- b) Engineering prototrophic yeast strain capable of expressing the roGFP2-Tsa2 Δ C_R biosensor from its genome.
- c) Interrogating whether H₂O₂ levels, peroxiredoxin oxidation, and the oxidation of peroxiredoxin target protein(s) oscillate during the YMC.
- d) Determining whether thiol disulfide changes influence or regulate metabolic clock function.
- e) Investigating if peroxiredoxins are crucial for YMC oscillation.
- f) Verifying whether cell division is synchronized with the YMC, and if metabolic oscillations are crucial for regulating cell cycle entry and exit.
- g) Examining whether loss or inactivation of peroxiredoxins affects coupling of cell metabolism to the cell division cycle.

2 RESULTS

Circadian and ultradian oscillations in the level of hyperoxidized peroxiredoxin proteins underlie cellular metabolic clocks. However, whether peroxiredoxins are important components of the clock mechanism or just convenient markers of oscillatory redox metabolism remained enigmatic. In this study, I sought to investigate whether peroxiredoxins are active participants in cellular timekeeping, using the YMC clock model. For this purpose, I established YMC-synchronized cultures and interrogated the role of peroxiredoxins using genetic and biochemical approaches.

2.1 Establishment of YMC-synchronized cultures

When prototrophic yeast cells are grown under nutrient-limited conditions in continuous culture using chemostat, they exhibit high amplitude periodic changes in oxygen consumption. These self-sustained oscillations are termed the Yeast Metabolic Cycle (YMC) and display periods ranging from approximately 40 minutes to over 10 hours, depending on the type of strain as well as growth conditions [46, 47, 52, 127, 128]. The YMC is the yeast ultradian metabolic clock, which consists of oscillations in cell metabolism, levels of cellular transcripts and the cell division cycle [47, 49, 56]. I used the YMC model because it shares features that are conserved with circadian rhythms in mammalian cells. The YMC exhibits oscillations that are temperature-compensated and are coupled with the cell division cycle. It also displays rhythmic oscillations in the cellular redox state (e.g. hyperoxidation of peroxiredoxin proteins) [40, 47].

2.1.1 The YMC consists of synchronized respiratory oscillations

To use the YMC as the model metabolic clock for my study, I cultured yeast cells under the chemostat conditions described by Tu *et al.* [47] with slight modifications, as described in Materials and Methods. After growth in a batch phase, starvation for at least 6 hours and continuous feed-in of fresh media into the culture vessel at a dilution rate of 0.05 h^{-1} , I observed self-synchronized oscillations in oxygen consumption by the yeast population. These oscillations consisted of long phases of low oxygen consumption (LOC) and short phases of high oxygen consumption (HOC), which persisted as long as media was available. The amplitude of each oscillation ranged between 60 – 80% of dissolved oxygen and the period of each wildtype YMC lasted approximately 5 hours (Fig. 1.7). Blocking respiratory activity with potassium cyanide (KCN) immediately halted oxygen consumption and returned YMC-synchronized cells to a ‘starvation mode’ that lasted until KCN was diluted out of the culture vessel (Fig. 2.1A). KCN inhibits complex IV of the mitochondrial electron transport chain. Addition of a bolus of respiratory substrate, ethanol, at the start of a LOC phase immediately triggered oxygen consumption that lasted for a longer period until the substrate was depleted (Fig. 2.1B). However, an inert solvent such as dimethyl sulfoxide (DMSO) had no observable effect on the YMC (Fig. 2.1C). Taken together, I have successfully established

the YMC for my study and shown that the oscillations in oxygen consumption observed during the YMC are largely respiratory in nature.

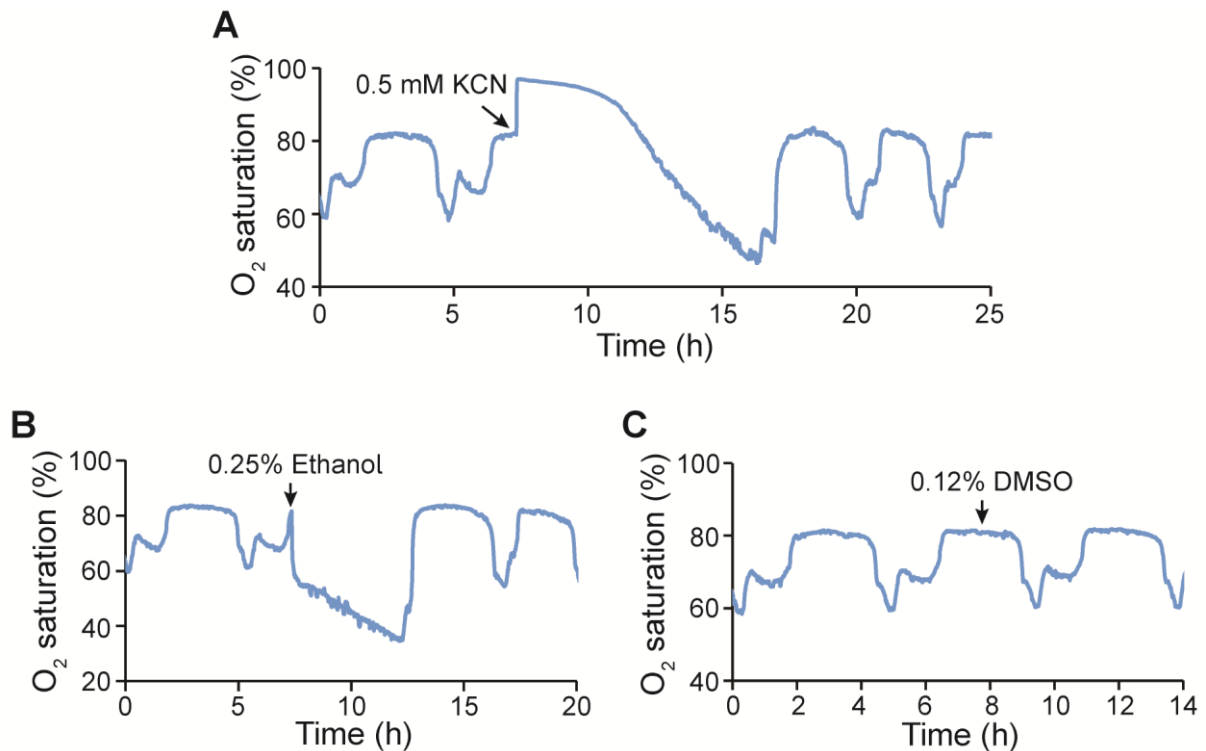


Figure 2.1: The yeast metabolic cycle consists of respiratory oscillations. (A) Representative oxygen trace showing how inhibition of respiration with 0.5 mM KCN immediately stops dissolved oxygen consumption and terminates oscillatory YMC for a prolonged period. Oscillatory behavior returns only after KCN is diluted out of the vessel. **(B)** Representative oxygen trace showing how ethanol, a respiratory substrate, forces synchronized cells to switch from fermentative to respiratory metabolism thereby inducing rapid dissolved oxygen consumption. **(C)** Representative oxygen trace showing that the organic solvent, DMSO, has no observable effect on yeast respiratory oscillations. All experiments were repeated at least twice with completely independent YMC-synchronized cultures.

2.1.2 Chemical inhibition of gene translation perturbs the YMC

It has been suggested that during the YMC, metabolic processes are temporally compartmentalized into phases that are tightly coordinated with gene expression and cell division [47, 50]. Gene expression analysis by microarray showed that periodic changes in the levels of more than 50% of cellular transcripts occur during the YMC. These periodic genes were grouped into three clusters. Based on these gene clusters, the YMC was classified into three phases: reductive building (RB), reductive charging (RC) and oxidative (Ox) [47].

I asked whether interfering with gene translation would have any impact upon the YMC. To answer this question, I performed chemical inhibition of translation using cyclohexamide and chloramphenicol. Cyclohexamide interferes with whole cell protein synthesis by blocking translation elongation whilst chloramphenicol specifically inhibits mitochondrial protein synthesis. Addition of cyclohexamide at the start of LOC initially triggered transient oxygen consumption and steadily slowed down oxygen consumption until the cells assumed a 'starvation mode' (Fig. 2.2A). Similarly, addition of chloramphenicol at the start of LOC destabilized the YMC and led to loss of oscillations in oxygen consumption (Fig. 2.2B).

In summary, these observations indicate that interfering with gene translation affects the YMC. Thus, cellular transcription/translation cycles are essential components of the YMC.

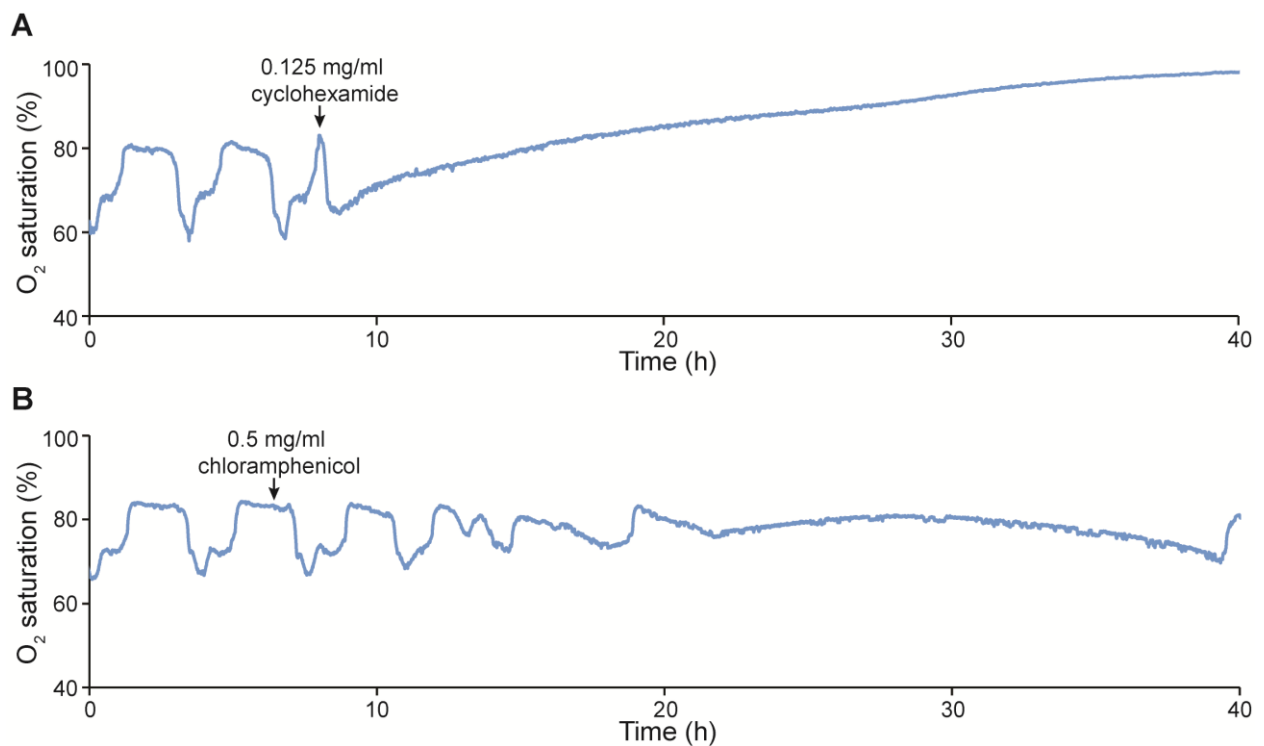


Figure 2.2: The YMC is coupled to cellular transcription/translation programs. (A) Representative oxygen trace showing that blocking cytosolic translation with 0.125 mg/ml cyclohexamide (dissolved in sterile milliQ-H₂O) has a prolonged effect of inhibiting dissolved oxygen consumption and halting oscillatory YMC. **(B)** Representative oxygen trace showing that inhibition of mitochondrial translation with 0.5 mg/ml chloramphenicol (dissolved in 0.12% DMSO) destabilizes the YMC. All experiments were repeated at least twice with completely independent YMC-synchronized cultures.

2.2 The YMC is responsive to and modulated by chemical redox changes

The YMC primarily exhibits rhythms in consumption of oxygen, an important redox molecule. The levels of several redox enzymes and metabolites also oscillate during the YMC. Moreover, genetic or chemical disruption of redox processes affects the YMC [49, 56]. These observations therefore position the YMC as a “redox clock”. Hence, I sought to ascertain how chemical perturbation of cellular redox processes would influence the YMC that I have established. In their study, Chen *et al.* showed that H₂O₂ and methionine advance the phase of the YMC of wildtype cells from RC to the Ox phase [49]. In this study, I applied the thiol reductant, dithiothreitol (DTT) and the thiol oxidant, N,N,N',N'-tetramethylazodicarboxamide (diamide) to wildtype YMC-synchronized cultures.

Addition of DTT at the start of LOC shortened time spent in LOC and facilitated switch to HOC in a concentration dependent manner. With 5 mM DTT, cells were forced to stay in a HOC phase for more than 10 hours, suggesting that a thiol reductant favors high oxygen consumption (Fig. 2.3).

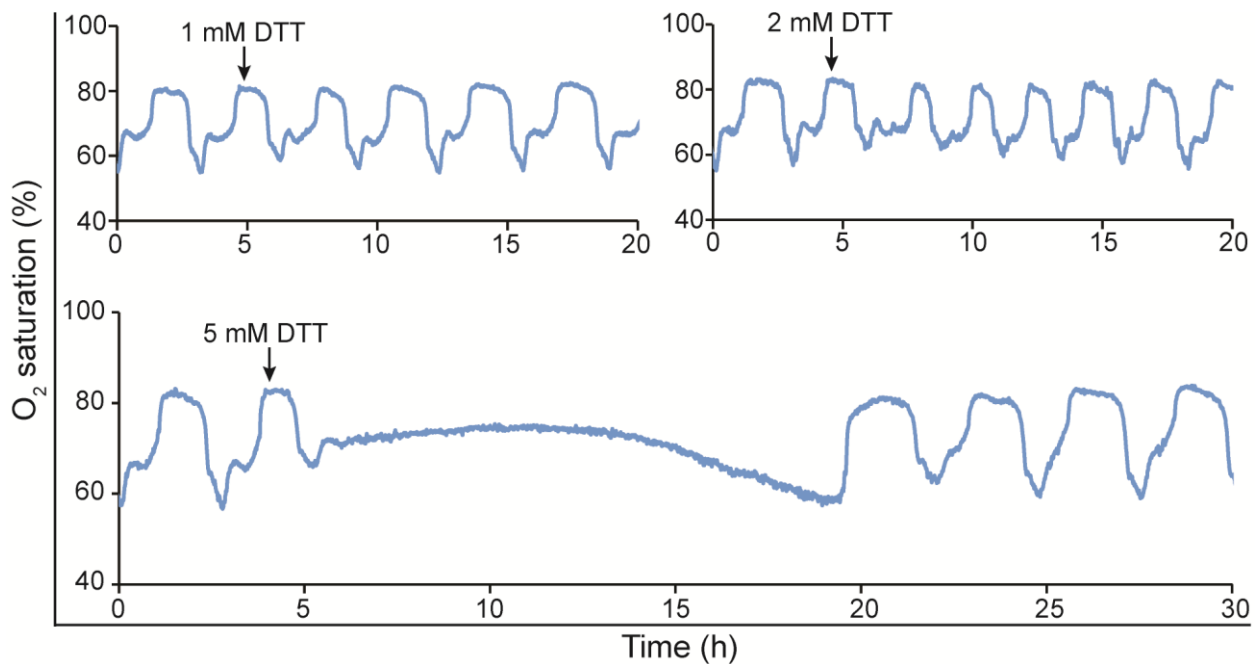


Figure 2.3: Reduction facilitates switch to high oxygen consumption. Representative oxygen trace showing the response of the YMC to the addition of DTT at the start of LOC, in a concentration dependent manner. With 5 mM DTT, oxygen consumption was sustained for a prolonged period. All experiments were repeated at least twice with completely independent YMC-synchronized cultures.

In contrast, addition of diamide at the start of LOC extended the duration of the LOC phase and delayed transition to HOC, in a concentration dependent manner (Fig. 2.4A-B). This suggests that a thiol oxidant promotes low oxygen consumption. Intriguingly, cells just about to initiate HOC could be forced to further stay longer in LOC for approximately 2 hours by addition of 2 mM diamide towards the end of

LOC (Fig. 2.4C). Taken together, these observations show that cellular respiratory rate, and thus the YMC, is responsive to and perhaps regulated by cellular redox changes.

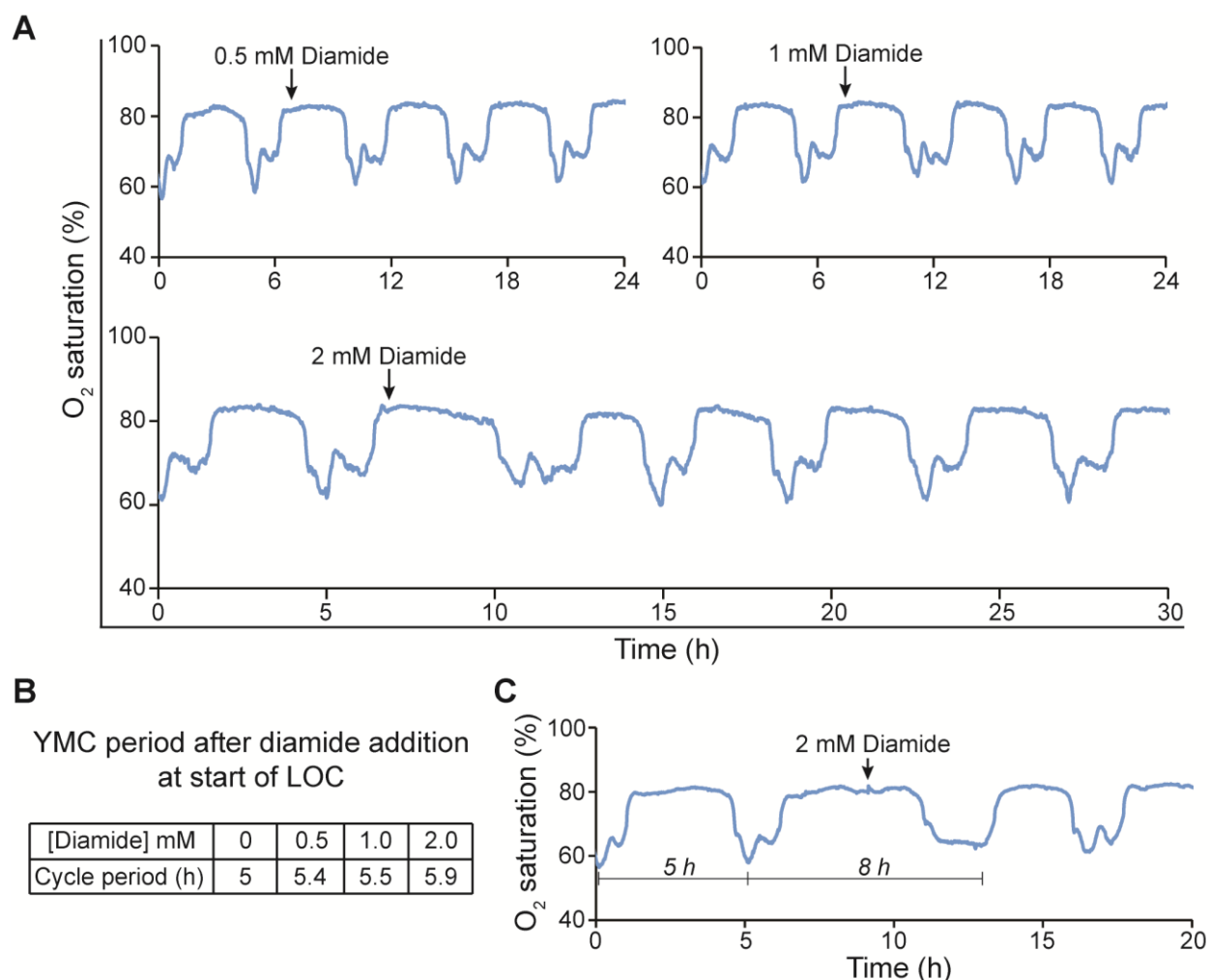


Figure 2.4: Oxidation delays switch to high oxygen consumption. (A) Representative oxygen trace showing the response of the YMC to the addition of diamide at the start of LOC, in a concentration dependent manner. **(B)** Table showing the period of a cycle of the YMC before and after addition of diamide at the indicated concentrations in (A). **(C)** Representative oxygen trace showing the response of the YMC to the addition of 2 mM diamide towards the end of LOC. Diamide delays switch to the HOC phase. All experiments were repeated at least twice with completely independent YMC-synchronized cultures.

2.3 Cyclical changes in cellular H₂O₂ occur during the YMC

Hydrogen peroxide (H₂O₂) is an important cellular redox metabolite that functions as a second messenger in a variety of cell signaling pathways and can elicit large-scale transcriptional responses [129]. By exogenous addition to YMC-synchronized cultures, H₂O₂ has been suggested as a signal that advances YMC phase and controls the gate for cell cycle entry [49]. However, until recently, no study had reported whether oscillations in H₂O₂ existed in circadian and ultradian metabolic clocks, under physiological conditions. I hypothesized that as a “redox clock”, oscillations in cellular H₂O₂ levels could occur during the YMC.

2.3.1 Integration of roGFP2-Tsa2ΔC_R biosensor into yeast genome

To test the above hypothesis, I integrated the roGFP2-Tsa2ΔC_R biosensor into yeast genome (Fig. 2.5A). This was done in part to circumvent the non-suitability of amino acid-based plasmid selection in the prototrophic CEN.PK yeast background. I specifically replaced the constitutive TEF promoter with a stronger expressing GPD promoter, coupled to a Kanamycin resistance marker gene (i.e. *KanMX4*) at its N-terminus for selection. This construct was re-constituted in a p415 plasmid and amplified by PCR using primer sequences that allowed integration into the intergenic region between hexose transporters *HXT6* and *HXT7*, just upstream of the conserved promoter region for *HXT7* [130]. This unusually long (~3kb) region was chosen in part because there are several other hexose transporters in the yeast genome, which render them functionally redundant in case of damage [131]. Moreover, this is the only region of the yeast genome that has been suggested to have no known function [47]. Successful construction and integration of the genomic sensor was confirmed by PCR and sequencing (Appendix A1). I could also confirm sensor expression and cytosolic localization by fluorescence microscopy (Fig. 2.5B). Additionally, the sensor exhibited an excitation spectra characteristic of roGFP2 with maxima at 405 (fully oxidized) and 488 nm (fully reduced), at an emission wavelength of 510 nm (Fig. 2.5C). The genomic sensor was also sensitive to changes in the cellular redox environment due to changing nutrient and oxygen availability (Fig. 2.5D).

Furthermore, the sensor could respond to a wide range of redox chemicals including H₂O₂, the organic *tert-butyl* hydroperoxide (*t*-BOOH), the thiol oxidant diamide and thiol reductant DTT, in a concentration dependent manner (Fig. 2.6). To ascertain whether the sensor was functional during the YMC, I collected cells from different phases of a YMC-synchronized culture of the biosensor expressing cells and treated them with different concentrations of H₂O₂ in a plate reader format. The biosensor was oxidized upon H₂O₂ in a concentration dependent manner, suggesting that the biosensor was active under continuous culture conditions in the fermenter (Appendix A2). Taken together, these results show that the genomic expression of the roGFP2-Tsa2ΔC_R biosensor was successful. This sensor also afforded me the opportunity to study peroxiredoxin function *in vivo* since roGFP2 redox state was dependent upon a functional Tsa2ΔC_R. More so, changes in roGFP2 redox state could reflect changes in the redox state of endogenous peroxiredoxin relay(s).

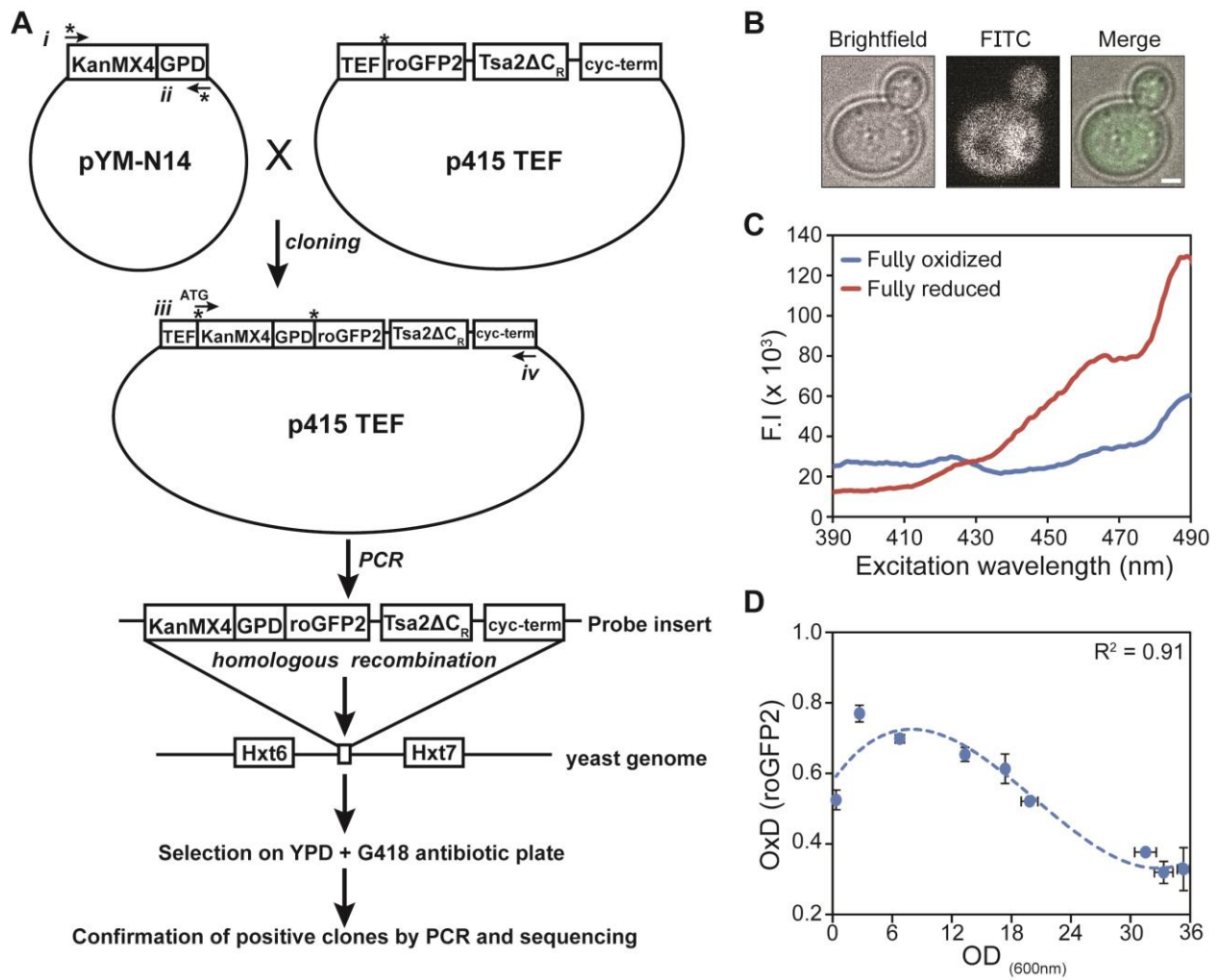


Figure 2.5: Construction and characterization of a genomically integrated roGFP2-Tsa2 Δ C_R sensor-expressing yeast strain. (A) Scheme illustrating the cloning strategy for generating CEN.PK113-1A strain with a genomically integrated construct for roGFP2-Tsa2 Δ C_R biosensor expression. (B) Fluorescence microscopy to show cytosolic localization of roGFP2-Tsa2 Δ C_R biosensor. (C) Fluorescence excitation spectra of CEN.PK cells expressing roGFP2-Tsa2 Δ C_R. Fully oxidized and fully reduced spectra were obtained by treating the cells with 20 mM diamide and 100 mM DTT respectively. (D) Sensor oxidation changes with cell density in glucose media. The degree of roGFP2 oxidation (OxD) was measured from YPD culture of the sensor-expressing strain every 2 hours. Data represent mean of three independent repeats, whilst error bars represent standard deviation. Note: (i) to (iv) in (A) represent primers P1 to P4 in Materials and Methods.

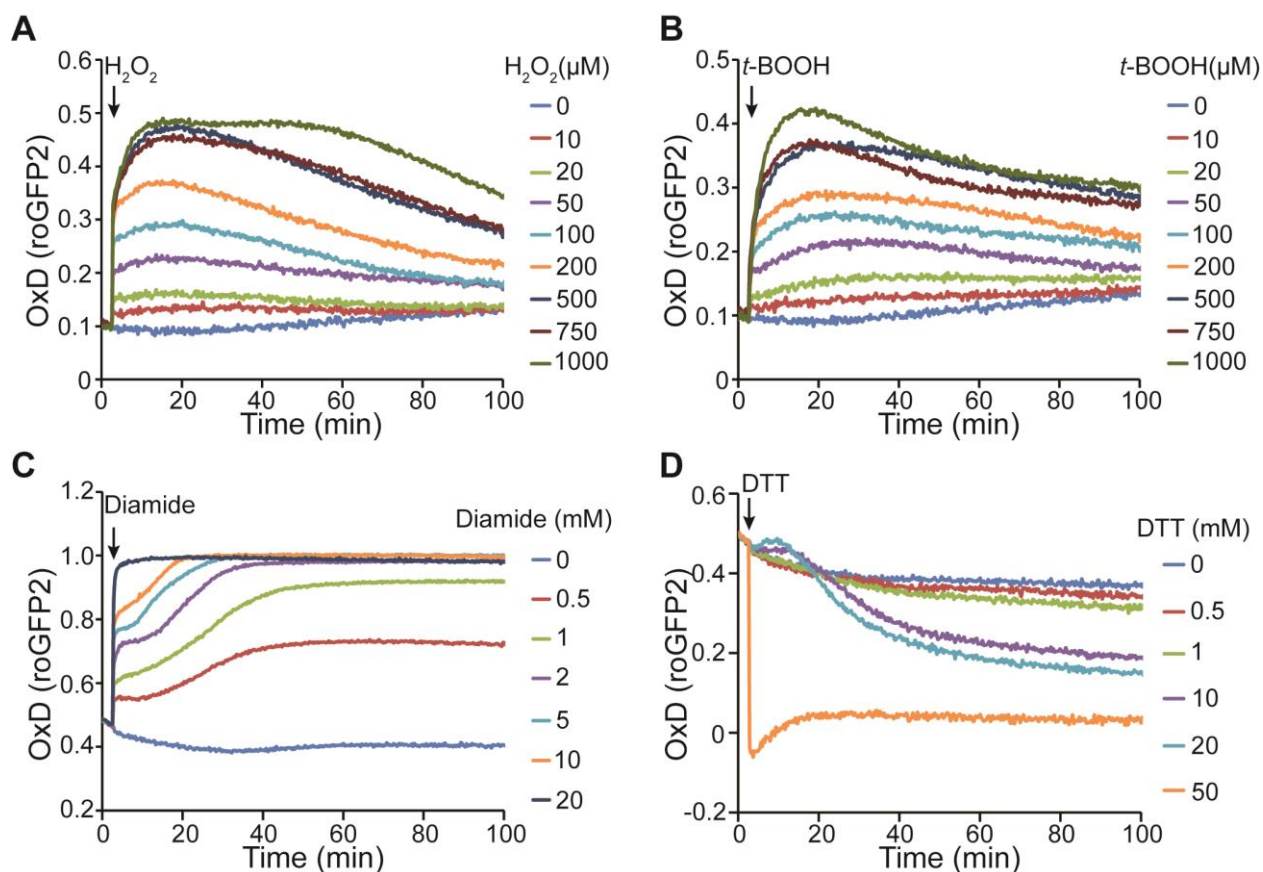


Figure 2.6: Genomically integrated roGFP2-Tsa2 Δ C_R sensor is sensitive to a variety of redox chemicals. Response of the roGFP2-Tsa2 Δ C_R biosensor, expressed in CEN.PK cells, to the addition of (A) H₂O₂, (B) *t*-BOOH, (C) diamide, and (D) DTT, at the indicated concentrations. All experiments were performed in triplicates.

2.3.2 Cyclical H₂O₂ changes are synchronized to YMC phase

To ascertain whether basal levels of H₂O₂ changed during the YMC, I cultured the sensor-expressing yeast strain under conditions for metabolic cycling. To monitor sensor fluorescence in real-time, I developed a system in-house, consisting of a flow cell placed in the chamber of a spectrofluorimeter and connected via tubes to the fermenter culture vessel (Fig. 2.7A). With the aid of a peristaltic pump, I drove cells from the culture vessel through the flow cell and back into the vessel. I measured the fluorescent intensity of cells at 425 nm and 488 nm excitation and 510 nm emission at 30 s intervals. By computing the ratio between fluorescent intensities at 425 nm and 488 nm, I could qualitatively monitor oxidation of the biosensor during the YMC. By overlaying biosensor fluorescence ratios and oxygen saturation curves from three metabolic cycles, I observed that oscillations in roGFP2 oxidation state accompanied the YMC. RoGFP2 oxidation peaked at the entry into LOC, whilst a reduction of roGFP2 correlated with the switch from LOC to HOC (Fig. 2.7B).

However, the signal to noise ratio from the real-time fluorescence measurements was high. As such, it was plausible that the observed oscillations in roGFP2 redox state was an artifact. To verify these oscillations in roGFP2 oxidation state, I collected samples from specific points of the YMC and analyzed their roGFP2 redox state via an N-Ethylmaleimide (NEM)-based trapping technique (Fig. 2.7C), as

described in Materials and Methods. NEM irreversibly alkylates cysteine residues to protect the redox state of protein thiols. By repeating this experiment for three independent metabolic cycles, calculating degree of sensor oxidation (OxD) and superimposing the results over one representative YMC, I could recapitulate the observations made with the flow-cell based real-time measurements (Fig. 2.7D). Taken together, these data demonstrate that oscillations in basal H_2O_2 levels occur during the YMC. Moreover, the redox state of peroxiredoxins as well as peroxiredoxin target protein(s) during the YMC is rhythmic.

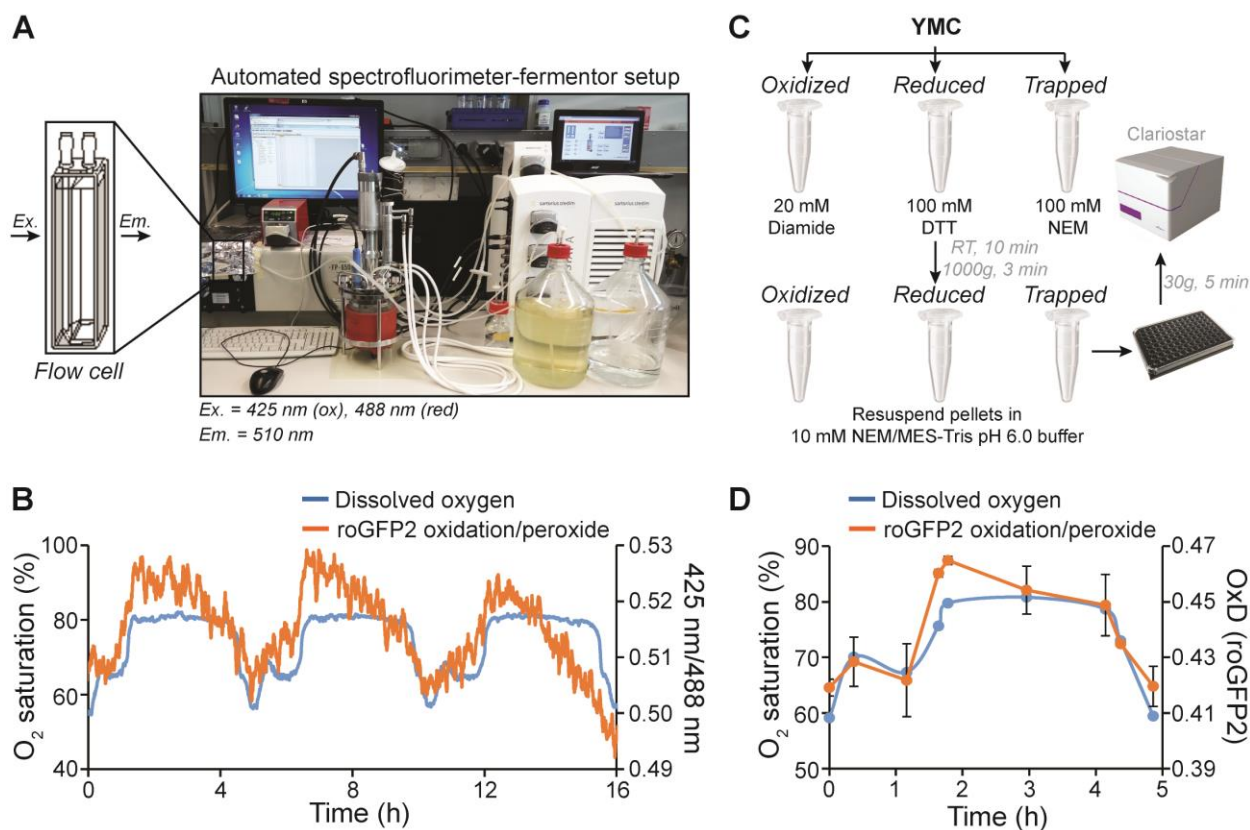


Figure 2.7: Oscillations in basal H_2O_2 levels during the YMC. (A) Setup of an automated system to monitor fluorescence of sensor-expressing cells during the YMC. (B) Representative trace of dissolved oxygen levels and roGFP2 fluorescence excitation ratio over three complete YMC cycles. (C) Experimental workflow for measuring steady-state roGFP2 oxidation by NEM-trapping, in a plate reader format. (D) The degree of roGFP2-Tsa2 Δ C_R oxidation measured from YMC-synchronized culture samples at the indicated time points, based on the NEM-trapping technique in (C). Data points represent average of three independent experiments while error bars represent standard deviation. Data points of percent oxygen saturation represent phase of YMC at which cell samples were taken.

2.3.3 H_2O_2 is not important for population synchrony

A model for signaling events during the YMC posits that liquidation of storage carbohydrates by a fraction of cells in HOC leads to the secretion of metabolites that trigger other cells to synchronously consume oxygen. These metabolites include ethanol, acetaldehyde and dihydrogen sulfide [58, 59, 115]. Having observed that H_2O_2 oscillates during the YMC, I asked whether it was secreted by cells into the medium to serve as a trigger for other cells to synchronously consume oxygen. To do this, I injected 12.5 μ g/ml of catalase into the culture vessel. Surprisingly, the YMC remained unperturbed for the entire course of fermenter run (Fig. 2.8). This suggests that H_2O_2 , even if exogenously secreted by cells into the surrounding medium, is not important for YMC synchrony.

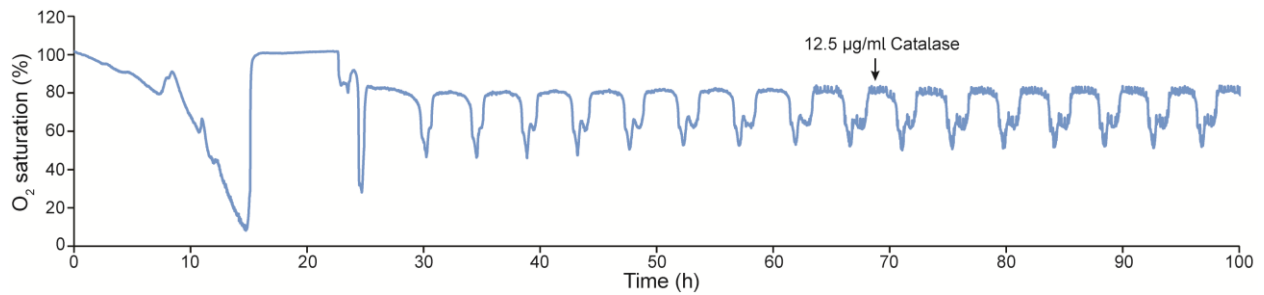


Figure 2.8: Effect of exogenous catalase on the YMC. Catalase solution at a final concentration of 12.5 µg/ml was added into the culture vessel at the start of a LOC phase as indicated, for exogenous H₂O₂ scavenging.

2.4 A signaling role for H₂O₂ and peroxiredoxins during the YMC

Having ruled out an inter-cellular communication function for H₂O₂, I asked whether H₂O₂ served an endogenous function during the YMC. If so, could peroxiredoxins act as mediators in such signaling event?

2.4.1 High exogenous H₂O₂ induces metabolic switch to HOC

To ascertain an endogenous role during the YMC, I added boli of H₂O₂ at different concentrations to the start of LOC of wildtype YMC-synchronized cultures. While 0.5 and 1 mM had no significant effect on the YMC, 5 mM H₂O₂ rapidly and transiently induced HOC, which lasted nearly 2 h before return to the LOC phase (Fig. 2.9A). However, addition of H₂O₂ to the culture vessel resulted in molecular oxygen production due to endogenous catalase activity, which could be detected by the dissolved oxygen (DO) probe, and thus interfered with my measurements. To circumvent this “side-effect”, I applied the organic hydroperoxide *t*-BOOH. Unlike H₂O₂, *t*-BOOH cannot be catabolized by catalase. Interestingly, I observed that 0.1 and 0.5 mM *t*-BOOH had no significant effect on the YMC, whilst 1 mM *t*-BOOH rapidly induced premature switch to HOC similar to 5 mM H₂O₂ (Fig. 2.9B). In sum, these observations indicate that peroxides can induce premature LOC-to-HOC transition when applied to YMC-synchronized cultures at high non-physiological concentrations.

2.4.2 High peroxide-induced switch to HOC during YMC is phase-independent

Having observed the induction of LOC-to-HOC transition upon high peroxide addition at the start of LOC of the YMC, I asked whether this response was phase-specific or could occur at any point of the YMC. To address this, I added either 5 mM H₂O₂ or 1 mM *t*-BOOH to different points of the YMC. Surprisingly, HOC could be induced independent of the phase of peroxide addition (Fig. 2.10).

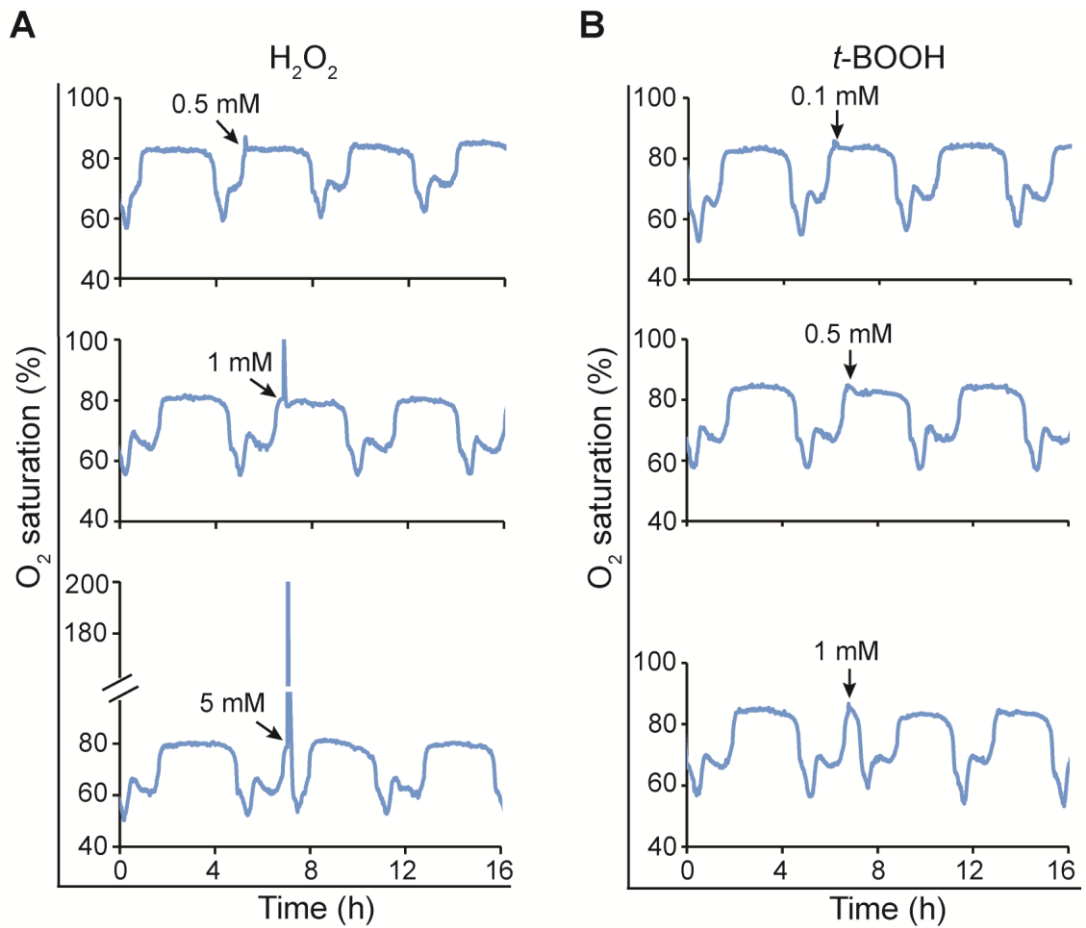


Figure 2.9: Effect of peroxides on the YMC. (A) Representative responses of YMC-synchronized culture of wildtype cells to the addition of H_2O_2 at the indicated concentrations. **(B)** Representative responses of YMC-synchronized cultures of wild-type cells to the addition of *t*-BOOH at the indicated concentrations.

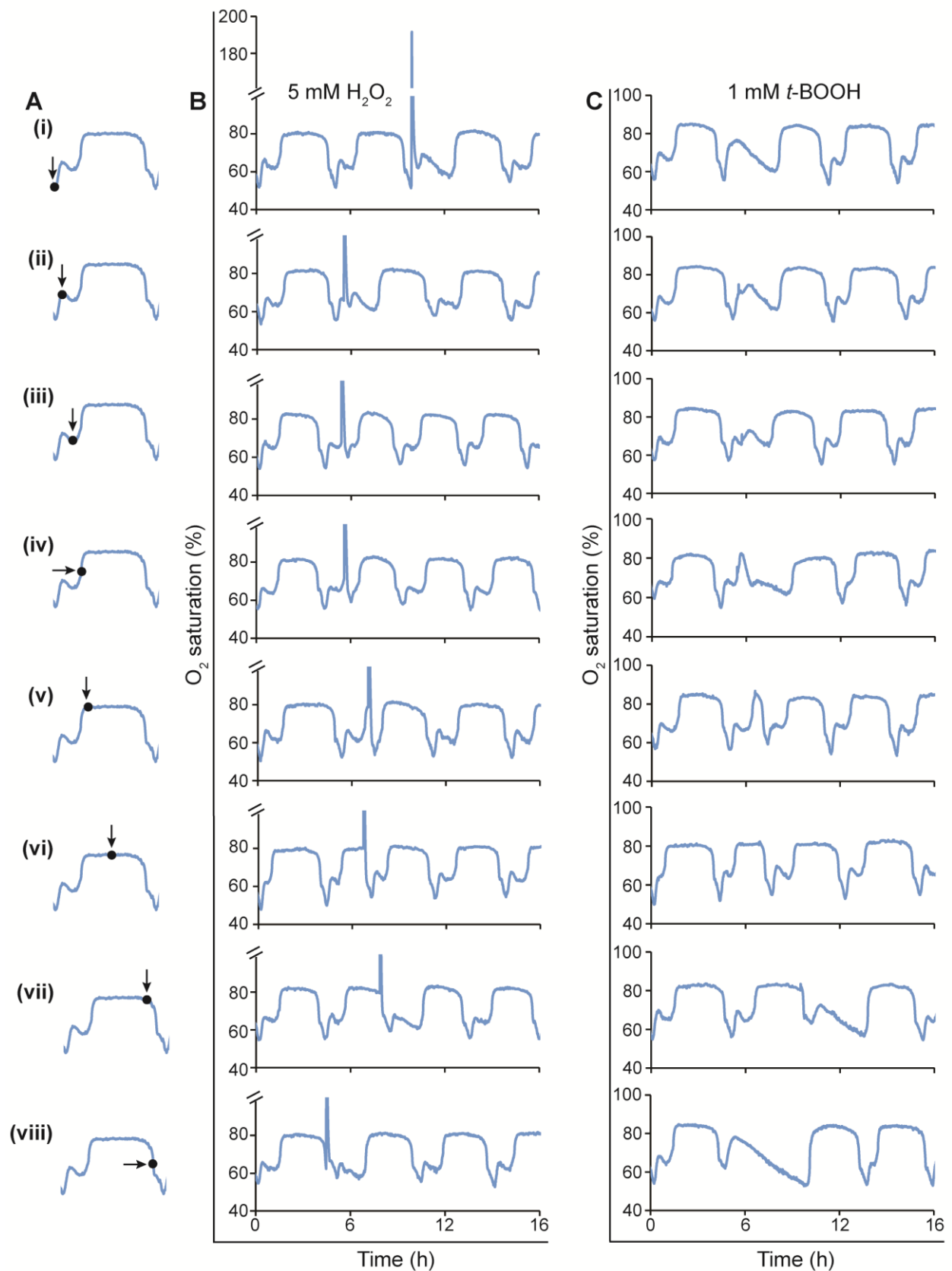


Figure 2.10: High amounts of peroxide can induce switch to HOC at any phase of the YMC. (A) Points on the YMC at which treatments were carried out. **(B)** Representative responses of YMC-synchronized cultures of wildtype cells to the addition of 5 mM H₂O₂. **(C)** Representative responses of YMC-synchronized cultures of wildtype cells to the addition of 1 mM *t*-BOOH.

2.4.3 Peroxiredoxin inactivation upon high peroxide mediates metabolic switch to HOC

Living cells respond to H_2O_2 via regulation of protein function leading to increased production of antioxidant enzymes and cofactors. The regulated proteins generally include kinases, phosphatases and transcription factors that mediate a variety of cellular processes such as transcription, growth, nutrient sensing and mitochondria biogenesis [132]. It has been suggested that the oxidation of most redox-regulated proteins by H_2O_2 is almost completely dependent on peroxiredoxins [72]. Accordingly, I sought to ascertain whether the premature LOC-to-HOC transition upon high peroxide could be mediated by peroxiredoxins. To do this, I cultured the sensor-expressing cells under YMC conditions and monitored sensor fluorescence in real-time before and upon addition of the different concentrations of *t*-BOOH previously used. At bolus concentrations of 0.1 and 0.5 mM *t*-BOOH, I observed roGFP2 oxidation, which gradually reduced to 'normal' levels before the switch to HOC. Counter-intuitively, upon 1 mM *t*-BOOH, roGFP2 oxidized transiently and reduced in a manner that correlated with increased oxygen consumption (i.e. LOC-to-HOC transition) (Fig. 2.11A-C(i)). Interestingly, roGFP2 appeared to have reduced to levels below the initial oxidation state (Fig. 2.11C(i)). This observation was indicative of hyperoxidation-based inactivation of the Tsa2 Δ C_R moiety of the roGFP2-Tsa2 Δ C_R sensor. This phenomenon is conceivable because upon excess peroxide, the C_P of the Tsa2 Δ C_R moiety becomes hyperoxidized and inactivated. Consequently, the transduction of oxidizing equivalents from peroxide to roGFP2 is inhibited. The redox state of roGFP2 thus depends on equilibration with the cellular glutathione pool (Fig. 2.12).

To verify whether the observed reduction of roGFP2 redox state upon high peroxide was due to hyperoxidation and inactivation of Tsa2 Δ C_R, I collected YMC-synchronized cells from the fermenter at the start of LOC, before and 30 mins after *t*-BOOH treatment. I then assessed roGFP2 fluorescence via the plate-reader method. This assay works on the principle that if the Tsa2 Δ C_R moiety of the sensor was still functional after *t*-BOOH addition to cells during the YMC, further oxidation of roGFP2 should be achieved upon exogenous addition of H_2O_2 to cells in a 96-well plate, in a concentration dependent manner. On the contrary, if the Tsa2 Δ C_R moiety of the sensor becomes inactivated upon *t*-BOOH addition to cells during the YMC, roGFP2 becomes unresponsive independent of the amount of exogenous H_2O_2 added to cells in the plate. In line with this reasoning, sensor-expressing cells collected after 30 mins of 0.1 and 0.5 mM *t*-BOOH addition to YMC-synchronized cultures were responsive to external H_2O_2 in a concentration dependent manner (Fig. 2.11A-B(ii)). On the other hand, sensor-expressing cells collected after 30 mins of 1 mM *t*-BOOH addition to YMC-synchronized cultures were unreactive to any concentration of external H_2O_2 (Fig. 2.11C(ii)). These observations confirmed that the peroxiredoxin of the biosensor was inactivated upon 1 mM *t*-BOOH addition to YMC-synchronized cells. Furthermore, the steady-state OxD of roGFP2 was rendered more reduced in 1 mM *t*-BOOH samples (Fig. 2.11D). Since the roGFP2-Tsa2 Δ C_R biosensor represented a reconstituted thiol peroxidase redox relay, I imagined that endogenous peroxiredoxin inactivation and subsequent reduction of the redox state of endogenous peroxiredoxin substrate(s) could be responsible for premature LOC-to-HOC transition upon high peroxide.

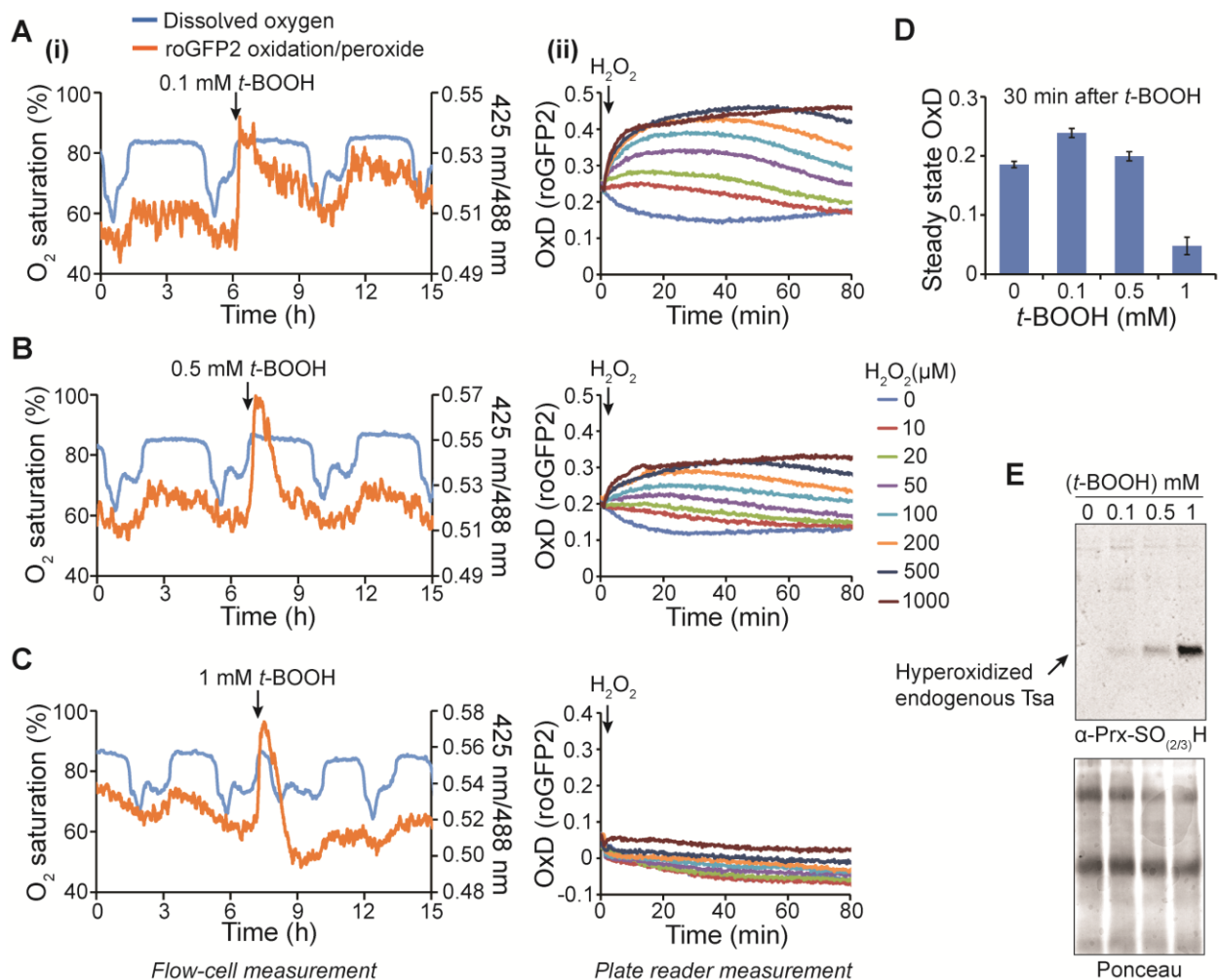


Figure 2.11: LOC-to-HOC transition upon high peroxide correlates with peroxiredoxin hyperoxidation. (A-C) Representative responses of a roGFP2-Tsa2 Δ C_R probe in YMC-synchronized cultures treated with either 0.1 mM, 0.5 mM or 1 mM *t*-BOOH. **(i)** Left panels represent traces of dissolved oxygen and roGFP2 fluorescence before and after treatment with *t*-BOOH in the fermenter at the indicated concentrations. **(ii)** Right panels represent sensor response to exogenous addition of the indicated concentrations of H₂O₂ in a plate-reader format, 30 mins after *t*-BOOH boli in the fermenter. **(D)** The steady-state oxidation of roGFP2 (substrate) was measured in a plate reader format. Data represent average of three independent experiments, while error bars represent standard deviation. **(E)** Western blot for hyperoxidized endogenous Tsa1 and Tsa2 following application of *t*-BOOH to continuous cultures at the indicated concentrations.

To test whether endogenous peroxiredoxins were hyperoxidized upon *t*-BOOH addition to YMC-synchronized cultures, the cell samples collected before and 30 mins after *t*-BOOH addition were assayed for endogenous peroxiredoxin hyperoxidation by Western blot. The antibody I used for this assay was raised against a Keyhole limpet hemocyanin (KLH)-coupled sulfonlated peptide corresponding to the active site sequence of human Prdx I to IV (AbFrontier, LF-PA004). This antibody was also shown to be specifically reactive towards yeast typical 2-Cys peroxiredoxins, Tsa1 and Tsa2 (Fig. 2.13, [90]). Intuitively, after assaying cells collected before and after addition of 0.1, 0.5 and 1 mM *t*-BOOH to YMC-synchronized cultures, I observed that the hyperoxidation of endogenous yeast typical 2-Cys peroxiredoxins, Tsa1 and Tsa2, occurred slightly in 0.5 mM and strongly in 1 mM *t*-BOOH treated samples (Fig. 2.11E). In addition, the pattern of endogenous peroxiredoxin hyperoxidation, as visualized on the Western blot, precisely mimicked the biosensor peroxiredoxin response observed with the plate-reader (compare Fig. 2.11C(ii) and

Fig. 2.11E). In sum, I have demonstrated that peroxide prematurely triggers LOC-to-HOC transition only when added at concentrations high enough to induce hyperoxidation of typical 2-Cys peroxiredoxins, a phenomenon that leads to reduction of the redox state of peroxiredoxin target protein(s). Although this concentration of peroxide is non-physiological, these observations suggest that peroxiredoxins have an important role in regulating LOC-to-HOC transition. Consequently, peroxiredoxins and peroxiredoxin target protein(s) constitute a molecular switch that regulate LOC-to-HOC transition and thus the YMC.

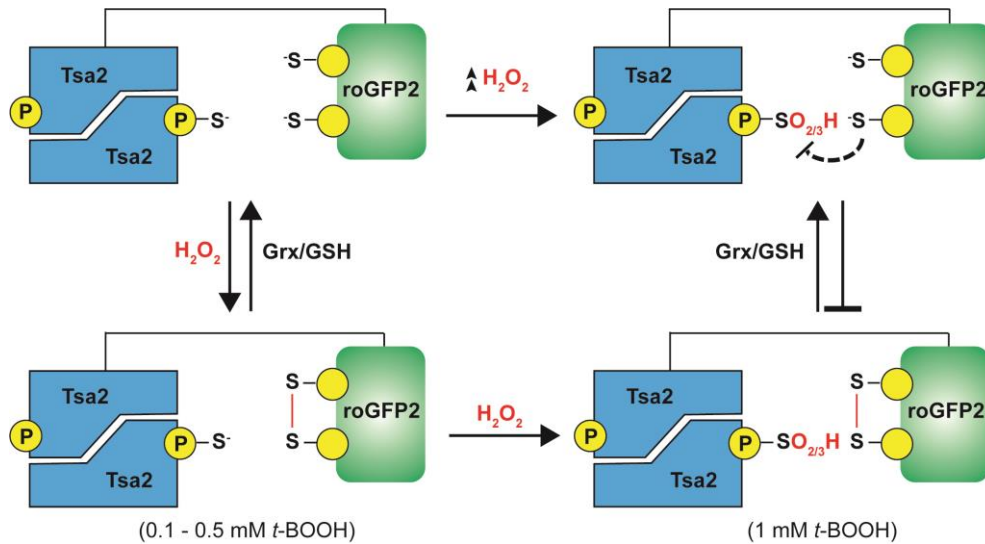


Figure 2.12: Scheme explaining sensor behavior after *t*-BOOH bolus in fermenter. At steady state, the sensor remains mostly in the reduced thiolate state. Upon encountering basal H_2O_2 , the ratio of oxidized to reduced probe levels change depending on the amount of H_2O_2 , as depicted by the cyclical changes during the YMC. RoGFP2 acts as substrate to receive oxidizing equivalents from H_2O_2 with the C_P of the $Tsa2\Delta C_R$ acting as the transducer. In this state, $Tsa2\Delta C_R$ remains very active in this role. Upon exogenous addition of 0.1 or 0.5 mM *t*-BOOH, the oxidized levels of the sensor increase and more oxidizing equivalents passed onto roGFP2 by an active $Tsa2\Delta C_R$. RoGFP2 stays more oxidized until peroxide is diluted out of the culture to basal levels, and thereafter reversed to a reduced thiolate state by Grxs using GSH. Upon excess peroxide (e.g. 1 mM *t*-BOOH), the sensor becomes only transiently oxidized and remains reduced thereafter. This is because the C_P of the $Tsa2\Delta C_R$ becomes overwhelmed by the amount of peroxide and therefore is inactivated by hyperoxidation. Subsequently, the transduction of oxidizing equivalents to roGFP2 is hindered, resulting immediately in the return to a more reduced thiolate roGFP2 via the action of Grxs using GSH.

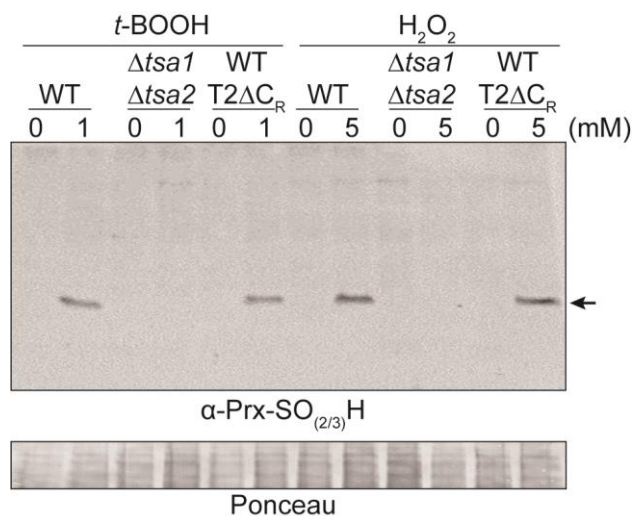


Figure 2.13: Antibody detection of peroxiredoxin hyperoxidation is Tsa-specific. Western blot showing specificity of Prx-SO_(2/3)H antibody towards the yeast typical 2-Cys peroxiredoxins, Tsa1 and Tsa2. Key: WT - wildtype CEN.PK cells, WT T2 ΔC_R - genomic sensor-expressing cells, $\Delta tsa1\Delta tsa2$ - cells deleted for *TSA1* and *TSA2*.

In fact, it was instructive to observe an apparent reduction of roGFP2 redox state upon 1 mM *t*-BOOH since peroxides function as oxidants. Therefore, I ascertained whether the thiol oxidant diamide caused a reduction in roGFP2 redox state under similar conditions. In contrast, by monitoring sensor response in real-time, diamide could only induce roGFP2 oxidation when added at the start of LOC. LOC-to-HOC transition was only achieved after diamide was removed from the culture vessel by dilution and roGFP2 redox state reduced to ‘normal’ levels (Fig. 2.14). Thus, unlike high levels of peroxides, diamide only induced roGFP2 oxidation, which was not required for LOC-to-HOC transition, suggesting that LOC-to-HOC transition is regulated by thiol reduction. This thiol reduction is achieved either via low signaling H₂O₂ levels under physiological conditions or upon high non-physiological peroxide levels that hyperoxidize and inactivate peroxiredxins, a phenomenon explainable by the ‘relay’ hypothesis.

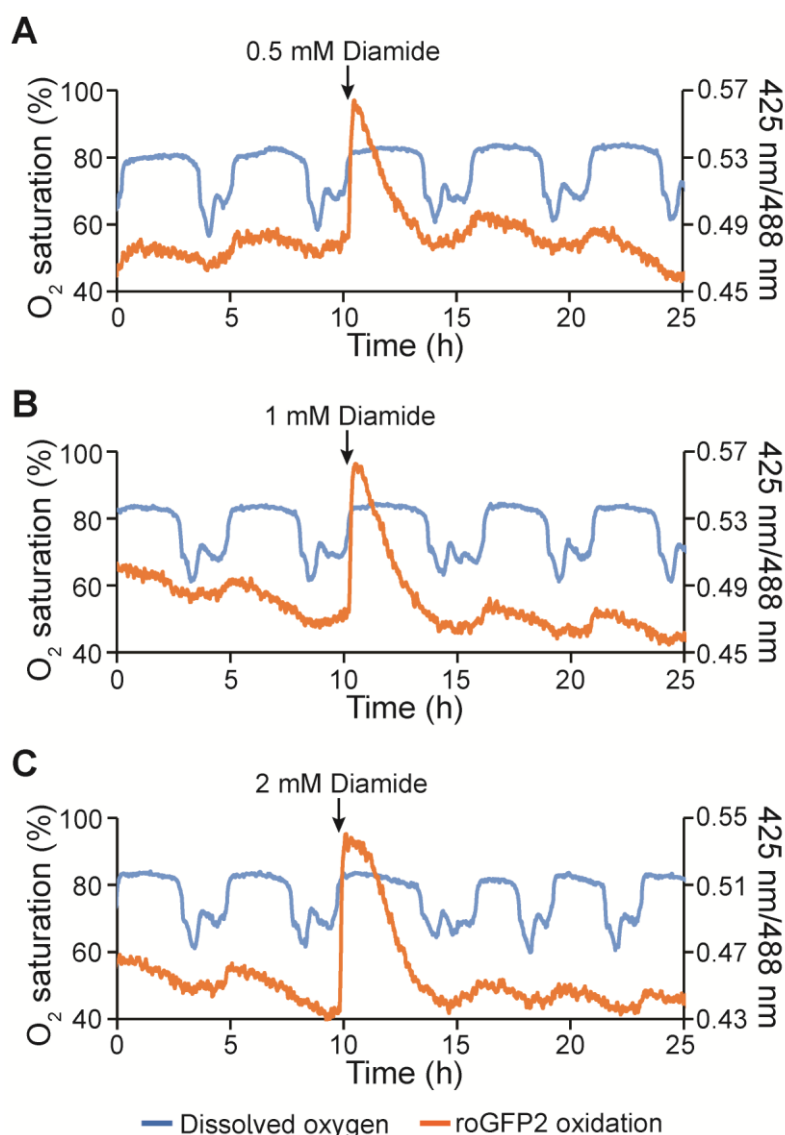


Figure 2.14: The oxidant diamide does not induce roGFP2 reduction as well as rapid LOC-to-HOC transition. Representative graphs showing YMC response to (A) 0.5 mM (B) 1 mM and (C) 2 mM diamide addition at start of LOC together with the response of the genomically integrated roGFP2-Tsa2ΔC_R probe. All experiments were repeated at least twice with completely independent YMC-synchronized cultures.

2.5 Cytosolic peroxiredoxins are essential for YMC regulation

Given that peroxiredoxin hyperoxidation correlated with the switch to HOC from LOC, I asked whether loss of peroxiredoxins would affect the YMC *per se*, as well as the response of YMC-synchronized cells to the levels of *t*-BOOH needed to induce LOC-to-HOC switching.

2.5.1 Loss of cytosolic 2-Cys peroxiredoxins is associated with decreased YMC period

To address the above question, I performed single and double deletions of peroxiredoxins in yeast cytosol or mitochondria. Loss of the mitochondria 1-Cys peroxiredoxin, *PRX1*, had no observable effect on YMC shape and period. However, a single deletion of the cytosolic atypical 2-Cys peroxiredoxin and alkylhydroperoxidase, *AHP1*, significantly affected YMC shape and decreased YMC period to approximately 2.7 hours. Similarly, double deletion of the cytosolic typical 2-Cys peroxiredoxins, *TSA1* and *TSA2* significantly affected YMC shape and decreased YMC period to approximately 2.5 hours (Fig. 2.15). Taken together, these observations suggest that cytosolic 2-Cys peroxiredoxins may be essential for YMC regulation.

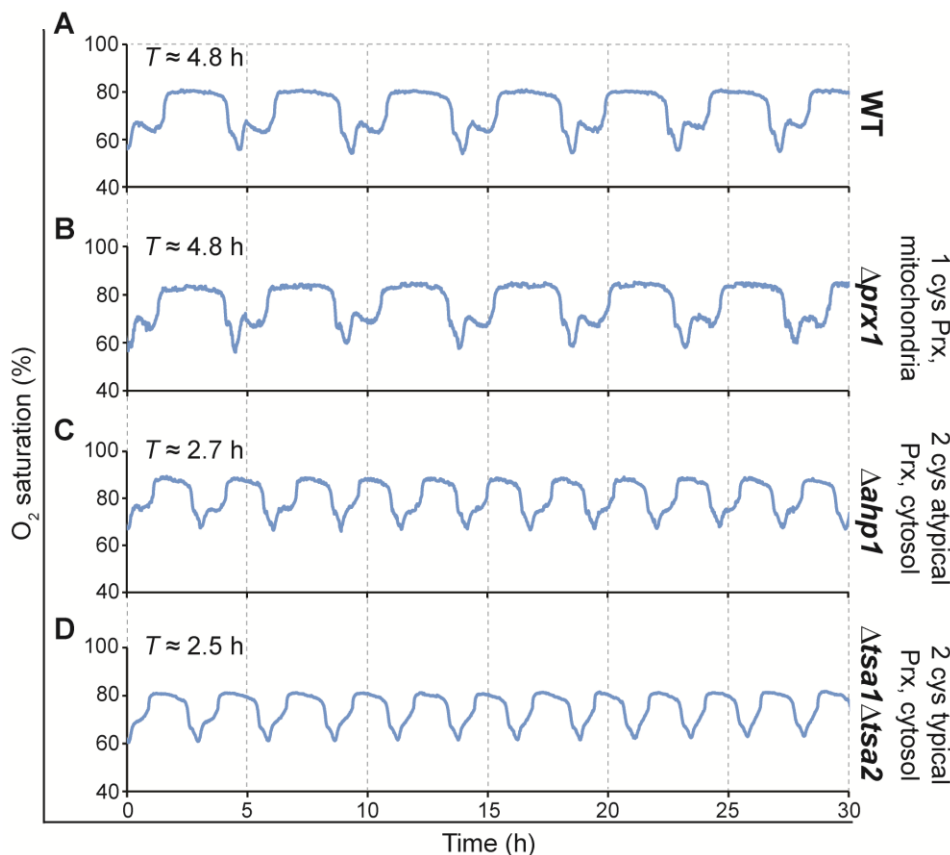


Figure 2.15: Effect of peroxiredoxin deletion on the YMC. Representative oxygen traces to show the YMC for (A) Wildtype CEN.PK113-1A, (B) Cells deleted for the mitochondrial 1-Cys peroxiredoxin *PRX1*, (C) Cells deleted for the cytosolic atypical 2-Cys peroxiredoxin *AHP1* and (D) Cells deleted for the cytosolic typical 2-Cys peroxiredoxins *TSA1* and *TSA2*. All experiments were repeated at least twice with completely independent YMC-synchronized cultures.

2.5.2 Multiple peroxiredoxins function to mediate peroxide-induced metabolic switch to HOC

Next, I sought to understand how loss of peroxiredoxins might modulate response to the peroxide levels needed to induce switch to HOC in wildtype cells, if any. To do this, I added 1 mM *t*-BOOH at points of the YMC described in Fig. 2.10A. At this concentration of *t*-BOOH, I observed induction of HOC in $\Delta prx1$ cells in a manner synonymous to wildtype cells (Fig. 2.16). However, this concentration was lethal to $\Delta tsa1\Delta tsa2$ cells and resulted in loss of oxygen consumption and metabolic cycles, probably due to the strongly diminished antioxidant capacity of these cells (Fig. 2.17A). Nonetheless, with 0.5 mM *t*-BOOH, HOC could still be induced similar to wildtype and $\Delta prx1$ cells (Fig. 2.17B).

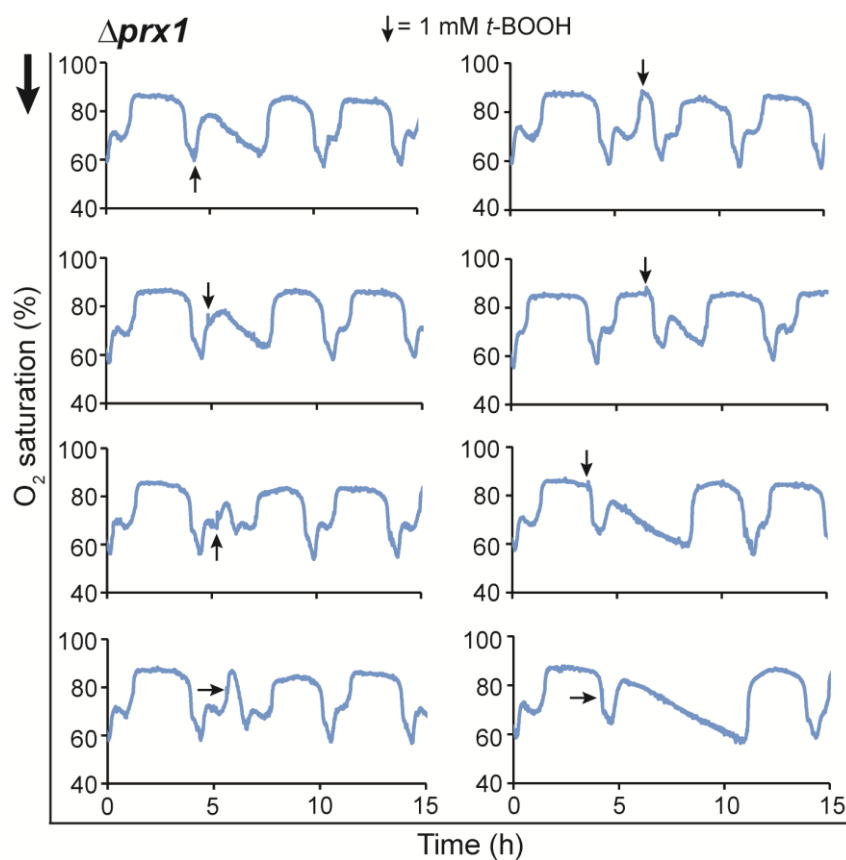


Figure 2.16: High peroxide induces switch to HOC in *PRX1*-deleted cells. Representative oxygen traces showing YMC response of $\Delta prx1$ cells to 1 mM *t*-BOOH. Thick black arrow indicates sequence of YMC phase of *t*-BOOH addition as depicted in Fig. 2.10A.

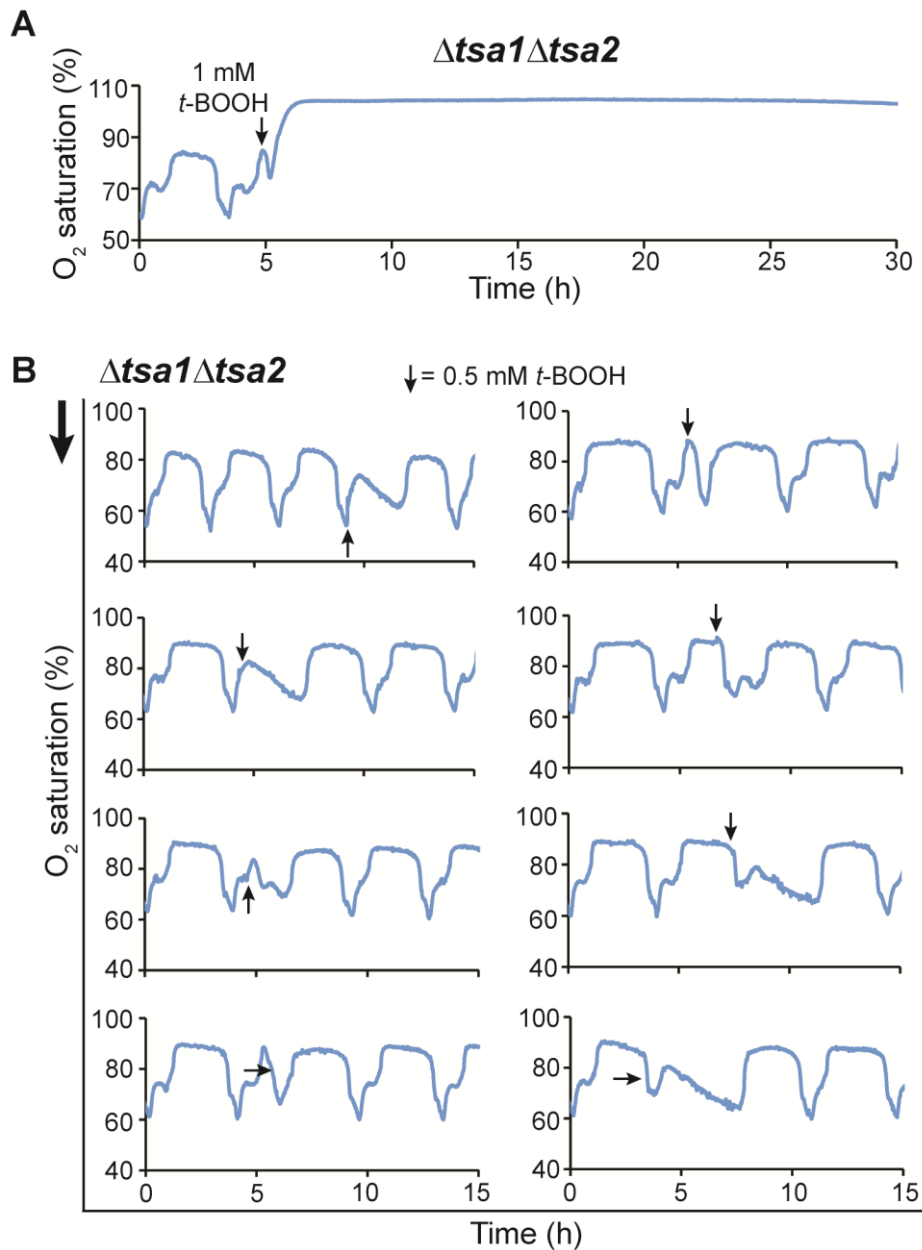


Figure 2.17: High peroxide induces switch to HOC in $\Delta tsa1\Delta tsa2$ cells. Representative oxygen traces showing YMC response of $\Delta tsa1\Delta tsa2$ cells to **(A)** 1 mM and **(B)** 0.5 mM *t*-BOOH. Thick black arrow indicates sequence of YMC phase of *t*-BOOH addition as depicted in Fig 2.10A.

It was instructive to note that YMC-synchronized cultures of $\Delta tsa1\Delta tsa2$ cells could exhibit LOC-to-HOC switching upon high amounts of *t*-BOOH, suggesting that peroxiredoxin hyperoxidation might have still occurred. This reasoning is not far-fetched since thiol peroxidases exhibit functional redundancy in their response to peroxides [129]. Given that $\Delta ahp1$ cells displayed YMC with shape and period similar to $\Delta tsa1\Delta tsa2$ cells, I asked whether endogenous Ahp1 might have been hyperoxidized and inactivated in wildtype as well as $\Delta tsa1\Delta tsa2$ cells to mediate peroxide-induced switch to HOC during the YMC. However, there was no easy and direct way to answer this question since there was no known antibody for detection of hyperoxidized Ahp1 levels by Western blot. Meanwhile, we had developed a sensor similar to roGFP2-Tsa2 Δ C_R, by fusing Ahp1 to the C-terminus of roGFP2 [90]. I therefore tested whether it was

possible to hyperoxidize the Ahp1 moiety of this biosensor in the BY4741 or BY4742 yeast backgrounds, using the plate reader assay. The principle behind this assay is that if Ahp1 becomes hyperoxidized upon peroxide, roGFP2 would be reduced. On the other hand, roGFP2 would stay oxidized in the absence of Ahp1 hyperoxidation upon peroxide (Fig. 2.18A). Interestingly in the BY4741 background, the roGFP2-Ahp1 sensor was rapidly reduced in a $\Delta ahp1$ compared to a wildtype strain, upon 1 mM *t*-BOOH (Fig. 2.18B). In a BY4742 $\Delta tsa1\Delta tsa2$ strain, the sensor could increasingly be oxidized with 0.5 and 1 mM *t*-BOOH. However, it was briefly oxidized and quickly reduced with 2 mM *t*-BOOH, an indication of rapid roGFP2 reduction upon Ahp1 hyperoxidation and inactivation (Fig. 2.18C). In a separate experiment, hyperoxidation of the roGFP2-Tsa ΔC_R sensor could be achieved with 0.75 mM *t*-BOOH in the wildtype background of these strains (data not shown). Summarily, these observations suggest that during the YMC, Tsa1 and Tsa2 are preferentially inactivated upon high peroxide, after which Ahp1 could take over such role. Interestingly, contributions of Ahp1 toward YMC regulation had not been considered in previous studies.

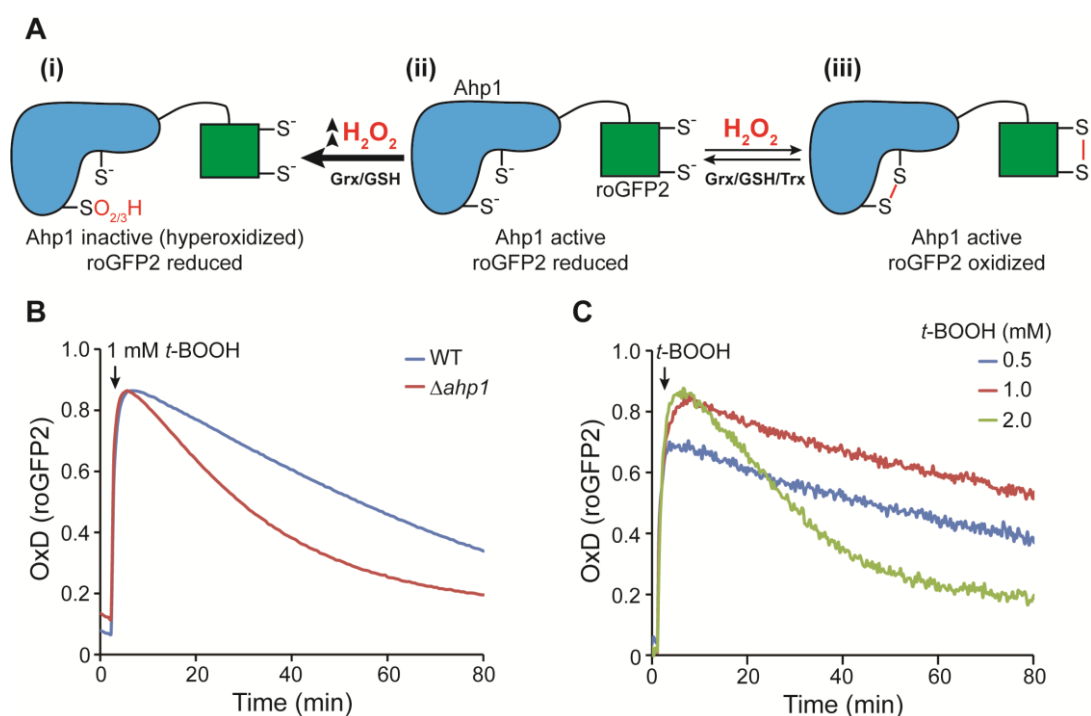


Figure 2.18: RoGFP2 fluorescence measurements reveal possible Ahp1 hyperoxidation upon high peroxide. (A) Scheme showing mechanism of an Ahp1 coupled roGFP2 sensor. Ahp1 acts as the transducer of oxidizing equivalents from peroxide to roGFP2. (ii) All cysteine residues of the roGFP2-Ahp1 sensor remain in a reduced thiolate state in the absence of peroxide. (iii) Upon encountering peroxide, oxidizing equivalents are transferred via the C_P of Ahp1, resulting ultimately in the formation of an intramolecular Ahp1 and roGFP2 disulfide bonds. (i) In the presence of excess peroxide, the C_P of Ahp1 becomes hyperoxidized and inactivated, rendering the transfer of oxidizing equivalents non-functional. Thus, Grxs return the cysteine residues of roGFP2 to a more reduced thiolate state using GSH. The presence of the C_R of Ahp1 in this sensor, unlike in the roGFP2-Tsa2 ΔC_R sensor, leads to competition between roGFP2 oxidation and intramolecular Ahp1 disulfide bond reduction by thioredoxins. (B) Degree of sensor oxidation in a BY4741 wildtype and $\Delta ahp1$ backgrounds upon 1 mM *t*-BOOH. (C) Degree of sensor oxidation in a BY4742 $\Delta tsa1\Delta tsa2$ background upon 0.5, 1 and 2 mM *t*-BOOH. Data represent mean of at least three independent experiments.

2.5.3 Combined loss of *TSA1* and *AHP1* in prototrophic yeast leads to non-viability

Previous works have demonstrated that yeast thiol peroxidases are functionally redundant; hence, it was possible to delete all eight thiol peroxidases in the BY4742 background and still have a viable yeast strain [129]. I therefore sought to ascertain the consequence on the YMC of deleting all three cytosolic 2-Cys peroxiredoxins together (i.e. *TSA1*, *TSA2* and *AHP1*). To do this, I intended to delete *AHP1* from the $\Delta tsa1\Delta tsa2$ background by the same homologous recombination-based gene deletion approach. Surprisingly, I was unable to generate either $\Delta tsa1\Delta ahp1$ or $\Delta tsa1\Delta tsa2\Delta ahp1$ mutants in the CEN.PK 113-1A background upon several attempts (data not shown). Similarly, I could not obtain a $\Delta tsa1\Delta ahp1$ strain by deleting *AHP1* in a $\Delta tsa1$ background using the same approach. Meanwhile, I could obtain the $\Delta tsa1\Delta ahp1$ and $\Delta tsa1\Delta tsa2\Delta ahp1$ strains in the BY4742 background by homologous recombination (data not shown).

To ensure that the supposed failure was not due to technical challenges, but perhaps, a biological phenomenon peculiar to the CEN.PK background, I sought to obtain the desired strains via mating, sporulation and tetrad dissection experiments as described in Materials and Methods. I crossed $\Delta tsa1\Delta tsa2$ from the CEN.PK113-1A (Mat- α) background with $\Delta ahp1$ from the CEN.PK113-7D (Mat-a) background (Fig. 2.19A). Interestingly, I could not obtain any viable $\Delta tsa1\Delta ahp1$ or $\Delta tsa1\Delta tsa2\Delta ahp1$ spores from any of the 33 tetrads dissected (Fig 2.19B-D). These observations suggest that combined loss of *TSA1* and *AHP1* is lethal in the CEN.PK background, an observation that is in sharp contrast with the common lab yeast strain BY4742.

The main difference between the CEN.PK and BY4742 is that the former is a prototrophic strain capable of synthesizing all its amino acids, whilst the latter is an auxotrophic strain that is incapable of synthesizing all of its amino acids and thus must be supplied in the media for growth. I therefore asked whether the difference between the two strains, with respect to the deletion of 2-Cys peroxiredoxins, could be explained by the differences in their auxotrophic markers. To answer this question, I transformed BY4742 $\Delta tsa1\Delta ahp1$ cells, as well as their wildtype counterparts with a pHLUK plasmid to replace all auxotrophic markers in order to assume a 'CEN.PK-like' state. I also independently transformed these cells with pHUK, p415 and p416 plasmids as controls. The pHUK plasmid replaced all auxotrophic makers except leucine, whilst the p415 and p416 plasmids replaced leucine and uracil, respectively. I then grew the transformed cells on Hartwell Complete (HC) agar plates lacking either leucine (L) or uracil (U) for selection. Interestingly, cells transformed with pHLUK were fully viable; suggesting that absence of viable $\Delta tsa1\Delta ahp1$ or $\Delta tsa1\Delta tsa2\Delta ahp1$ spores in the CEN.PK background could not be due to their amino acid prototrophy (Fig 2.20).

It is plausible that in the CEN.PK background, *TSA1* and *AHP1* may be essential for spore formation or viability although I do not have direct evidence for this. It is also possible that peroxiredoxins will have a much broader role for the survival of CEN.PK yeast, independent of antioxidant defense, although this is yet to be proven. Furthermore, another difference between CEN.PK and most laboratory

strains, such as BY4742 and W303, is that the latter are known to be unable to establish synchronized metabolic oscillations [47, 56]. Based on the above reasoning, it is tempting to speculate that the differential requirement for peroxiredoxins in typical laboratory strains versus ‘less domesticated’, prototrophic yeast strains, such as CEN.PK is related to the ability to establish synchronized metabolic cycles.

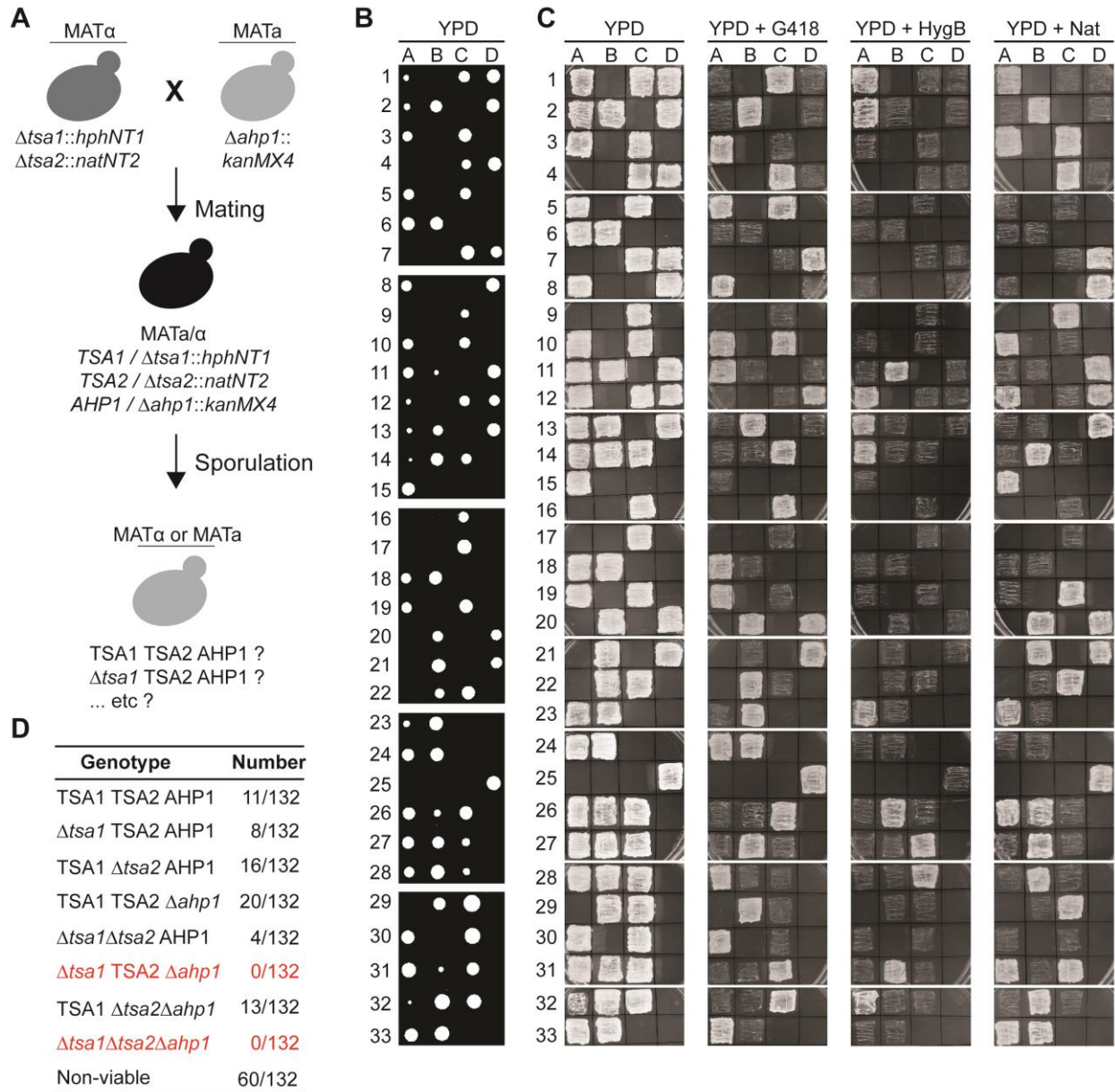


Figure 2.19: Double deletions of *TSA1* and *AHP1* leads to loss of viability in prototrophic yeast. (A) Scheme illustrating the mating, sporulation and tetrad dissection procedure. **(B)** Images of tetrad dissection plates for all 33 tetrads dissected. **(C)** Images showing growth of cells from all recovered viable spores on media containing the indicated antibiotics to assess for the presence of the antibiotic resistance cassettes used for gene deletion. **(D)** Table showing the eight possible genotypes and the number of spores recovered with each genotype.

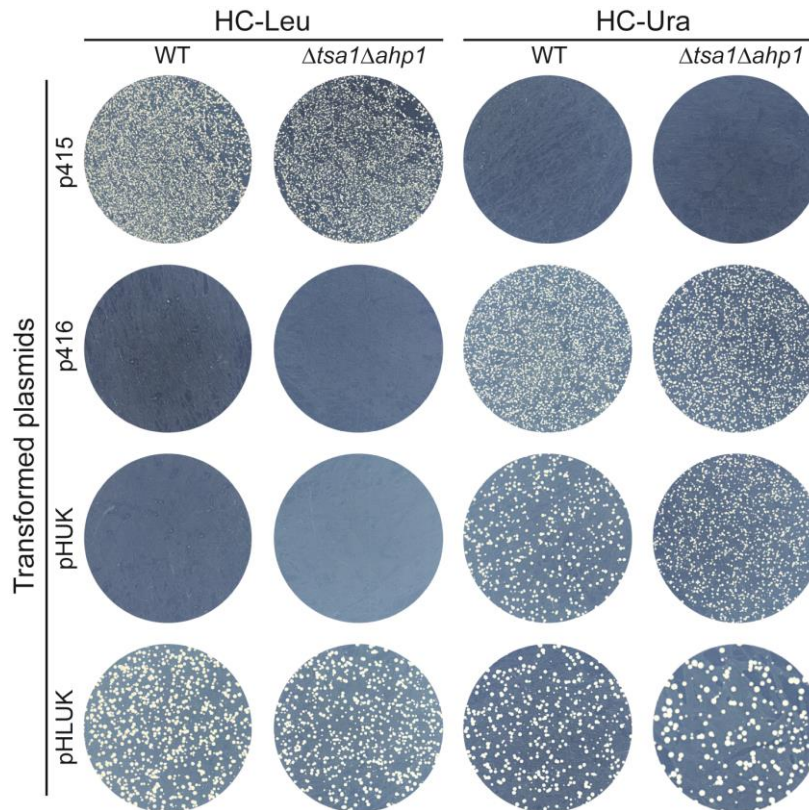


Figure 2.20: Non-viability of $\Delta tsa1\Delta ahp1$ cells in a CEN.PK background is not due to prototrophy. Images of colonies of BY4742 wildtype and $\Delta tsa1\Delta ahp1$ cells formed on indicated selective plates following transformation with the indicated plasmids. BY4742 cells are uracil and leucine auxotrophs. Therefore, cells transformed with p416 and pHUK plasmids, which both harbor URA3 as a selective marker, would not be expected to grow on media lacking leucine. Likewise, cells transformed with p415 (LEU2 as selective marker) should not grow on plates lacking uracil. These conditions therefore serve as controls. Cells transformed with a pHLUK plasmid to replace all four auxotrophic markers grow well on media lacking either leucine or uracil. Key: H – histidine, L – leucine, U – uracil, K – lysine.

2.5.4 An auxin-inducible degron system reveals toxicity of Ahp1 degradation in a *Atsa1* background

Since I could obtain neither a viable *Atsa1Δahp1* nor *Atsa1Atsa2Δahp1* strain by both homologous recombination and tetrad dissection experiments, I genomically fused *AHP1* with an auxin regulable degron (AID) in a *Atsa1Atsa2* background. This approach was used in order to first, verify the viability phenotype due to the combined loss of *TSA1* and *AHP1* in the CEN.PK background, and second, to assess the effect on the YMC of the combined loss of *TSA1* and Ahp1. This technique allows for rapid degradation of AID-fusion proteins upon supplementation with the auxin hormone indole-3-acetic acid (IAA) [133, 134]. The *Arabidopsis thaliana* F-box protein, *AtTIR1*, which is coupled to the AID construct functions as part of the ubiquitin ligase system to ubiquitinate and deliver AID-fusion proteins to the proteasome for degradation (Fig. 2.21A). I obtained the AID/*AtTIR1* construct on a plasmid from the lab of Prof. Blanche Schwappach (Göttingen, Germany). I amplified this construct by PCR and transformed it into yeast for genomic integration and fusion to the N-terminus of *AHP1* (Appendix A3). After successful strain construction, I tested the effect of this technique in a drop dilution growth assay, performed on YPD plates supplemented with either 0.2 mM IAA or 0.1% DMSO as vehicle control. Interestingly, *Atsa1* and *Atsa1Atsa2* strains

harboring the Ahp1 degron exhibited decreased viability on plates supplemented with IAA, as compared with their wildtype or *Atsa2* counterparts (Fig. 2.21B). This result demonstrates that depletion of Ahp1 in a CEN.PK *Atsa1* or *Atsa1Atsa2* background is detrimental for growth.

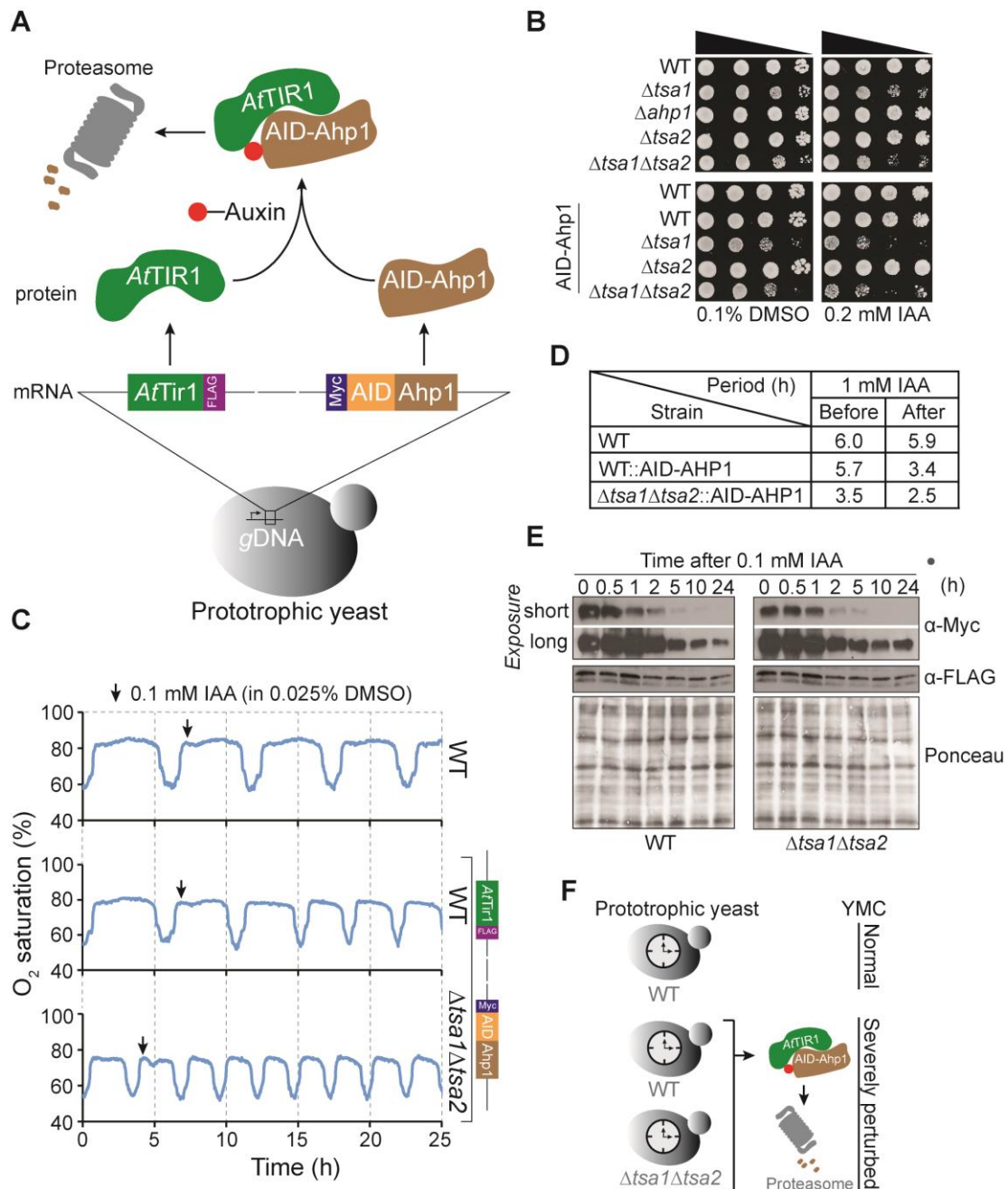


Figure 2.21: Conditional depletion of Ahp1 is lethal in $\Delta tsa1$ cells and severely perturbs the YMC. (A) Scheme illustrating the mechanism of Ahp1 depletion by the AID system. Both *AfTIR1* and *AID-Ahp1* are expressed from the genome of prototrophic yeast. Auxin binding to *AfTIR1* promotes the interaction between *AfTIR1* and *AID-Ahp1*. Subsequently, *AfTIR1* acts as an E3 ubiquitin ligase to recruit an E2 ligase resulting in polyubiquitination of *AID-Ahp1* (not shown). *Ahp1* is then delivered to the proteasome for degradation. **(B)** Drop dilution assay showing the growth of the indicated yeast strains on YPD plates containing either 0.1% DMSO as a vehicle control or 0.2 mM indole-3-acetic acid (IAA). Growth inhibition was monitored by incubation at 30 °C for 48 h. **(C)** Representative oxygen traces showing the effect of treating YMC-synchronized cultures of wildtype cells or wildtype and $\Delta tsa1\Delta tsa2$ cells expressing *Ahp1* genetically fused to an auxin inducible degron, with 0.1 mM indole-3-acetic acid (auxin). **(D)** Table illustrating effect of IAA on YMC period. **(E)** Western blot of *Ahp1* degradation after IAA treatment. Samples were taken at 0, 0.5, 1, 2, 5, 10 and 24 h after treatment to test for *Ahp1* degradation by Western blot. **(F)** Schematic explaining effect of IAA on the YMC of the cell types used. WT YMC remains unaffected whilst YMC of *AID-Ahp1/AfTIR1* expressing cells are severely perturbed upon IAA, due to gradual *Ahp1* degradation. All experiments were repeated at least twice with completely independent YMC-synchronized cultures.

2.5.5 Repression of Ahp1 in a $\Delta tsa1\Delta tsa2$ background perturbs the YMC

Further, I tested the effect of auxin on the YMC of wildtype- and $\Delta tsa1\Delta tsa2$ - AID-*AHP1*/*AtTIR1* expressing cells in comparison with their wildtype non-construct expressing counterpart. I cultured these cells under metabolic cycling conditions and added IAA at a final concentration of 0.1 mM at the start of LOC. The cycles of wildtype and $\Delta tsa1\Delta tsa2$ cells expressing the AID construct had periods remarkably shortened from 5.7 to 3.4 hours and 3.5 to 2.5 hours respectively, upon 0.1 mM IAA. The YMC of non-construct expressing wildtype cells was barely affected, maintaining periods of about 6 hours before and after 0.1 mM IAA (Fig. 2.21C-D). The reduction of YMC period in the AID-construct expressing cells was consistent with Ahp1 protein degradation as visualized by Western blot (Fig. 2.21E). The cycles could not be completely abolished as I anticipated. This was explainable by the incomplete removal of Ahp1 upon film visualization at long exposure. In short, these observations taken together demonstrate that cytosolic 2-Cys peroxiredoxins, especially Tsa1 and Ahp1, regulate the YMC and are important for the yeast timekeeping mechanism (Fig. 2.21F).

2.6 Peroxiredoxin-mediated YMC regulation is thioredoxin dependent

Thioredoxins (Trxs) are evolutionarily conserved proteins that facilitate protein thiol-disulfide reduction on specific target proteins, including peroxiredoxins [135]. Budding yeast harbors three thioredoxins; two in the cytosol, Trx1 and Trx2, and one in the mitochondria, Trx3. Thioredoxins and the NADPH-dependent thioredoxin reductase (TrxR) form a protein reductive system that mediate maintenance of cellular redox homeostasis and repair of oxidatively modified proteins, such as PTPs and STAT3 [69, 73]. Active peroxiredoxin catalysis requires disulfide reduction by thioredoxins. Similarly, active recycling of peroxiredoxins via the Trx/TrxR system is essential for hyperoxidation since the peroxiredoxin disulfide is protected from further oxidation [136].

I imagined two mechanisms by which thioredoxins could be important during the YMC: first, thioredoxins may reduce/repair/recycle target protein(s) oxidatively modified by peroxiredoxins, and second, they might directly reduce oxidized peroxiredoxins to limit oxidation of target protein(s). These plausible mechanisms could be affected in the absence of thioredoxins and possibly perturb the YMC, especially if peroxiredoxin relay(s) that regulate YMC oscillation become modulated. Therefore, I asked whether loss of thioredoxins (especially Trx1 and Trx2) could affect the YMC. I tested the impact of loss of *TRX2* on the YMC *per se*, and in response of the YMC to *t*-BOOH. Remarkably, *TRX2* deletion shortens YMC period similar to combined loss of *TSA1* and *TSA2* or loss of *AHP1* alone (Fig. 2.22A). Moreover, 0.5 mM *t*-BOOH was enough to trigger “hyperoxidation-based” LOC-to-HOC transition (Fig. 2.22B). In

contrast to wildtype and $\Delta tsa1\Delta tsa2$ cells, 1 mM *t*-BOOH only triggered transient HOC and an immediate return of the YMC to a prolonged LOC phase that lasted more than 6 hours (Fig. 2.22B).

Having earlier observed that an oxidative process (e.g. diamide) was required to keep cells in the LOC phase, I hypothesized that the prolonged LOC in $\Delta trx2$ cells upon 1 mM *t*-BOOH could be due to direct oxidation of protein thiols by *t*-BOOH. This situation is plausible because $\Delta trx2$ cells may have a diminished ‘reductive capacity’ occasioned by the loss of *TRX2*, thus, frustrating their ability to facilitate effective removal of *t*-BOOH. Furthermore, unlike H_2O_2 that is largely dependent on peroxiredoxins to effectively oxidize protein thiols [72]; *t*-BOOH on the other hand can directly oxidize protein thiols in the absence of peroxiredoxins. To test the latter claim, I collected samples from the YMC of wildtype cells expressing the genomic roGFP2-Tsa $\Delta 2C_R$ sensor, 30 mins after 1 mM *t*-BOOH-mediated hyperoxidation-based LOC-to-HOC transition. Samples were processed for fluorescence measurements in a plate-reader format, and further treated with either 1 mM H_2O_2 or 1 mM *t*-BOOH (Fig. 2.23A). Interestingly, 1 mM *t*-BOOH could directly oxidize roGFP2 despite Tsa $\Delta 2C_R$ inactivation, whilst 1 mM H_2O_2 could not (Fig. 2.23B-C).

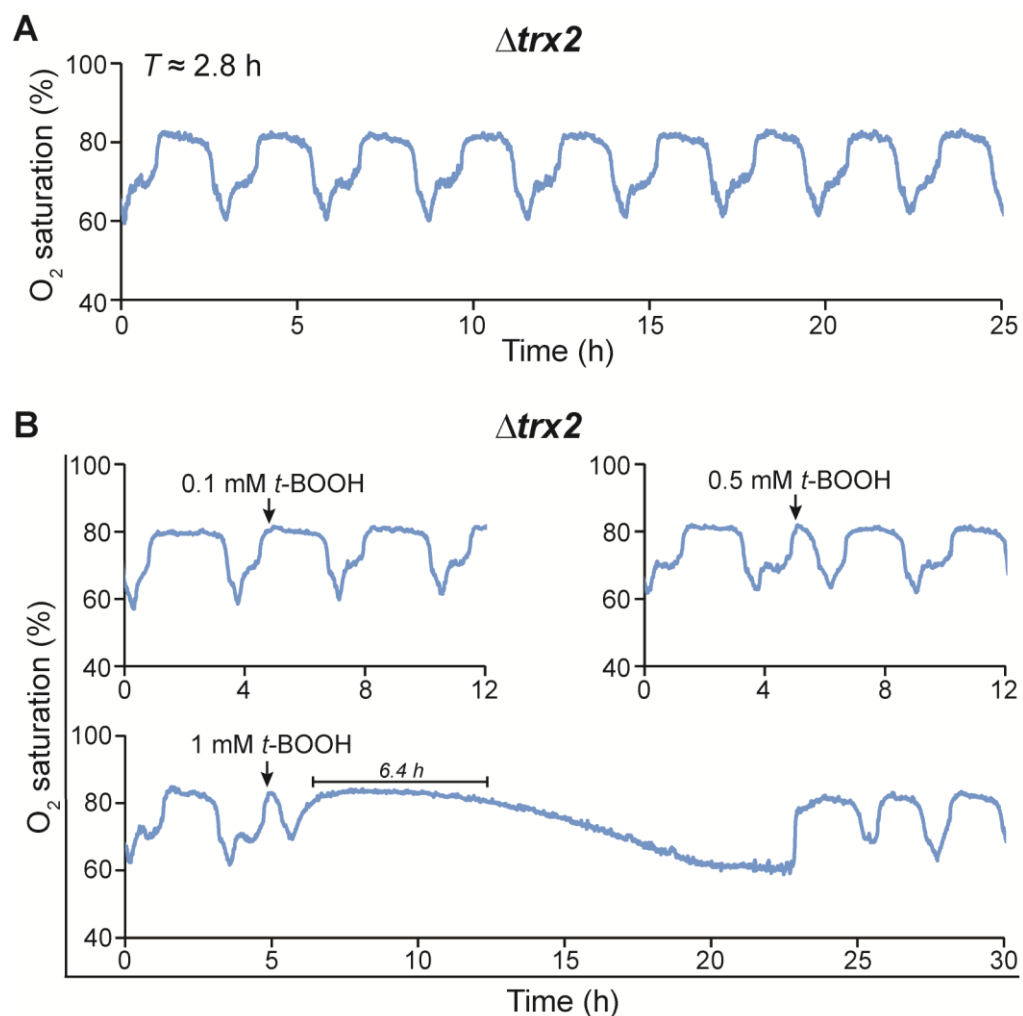


Figure 2.22: Loss of *TRX2* affects the YMC *per se*, as well as YMC response to *t*-BOOH upon peroxiredoxin hyperoxidation during the YMC. (A) Representative oxygen traces to show the YMC for $\Delta trx2$ cells. (B) Representative oxygen traces showing the effect of *t*-BOOH on YMC-synchronized cultures of a $\Delta trx2$ strain at the indicated concentrations.

To test the consequence of loss of both cytosolic *TRXs* on the YMC, I sought to delete *TRX2* in a $\Delta trx1$ background or *vice versa*, by the homologous recombination-based gene deletion approach. This attempt was unsuccessful; however, the $\Delta trx1\Delta trx2$ strain could be obtained by subsequent mating, sporulation and tetrad dissection (Shamala Riemann, data not shown). That notwithstanding, the $\Delta trx1\Delta trx2$ culture could only grow in a batch phase without the ability to consume the levels of dissolved oxygen in the culture vessel, hence, could not establish synchronized metabolic cycles (Fig. 2.24). Taken together, these observations indicate that thioredoxins are important for YMC regulation. These results further speak in favor of function(s) for the peroxiredoxin and thioredoxin systems in the yeast metabolic clock.

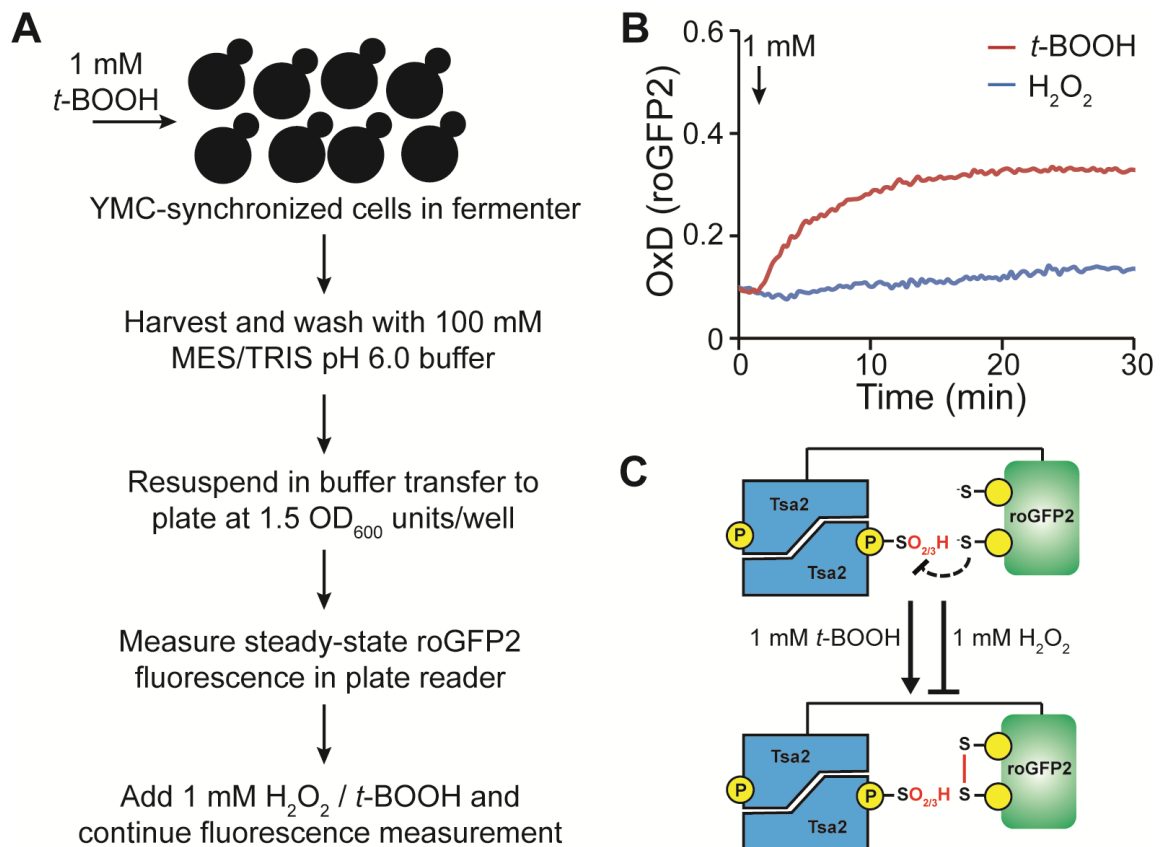


Figure 2.23: Unlike H₂O₂, *t*-BOOH mediates direct protein thiol oxidation upon peroxiredoxin hyperoxidation. (A) Schematic describing procedure by which sensor-expressing cells treated with *t*-BOOH during the YMC were processed to test for further peroxide response by the plate reader method. (B) Sensor expressing cells respond differently to *t*-BOOH and H₂O₂ after peroxiredoxin hyperoxidation in the fermenter. (C) Schematic explaining hyperoxidized probe response upon further *t*-BOOH or H₂O₂. Note: Unlike H₂O₂, *t*-BOOH can bypass the inactivated Tsa2 Δ C_R and react directly with roGFP2 to keep it oxidized. Therefore, in the absence or decreased levels of reducing equivalents from cellular thioredoxins, *t*-BOOH mediates hyperoxidation of peroxiredoxins during the YMC to induce switch to HOC, which is only short-lived, and immediately returned to a prolonged LOC phase possibly via direct oxidation of endogenous peroxiredoxin target protein(s).

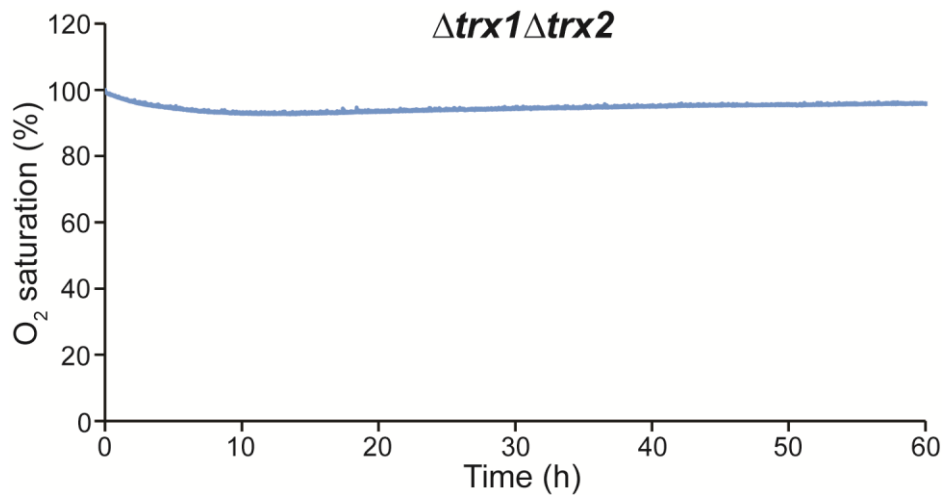


Figure 2.24: $\Delta trx1\Delta trx2$ cells do not generate synchronized metabolic cycles. Representative oxygen trace showing that $\Delta trx1\Delta trx2$ cells only grow in a batch phase and could not effectively consume dissolved oxygen to generate synchronized metabolic cycles.

2.7 Peroxiredoxins couple metabolic oscillations in yeast to the cell division cycle (CDC)

Circadian and ultradian clocks are coupled to the cell division cycle (CDC) in a variety of species [50, 53-55]. In cyanobacteria, algae, fungi and mammals, the circadian clock gates the CDC such that cell cycle events are arrested at checkpoints during prohibitive circadian phases [53, 55, 137-139]. It has also been suggested that DNA replication and cell division are synchronized to, and temporally regulated by the YMC [49]. In other words, metabolism gates the decision to undergo division, as such; cells lacking essential metabolites will not bypass the ‘committed step’ to cell division [111, 140-142].

However, the mechanistic details on how metabolic changes may temporally be coordinated with the CDC remains unresolved. Moreover, some evidence point to the existence of a regulatory redox cycle within the cell cycle [143, 144]. This proposition is strengthened by the presence of redox-sensitive motifs in a variety of cell cycle regulatory proteins, suggesting that periodic oscillations in intracellular redox state could play a significant role in regulating cell cycle progression [119, 123]. However, it is not completely clear whether peroxiredoxins are involved in cell cycle regulation. I hypothesized that oscillations in the intracellular redox state (e.g. H₂O₂ levels) during the YMC could represent a fundamental mechanism linking cell metabolism to cell cycle regulation. If so, this mechanism might rely on peroxiredoxins as transducers of H₂O₂.

2.7.1 Oscillatory metabolism is coordinated with cell division

To explore the relationship between the YMC and the CDC, I monitored the progression of DNA replication throughout the YMC, by performing propidium iodide (PI) staining of ethanol-fixed cells collected from YMC-synchronized cultures. I then subjected these samples to flow cytometry analysis. By sampling cells at specific phases of the YMC of wildtype cells, I observed that nuclear DNA replication was initiated during HOC, with increasing proportion of cells acquiring twice (2N) their DNA content before the LOC phase. The proportion of cells with 2N DNA content then decreased gradually towards the end of LOC and into the next HOC (Fig. 2.25A-C). This increase and decrease in DNA replication during the YMC correlated precisely with the increase and decrease in cellular H₂O₂ levels as well as roGFP2 oxidation demonstrated earlier (see Fig. 2.7B,D), suggesting a communication between the redox and cell division cycles. Thus, it appears that increasing cellular H₂O₂ levels may be required for DNA synthesis and cell cycle entry, whilst decreasing H₂O₂ levels permit cell division and cell cycle exit. This reasoning aligns with the suggestion by Chen *et al.* that H₂O₂ might regulate cell cycle entry [49].

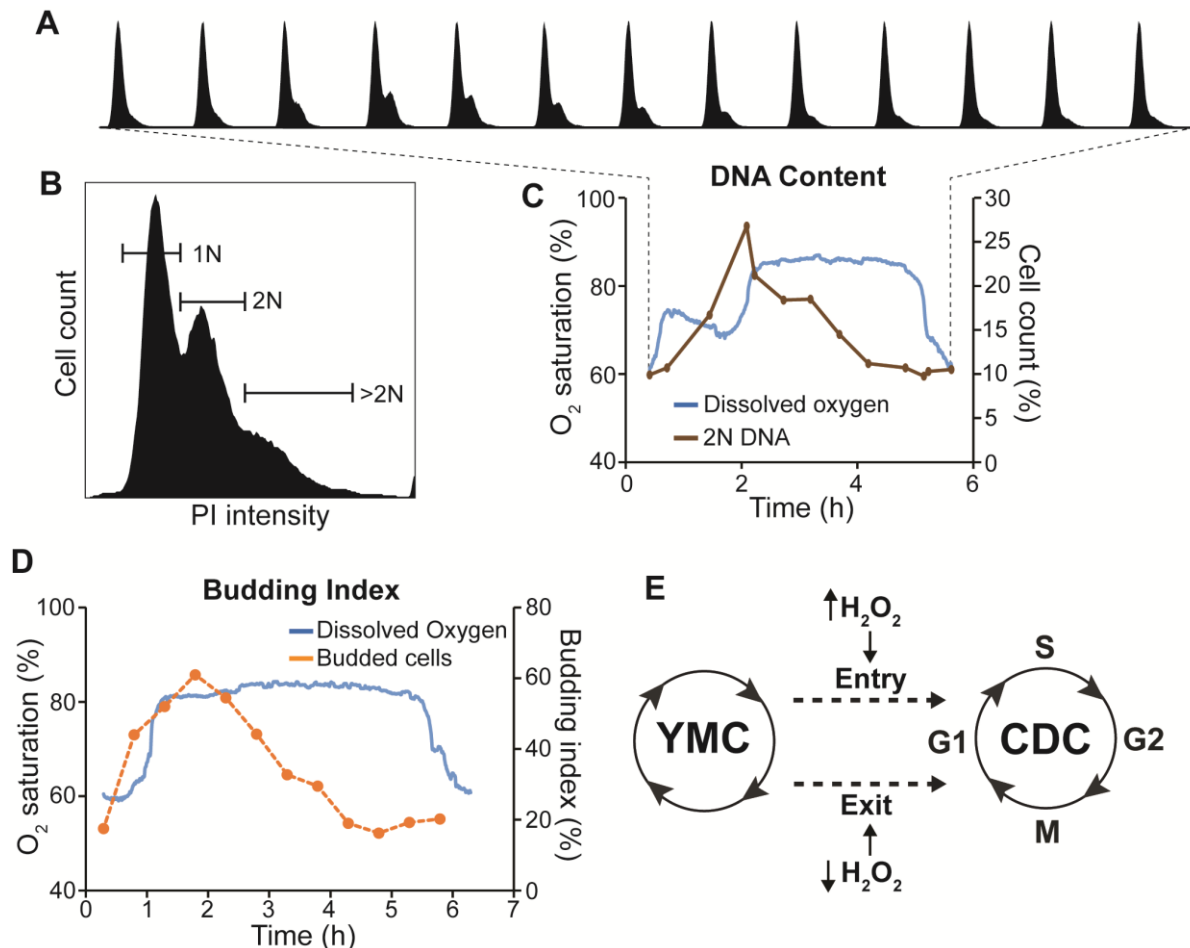


Figure 2.25: Coupling of YMC and CDC during the YMC. (A) Representative flow cytometry histograms showing DNA content in samples harvested from a culture of YMC-synchronized wildtype cells. (B) Illustration showing how flow cytometry histograms were assessed for DNA content. (C) Change in DNA content during the YMC for wildtype cells, determined based on the histograms in (A). (D) Representative graph showing the budding index determined in samples of wildtype yeast cells collected at the indicated time points from YMC-synchronized cultures. (E) Scheme summarizing mode of coupling between the YMC and CDC.

To verify this supposed YMC-CDC coordination, I collected samples from an independent YMC-synchronized culture of wildtype cells, fixed them in 70% ethanol and determined cell budding index by microscopy, in collaboration with Dr. Galal Metwally (Molecular Genetics, TU Kaiserslautern). Interestingly, I observed that the proportion of budding cells increased and decreased in correlation with the proportion of cells acquiring 2N DNA content (Fig. 2.25D). I therefore opined that redox/H₂O₂ changes during the YMC might in part be coupled to modulate target-protein activity to regulate the cell division cycle (Fig. 2.25E). In other words, under physiological conditions DNA replication might not necessarily be restricted to the non-respiratory phase of the YMC in order to prevent oxidative DNA damage as previously suggested [47, 49], rather, increasing H₂O₂ levels may be necessary to trigger DNA synthesis and entry into the CDC. Alternatively, redox/H₂O₂ changes might control the metabolic state of cells, which in turn gates the CDC.

2.7.2 Temporary inactivation or loss of peroxiredoxins leads to decoupling of CDC from YMC

Next, I sought to ascertain whether peroxiredoxins might be essential to the synchrony between the YMC and CDC. To do this, I collected samples from YMC-synchronized cultures of wildtype cells before and after treatment with 1 mM *t*-BOOH at the start of LOC. I then analyzed the DNA content by flow cytometry as described earlier. I observed once again that the proportion of cells with 2N DNA content peaked before entry to LOC; however, upon 1 mM *t*-BOOH and peroxiredoxin hyperoxidation, the proportion of cells with 2N DNA content began to decrease and correlated with switch to HOC. The proportion of cells with 2N DNA content remained low on the next immediate cycle, suggesting a temporary loss of coupling between the YMC and CDC. Synchrony between the YMC and CDC returned upon the second next cycle, presumably when active peroxiredoxin catalysis was restored (Fig. 2.26A,B).

To ascertain what the combined loss of *TSA1* and *TSA2* could mean for YMC-CDC synchrony, I further collected samples from YMC-synchronized cultures of $\Delta tsa1\Delta tsa2$ cells and analyzed their DNA content by flow cytometry. Interestingly, nuclear DNA replication stayed constant over the two metabolic cycles sampled, suggesting a decoupling of CDC from the YMC (Fig. 2.26C,D). Subsequently, I collected samples from an independent YMC-synchronized culture and fixed them in 70% ethanol for budding index determination. Here, I also observed equal number of budding cells at every stage of the YMC from which samples were taken (Fig. 2.26E). Taken together, these data suggest that peroxiredoxins may be crucial in coupling metabolic/redox changes during the YMC to regulate DNA replication and cell division

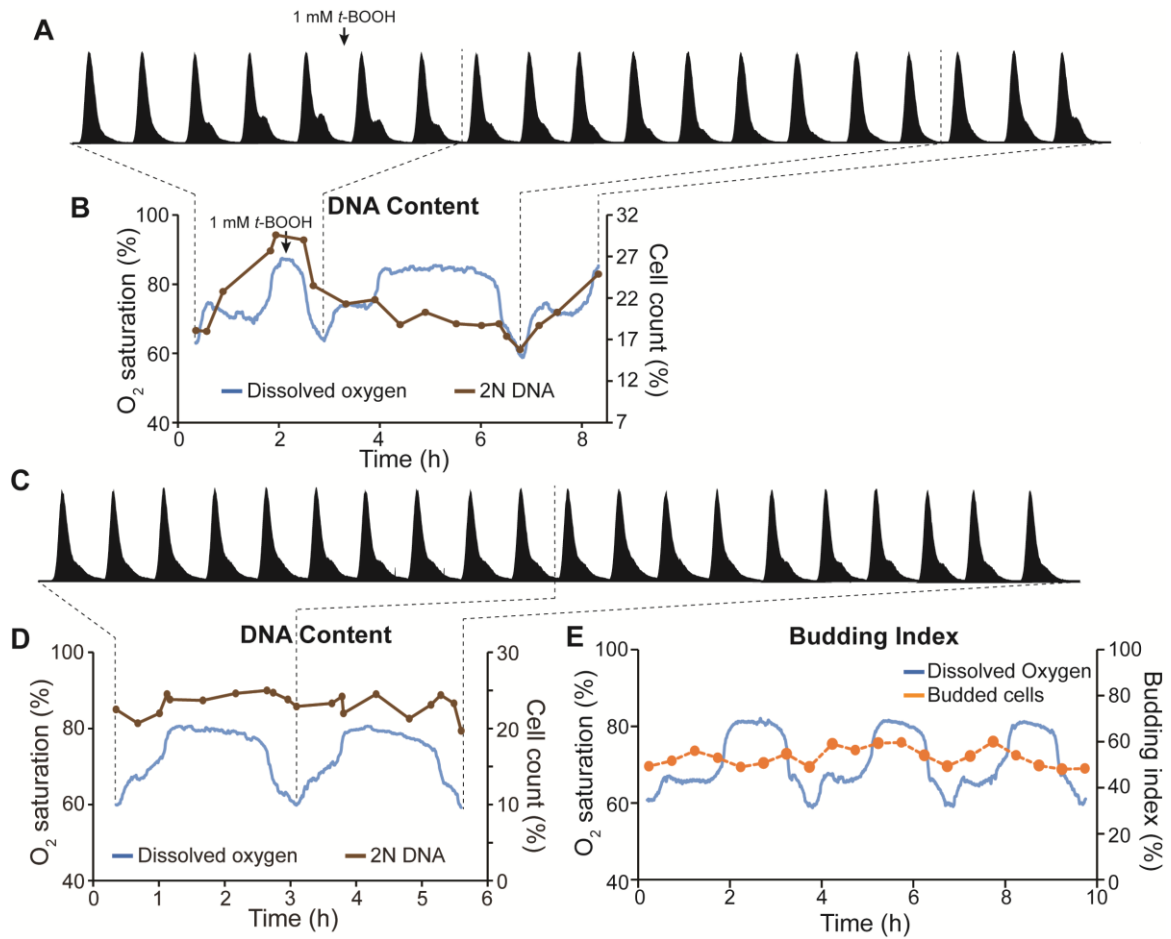


Figure 2.26: Coupling of YMC to CDC is mediated by peroxiredoxins. (A) Representative flow cytometry histograms showing DNA content in samples harvested from a culture of YMC-synchronized wildtype cells before and after 1 mM t -BOOH. (B) Change in DNA content during the YMC for wildtype cells treated with 1 mM t -BOOH, determined based on the histograms in (A). (C) Representative flow cytometry histograms showing DNA content in samples collected from a culture of YMC-synchronized $\Delta tsa1\Delta tsa2$ cells at the indicated time points. (D) Change in DNA content during the YMC for $\Delta tsa1\Delta tsa2$ cells, as determined based on the data in (C). (E) Graph showing the budding index determined in samples of $\Delta tsa1\Delta tsa2$ yeast cells collected at the indicated time points from YMC-synchronized cultures. All experiments were repeated at least twice with completely independent YMC-synchronized cultures.

2.8 Chemical redox perturbations of the YMC modulate entry into and exit from the cell division cycle

Given that, I could predictably manipulate switching between LOC and HOC of the YMC by applying thiol redox compounds such as diamide and DTT: i.e. diamide delays switch to HOC, whilst DTT promotes switch to HOC, I asked what the consequence would be of these molecules, on the coordination of the YMC to the CDC.

2.8.1 Induction of HOC upon thiol disulfide reduction promotes cell cycle entry

To address this question, I first treated YMC-synchronized cultures of wildtype cells with 5 mM DTT at the start of LOC to induce switch to HOC. Subsequently, I collected cell samples at defined time points before and after, and analyzed their DNA content by flow cytometry (Fig. 2.27A,B). Strikingly, upon DTT addition to induce LOC-to-HOC transition and a prolonged HOC phase for more than 10 hours, I observed a consistent increase in the proportion of cells with 2N DNA content. Interestingly, nearly 4 hours after DTT treatment, I also observed the presence of cells that appear to contain more than 2N DNA content (Fig. 2.27A,B).

To confirm the above observation, I setup an independent YMC-synchronized wildtype culture, collected samples in similar fashion as before and fixed them in 70% ethanol for microscopic analysis and budding index determination. Upon determination of budding index, I observed a consistent increase in the proportion of cells with one bud after DTT treatment. Surprisingly, I also saw cells with more than one bud appearing nearly 4 hours after DTT addition (Fig. 2.27C-D). Upon DAPI staining of nuclear DNA and microscopic analysis, I could show that cells with more than one bud possessed more than 2N DNA content (Fig. 2.27E). Importantly, in budding yeast the occurrence of a new bud is timed with initiation of DNA replication [145]. Thus, the above observations suggest that artificially inducing YMC-synchronized cells to remain in a prolonged HOC phase compels them to trigger DNA synthesis and start a new cell cycle irrespective of whether the previous cell division had been fully accomplished. This therefore results in the accumulation of cells with increasing DNA content and more than one bud. Consequently, switching to HOC appears to be a prerequisite for initiation of cell division.

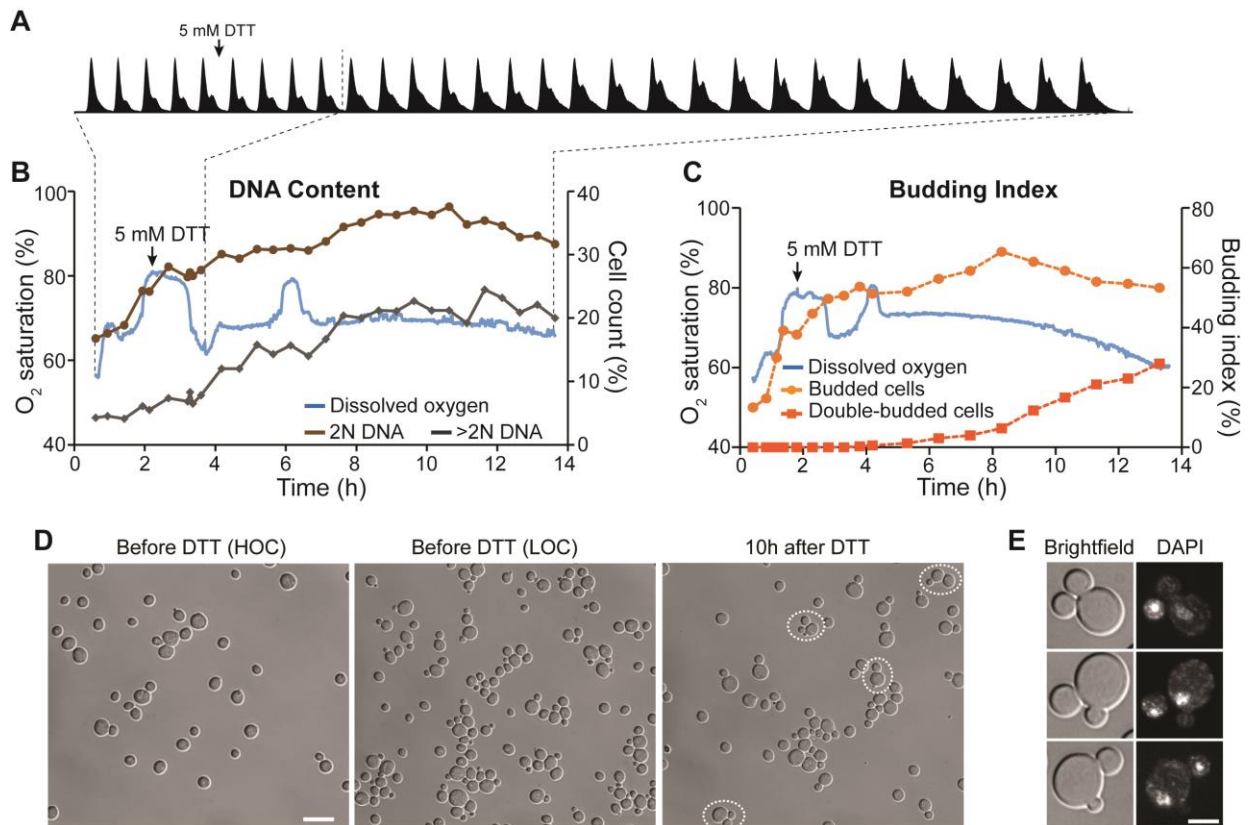


Figure 2.27: Effect of thiol reduction on DNA replication and cell budding. (A) Representative flow cytometry histograms showing change in cellular DNA content before and after addition of 5 mM DTT to YMC-synchronized cultures of wildtype cells. (B) Graph showing the impact of 5 mM DTT treatment on the YMC as assessed by monitoring of oxygen consumption as well as the impact on cell cycle based upon cellular DNA content determined from the histograms in (A). (C) Graph showing the change in budding index of YMC-synchronized wildtype cells before and after the addition of 5 mM DTT. (D) Representative microscopy images of yeast cells before and ~10 h after 5 mM DTT addition to YMC-synchronized wildtype cells. (E) Representative microscopy images of DAPI stained cells with 2 buds, isolated from YMC-synchronized cultures ~10 h after addition of 5 mM DTT. Scale bar is 2 μ m.

2.8.2 Prolongation of LOC upon thiol disulfide oxidation delays cell cycle entry

Similarly, I treated YMC-synchronized wildtype cells with 2 mM diamide towards the end of LOC and collected samples at defined time points for DNA content analysis by flow cytometry (Fig. 2.28A,B). In contrast to DTT, addition of 2 mM diamide towards the end of LOC of YMC-synchronized wildtype cells delayed LOC-to-HOC transition as well as start of DNA replication by nearly 2 hours (Fig. 2.28A,B). I then subjected these samples to microscopic analysis to determine their budding index. Strikingly, the proportion of budding cells stayed low during the period of LOC extension and into the next HOC (Fig. 2.28C).

During cell division, proteins that control the activity of cyclin-dependent kinases (Cdks) regulate cell cycle entry and exit. For example, Sic1 is a Cdk inhibitor that blocks initiation of S-phase and must be degraded at the G₁-S transition to facilitate cell cycle entry [146, 147]. Likewise, Clb2 is a B-type cyclin that accumulates during G₂ and M phases of the cell cycle and repressed by the end of mitosis; it activates Cdc28p to promote the transition from G₂ to M phase [148, 149] (Fig. 2.28D).

To ascertain what was happening to these regulatory protein levels during the YMC and upon diamide treatment, I performed Western blot analysis against Sic1 and Clb2 in collaboration with Galal, using the above cells. I observed that upon diamide treatment, Sic1 levels increased whilst Clb2 levels that were diminished shortly before treatment did not reappear over the duration of the experiment (Fig. 2.28E). Taken together, these observations suggest that switching to LOC seems to be a pre-requisite for completion of cell division, as such; a prolonged LOC phase upon diamide treatment appears to trap cells that have exited mitosis in the G₁ phase, unable to initiate a new cell cycle.

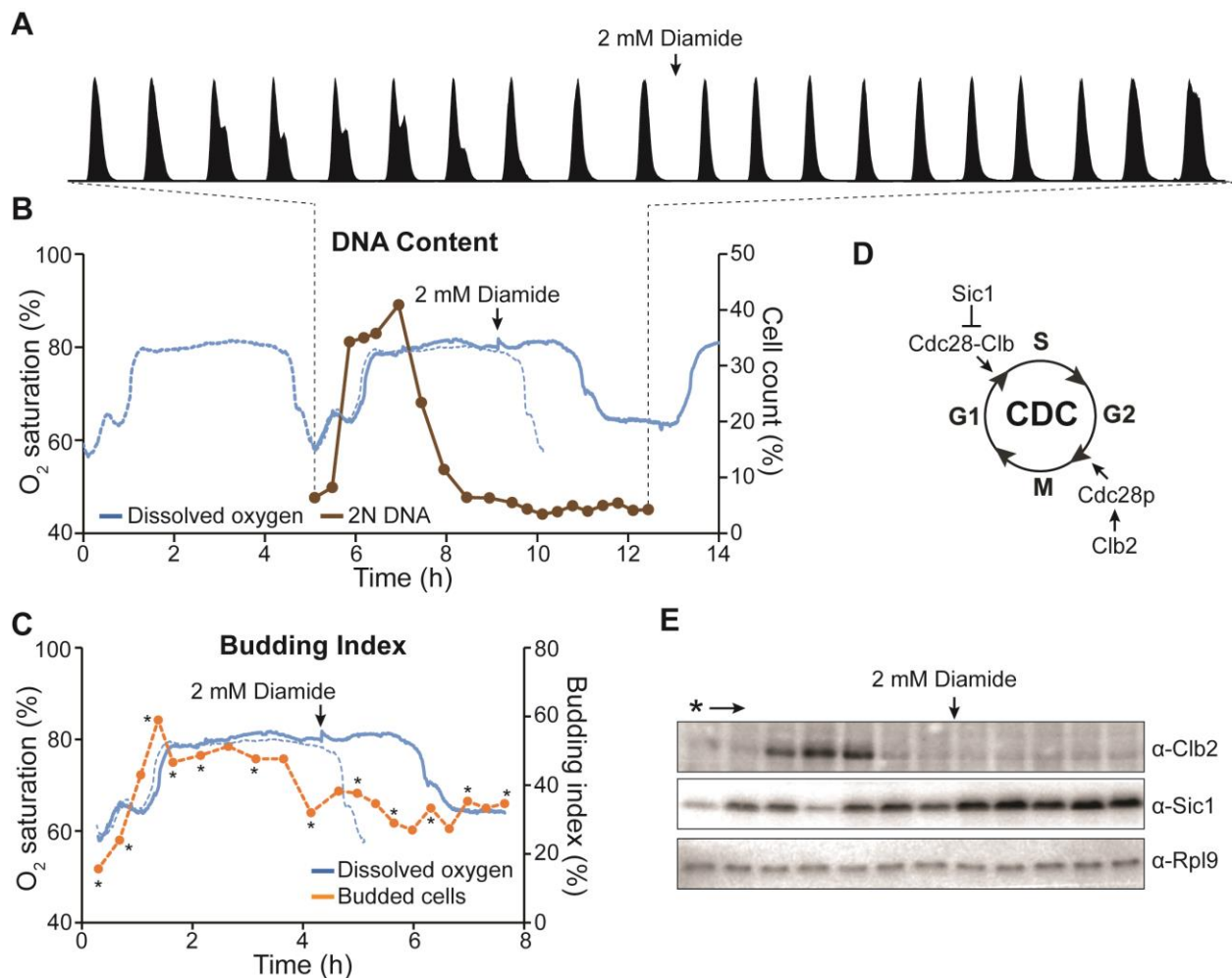


Figure 2.28: Effect of thiol oxidation on DNA replication and cell budding. (A) Representative flow cytometry histograms showing change in cellular DNA content before and after addition of 2 mM diamide to YMC-synchronized cultures of wildtype cells. (B) Graph showing the impact of 2 mM diamide treatment on the YMC as assessed by monitoring of oxygen consumption, as well as the impact on cell cycle based upon cellular DNA content determined from the histograms in (A). (C) Graph showing the change in budding index of YMC-synchronized wildtype cells before and after the addition of 2 mM diamide. Dotted blue lines in (B) and (C) represent an overlay of the YMC cycle immediately prior to the one indicated with the continuous blue line. (D) Scheme showing some proteins involved in regulating cell cycle progression. (E) Western blot using anti-Sic1 and anti-Clb2 antibodies. Rpl9 was used as a loading control. Samples were collected as indicated by (*) in (C).

3 DISCUSSION

The aim of this study was to investigate whether peroxiredoxins are active players in the cellular timekeeping mechanism, using the yeast metabolic clock as a model. I utilized the reconstituted peroxiredoxin redox relay, roGFP2-Tsa2 Δ C_R, and performed genetic manipulations and biochemical assays to show that yeast 2-Cys peroxiredoxins are crucial for regulating the yeast metabolic clock. This, I propose they do by coupling cyclical changes in H₂O₂ during the yeast metabolic cycle (YMC) to regulate the redox state of redox-regulated proteins. I have also shown that metabolic oscillations are coupled with the cell division cycle, an important feature of circadian and ultradian metabolic clocks. As such, perturbation of cell metabolism with thiol redox modifiers influences entry into and exit from the cell division cycle. More importantly, I demonstrate that 2-Cys peroxiredoxins are essential for coordinating metabolic changes to the cell division cycle. In this section, I discuss the above findings and summarize this novel role for peroxiredoxins in the cellular clockwork.

3.1 The YMC is a redox clock that is regulated by thiol switch(es)

I have engineered prototrophic yeast to genomically harbor a genetically encoded biosensor that allows real-time, dynamic monitoring of the flux of oxidation through a peroxiredoxin redox relay during the YMC. My observations principally reveal that: (1) oscillations in basal H₂O₂ levels accompany oscillatory metabolism, (2) there exist in the yeast metabolic clock, changes in the flux of oxidation through a peroxiredoxin redox relay, (3) these flux changes are large enough to induce changes in the oxidation state of peroxiredoxin target protein(s). The yeast metabolic clock is characterized by two phases dependent upon the rate of oxygen consumption, namely; a high oxygen consumption (HOC) phase in which dissolved oxygen levels decrease and a low oxygen consumption (LOC) phase where the levels of dissolved oxygen are high (Fig 1.7). My observations indicate that H₂O₂ levels rise during ‘decreasing’ HOC and peak before HOC-to-LOC transition thereby inducing peroxiredoxin and peroxiredoxin target protein(s) oxidation. H₂O₂ then decreases gradually during LOC to levels that render peroxiredoxin and peroxiredoxin target(s) more reduced to trigger LOC-to-HOC switching. A decrease in HOC is triggered once again by accumulating H₂O₂ levels and subsequent peroxiredoxin and peroxiredoxin target protein(s) oxidation (Fig. 2.7 and 3.1).

In *N. crassa* and cyanobacteria, the daily expression pattern of clock and clock-controlled genes involved in coordinating photosynthesis is influenced by H₂O₂ [96-98]. It has also been shown that visible light alters the YMC by inhibiting respiration [150]. In cultured mouse, monkey and humans cells, light stimulates H₂O₂ production via photoreduction of flavin-containing enzymes such as peroxisomal acyl-coenzyme A (CoA) oxidase [151]. Recent evidence suggests that yeast peroxisomal flavin-containing fatty acyl CoA oxidase, Pox1, converts visible light into H₂O₂ signal that is sensed by the peroxiredoxin Tsa1 and transduced to thioredoxin, to counteract PKA-dependent Msn2 phosphorylation [152]. Additionally,

Tu *et al.* demonstrated that the levels of *POX1* transcripts oscillate during the YMC [47]. Moreover, zebrafish circadian clock is coupled to light signals via H_2O_2 [95]. Thus, it is tempting to speculate that by oscillating during the YMC, H_2O_2 acts as a signal to entrain the yeast metabolic clock. The oscillations in H_2O_2 levels that underlie the yeast metabolic clock as I have demonstrated, may not only be unique to this clock model, but rather, represent an important feature of all circadian and ultradian metabolic clocks. In support of this reasoning, recent studies by Liu and colleagues suggest that oscillations in H_2O_2 levels occur in single N2a murine neuroblastoma and human U2OS cells in a circadian manner [153]. They also observed diurnal oscillations in H_2O_2 levels in the liver of mice [153]. I envisage that these observations would be replicated in several metabolic clock models in the near future.

Furthermore, I note that oscillations in H_2O_2 levels during the YMC serve a causative role, rather than being just a by-product of cell metabolism. I propose that this causative function may be intrinsic to each yeast cell, but the outcome may be orchestrated on the population level to achieve metabolic synchrony. Although it has been suggested that population synchrony of budding yeast in low-glucose bioreactors could arise from signaling between cells due to secreted metabolites such as ethanol, acetaldehyde and dihydrogen sulfide [58, 59], secreted H_2O_2 molecules do not play a role in such intercellular communications. This reasoning was confirmed by catalase-mediated H_2O_2 scavenging activity in the culture vessel, which had no observable effect on the YMC (Fig 2.8). Like H_2O_2 , oscillations in other redox metabolites such as GSH/GSSG, $NAD^+/NADH$ and $NADP^+/NADPH$ accompany the YMC [56, 154, 155]. Moreover, transcript levels of redox proteins and enzymes oscillate during the YMC [47]. These observations, taken together, affirm that the YMC is indeed a redox clock.

Although I could report oscillations in H_2O_2 levels during the YMC using two different approaches, i.e. thiol-based NEM-trapping technique and real-time measurements with a flow cell (Fig 2.7), the amplitude of change was small. Nonetheless, an $\approx 5\%$ oscillation in basal H_2O_2 levels or physiological oxidations during the YMC, as I have demonstrated herein, is not trivial. Sobotta *et al.* showed that in the PRDX2-STAT3 redox relay in mammalian cells, only a very small subpopulation of STAT3 is oxidatively modified to compromise STAT3 transcriptional activity, in response to cytokines [73]. Therefore, it is conceivable that an $\approx 5\%$ change in the redox state of yet to be identified peroxiredoxin redox relay(s) may be enough to regulate the YMC.

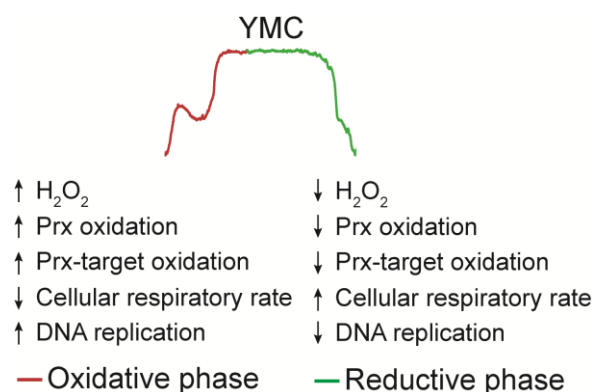
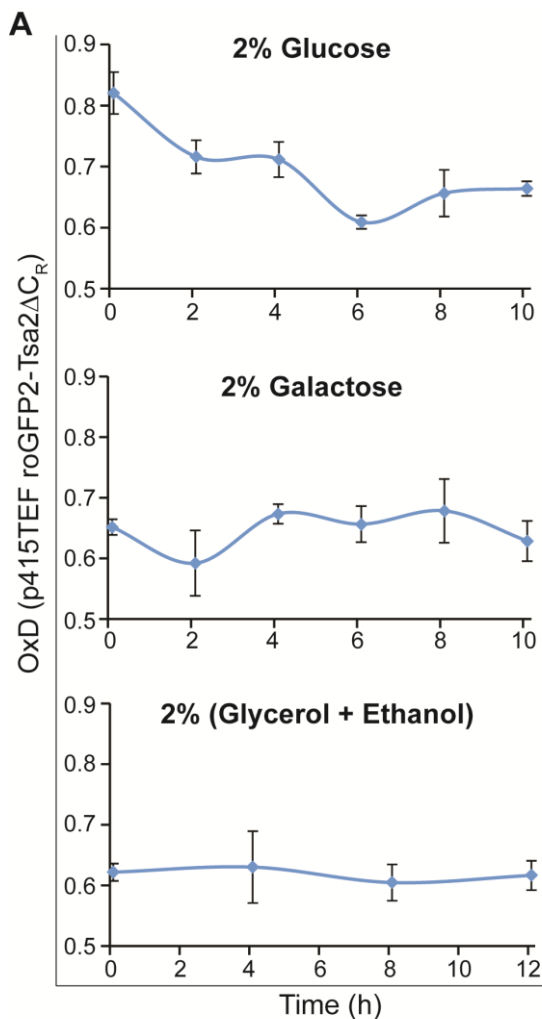


Figure 3.1: The YMC is a redox clock. Scheme describing events occurring at each phase of the yeast metabolic cycle as observed in this study.

On the other hand, the observed “small” amplitude of change in physiological oxidations could be explained with respect to cellular physiology and technical/experimental conditions. First, the biosensor used to monitor cellular H_2O_2 was localized to the cell’s cytoplasm. Oscillations in cytoplasm-localized H_2O_2 levels could most likely be counteracted by the high reducing capacity of the cytoplasm. Reducing molecules such as GSH and NADPH are highly abundant within the cytoplasm of cells to mitigate any significant rise in physiological oxidations. Nonetheless, this reductive capacity does not completely eliminate signaling H_2O_2 levels that could be detected and transduced by peroxiredoxins to regulate protein thiols, as observed with the biosensor. Secondly, during real-time biosensor fluorescence measurements, experimental conditions such as the distance or time it takes for cells to travel from the culture vessel into the spectrofluorimeter, as well as air bubbles arising from culture aeration and stirring could frustrate ‘actual’ fluorescence signals. Thirdly, although I tried to immediately ‘trap’ the redox state of the biosensor after collecting cell samples from the fermenter, it is plausible that the NEM-trapping technique might not have been effective as envisaged, to monitor fluctuations in basal H_2O_2 levels on such a huge time-scale. It is also plausible that some thiol alkylation might have been lost during sample processing. Since this is the first study utilizing the flow cell technique to measure oscillations in basal H_2O_2 levels in real-time, it could be improved upon and standardized for future studies. These notwithstanding, the $\approx 50\%$ oxidation state of roGFP2 as observed with the NEM-trapping technique accurately reflects the steady-state degree of oxidation of the roGFP2-Tsa2 ΔC_R biosensor under physiological conditions in wildtype cells, as have been previously reported [90]. The real-time flow cell measurements also qualitatively reveal $\approx 50\%$ roGFP2 oxidation ratio.

An outstanding question that remains to be fully answered is how these H_2O_2 oscillations are generated and sustained. In other words, how is H_2O_2 produced during the YMC? Are the observed oscillations due to H_2O_2 production or consumption? While these questions could be the subject of future investigations, some explanations can be attempted. First, I note that when the sensor redox state of genomically engineered yeast cells grown in glucose batch culture was trapped with NEM and roGFP2 fluorescence measured, the oxidation state of roGFP2 decreased with culture density (Fig. 2.5D). This suggests that once glucose became limiting, H_2O_2 production gradually decreased and roGFP2 consistently became reduced. Secondly, in a comparative measurement of roGFP2 fluorescence in wildtype BY4742 yeast cells transformed with a plasmid expressing the roGFP2-Tsa2 ΔC_R sensor and grown in media supplemented separately with three different carbon sources (i.e. glucose, galactose and glycerol/ethanol); I could observe only in glucose media, change in roGFP2 oxidation state with respect to culture duration. The sensor was almost 80% oxidized in fresh glucose and gradually reduced to about 60% oxidation over time, probably when glucose was depleted. This nearly 60% oxidation state was what was consistently achieved in galactose and glycerol/ethanol media over the duration of the experiment (Fig 3.2A). Similarly, by growing the plasmid expressing cells in glucose to mid-log phase, harvesting, diluting and further growing them separately in the three media described above, for NEM trapping experiments over a period

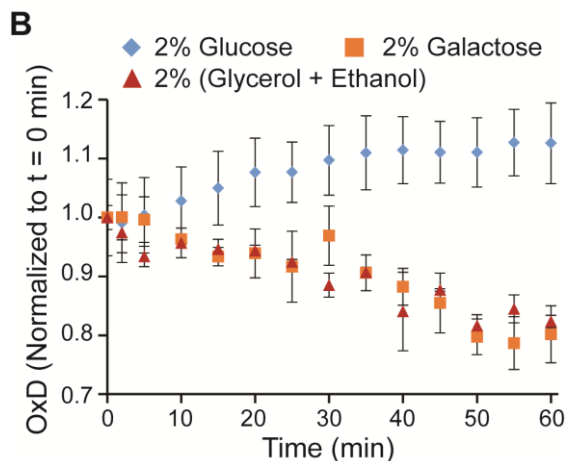
of 1 hour, I observed a consistent increase in the degree of roGFP2 oxidation only in glucose media (Fig.



3.2B). Based on these observations, I concluded that glucose stimulated H_2O_2 production.

Consequently, the controlled but consistent supply of glucose during continuous culture could be responsible for the generation of H_2O_2 that underlie the YMC. This reasoning is also supported by the fact that interference with cellular H_2O_2 generation systems inhibits the generation of, or perturbs the YMC. For instance, deletion of yeast cytosolic Cu-Zn superoxide dismutase 1 (*SOD1*) – an enzyme that catalyzes the breakdown of superoxide radical to molecular oxygen and H_2O_2 – inhibits respiratory growth and YMC generation (Fig. 3.3A). Moreover, deletion of yeast superoxide-generating NADPH oxidase, *YNO1*, strongly perturbs the YMC (Fig. 3.3B).

Figure 3.2: Glucose stimulates H_2O_2 production. WT BY4742 cells expressing the roGFP2-Tsa2 Δ C_R plasmid were (A) cultured in the respective media at OD₆₀₀ = 0.25 and trapped with NEM to monitor steady-state roGFP2 oxidation over the stated duration. (B) grown in 2% glucose media to OD₆₀₀ = 3.5, diluted in the respective media and trapped in NEM at specific time intervals for 1 h. Data represent at least three independent replicates and error bars represent standard deviation.



Another important source of H_2O_2 within the cell is the mitochondria. Mitochondrial ROS are mainly generated at complexes I and III of the ETC in the form of superoxide, which is then converted to H_2O_2 by the superoxide dismutase Sod2 [156]. In mammalian cells, the protein product of an mRNA isoform of the mitochondrial *SHC1* gene, p66^{Shc}, has been implicated in the generation of H_2O_2 that oxidizes the circadian clock protein, CLOCK [153]. It is believed that p66^{Shc} functions

as an oxidoreductase to transfer electrons from cytochrome c to molecular oxygen, leading to the generation of mitochondrial H_2O_2 [157]. Liu and colleagues showed that both p66^{Shc} mRNA and protein products are expressed in a circadian manner, and that knockout of p66^{Shc} compromises circadian H_2O_2 oscillations in hepatocytes and SCN neurons [153]. The significance of a functional ETC in the generation of H_2O_2 is also underscored by the fact that loss of a subunit of yeast cytochrome c oxidase (complex IV) of the ETC, *COX6*, decreases the starting OxD of roGFP2 and eliminates the H_2O_2 dynamics observed in 2% glucose batch culture of wildtype BY4742 cells (Fig 3.4).

Conversely, culture aeration and glucose supply remained constant during the YMC, although dissolved oxygen levels changed. It is plausible that H_2O_2 is constantly produced during the YMC. It is also conceivable that the oscillations in H_2O_2 during the YMC is underscored by H_2O_2 consumption or removal, rather than production. One major enzyme involved in H_2O_2 removal or transduction in budding yeast is the peroxiredoxin Tsa1. Strikingly, I observed that the levels of endogenous Tsa1 protein peaked during phases of decreasing H_2O_2 levels (Fig. 3.5A). In line with this observation, Tu *et al.* reported changes in *TSA1* transcript levels during the YMC, which levels peaked during the ‘reductive charging’ phase [47] (Fig. 3.5B). The ‘reductive charging’ phase described by Tu *et al.* is the phase of decreasing H_2O_2 levels in this study. Furthermore, the study by Tu *et al.* also showed that the transcription factor Yap1 translocated into and accumulated in the nucleus during the ‘oxidative’ phase of the YMC [47]. Nuclear translocation of Yap1 leads to elevated expression of genes encoding most antioxidants and components of the cellular thiol-reducing pathways [158, 159]. These elevated antioxidant defense mechanisms during the so-called ‘oxidative’ phase, I propose, was responsible for the decreased H_2O_2 and roGFP2 oxidation levels I observed in this study during this phase of the YMC. Therefore, in contrast to their characterization, I propose a YMC consisting of two phases – oxidative and reductive – based on the mode of H_2O_2 changes (Fig. 3.1).

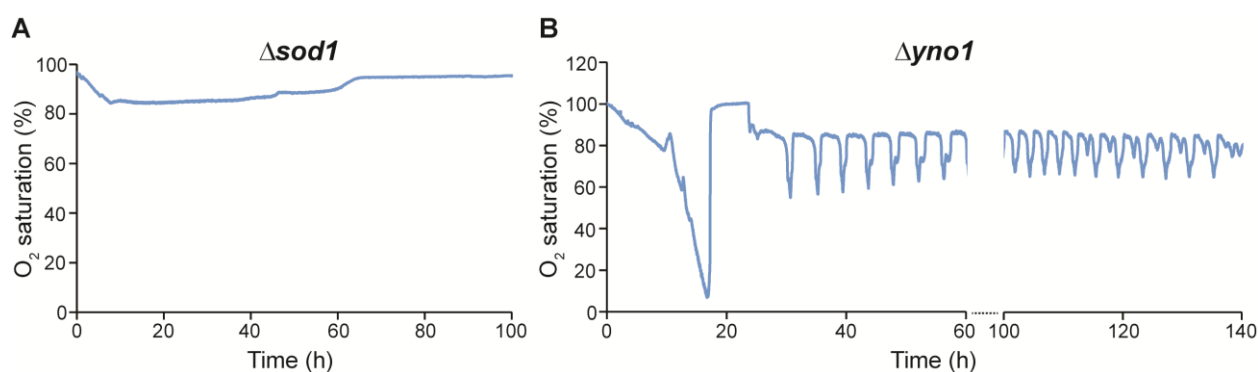


Figure 3.3: Interference with H_2O_2 generating pathways affect the YMC. (A) Representative oxygen trace showing that $\Delta sod1$ cells only grow in a batch phase and could not effectively consume dissolved oxygen to generate synchronized metabolic cycles. (B) Representative oxygen trace showing that loss of *YNO1* perturbs the YMC.

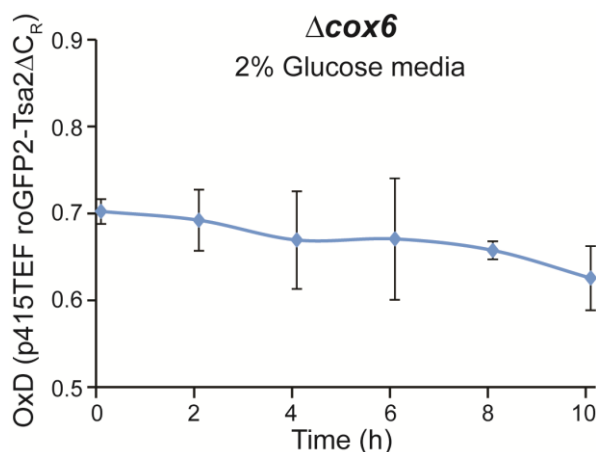


Figure 3.4: Glucose-stimulated H_2O_2 dynamics is eliminated in $\Delta cox6$ cells. BY4742 $\Delta cox6$ cells expressing the roGFP2-Tsa2 ΔC_R plasmid were cultured in glucose media at $OD_{600} = 0.25$ and trapped with NEM to monitor steady-state roGFP2 oxidation over the stated duration. Data represent at least three independent replicates and error bars represent standard deviation.

The YMC has historically been studied in low-glucose chemostats. Burnett *et al.* propose that this is so because the budding yeast population self-synchronizes in low-glucose conditions [115]. I propose that such self-synchronization in low-glucose chemostats may be achieved in part via glucose stimulated H₂O₂ generation. On the other hand, it has also been proven that yeast metabolic oscillations can occur on the population level, outside chemostat conditions and in non-glucose media. For instance, metabolic oscillations occurred in a batch culture upon diauxic shift to pure respiration on ethanol from aerobic fermentation [160]. Moreover, batch-grown and phosphate-starved yeast cells with ethanol as a sole carbon source exhibited metabolic oscillations [161].

The causative role for H₂O₂ during the YMC was reinforced by exogenous addition of non-physiological peroxide levels that was enough to trigger phase shifting of the YMC from LOC to HOC (Fig 2.9). Interestingly, this observation was independent of the phase of peroxide addition (Fig 2.10). More importantly, hyperoxidation and inactivation of endogenous typical 2-Cys peroxiredoxins as well as the 2-Cys peroxiredoxin of the H₂O₂ biosensor accompanied the switch from LOC to HOC, upon high peroxide (Fig 2.11). This peroxide-induced peroxiredoxin hyperoxidation was also reflected in the reduction of the redox state of the peroxiredoxin target reporter, roGFP2, and in extension, endogenous peroxiredoxin protein target(s), although I did not provide direct evidence for the latter.

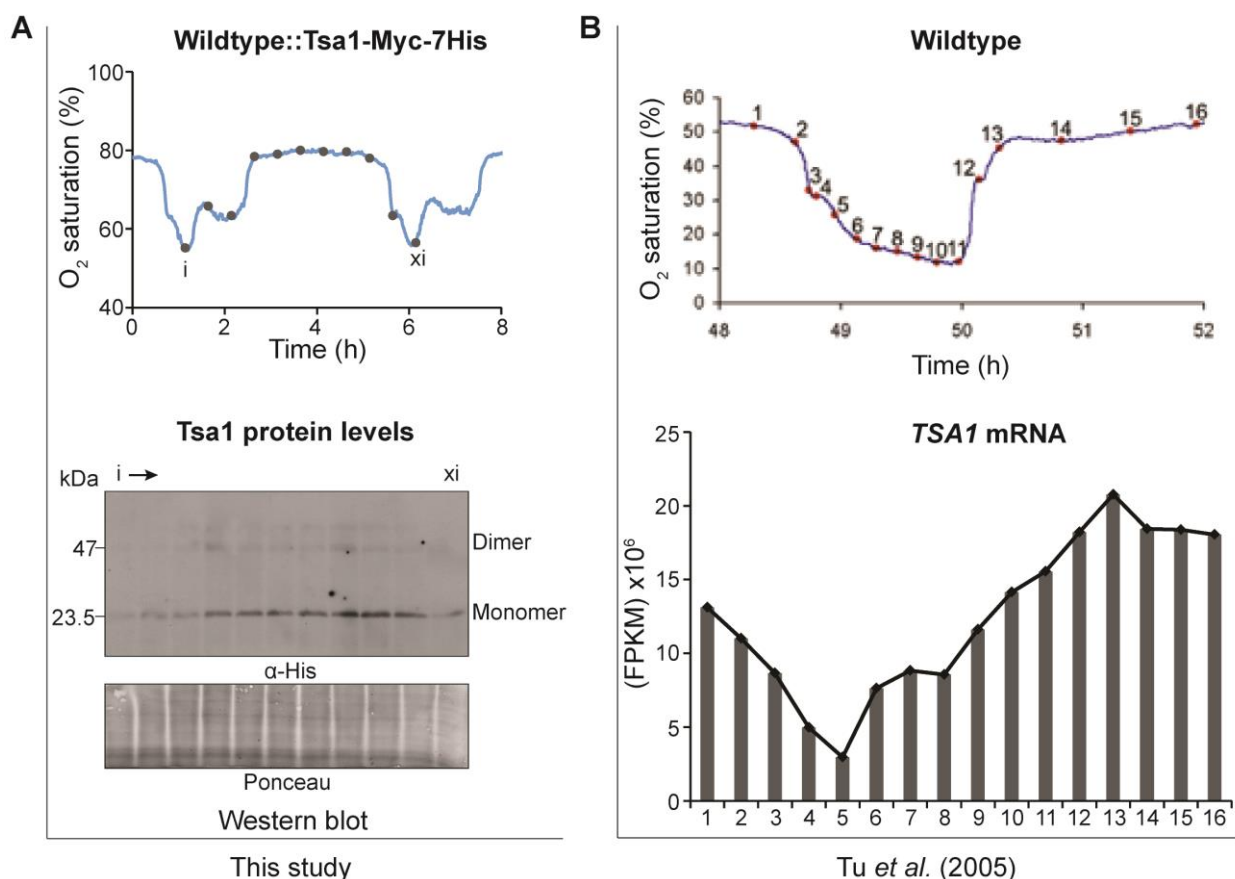


Figure 3.5: Tsa1 protein and transcript levels peak during the LOC phase, before entry to HOC. (A) Representative oxygen trace (top) and Western blot (bottom) indicating points of sampling and Tsa1 protein levels, respectively, as observed in this study. (B) Representative oxygen trace (top) and TSA1 mRNA levels (bottom) as reported by Tu *et al.* [47].

Based on the above observations, I concluded that the YMC is regulated by thiol redox switch(es) that are controlled by peroxiredoxins. In other words, cyclical H_2O_2 changes are transduced by peroxiredoxins to regulate the redox state of protein target(s) that control oscillatory metabolism. I opined that if this hypothesis held true, then two predictions could easily be tested: Firstly, the addition of thiol oxidants and reductants should predictably perturb the YMC. Meaning, a thiol oxidant should directly oxidize protein thiols and thus prolong the LOC phase, whilst, a thiol reductant should directly reduce protein thiols and trigger HOC. This prediction works independent of peroxiredoxin activity. Secondly, peroxiredoxin deletion should strongly affect the YMC.

The first prediction was tested by separate additions of 0.5, 1 and 2 mM diamide to independent wildtype YMC-synchronized cultures at the start of LOC, which extended the duration of LOC in a concentration dependent manner. Strikingly, addition of 2 mM diamide just before the switch from LOC to HOC extended the duration of LOC and profoundly delayed switch to HOC (Fig 2.4). Furthermore, DTT at 1, 2 and 5 mM shortened time in LOC and mediated rapid switch to HOC in a concentration dependent manner when added at the start of LOC in independent wildtype YMC-synchronized cultures. Importantly, 5 mM DTT profoundly extended the duration of HOC beyond 10 hours – the time needed to complete two metabolic cycles (Fig 2.3). Hence, by applying thiol redox modifiers, the YMC could be switched between LOC and HOC metabolic states.

In conclusion, I could demonstrate that redox processes that include thiol disulfide exchanges or switches regulate the yeast metabolic clock (Fig. 3.6). Identification of the specific thiol switch(es) involved could be an interesting subject for future investigations.

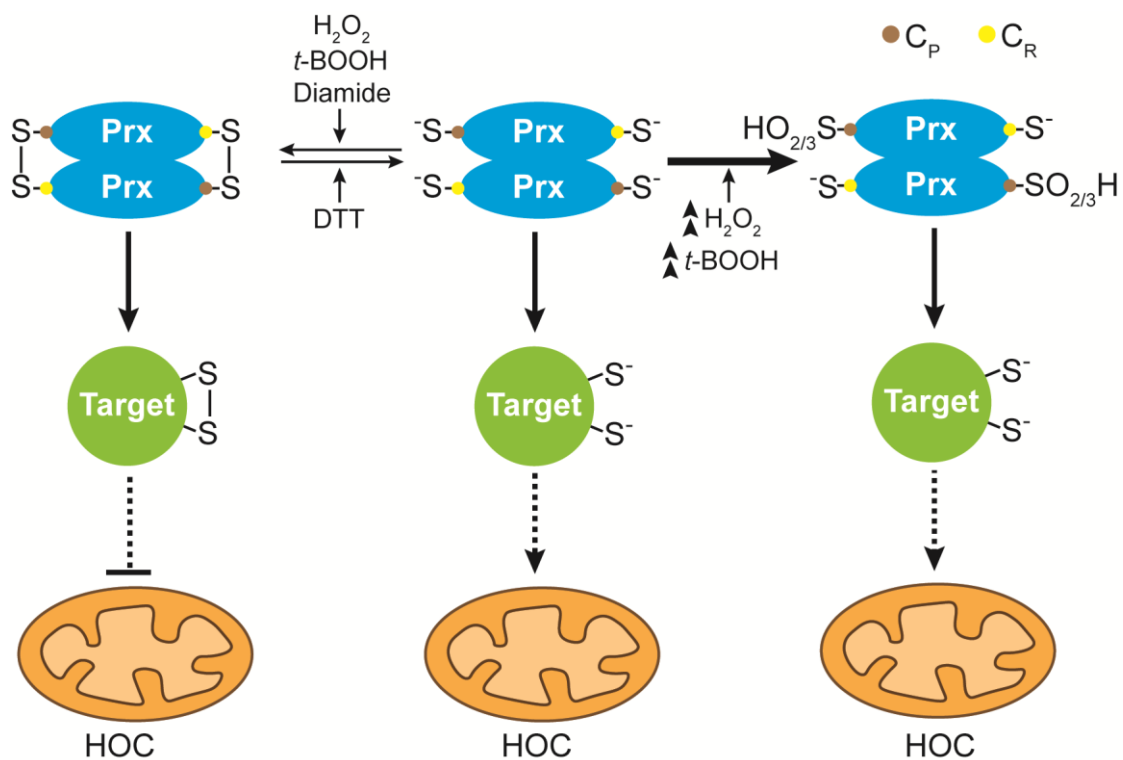


Figure 3.6: Peroxiredoxin-mediated thiol-disulfide exchanges regulate the yeast metabolic clock. Scheme describing the effect of chemical redox perturbations on the yeast metabolic cycle.

3.2 Peroxiredoxins and thioredoxins are crucial for stable metabolic clock function

The second prediction stated above was tested by deleting one or more peroxiredoxins from the yeast genome by homologous recombination of an antibiotic resistance cassette. By this method, I successfully generated cells lacking the mitochondrial matrix 1-Cys peroxiredoxin – i.e. $\Delta prx1$, cells lacking the cytosolic atypical 2-Cys peroxiredoxin – i.e. $\Delta ahp1$, and cells lacking both cytosolic typical 2-Cys peroxiredoxins – i.e. $\Delta tsa1\Delta tsa2$. In comparison to wildtype YMC-synchronized cultures, cells lacking the cytosolic 2-Cys peroxiredoxins displayed YMCs with shortened periods and diminished shapes, whilst $\Delta prx1$ YMC remained virtually unaffected (Fig 2.15). In other words, loss of one or more cytosolic 2-Cys peroxiredoxin(s) profoundly affects the stability of the yeast metabolic clock.

The importance of peroxiredoxins for yeast metabolic clock function could further be deduced from the observation that combined loss of *TSA1* and *AHP1* leads to non-viability of the CEN.PK strain (Fig. 2.19). In fact, conditional depletion of Ahp1 in a $\Delta tsa1\Delta tsa2$ strain further affects YMC stability (Fig. 2.21). Peroxiredoxin-mediated YMC regulation was mirrored in the behavior of the YMC upon temporary inactivation of peroxiredoxins with excess peroxide. Of note, is the correlation between peroxiredoxin hyperoxidation and immediate switch from LOC to HOC upon 1 mM *t*-BOOH or 5 mM H_2O_2 (Fig. 2.9 and Fig. 2.11). Meanwhile, this peroxide-induced HOC could also occur in a $\Delta prx1$ or $\Delta tsa1\Delta tsa2$ strain, although at different peroxide concentrations (Fig. 2.16 and Fig. 2.17). Thus, it is possible that multiple peroxiredoxins were hyperoxidized simultaneously during the peroxide-induced HOC in wildtype cells. To buttress this point, I have shown that the endogenous cytosolic typical 2-Cys peroxiredoxins, Tsa1 and Tsa2, were hyperoxidized via Western blots (Fig. 2.11D). Additionally, the hyperoxidation of the Tsa2 ΔC_R and Ahp1 moieties of the biosensors upon excess peroxide, could be demonstrated (Fig. 2.11C(ii) and Fig. 2.18). Therefore, it was not surprising that similar peroxide-induced HOC could be achieved in $\Delta prx1$ and $\Delta tsa1\Delta tsa2$ cells. It would be interesting to test in future studies, the contribution of the nuclear peroxiredoxin, Dot5, to YMC regulation. Additionally, raising antibodies against the hyperoxidized forms of other peroxiredoxins could augment our understanding of the contributions of each enzyme to the observed phenomenon. Taken together, these results confirm the functional redundancy between the different peroxiredoxins with respect to YMC control, and support the conclusion that peroxiredoxins and peroxiredoxin redox relays are crucial for YMC regulation.

I have proposed that peroxiredoxins control thiol switch(es) that mediate YMC regulation. By using roGFP2 as a substrate, I have demonstrated that: (1) roGFP2 reduction in a ‘normal’ metabolic cycle correlates with switch to HOC, and (2) hyperoxidation of peroxiredoxins leads to reduced roGFP2, which correlates with switch from LOC to HOC. Next, I asked if indeed peroxiredoxin redox relays are crucial for YMC regulation, what might the target proteins of these relays be? Although numerous targets of peroxiredoxin relays have been identified in other organisms, only a few have so far been described in yeast. These include the transcription factor Yap1, which is oxidized by the glutathione peroxidase homolog

Orp1 [74], and the transcription factor Cad1, which was suggested to be oxidized by Ahp1 [162]. Indirect evidence suggests that there are many more unidentified targets of peroxiredoxin redox relays. For instance, a study from the lab of Vadim Gladyshev showed that about 50% of all yeast transcripts respond to H₂O₂ in a manner that is almost completely dependent on the presence of peroxiredoxins [129]. Interestingly, it was recently reported that Tsa1 can regulate redox modifications on the yeast protein kinase A (PKA) subunit, Tpk1 [163]. The general stress responsive transcription factor, Msn2, is a target of PKA, and Msn2 deletion has been shown to strongly disrupt the YMC, particularly the switching from LOC to HOC [164]. Other targets of PKA include the general heat shock response transcription factor, Hsf1, and metabolic enzymes, such as Pfk2, encoding phosphofructokinase. Thus, it is possible that peroxiredoxins, via redox regulation of PKA, enable cells to regulate a wide range of transcriptional and metabolic processes in response to changing H₂O₂ levels. Elucidating the mechanistic underpinnings and their relevance, for example, in coupling metabolic changes with the cell cycle, would be an interesting subject of future investigations.

Active peroxiredoxin catalysis endogenously require thioredoxins – enzymes that facilitate the reduction of proteins by catalyzing cysteine thiol-disulfide exchange reactions [165]. Thus, in place of the artificial roGFP2, thioredoxins represent endogenous substrates of peroxiredoxins. Although I did not directly identify in this study, the specific thiol switch(es) involved in regulating the yeast metabolic clock, I opined that thioredoxins could be of interest if indeed peroxiredoxin relay(s) was/were crucial for YMC regulation. Mechanistically, thioredoxins contain two conserved cysteines that either exist in a reduced (-SH) or an oxidized (S-S) form. They donate electrons from their active site dithiol to protein disulfide bonds, which are then reduced to dithiols. The resulting oxidized thioredoxin disulfide is reduced by thioredoxin reductase with electrons donated by NADPH [165]. I imagined that this catalytic mechanism could be important for regenerating oxidized peroxiredoxins to mediate the oscillatory H₂O₂ signaling phenomenon observed during the YMC. Consequently, loss of either cytosolic thioredoxins, ie. *TRX1* or *TRX2* should have an effect on the YMC. Intuitively, a $\Delta trx2$ strain exhibited cycles similar to that of *Atsa1Atsa2* and *Aahp1* strains, suggesting that loss of *TRX2* affects YMC regulation (Fig. 2.22A). More importantly, a *Atrx1Atrx2* strain could not generate metabolic cycles (Fig. 2.24).

Furthermore, loss of *TRX2* affected hyperoxidation-based LOC-to-HOC switching in a significant way. I noted that unlike wildtype YMC-synchronized cultures, 0.5 mM *t*-BOOH was enough to induce rapid LOC-to-HOC transition in $\Delta trx2$ cultures. Strikingly, 1 mM *t*-BOOH induced a short LOC-to-HOC and immediately returned the YMC to a prolonged LOC phase spanning more than 6 hours (Fig. 2.22B). This observation is explainable as follows: unlike wildtype cells, loss of *TRX2* diminishes the cellular ‘reductive capacity’; hence, 0.5 mM *t*-BOOH was enough to achieve peroxiredoxin hyperoxidation. This concentration of *t*-BOOH however does not overwhelm Trx1-mediated reduction of protein thiols, hence HOC induction occurred ‘normally’ and the YMC was returned to ‘normal’ wildtype behavior. On the other hand, 1 mM *t*-BOOH overpowers rapid Trx1-mediated thiol reductions, as such, LOC-to-HOC transition is short-lived and cells are returned to a prolonged LOC phase, possibly due to direct oxidation of

peroxiredoxin-regulated thiol switch(es) by *t*-BOOH (Fig. 3.7), in ways similar to diamide. Indeed, unlike H₂O₂, which essentially depends on peroxiredoxins to mediate protein thiol oxidations [72, 166]; *t*-BOOH can directly react with protein thiols with or without peroxiredoxins. This was revealed in the response of roGFP2 to further addition of either 1 mM H₂O₂ or *t*-BOOH upon hyperoxidation of the Tsa2ΔC_R moiety of the biosensor (Fig. 2.23).

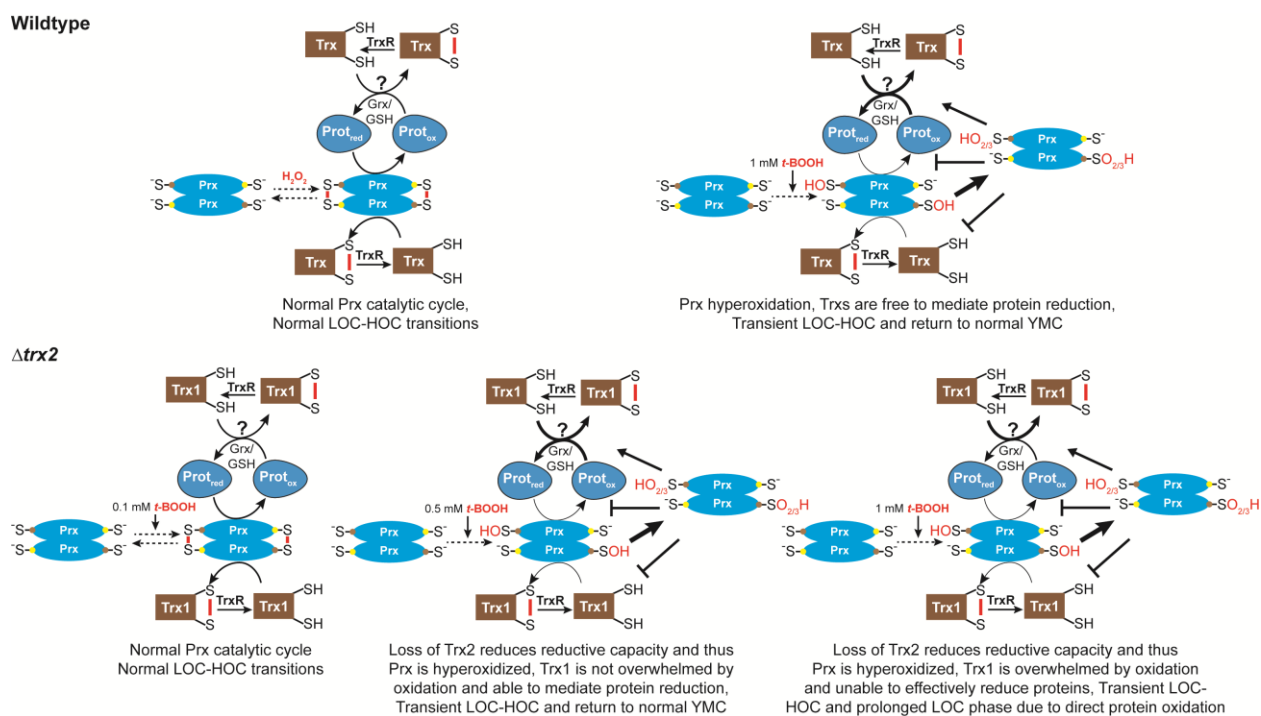


Figure 3.7: Scheme explaining YMC behavior in wildtype and Δ *trx2* cells upon peroxide. Loss of *TRX2* decreases cellular reductive capacity and facilitates a prolonged LOC phase upon peroxiredoxin hyperoxidation due to direct target protein oxidation by excess *t*-BOOH.

A conceivable role for thioredoxins in circadian clock function was occasioned by the observation that mammalian AMP-activated protein kinase (AMPK), the master regulator of metabolism, is a direct target of Trx1 – i.e. Trx1 regulates the redox state and activation of AMPK during energy metabolism [167]. AMPK has been shown to regulate the circadian metabolic clock in mammals via cryptochrome (Cry) phosphorylation and degradation [168]. Snf1 is the yeast homolog of mammalian AMPK. In budding yeast, Snf1 is important for increased transcription of genes required for metabolic adaptation in low-glucose or non-glucose media [169]. Snf1 activation requires phosphorylation by Sak1/Elm1/Tos3 kinases, of a threonine residue (Thr210) in the activation loop of the kinase domain [170, 171]. Inside the kinase domain are four cysteine residues; Cys168, Cys212, Cys238 and Cys247, two of which directly flank Thr210 (Fig. 3.8A). Shao *et al.* showed that AMPK forms oxidative aggregates in response to energy stress, via intermolecular disulfide bonds at the conserved Cys130 (Cys168 in *S. cerevisiae*) and Cys174 (Cys212 in *S. cerevisiae*) residues, which inhibit activating phosphorylation of AMPK. Consequently, AMPK activation by phosphorylation is restored by Trx1-mediated reduction of these cysteine residues [167]. Crystal structure analysis shows that formation of Snf1 dimer involves segments around Thr210 and

Cys212, predominantly via hydrophobic interactions [172]. Based on their results, Shao *et al.* suggested that disulfide bond formation might be involved in both Snf1 and AMPK dimerization [167]. Upon dimerization, the activation loop and substrate-binding site of Snf1 are buried inside the dimer, resulting in an inactive protein [172]. I imagined that such a disulfide bond could modulate Snf1 function as shown (Fig. 3.8B).

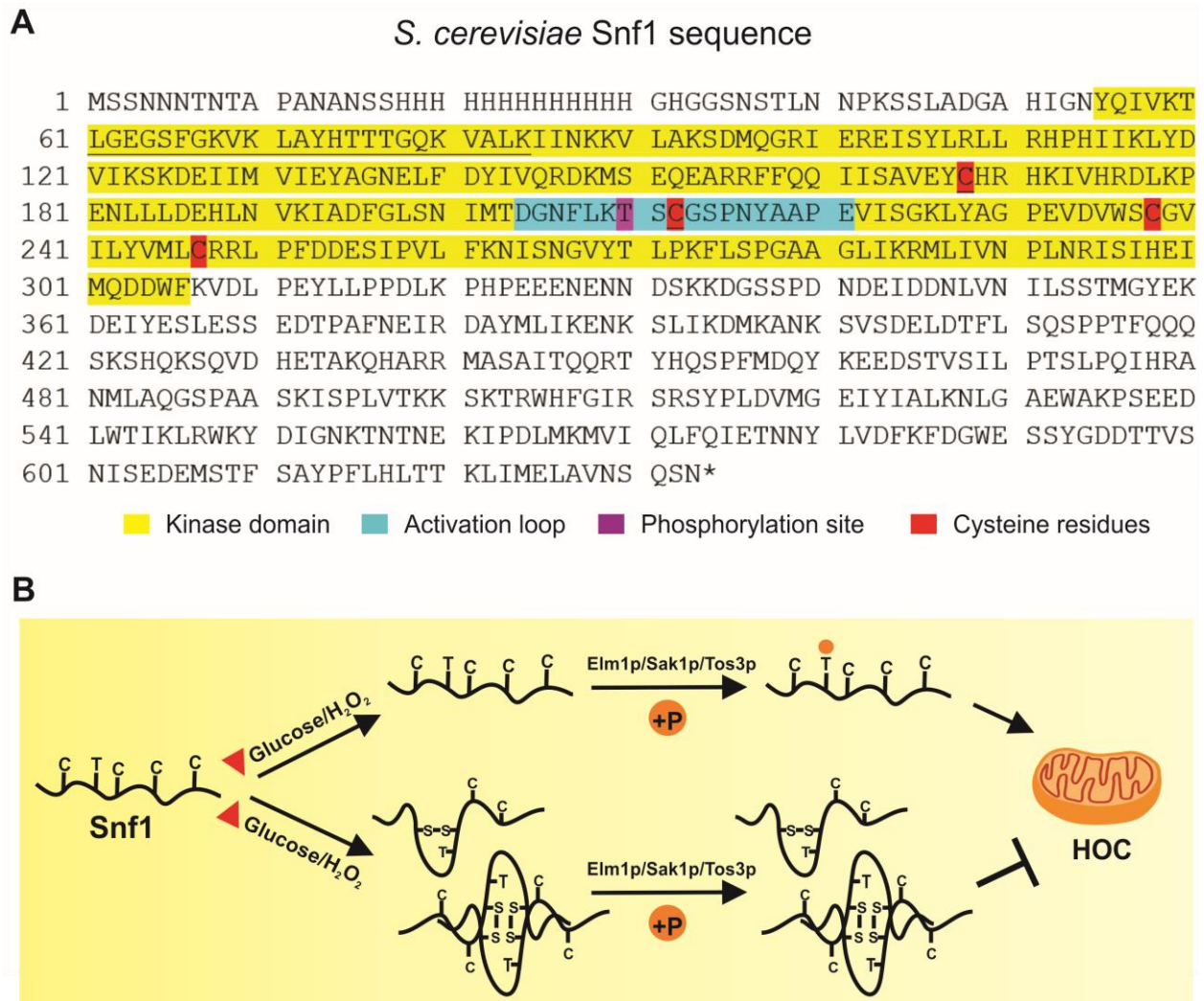


Figure 3.8: Snf1 could potentially be redox regulated. (A) Annotated sequence of Snf1. Sequence was obtained from the Yeast Genome Database. (B) Inter- or intra-molecular disulfide bond formation at Cys168 and/or Cys212 under high physiological H_2O_2 or high glucose could inhibit Snf1 activation by phosphorylation. Consequently, expression of genes required for respiration and HOC could be suppressed.

It is plausible that Snf1 function may be required for metabolic cycling in low-glucose chemostats, since a $\Delta snf1$ strain could not grow in batch culture to establish the YMC (Fig. 3.9). Such a function could probably be mediated via thiol redox modifications at Cys168 and/or Cys212, in response to changing metabolic states, which ultimately affect activating phosphorylation at Thr210. During the YMC, these Snf1 thiol disulfide modifications might occur in a cyclical manner in response to oscillations in H_2O_2 , and possibly be regulated by the peroxiredoxin and thioredoxin systems. Consequently, shuttling of Snf1 in and out of the nucleus would influence changes in expression of genes that are needed for respiration, as well

as to mediate LOC and HOC metabolic states of the YMC (Fig 3.10). It would be interesting to pursue this hypothesis in the future and test the impact of Snf1 cysteine mutants on YMC oscillation.

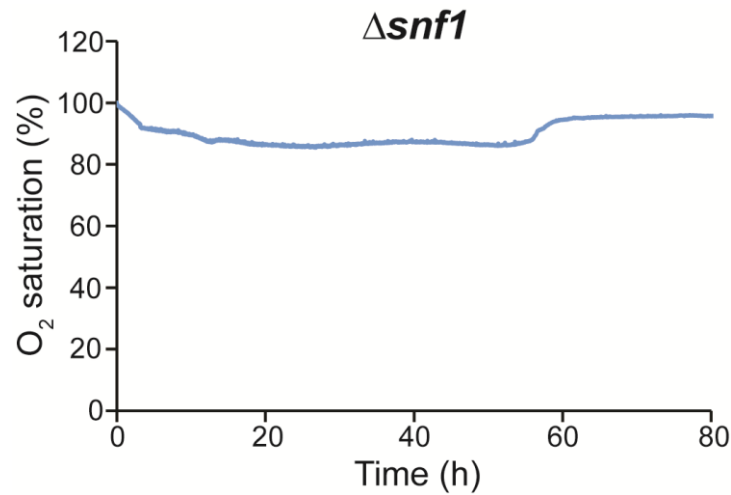


Figure 3.9: Loss of *SNF1* affects generation of the YMC. Representative oxygen trace showing that $\Delta snf1$ cells only grow in a batch phase and could not effectively consume dissolved oxygen to generate synchronized metabolic cycles.

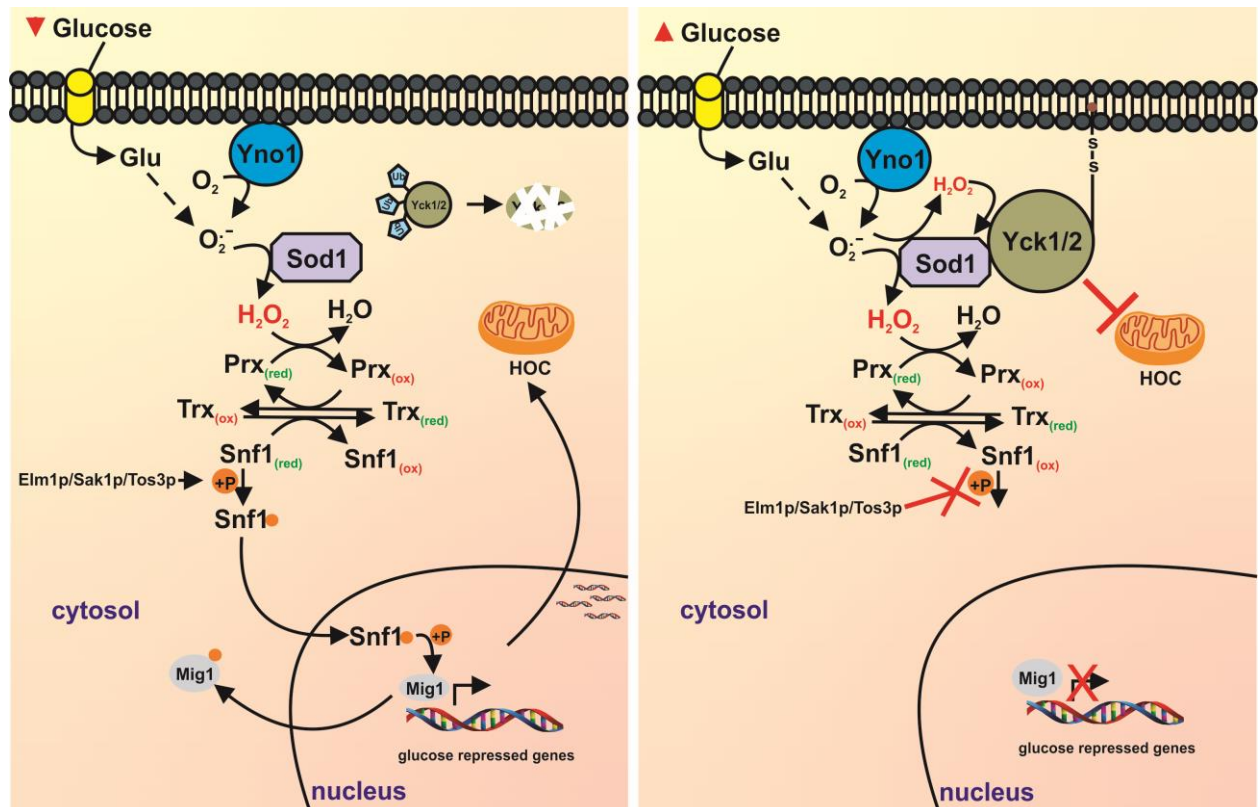


Figure 3.10: Redox regulation of Snf1 could be essential for YMC oscillation. Scheme illustrating a possible mode of Snf1 regulation in low-glucose or low signaling H_2O_2 conditions (left), as well as in high-glucose or high signaling H_2O_2 conditions (right). Under low-glucose, Snf1 stays reduced due to low signaling levels of H_2O_2 . Consequently, Snf1 could be activated by phosphorylation to translocate into the nucleus to induce expression of genes required for respiration and HOC. Under high-glucose, Snf1 becomes oxidized due to high signaling levels of H_2O_2 . Consequently, phosphorylation of Snf1 is inhibited and Snf1 stays in the cytoplasm. Sod1-mediated stabilization of Yck1p1/Yck2p under high signaling levels of H_2O_2 leads to repression of respiration [173].

3.3 The cellular redox/metabolic state regulates the cell division cycle

Herein, I have shown that during the YMC, levels of H_2O_2 begin to rise at the height of oxygen consumption (i.e. trough of the YMC) and peak just before the entry into LOC. During LOC, H_2O_2 levels begin to decrease and is lowest at LOC-to-HOC transition. Simultaneously, accumulation of 2N DNA content was observed to begin in correlation with rising H_2O_2 levels and peaked just before the entry into LOC. Thereafter, the proportion of cells with 2N DNA content decreased and was lowest during LOC-to-HOC transition. Furthermore, cell budding was highest before entry to LOC and cell division was completed before entry into HOC (Fig. 2.25 and Fig. 3.1). These observations suggest that changes in H_2O_2 signals during oscillatory metabolism is required to synchronously drive cells through the cell division cycle. I therefore hypothesized that initiation of DNA synthesis might require input signals from H_2O_2 . For a successful completion of cell division however, signaling levels of H_2O_2 must decrease.

In line with this reasoning, it was suggested that oscillations in the intracellular redox state during cell cycle progression represents a fundamental mechanism that may link oxidative metabolism to cell cycle regulation [119]. The idea that redox changes may regulate the cell division cycle is supported by evidence from Tu *et al.* who demonstrated that several DNA replication and cell cycle regulatory genes are expressed during a reductive non-respiratory phase of the YMC (i.e. LOC) whilst cell cycle initiation occurs very late during a respiratory oxidative phase (i.e. peak of HOC or trough of the YMC) [47]. Although it is not entirely clear which redox half-reactions control either cell cycle entry or exit, it has been suggested that transient increase in oxidation early in G_1 is necessary for G_1 -to-S phase transition and thus inhibiting this transient increase in oxidation causes cell cycle arrests in the G_1 phase [122]. Similarly, GSH levels were reported to be significantly higher in the G_2 and M phases of the cell cycle compared to G_1 , suggesting that cells in the G_2 and M phases are at a more reduced redox state compared to G_1 phase cells [125]

The plausibility of periodic oscillations in the intracellular redox state playing a crucial role in regulating cell cycle progression is not far-fetched since several cell cycle regulatory proteins harbor redox-sensitive motifs [125]. These proteins include but not limited to cyclins, Cdks and Cdk inhibitors. For instance, the activity of the 20S proteasome in *S. cerevisiae* is inhibited by S-glutathionylation following H_2O_2 treatment, meanwhile, proteasomal degradation of cyclins is central to cell cycle regulation [174]. In line with this, it has been shown in Her14 fibroblasts that exposure to H_2O_2 leads to accumulation of cyclin D1 at G_1 phase, due to the inhibition of cyclin D1 protein degradation [175]. Moreover, direct redox modification of cyclin D1 itself has been proposed as an alternative mechanism for its regulation. Cyclin D1 contains two phosphorylation sites – Thr286 and Thr288 – that can be phosphorylated by glycogen synthase kinase (GSK-3 β) and Mirk/dyrk kinase, for proteasomal degradation [176, 177]. It is suggested that redox thiol modification of cyclin D1 at Cys285 could induce a conformational change that might influence degradation phosphorylation at Thr286 and/or Thr288 [119]. Furthermore, Cdc25, an activator of cyclin–Cdk complex kinase activity could be inhibited either by the thiol-alkylating agent NEM or via

mutation of a single conserved cysteine residue [178, 179]. In addition, H₂O₂ induced degradation of Cdc25c proteins via formation of intramolecular disulfide bond at Cys377 and Cys330, whilst double mutants of Cys377 and Cys330 were resistant to H₂O₂-induced degradation [180].

Recent observations suggest that metabolic cycles are crucial for regulating cell cycle entry and exit [114, 115]. I imagined that the redox state *per se* might not only be necessary to modulate cell cycle regulatory proteins and thereby controlling the cell cycle, rather, the redox state may influence the metabolic state that eventually determines whether cells are ready to initiate the cell cycle or not. In other words, cell cycle initiation is dictated by the metabolic state, which in itself is controlled by the cellular redox environment (Fig 3.11). I have shown that HOC is a trigger for DNA synthesis, and LOC-to-HOC transition is characterized by low H₂O₂ (or oxidation) levels under physiological conditions. Intriguingly, inducing a reducing environment with DTT is enough to artificially maintain a prolonged HOC phase and cause multiple rounds of DNA synthesis and cell cycle initiation even though a previous cell division cycle remains uncompleted (Fig. 2.27). Conversely, a LOC phase was critical for cell cycle completion and exit, and entry into LOC was triggered by high H₂O₂ (or oxidation) levels under physiological conditions. Accordingly, temporarily prolonging the LOC phase and delaying LOC-to-HOC transition with diamide delays initiation of DNA synthesis and start of a new cell cycle (Fig. 2.28).

It has been shown that more than 50% of yeast metabolome changes during cell cycle progression downstream of *Start*, causally linking global metabolism changes to cell division [181]. The mechanistic details on how metabolic changes might regulate cell division or *vice versa* remains to be fully explored. Cell division in itself is suggested to involve several coupled, but nonetheless independent oscillators, in addition to the classic and well understood cyclin-Cdk system. Recent observations suggest that Cdk1 directly modulates metabolism of storage carbohydrates via activation of trehalase, Nth1, and glycogen phosphorylase, Gph1, thus coordinating carbohydrate metabolism and the cell cycle in yeast [181, 182]. I have proposed earlier that peroxiredoxins might regulate PKA to trigger a wide range of transcriptional and metabolic processes in response to changing H₂O₂ levels. Interestingly, it has been shown that Gph1 and Nth1 are not only targets of Cdk1, but also of PKA [182, 183]. Moreover, some studies have identified Bcy1, the regulatory subunit of PKA, as a Cdk substrate [184, 185]. More importantly, PKA has been shown to regulate the activity of Cln-Cdc28 at G₁ and multiple G₁ cyclins (i.e. Cln1, Cln2, and Cln3) harbor consensus PKA phosphorylation sites [182, 186]. It is plausible that Cdk and PKA not only interact with similar substrates, but also regulate each other. This believe stems from the observation that PKA and Cdk activity peak at the same time during cell cycle *Start* [187]. Thus, peroxiredoxins, PKA, Cdk and their substrates might form a regulatory circuit that mediate the coordination of metabolism with cell division in the yeast metabolic cycle.

3.4 Peroxiredoxins couple changes in cell metabolism to cell division

My own observations, as well as previous reports show that metabolic clocks are coupled to cellular programs such as transcription/translation and cell division [47, 49, 56]. Intriguingly, I find that temporary inactivation or loss of the cytosolic typical 2-Cys peroxiredoxins, Tsa1 and Tsa2, do not only affect the yeast metabolic cycle, but also profoundly upsets coordination of the metabolic cycle with the cell division cycle (Fig. 2.26). Consequently, the mechanism by which the metabolic state controls cell division might be governed by peroxiredoxins.

I propose that under physiological conditions in the yeast metabolic cycle, peroxiredoxins sense oscillations in H₂O₂ levels to regulate cellular metabolism [188] and possibly the redox state of cell cycle modulators. During periods of low signaling H₂O₂ levels, peroxiredoxins become less oxidized and their target(s) stay(s) reduced. Reduced peroxiredoxin target(s) induce(s) a HOC state, which is a pre-requisite for DNA synthesis and cell cycle entry. Upon high signaling H₂O₂ levels, peroxiredoxins become oxidized and transfer oxidizing equivalents to their target(s). Oxidized peroxiredoxin target(s) induce(s) a LOC state, which is a pre-requisite for cell division and cell cycle exit. By artificially modulating the redox state of peroxiredoxin target(s) directly or indirectly either via peroxiredoxin hyperoxidation with excess *t*-BOOH, oxidation with diamide or reduction with DTT, a HOC or LOC metabolic state can be achieved to trigger entry into or exit from the cell division cycle (Fig. 3.11). Importantly, a prolonged LOC phase prolongs duration of cell cycle exit and inhibits entry, whilst a prolonged HOC phase favors DNA replication and cell cycle entry and inhibits cell cycle exit.

The involvement of peroxiredoxins in regulation of cell cycle processes may represent a novel and exciting area of scientific research. Recent observations suggest this ‘new’ role for peroxiredoxins may either be achieved indirectly via endogenous substrates such as thioredoxins or through direct redox modulation of cell cycle regulators. For instance, the rate-limiting enzyme of deoxyribonucleotide triphosphate (dNTP) biogenesis – ribonucleotide reductase (RNR) – relies on electrons from thioredoxins or glutaredoxins for recycling during DNA replication and repair in the cell cycle [189, 190]. Boronat and colleagues demonstrated that the cytosolic thioredoxin, Trx1, is the primary electron donor for the RNR large subunit, Cdc22, in *S. pombe*. Genetic depletion of *TRX1* and *TRX3* leads to severe replication stress that is partially overcome by activation of the Rad3-Cds1 DNA replication checkpoint to induce transcription of Cdc22. However, loss of the peroxiredoxin Tpx1, a major substrate of Trx1, in a *Δtrr1Δgrx1* strain favored the reduction and functionality of RNR to allow DNA synthesis, cell cycle progression and cell growth [191].

Furthermore, it has been proposed that the replication of DNA requires coordination between replication fork progression and metabolic pathways involved in dNTP biogenesis. In the absence of such coordination or during adverse metabolic conditions such as elevated ROS production, replication fork integrity might be compromised, thereby undermining the fidelity of genome duplication [49, 192].

Perturbation of RNR leads to elevated ROS levels and an imbalance of dNTPs in human cells, which can affect genome integrity by inducing replication fork stalling, DNA breaks and impairment of polymerase proofreading activity [193]. Somyajit *et al.* proposed a mechanism by which redox signaling couples fluctuations of dNTP biogenesis with replisome activity to reduce stress during genome duplication. This mechanism is mediated by the interaction between a component of the replisome, TIMELESS and peroxiredoxin 2 (PRDX2). In low ROS levels, PRDX2 binds TIMELESS to accelerate the replication fork and enable timely genome duplication. In elevated ROS levels, PRDX2 oxidization disrupts this binding and compels the displacement of TIMELESS from the replisome leading to replication fork slowdown [193, 194].

Cell cycle progression through mitosis depends upon the activation of the Cdk1-cyclin B complex in early mitosis [195]. This activation occurs first at the centrosome during prophase and amplified via multiple feedback loops involving kinases such as cyclin B, Cdc25 and Aurora A [196-198]. The activity of these kinases are in turn regulated by anaphase-promoting complex/cyclosome (APC/C)-mediated ubiquitination and subsequent degradation in the proteasome. Meanwhile, APC/C activation is dependent upon Cdh1, whose phosphorylation by Cdk1 inhibits this interaction [199, 200]. Cdk-opposing phosphatases such as Cdc14B, PP1 and PP2A restore Cdh1 activation via de-phosphorylation [201-203].

It is suggested that the intracellular concentration of H₂O₂, especially at the centrosome, increases as the cell cycle progresses. Recent reports show that this local accumulation of H₂O₂ results from Cdk1-mediated inhibition of PrxI oxidase activity via phosphorylation [204, 205]. At the centrosome, H₂O₂ is believed to oxidatively inhibit Cdk1-opposing phosphatases such as Cdc14B at Cys228 and Cys314, leading to the accumulation of phosphorylated Cdh1 [205]. Accordingly, by Cdk1-mediated phosphorylation and inhibition of PrxI at the centrosome, H₂O₂ locally accumulates to control the activity of Cdk1 regulators to promote mitotic entry. My observation that H₂O₂ levels peak just before entry into LOC, a phase characterized by cell division, underscores the above reports. It will be interesting to elucidate the exact mechanisms involved during the YMC.

My observations also show that the YMC persisted, albeit in a perturbed manner, upon deletion of the genes encoding the two cytosolic typical 2-Cys peroxiredoxins, Tsa1 and Tsa2. The mutant cells divide completely asynchronously from the metabolic cycles and from each other. Although the consequence of the loss of YMC-CDC coupling in 2-Cys peroxiredoxin-deleted cells remains to be fully elucidated, this loss of synchrony could explain why for example, thiol peroxidase-deficient (e.g. *Δtsa1*) cells exhibit decreased growth fitness and are prone to spontaneous genetic mutations and gross chromosomal rearrangements, compared to their wildtype counterparts [206-208]. More so, deletion of peroxiredoxins is associated with an increased incidence of cancer in higher organisms [207, 209]. These phenotypes are typically attributed to supposedly higher levels of ROS in peroxiredoxin deficient cells. However, an attractive alternative hypothesis arising from this study is that in the absence of peroxiredoxins, the uncoupling of cell division from metabolism allows cells to divide at 'inappropriate' times, with respect for example to metabolite availability and prevailing metabolic conditions.

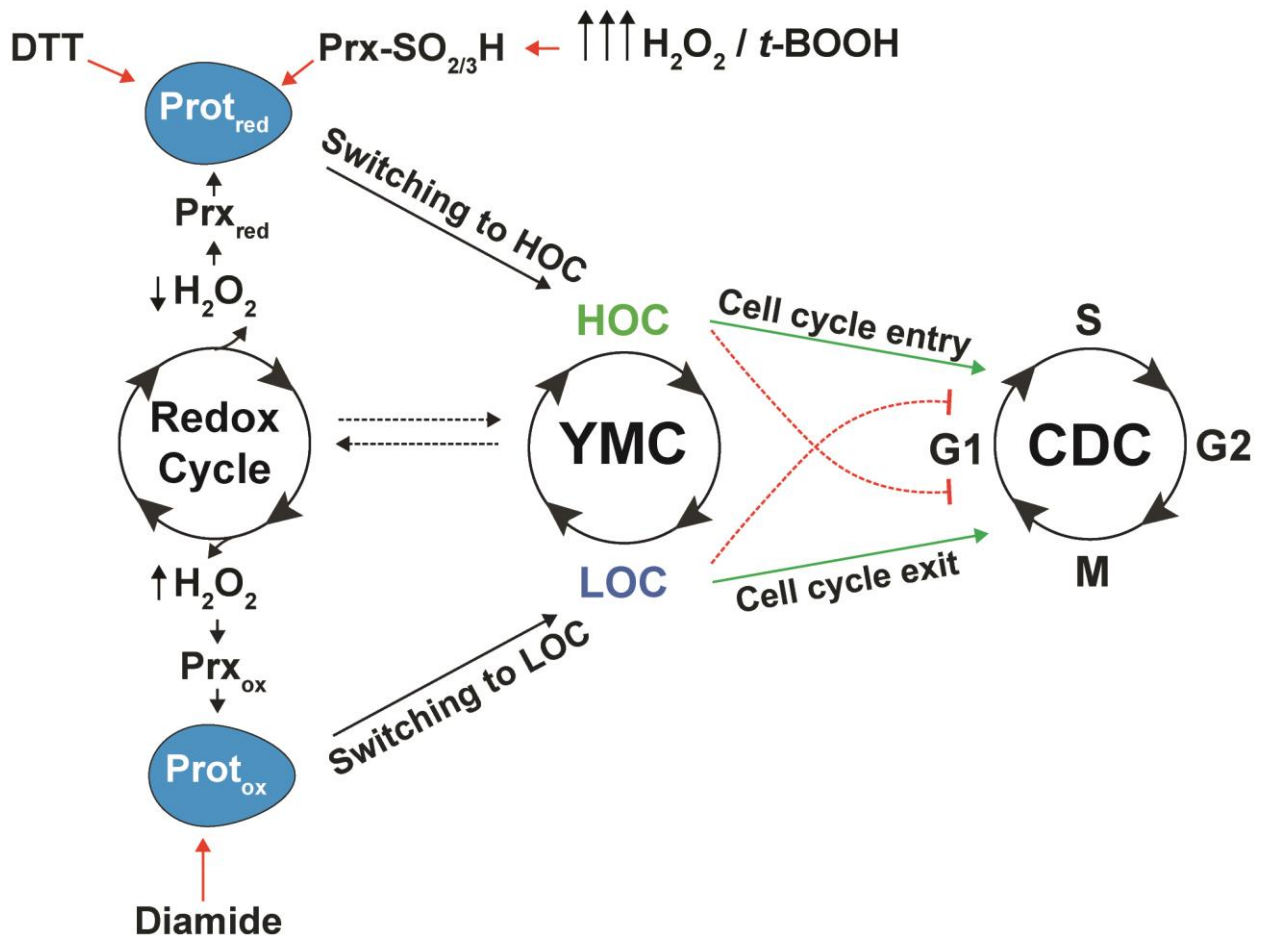


Figure 3.11: Model illustrating the role of peroxiredoxins in the YMC. A proposed role for peroxiredoxins in regulation of metabolic cycling and the coordination of metabolism with cell division. Red arrows indicate non-physiological treatments that have been used in this study to test the model.

4 OUTLOOK

In this study, I have demonstrated that peroxiredoxins and peroxiredoxin redox relays are important for metabolic clock function, and in coupling of metabolism to the cell division cycle. I was able to demonstrate that 2-Cys peroxiredoxins, especially Tsa1 and Ahp1, are crucial for this function, loss of both being detrimental for prototrophic yeast viability.

I could not in this study identify specific redox relays important for YMC control and CDC coupling, although previous reports provide some insights into this [74, 162, 164]. It would therefore be interesting for future studies to use high throughput approaches to identify some of these relays. Protein-protein interaction techniques such as proximity biotinylation could be helpful in this regard. Fusion and coexpression of Tsa1 with the biotin affinity tag and biotin-ligase BirA*, for instance, and treating a YMC-synchronized culture of the tagged yeast strain with appropriate amounts of commercially available biotin would lead to promiscuous biotinylation of Tsa1 interacting partners [210-212]. By phase-specific sampling and proteomic analysis, it would be possible to analyze in an unbiased manner, phase-specific expression changes of such relays or interactions. An alternative strategy would be to trap the thiol redox state of samples collected at specific phases of the YMC and subject them to redox proteomic analysis techniques such as OxICAT [213, 214] or SICyLIA [215].

Changes to cellular transcript levels during the YMC have been investigated [47]. One subject that would be interesting to explore in the future would be to compare transcriptomic profiles to proteomic profiles during the same YMC. It is plausible that oscillatory changes in transcript levels are reflected at the proteomic level, or not. However, this is yet to be demonstrated. It would also be interesting to know how these transcriptome and proteome profiles are altered in response to the concentrations of peroxides used in this study. A proper experimental protocol would be to extract both mRNAs and proteins simultaneously from same cell aliquots in an assay and subject them to transcriptomics and non-targeted proteomic analysis. The GenElute™ RNA/DNA/Protein Purification Plus Kit (RDP300) from Sigma-Aldrich would be helpful for this purpose.

The requirement of Tsa1 and Ahp1 for prototrophic yeast viability is a novel observation that warrants further interrogations in the future. It would be interesting to know if the differential requirement for Tsa1 and Ahp1 is idiosyncratic of all prototrophic yeast strains that undergo metabolic cycling. It is also plausible that the more domesticated lab strains, such as BY4742 and W303, might have lost other important biological features that are essential for understanding cellular mechanisms on the systems biology level (e.g. Proteostasis). The challenge for yeast biologists, which is worthy of debate, is whether before drawing conclusions from experiments performed in auxotrophic yeast strains, it would be necessary to confirm same in their prototrophic counterparts, in similar fashion as cell culture experiments are verified in primary cells or animal models.

The importance of thioredoxins in redox processes and ribonucleotide biosynthesis position these enzymes at the interface of YMC-CDC coupling. My 'biased' selection of *TRX2* for scrutiny of its impact

in YMC regulation revealed an important finding that is worth pursuing. The requirement of thioredoxins for peroxiredoxin recycling was reflected in the effect on the YMC, of the loss of *TRX2*. It is possible that $\Delta trx2$ cells will exhibit CDCs decoupled from the YMC, although yet to be proven. In their review, Chen and McKnight argued as follows: “Based on the redox nature of cell cycle gating by the YMC, the regulatory factor(s) might possess the following attributes: (1) redox sensitivity; (2) expression and/or activity that is switched on or off at the oxidative-reductive transition point; and (3) direct or indirect interaction with key factors controlling DNA replication” [216]. It is my view that thioredoxins meet these criteria. A careful dissection of the contributions of thioredoxins and thioredoxin reductases to YMC regulation is worth pursuing. Moreover, the mechanisms that underlie YMC-CDC coupling as well as impacts of the loss of such coupling on cell physiology could become clearer upon identification of the redox relays that govern such process using the techniques aforementioned.

Although other redox metabolites such as NADP(H) and GSH/GSSG have been shown to oscillate during the YMC [56], the approach used to interrogate H_2O_2 dynamics in this study is novel and less prone to direct human manipulations. Real-time measurements provide high resolution, second to second interval snapshots of redox metabolite dynamics. During the course of this study, I have also engineered CEN.PK yeast strain expressing a genomically integrated roGFP2-Grx1 biosensor, capable of monitoring in real-time, oscillations in the GSH/GSSG couple during the YMC. It would be good to use this strain in the future to monitor GSH/GSSG dynamics during the YMC. While expression of plasmids in the CEN.PK background was assumed impossible due to the inability for plasmid selection, I devised a technique, by deleting the *HIS3* gene from the CEN.PK genome and supplementing this with a *HIS3* plasmid. By so doing, it was possible to develop a $\Delta his3$ CEN.PK strain expressing a *HIS3* plasmid and capable of generating synchronized YMCs just like a wildtype strain (data not shown). I am aware that plans are advanced by the Morgan lab to develop plasmid-based genetically encoded biosensors to monitor cellular NADP(H) in yeast. Such plasmids, when ready, can be expressed in the $\Delta his3$ CEN.PK strain to monitor cycling changes in this metabolite during the YMC, if any. Such NADPH oscillations are expected to run anti-phasic to H_2O_2 changes, owing to the antioxidant role of NADPH. It would be interesting to see how this turns out in the future. The source of H_2O_2 during the YMC, as well as the mechanisms by which their oscillations are generated and maintained is worth following up on.

5 MATERIALS AND METHODS

This section contains methods that are standard protocols in the Morgan lab. Methods that were developed by me as part of this project are described in details. Methods modified from other publications are duly cited and referenced.

5.1 Molecular Biology Methods

5.1.1 Plasmid DNA isolation from *Escherichia coli* (*E. coli*)

I isolated plasmid DNA from *E. coli* cells after cloning of vectors. To do this, I inoculated 5 ml of selective LB-media with a single bacteria colony and incubated at 37 °C with shaking at 140 rpm overnight. I harvested and extracted DNA from 2 ml of *E. coli* culture using the NucleoSpin Plasmid-Kit (Macherey-Nagel, #740609.250) according to the manufacturer's instructions.

5.1.2 Determination of DNA concentration

I used the NanoDrop™ 1000 Spectrophotometer (Thermo Fisher Scientific) to evaluate DNA concentration and purity. This was done with 1 µl of DNA after cleaning and blanking of instrument with milliQ-H₂O. I measured absorbance at 280, 260 or 230 nm. The ratios of 280/230 and 260/230 were used to determine contamination by proteins, RNA and organic compounds. For low contamination, a ratio of around 2 was sufficient.

5.1.3 Polymerase chain reaction for DNA amplification

I performed polymerase chain reaction (PCR) to amplify DNA for homologous recombination, plasmid construction and successful clone verification. For homologous recombination and plasmid construction, the PCR reaction volume was 50 µl, consisting of 100 ng template DNA, 40 pmol each of forward and reverse primers, 0.2 mM dNTPs, 1 U polymerase and 1x reaction buffer, and made up with milliQ-H₂O. For verifications after cloning, the PCR reaction volume was scaled down to 25 µl.

Successful integration of antibiotic resistance cassette by homologous recombination was confirmed by colony PCR. To do this, one colony of yeast was dissolved in 30 µl of 0.2 % SDS and boiled for 10 min at 95 °C. Afterwards, cell debris and intact cells were pelleted using a small tabletop centrifuge at 17,000g for 1 min. Thereafter, 1 µl of the supernatant was used as template DNA for PCR.

All reactions were performed with the Phusion High-Fidelity DNA Polymerase kit (New England BioLabs or NEB, #M0530L). The PCR was run under the following conditions: initial denaturation at 98°C for 3 min, 30 cycles of denaturation at 98 °C for 30 s, followed by annealing at 60 °C for 20 s and extension

at 72 °C for 1 min/kb. The final extension of PCR product was carried out at 72 °C for 10 min and cooling to 4 °C.

5.1.4 Restriction digestion of DNA

Restriction digestion was used to confirm plasmid construct before and after cloning. PCR products or plasmids were digested in a 50 µl reaction volume containing 15 U of restriction enzyme and 1x reaction buffer (CutSmart, NEB, #B7204S) as recommended by the manufacturer. To avoid self-ligation, 1 U of calf intestinal phosphatase (CIP, NEB, #M0290S) was added to the reaction where necessary. The reaction mixture was incubated at 37 °C for 2 h and analyzed in agarose gel electrophoresis. The respective DNA fragment was purified after electrophoresis or directly after the digestion reaction using the NucleoSpin® PCR Clean-up kit (Macherey-Nagel) according to the manufacturer's instructions. For analytic purposes, 500 ng of plasmid DNA was digested for 30 min at 37 °C in a 20 µl reaction volume and analyzed by agarose gel electrophoresis.

5.1.5 Ligation of DNA fragments with vectors

Insert fragments were ligated into vector plasmid DNA in a 3:1 ratio in a reaction volume of 20 µl. This consisted of 100 ng of vector, 2 µl of *T4 DNA ligase* (NEB, #M0202S), 2 µl of 10x ligase reaction buffer (NEB, #E6289), and made up with milliQ-H₂O. The reaction was performed at 16 °C overnight and 2 µl of the ligation reaction was transformed into *E. coli* cells.

5.1.6 Agarose gel electrophoresis

Agarose was used for verification of DNA fragments after restriction digest and cloning. The gel was prepared at 1% (w/v) in 1x TAE buffer (40 mM Tris, 1.14% acetic acid, 10 mM EDTA pH 8.0) by heating in a microwave. The gel was casted into a slide and 0.5 µg/ml ethidium bromide was added to visualize DNA under ultra violet (UV) light. Samples were mixed with 6x loading dye (60 mM Tris/HCl pH 7.5, 30 mM sodium acetate, 12 mM EDTA, 60% (v/v) glycerol, 0.36% (w/v) orange G) and loaded onto wells in the gel. The electrophoresis was performed in 1x TAE buffer at 10 V/cm. The gels were analyzed under UV light.

5.1.7 Chemical transformation of *E. coli* cells

Chemo competent *E. coli* cells were transformed for the amplification of plasmid DNA. Cells were thawed slowly on ice and mixed with either 2 µl of a ligation reaction or 20 ng of plasmid DNA. The mixture was further incubated on ice for 30 min followed by a 45 s heat shock at 42 °C and incubation on ice for another 1 min. Afterwards, 100 µl LB-media was added and the suspension incubated further at 37°C for 1 h on 750 rpm shaking. The cell suspension was immediately plated onto LB agar plates supplemented with 100 µg/ml Ampicillin and incubated at 37 °C overnight until colonies appeared. The *E. coli* cells used in this study are described in Table 5.1.

5.1.8 One-step transformation of *S. cerevisiae* cells

One milliliter of log phase yeast cells were harvested at 900g for 3 min. For homologous recombination to genomically integrate a DNA cassette, cell pellet was washed with 1 ml sterile milliQ-H₂O and re-suspended in 200 µl of one-step buffer (0.2 M Li-Acetate, 40 % PEG 3350, 100 mM DTT), 10µl of 100 mg/ml single strand DNA from Salmon sperm (denatured at 95 °C for 5 min) and 500 ng of PCR product. In case of transformation with plasmid DNA for sensor expression, cell pellet was washed with 1 ml sterile milliQ-H₂O and re-suspended in 100 µl one-step buffer, 5 µl Salmon sperm DNA and 100ng of plasmid DNA. The mixture was vortexed briefly and incubated at 45 °C for 30 min on 750 rpm shaking.

With plasmid transformations, the suspension was immediately spread onto HC agar plates lacking the respective amino acid for selection. For homologous recombination, cells were pelleted at 900g for 3min, re-suspended in 1 ml of fresh YPD media and transferred into flasks containing 4 ml of fresh YPD media. The cell suspension was then incubated overnight in a shaking incubator at 30 °C. Thereafter, cells were harvested at 900g for 3 min and re-suspended in 200 µl of fresh YPD media. The cells were then plated onto the appropriate selective media as follows: 180 µl of the immediate suspension was spread on a YPD agar plate (90% plate), and the remaining 20 µl suspension was further diluted with 180 µl of fresh YPD media and plated onto another agar plate (10% plate). All plates were incubated at 30 °C for 2-3 days until colonies appeared.

5.1.9 Plasmids and primers

Plasmids used in this thesis are described in Table 5.2, whilst primers used in plasmid and strain construction are listed in Table 5.3. Plasmids were designed for expression in yeast. In some instances, primer names are denoted by the yeast strain they were used to construct and confirm.

5.2 Cell Biology Methods

5.2.1 Yeast strains

The CEN.PK 113-1A strain background was used to perform all experiments using the fermenter. Most deletion mutants were created in this background, unless otherwise stated. The BY4741 and BY4742 backgrounds were also used for some experiments. Gene deletion strains were created using a standard, homologous recombination-based gene deletion approach (Table 5.4). All deletion strains were confirmed by PCR on isolated genomic DNA using primers designed to anneal 100–200 base pairs up- and downstream of the gene of interest (Table 5.3).

5.2.2 Construction of a genomically integrated roGFP2-Tsa2 Δ C_R expressing yeast strain

The peroxiredoxin-based H₂O₂ sensor, roGFP2-Tsa2 Δ C_R, was modified for integration and expression from the yeast genome. Briefly, the coding sequence for roGFP2-Tsa2 Δ C_R was genetically fused to the KanMX4 resistance cassette and a strong constitutive promoter, GPD, both derived from a pYM-N14 plasmid [217]. The KanMX4-GFP fragment was amplified by PCR using primers P1 and P2, which possess a *NheI* restriction site to enable annealing to the *XbaI* restriction site of the p415TEF roGFP2-Tsa2 Δ C_R plasmid. The complete construct was assembled in a p415TEF plasmid and confirmed by sequencing. The entire KanMX4-GPD-roGFP2-Tsa2 Δ C_R construct was then amplified by PCR using primers P3 and P4, which were designed to have overhangs complementary to a non-coding genome region between the *HXT6* and *HXT7* genes. The PCR product was transformed into yeast for homologous recombination, positive colonies were selected on YPD agar plates supplemented with G-418 antibiotic, and confirmed by PCR of the genomic DNA using primers P5 and P6 (see Appendix A1).

5.2.3 Construction of yeast strains capable of conditional genomic Ahp1 depletion via an auxin-inducible degron (AID) system

A plasmid construct (AP2099) of both the auxin-inducible degron and *Arabidopsis thaliana* F-box protein, transport inhibitor response 1 (*AtTir1*), was a generous gift from Prof. Dr. Blanche Schwappach (Göttingen, Germany). The construct was modified and amplified by PCR for genomic integration and fusion to the N-terminus of *AHP1*, using primers P7 and P8. Positive clones were selected on YPD agar plates supplemented with G-418 antibiotic and verified by PCR using primers P9 and P10 or P9 and KanMX4 REV (see Appendix A3). Sensitivity to auxin was determined by spotting serial dilutions of exponentially growing yeast cultures on YPD plates containing 0.2 mM of auxin.

5.2.4 Yeast mating, sporulation and tetrad dissection

A CEN.PK113-1A $\Delta tsa1\Delta tsa2$ strain was crossed with CEN.PK113-7D $\Delta ahp1$ strain on YPD agar plate. The resultant diploid cells were selected and enriched by growth on YPD plates supplemented with G418, nourseothricin and hygromycin antibiotics. These cells were subsequently inoculated into 10 ml of fresh YPD media and incubated overnight with shaking at 140 rpm, 30 °C. Next, 500 μ l of YPD culture was harvested by centrifugation at 900g for 3 min and re-suspended in 10 ml of sporulation media (10 g/l Potassium acetate, 1 g/l yeast extract, 0.5 g/l glucose). The cell suspension was further incubated at 30 °C for 4 days to allow for sporulation. About 500 μ l of sporulated cell suspension was harvested by centrifugation at 900g for 3 min and re-suspended in 100 μ l of 1.2 M sorbitol buffer supplemented with zymolyase and incubated for 15 min at room temperature (RT). Zymolyase-treated cells were further diluted 1:50 in 1.2 M sorbitol buffer and a few microliters of the suspension transferred onto the side of a dried YPD plate under sterile conditions. The plate was dried for a further 10 min and tetrads dissected using a tetrad dissection microscope (Nikon ECLIPSE 50i). Dissected tetrads were incubated at 30 °C for 48 h and characterized by growth on appropriate antibiotic containing media.

5.2.5 Media for *E. coli* cultivation

Bacteria was cultivated in liquid culture or on agar plates. LB medium (1% bacto-tryptone, 0.5% yeast extract, 1% sodium chloride, pH was adjusted to 7.5 with NaOH) supplemented with 100 μ g/ml ampicillin was used for liquid culture and plasmid selection. For agar plates, 2% bacto-agar (w/v) was dissolved in LB medium and autoclaved. After cooling of the agar solution, 100 μ g/ml of ampicillin was added prior to pouring in plates.

5.2.6 Media for *S. cerevisiae* cultivation

Yeast cells were cultured in full YP-media (1% yeast extract, 2% peptone, pH was adjusted to 5.5 with HCl) supplemented with 2% glucose as carbon source. YPD agar plates were prepared by mixing 2% agar, 1% yeast extract and 2% peptone, adjusted to pH 5.5 with HCl and autoclaved. Autoclaved media was supplemented with 2% of glucose and 100 μ g/ml of G418, Nourseothricin or Hygromycin B solution for selection where necessary. The mixture was poured into petri dishes.

Yeast strains were streaked onto YPD agar plates for growth before culture in liquid media. Cells streaked on agar plates were grown in a stationary incubator, whilst cells cultured in liquid media were grown in a shaking incubator (140 rpm) at 30 °C. Yeast transformed for gene deletion by homologous recombination was grown on YPD agar plates supplemented with the respective antibiotic for selection. Backgrounds transformed with plasmids were grown in Hartwell's complete (HC) media lacking the appropriate amino acids for plasmid selection, with 2% glucose as carbon source. The composition of HC media is described in Table 5.5. All media components were sterile filtered before use.

5.2.7 Establishment of continuous culture

A Biostat® A fermenter (Module BB-8822002, Serial # 00337/16, Sartorius Stedim Systems, Guxhagen, Germany) was used for all continuous culture experiments. Fermenter runs were initiated by the addition of a 20 ml starter culture, which had been grown to stationary phase in YPD media at 30 °C. The culture working volume was 800 ml. The fermenter was run at a constant temperature of 30 °C, with a constant pH of 3.4 maintained by automated addition of 10% (w/v) NaOH. The culture was continuously aerated at 1 L/min with stirring at 530 rpm. After growth to stationary phase as a batch culture, continuous culture was initiated by the addition of growth media at a constant dilution rate of 0.05 h⁻¹.

Growth media consisted of 10 g/l glucose, 1 g/l yeast extract (SERVA, #24540.03), 5 g/l (NH₄)₂SO₄, 2 g/l KH₂PO₄, 0.5 g/l MgSO₄·7H₂O, 0.1 g/l CaCl₂·2H₂O, 0.02 g/l FeSO₄·7H₂O, 0.01 g/l ZnSO₄·7H₂O, 0.005 g/l CuSO₄·5H₂O, 0.001 g/l MnCl₂·4H₂O, 2.5 ml 70% H₂SO₄ and 0.5 ml/l Antifoam 204 (Sigma). Media components and trace metals were separately prepared, sterilized and re-constituted to a total volume of 5L. Briefly, a solution consisting of 1 g/l yeast extract (SERVA), 5 g/l (NH₄)₂SO₄, 2 g/l KH₂PO₄, 0.5 g/l MgSO₄·7H₂O, 0.1 g/l CaCl₂·2H₂O was prepared to the appropriate volume and autoclaved. To this solution were added the appropriate amounts of separately autoclaved 100 g/l glucose solution and 70 % H₂SO₄ solution. ZnSO₄·7H₂O, CuSO₄·5H₂O and MnCl₂·4H₂O were prepared as a 1000x trace metal stock and separately autoclaved. Finally, FeSO₄·7H₂O was dissolved to 10 mg/ml in water, sterile filtered, and the appropriate amount added to the media mix, together with the appropriate volume of antifoam 204.

5.2.8 Online monitoring of roGFP2-Tsa2ΔC_R

To enable the continuous ‘on-line’ monitoring of roGFP2-Tsa2ΔC_R fluorescence, I developed an in-house system. Briefly, a peristaltic pump was used to continuously pump culture from the fermenter, through a flow-cell (Type 71-F, Starna GmbH, Göttingen) inserted into a JASCO FP-6500 spectrofluorimeter. Fluorescence was measured at fixed excitation wavelengths of 425 nm and 488 nm with emission monitored at 510 nm. The excitation and emission bandwidths were set to 5 nm. A measurement was recorded every 30 s. RoGFP2 oxidation was qualitatively determined by computing the ratio between fluorescence intensities at 425 nm and 488 nm

5.2.9 NEM-based alkylation for degree of oxidation of roGFP2-Tsa2ΔC_R determination

To monitor changes in roGFP2-Tsa2ΔC_R oxidation during the YMC an NEM-based probe oxidation ‘trapping’ method was used. Briefly, cells were removed from the culture vessel at the indicated time points. Aliquots of 450 μl were immediately added to separate Eppendorf tubes containing either 50 μl 1 M NEM (i.e. 100 mM final), 50 μl 1 M DTT (i.e. 100 mM final) or 50 μl 0.2 M diamide (i.e. 20 mM final). The samples were incubated at RT for 10 mins. Cells were subsequently harvested by centrifugation

at 900g for 3 min and re-suspended in 100 mM MES-Tris buffer (pH 6.0) containing 10 mM NEM. Cells were then transferred to a 96-well plate and probe oxidation was measured using a BMG Labtech CLARIOstar fluorescence plate reader. The degree of sensor oxidation was determined according to Equation 1, as previously described, based on the fluorescence emission intensity at 510 nm with excitation at both 405 nm and 488 nm for the fully oxidized, fully reduced and control samples respectively [90, 93, 218].

Equation 1

$$\text{OxD}_{\text{roGFP2}} = \frac{(I_{405_{\text{sample}}} * I_{488_{\text{red}}}) - (I_{405_{\text{red}}} * I_{488_{\text{sample}}})}{(I_{405_{\text{sample}}} * I_{488_{\text{red}}} - I_{405_{\text{sample}}} * I_{488_{\text{ox}}}) + (I_{405_{\text{ox}}} * I_{488_{\text{sample}}} - I_{405_{\text{red}}} * I_{488_{\text{sample}}})}$$

5.2.10 Flow cytometry analysis of DNA content

Aliquots of 1.0 OD₆₀₀ units of fermenter cultures (~1 x 10⁷ cells) were harvested at 6,000g for 1min. Cells were re-suspended and fixed in 1 ml 70 % (v/v) ethanol at 4 °C overnight. Fixed cells were then pelleted at 6,000g for 1 min and washed with milliQ-H₂O. Cells were subsequently re-suspended in 250 µl FxCycle™ PI/RNase staining solution (Life Technologies, #F10797), incubated at RT in the dark for 30min and then stored at 4 °C for 72 h. Samples were sonicated at 30 % amplitude for 20 s and run on an Attune™ Flow Cytometer. Data analyses was performed using the FlowJo™ software (v.10). Samples were gated for single cells and a histogram of cell count against PI intensity plotted. The percentage of cells with 1N DNA and 2N DNA content were determined as follows: 1N; area under the histogram from 2.7 to 4.5 x 10⁵ PI intensity and 2N; area under the histogram from 4.5 to 7 x 10⁵ PI intensity. Cell populations with PI intensity greater than 7 x 10⁵ were considered to have more than 2N DNA content.

5.2.11 Budding index determination and DNA visualization by DAPI staining and microscopy

Fermenter culture samples were harvested at the indicated times and fixed with 70% (v/v) ethanol at 4 °C for 30 min. Cells were washed twice with 1x phosphate-buffered saline (PBS). Budded and non-budded cells in several random fields were scored to calculate budding index. To visualize DNA 4,6-diamidino-2-phenylindole (DAPI) was added to the harvested cells at a final concentration of 1 µg/ml in PBS and incubated in the dark for 10 mins. Cells were then washed and re-suspended in PBS for visualization. Cells were visualized with a fully automated Zeiss inverted microscope (AxioObserver Z1) equipped with the CSU-X1 spinning disk confocal head (Yokogawa). Image acquisition was performed using a CoolSnap HQ camera (Roper Scientific) and a 40x air or 63x oil objective under the control of the Slidebook software (Intelligent Imaging Innovations, Denver, CO).

5.2.12 Fluorescence Microscopy

Genomically integrated sensor-expressing strains were grown to mid-log phase in YPD. About 1 μ l of the culture was placed on a microscopic slide and covered with a cover slip. Cells were viewed using a Nikon ECLIPSE E600 fluorescent microscope. Images were acquired with a 100 \times oil immersion lens and Nikon equipped camera using NIS-Elements D 4.50.00 software. Images were then transferred to PhotoScape (version 3.7) or ImageJ (version 1.52a) for processing.

5.3 Protein biochemistry methods

5.3.1 Protein extraction

For detection of hyperoxidized peroxiredoxin proteins, 2.0 OD₆₀₀ units of cells were collected from the fermenter 30 min after *t*-BOOH treatment and immediately treated with 100 mM NEM for 10 min at RT. Subsequently, cells were isolated by centrifugation at 900g for 3 min, re-suspended in 100 μ l of 100 mM NaOH and incubated for 10 min at RT. Cells were then centrifuged at 900g for 3 mins, re-suspended in 15 μ l of lysis buffer (50 mM HEPES, pH 8.0, 50 mM NaCl, 1% SDS, 10 μ M EDTA, 20 mM NEM) and mixed with 15 μ l of 2 \times non-reducing SDS-PAGE sample loading buffer (50 mM Tris-HCl pH 6.8, 10% glycerine, 2% SDS, 0.01% bromophenol blue).

For western blots against Myc-, FLAG- and His- tagged proteins, 1.0 OD₆₀₀ units of cells were harvested at the indicated time points, re-suspended in lysis buffer and mixed with an equal volume of 2 x SDS-PAGE sample loading buffer.

To control for specificity of anti-Prx-SO_{2/3}H antibody towards Tsa, CEN.PK113-1A wildtype, Δ *tsa1* Δ *tsa2* and sensor-expressing cells were grown to mid log phase (OD₆₀₀ of 3-3.5) in fermenter media at 30 °C in a shaking incubator. About 2.0 OD₆₀₀ units of cells were aliquoted into eppis containing a final of 0 and 1 mM *t*-BOOH or 0 and 5 mM H₂O₂.

5.3.2 SDS-polyacrylamide gel electrophoresis (SDS-PAGE)

Sodium dodecyl sulfate polyacrylamide gel electrophoresis (SDS-PAGE) separates proteins by their size. In this method, proteins are denatured and assume a negative charge due to the SDS detergent. This allows protein migration through an electric field towards the anode of the gel chamber. The network of acrylamide fibers leads to a slow migration of unfolded and large proteins whereas small or partially folded proteins run faster through the gel. Gels were casted in-house using the components shown in Table 5.6. Samples were mixed with appropriate sample buffer prior to loading in gels. Protein sizes were determined with the aid of an unstained marker from peQLab or PageRuler™ Prestained Protein Ladder from ThermoFisher Scientific. Each gel was run at 25 mA for 2 h in SDS running buffer (25 mM Tris-HCl pH 8.3, 190 mM glycine, 0.1% SDS).

5.3.3 Western blot transfer and detection

Proteins separated in SDS-PAGE were transferred onto a cellulose membrane using the semi-dry method. Two whatman papers (sized 17 cm x 12 cm) were briefly incubated in blotting buffer (20 mM Tris, 150 mM glycine, 0.08% SDS, 20% methanol) and placed in the blotting chamber. Nitrocellulose membrane (sized 15 cm x 10 cm) and the SDS-gel were also incubated in the blotting buffer. The cellulose membrane was placed on top of the whatman paper followed by the gel. An additional Whatman paper was placed on top of the gel and the chamber was tightly closed. All processes were performed to avoid air bubbles. Proteins were transferred onto the membrane at 200 mA for 1.5 h. Membrane-transferred proteins were visualized by staining in Ponceau S solution (0.2% (w/v) Ponceau S, 3% (w/v) acetic acid) for 2 – 5 mins.

Next, membranes were incubated reeling for 30 min in 5 % milk or BSA in 1x TBS buffer (10 mM Tris/HCl pH 7.5, 150 mM NaCl) to prevent unspecific binding of antibodies. Afterwards, the membranes were incubated with the primary antibody (as indicated below) overnight reeling at 4°C. The membranes were washed three times for 10 mins with TBS buffer. Afterwards, the membranes were incubated for at least 30 min, reeling at RT with horse reddish peroxidase-coupled secondary antibodies (anti-mouse or anti-rabbit, 1:10,000 in 5 % milk or BSA in TBS). Membranes were thereafter washed again thrice for 10 mins. Membranes were then visualized by chemiluminescence using a 1:1 ratio of ECL 1 (100 mM Tris/HCl pH 8.5, 0.044% (w/v) luminol, 0.0066% p-coumaric acid) and ECL 2 (100 mM Tris/HCl pH 8.5, 0.03% H₂O₂) solutions. The primary antibodies used include rabbit polyclonal α -Prx-SO₃ (LF-PA0004, AbFRONTIER, 1:1000 in 5 % Milk), mouse monoclonal α -FLAG M2 (F3165, SIGMA, 1:500, 5 % Milk), mouse monoclonal α -Myc Tag (9E11) (MAI-16637, Invitrogen, 1:500 in 5% Milk) and rabbit polyclonal α -His (Herrmann lab, 1.000 in 5% BSA).

5.3.4 Autoradiography

Luminescent membranes were detected by autoradiography, by placing radiosensitive films (Fuji Medical X-Ray Film Super RX or Kodak BioMax MR Film) on top of the dried cellulose membrane. After the desired exposure time, the films were developed using the Optimax TR (MS Laborgeräte) machine.

Table 5.1: Genotypes of the different *E. coli* strains used in this study

Strain	Genotype	Use	Reference
MH1	MC1061 derivative; araD139, lacX74, <i>galU</i> , <i>galK</i> , <i>hsr</i> , <i>hsm+</i> , <i>strA</i>	Plasmid amplification	[219]
DH5 α	K12 derivative; F ⁻ ϕ 80 <i>dlacZ</i> Δ M15, Δ (<i>lacZYA-argF</i>)U169, <i>deoR</i> , <i>recA1</i> , <i>endA1</i> , <i>hsdR17</i> (rk ⁻ mk ⁺), <i>phoA</i> , <i>supE44</i> , λ^- , <i>thi-1</i> , <i>gyrA96</i> , <i>relA1</i>	Plasmid amplification	[220]

Table 5.2: List of plasmids used in this study

Name	Resistance/ Selection marker	Backbone	Insert	Reference
pYM-N14	<i>Amp^R/kanMX4</i>	p413-GPD	KanMX4-GPD	[217]
pYM46	<i>Amp^R/kanMX4</i>	pYM1	MYC-7His	[217]
p415GPD roGFP2-Tsa2 Δ C _R	<i>Amp^R/LEU2</i>	p415-GPD	roGFP2-Tsa2 Δ C _R	This study
p415TEF roGFP2-Tsa2 Δ C _R	<i>Amp^R/LEU2</i>	p415-TEF	roGFP2-Tsa2 Δ C _R	[90]
p415TEF roGFP2-Ahp1	<i>Amp^R/LEU2</i>	p415-TEF	roGFP2-Ahp1	[90]
AP2099	<i>Amp^R/kanMX4</i>	pCEV-Nop1	mycAID-ArTir1-Flag	Blanche, Göttingen
pFA6 α - <i>natNT2</i>	<i>Amp^R/natNT2</i>	pEG202	natNT2	[217]
pFA6 α - <i>hphNTI</i>	<i>Amp^R/hphNTI</i>	p425-GalI	hphNTI	[217]
pFA6 α - <i>kanMX4</i>	<i>Amp^R/kanMX4</i>	pYM3	kanMX4	[221, 222]
PHUK	<i>Amp^R</i>	N/A	HUK	Addgene
PHLUK	<i>Amp^R</i>	N/A	HLUK	Addgene

Table 5.3: List of primers used in this study

Primer name	5' → 3' Sequence
P1	GGTCCCGCGGCTAGCCGTACGCTGCAGGTCG
P2	GGCAAAGGGCTAGCCATCGATGAATTCTCTGTCG
P3	CCATTTAATTCCACCTTCGGATTTTTTTGCATAAACTCTCAATTT CCCCGCGATCCATCTGCCGAATGCGTACGCTGCAGGTCGAC
P4	CGTTCCTGTCAATCTAAGACTTGAAGATTACAGGACTTTTTTTTT TCTTACTGTATTTTTCCGTAGAGTGGTACCGGCCGCAAATTAAG G
P5	CGATTTGTTGATTCTATCCCAAGATTGAG
P6	CTCTTTCAGCCTTGTTTGATGGTGTAGATAAAACC
P7	GAAATTTCAACAAACCAGAACAACAAGTACTACCAATAACC ACAACAAAACATGCTTCGAGCGTCCCAAAACC
P8	GCAATGTATTGGAATTTGTAGTCGCCAGCTGGGAATTTCTTGTT AACTAAGTCAGAACCTGATACCTTCACGAACGC
P9	TTTCTGATTTGTAATTATACGGGGA
P10	ATTTTGTTCGAAACGCATATAATGT
KanMX4 confirm FWD	TGATTTTGATGACGAGCGTAAT
KanMX4 confirm REV	CTGCAGCGAGGAGCCGTAAT
HphNTI confirm FWD	GGCTTGTATGGAGCAGCAGAC
HphNTI confirm REV	CAAAGCATCAGCTCATCGAGAG
natNT2 confirm FWD	GCGCTCTACATGAGCATGCC
natNT2 confirm REV	CATCCAGTGCCTCGATG
Tsa1-S1	CTCGTTCAATTGCTCACAACCAACCACAACACTACATACACATACA TACACAATGcgtacgctgcaggtcgac
Tsa1-S2	CGTAAAGAGTGAATTTTAAATAAGTAGTCATTTAGACAACCTCTG CAAGCGTCTTAATCGATGAATTCGAGCTCG
Tsa1-S3	CCATCAAGCCAACCGTTGAAGACTCCAAGGAATACTTCGAAGC TGCCAACAAACGTACGCTGCAGGTCGAC
Tsa1 confirm FWD	TGCGTTTAAGGTGTACGAAAACCC
Tsa1 confirm REV	GGTTTACGCGTTTTAGAGCCAGAC
Tsa2-S1	CACTATTACTGTTTTTTGCTCAAGAATATATTAGCCTTACAAGA ACGTAAAAACCAATCATG cgtacgctgcaggtcgac
Tsa2-S2	CATATATAGGGTGTATTTTTTAATTATTTAATAGGGCCTAGC GTTATCGTGCGAAGATTAatcgatgaattcgagctcg
Tsa2 confirm FWD	GTTACCCGAGTAATCAAGGATCAACTATGG

Tsa2 confirm REV	GGTCATTTGCGTCTTCTGGATATAAAGATG
Ahp1-S1	CGAAATTTCAACAAACCAGAACAACACAAGTACTACCAATAAC CACAACAAAACATGcgtacgctgcaggtcgac
Ahp1-S2	CCTTGTACAGAATCGTTTTCTATTTTGAATTTTTTTATATAAAC ATGGTTTTATTGTCTATTACATAGCATCTAatcgaatcgagctcg
Ahp1 confirm FWD	TTTCTGATTTGTAATTATACGGGGA
Ahp1 confirm REV	ATTTTGTTCGAAACGCATATAATGT
Prx1-S1	GTGCTTCTAGATTCTCGCAGTAGGATGAGATAAATTTCAAAGA AGCAGGAAGCAAAGGATGCGTACGCTGCAGGTCGAC
Prx1-S2	GATAAAAGTTTTAGTTAGAGATACTTCATATACCTGTATATAGT AAAGTCGTTTTATTCAAAGCTTAATCGATGAATTCGAGCTCG
Prx1 confirm FWD	GTTTATCTTTATACAATATACAAAAGGTCACCCAG
Prx1 confirm REV	GGTCTTGGTCAGAATCTCGATTATC
Sod1-S1	GGAAAAACAGGCAAGAAAGCAATCGCGCAAACAAATAAAACA TAATTAATTTATAATGCGTACGCTGCAGGTCGAC
Sod1-S2	GCGCTTACTACTTACTTACATACGGTTTTTATTCAAGTATATTAT CATTAAACATTAATCGATGAATTCGAGCTCG
Sod1 confirm FWD	GTAAACCGGTGTGTCGGAATTAGTAAG
Sod1 confirm REV	CTGGAACCATCAAGACCGTTTTG
Yno1-S1	ATATCTCGTCGCCAGAACTTCTAATTTGGTAAGCCTTCCAATA AATATGCGTACGCTGCAGGTCGAC
Yno1-S2	ATTTCCGAGCATATTGCGTAAGACATTATTATTCTTTTCTTTTCC CCTCAATCGATGAATTCGAGCTCG
Yno1 confirm FWD	GATCGCTGCTCCGTAATACCGATATAC
Yno1 confirm REV	CCGATTAATAATGCGTACAACCTGTCAAG
Trx1-S1	CCCTGAAACTGCATTAGTGTAATAGAAGACTAGACACCTCGAT ACAAATAATGCGTACGCTGCAGGTCGAC
Trx1-S2	TATAACAAACACAGTATAGAAACACAATATATCGGTCATTGGG TGAGTTAATCGATGAATTCGAGCTCG
Trx1 confirm FWD	CGATATGTATATTCTTTTCGTTGGAAAAGATGTC
Trx1 confirm REV	CCTCTTGTGTGAAAAATTAATTGTTTCCTCC
Trx2-S1	GAATTATACACGCACACATACACGAGAGTCTACGATATCTTTA AATAACACATCAATAATGcgtacgctgcaggtcgac
Trx2-S2	GTTTATTTAAACTGGTAAACATGATGTACTTTACGTAGCGTTAA TATACCGGCAACTAatcgaatcgagctcg
Trx2 confirm FWD	CTCCCTACAAGGTGGCTCTTTTCTTACTAAGC

Trx2 confirm REV	CAAAGGTGCAGAAAGCTGCACCTTGTAAG
Cox6-S1	CGAACAATTGTATTTGACACATAAACTAATAAATATACAACAA TGC GTACGCTGCAGGTCGAC
Cox6-S2	ACAACAAATTACAGACGTTGTGTGGTAGCTTTTTCCTTATTATT AATCGATGAATTCGAGCTCG
Cox6 confirm FWD	GCCAGATCTCAAGGTTACCTCATTTTC
Cox6 confirm REV	TTCTGAGTGGATGAATATCCATAAAGGG

Table 5.4: Genetic composition of yeast strains used in this study

Strain	Genotype	References
CEN.PK113-1A	<i>MATα</i>	P. Kötter, Frankfurt
CEN.PK113-7D	<i>MATα</i>	P. Kötter, Frankfurt
BY4741	<i>MATα his3Δ1 leu2Δ0 met15Δ0 ura3Δ0</i>	Euroscarf
BY4742	<i>MATα his3Δ1 leu2Δ0 lys2Δ0 ura3Δ0</i>	Euroscarf
Δ <i>prx1</i>	CEN.PK113-1A <i>Δprx1::hphNT1</i>	This study
Δ <i>tsa1</i>	CEN.PK113-1A <i>Δtsa1::hphNT1</i>	This study
Δ <i>tsa2</i>	CEN.PK113-1A <i>Δtsa2::natNT2</i>	This study
Δ <i>tsa1Δ<i>tsa2</i></i>	CEN.PK113-1A <i>Δtsa1::hphNT1 Δtsa2::natNT2</i>	This study
Δ <i>tsa1Δ<i>tsa2</i></i>	BY4742 <i>Δtsa1::natNT2 Δtsa2::kanMX4</i>	[90]
Δ <i>ahp1</i>	CEN.PK113-1A <i>Δahp1::hphNT1</i>	This study
Δ <i>ahp1</i>	CEN.PK113-7D <i>Δahp1::kanMX4</i>	This study
Δ <i>ahp1</i>	BY4741 <i>Δahp1::kanMX4</i>	Euroscarf
CEN.PK T2- Δ C _R	CEN.PK113-1A <i>kanMX4-P_{GPD}-roGFP2-Tsa2ΔC_R</i>	This study
WT::AID-AHP1	CEN.PK113-1A <i>Af-Tir1-FLAG-Myc-kanMX4-AID-AHP1</i>	This study
Δ <i>tsa1</i> ::AID-AHP1	CEN.PK113-1A <i>Δtsa1::hphNT1 Af-Tir1-FLAG-Myc-kanMX4-AID-AHP1</i>	This study
Δ <i>tsa2</i> ::AID-AHP1	CEN.PK113-1A <i>Δtsa2::natNT2 Af-Tir1-FLAG-Myc-kanMX4-AID-AHP1</i>	This study
Δ <i>tsa1Δ<i>tsa2</i>::AID-AHP1</i>	CEN.PK113-1A <i>Δtsa1::hphNT1 Δtsa2::natNT2 Af-Tir1-FLAG-Myc-kanMX4-AID-AHP1</i>	This study
Δ <i>sod1</i>	CEN.PK113-1A <i>Δsod1::hphNT1</i>	This study
Δ <i>yno1</i>	CEN.PK113-1A <i>Δyno1::natNT2</i>	This study
Δ <i>cox6</i>	BY4742 <i>Δcox6::kanMX4</i>	[90]
Δ <i>snf1</i>	CEN.PK113-1A <i>Δsnf1::kanMX4</i>	This study

Table 5.5: Composition of Hartwell's Complete (HC) media for growth of plasmid transformed yeast strains

HC Media		Dropout mix (DOM)	
Component	Amount/L (ml)	Amino acids	10x (g/l)
10 x DOM	100	Methionine	0.2
10 x YNB	100	Tyrosine	0.6
ml 40% Glucose	50	Isoleucine	0.8
1g/l Uracil	35	Phenylalanine	0.5
1g/l Adenine	20	Glutamic acid	1.0
10g/l Lysine	12	Threonine	2.0
10g/L Tryptophan	8	Aspartic acid	1.0
20g/l Leucine	4	Valine	1.5
10g/l Histidine	2	Serine	4.0
milliQ-H ₂ O	669	Arginine	0.2

Table 5.6: Composition of SDS-PAGE gels

Gel	Composition
Running gel	16% acrylamide/14% acrylamide 0.11% bisacrylamide 375 mM Tris-HCl pH 8.8 0.1% SDS 0.1% ammonium persulfate (APS) 0.03% N,N,N',N'-Tetramethylethylenediamine (TEMED)
Stacking gel	5% acrylamide 0.03% bisacrylamide 60 mM Tris-HCl pH 6.8 0.1% SDS 0.05% APS 0.1% TEMED
Base gel	20% acrylamide 0.13% bisacrylamide 375 mM Tris-HCl pH 8.8 0.1% SDS 0.05% APS 0.1% TEMED

REFERENCES

1. Johnson, C.H., *Precise circadian clocks in prokaryotic cyanobacteria*. Curr Issues Mol Biol, 2004. **6**(2): p. 103-10.
2. Reddy, A.B. and G. Rey, *Metabolic and nontranscriptional circadian clocks: eukaryotes*. Annu Rev Biochem, 2014. **83**: p. 165-89.
3. Halberg, F., et al., *Transdisciplinary unifying implications of circadian findings in the 1950s*. J Circadian Rhythms, 2003. **1**(1): p. 2.
4. Gardner, M.J., et al., *How plants tell the time*. Biochemical Journal, 2006. **397**: p. 15-24.
5. Zuccarelli, L., et al., *Human Physiology During Exposure to the Cave Environment: A Systematic Review With Implications for Aerospace Medicine*. Frontiers in Physiology, 2019. **10**.
6. Foer, J. and M. Siffre, *CAVEMAN: AN INTERVIEW WITH MICHEL SIFFRE (Living beyond time)*. Cabinet Magazine, 2008(30).
7. Aschoff, J., *Circadian Rhythms in Man - a Self-Sustained Oscillator with an Inherent Frequency Underlies Human 24-Hour Periodicity*. Science, 1965. **148**(3676): p. 1427-+.
8. Antle, M.C. and R. Silver, *Neural basis of timing and anticipatory behaviors*. European Journal of Neuroscience, 2009. **30**(9): p. 1643-1649.
9. Bruce, V.G. and C.S. Pittendrigh, *Endogenous Rhythms in Insects and Microorganisms*. American Naturalist, 1957. **91**(858): p. 179-195.
10. Pittendrigh, C.S., *Temporal Organization - Reflections of a Darwinian Clock-Watcher*. Annual Review of Physiology, 1993. **55**: p. 16-54.
11. Hardin, P.E., J.C. Hall, and M. Rosbash, *Feedback of the Drosophila Period Gene-Product on Circadian Cycling of Its Messenger-Rna Levels*. Nature, 1990. **343**(6258): p. 536-540.
12. Young, M.W. and S.A. Kay, *Time zones: A comparative genetics of circadian clocks*. Nature Reviews Genetics, 2001. **2**(9): p. 702-715.
13. Lakin-Thomas, P.L., *Circadian clock genes frequency and white collar-1 are not essential for entrainment to temperature cycles in Neurospora crassa*. Proceedings of the National Academy of Sciences of the United States of America, 2006. **103**(12): p. 4469-4474.
14. Konopka, R.J. and S. Benzer, *Clock Mutants of Drosophila-Melanogaster*. Proceedings of the National Academy of Sciences of the United States of America, 1971. **68**(9): p. 2112-+.
15. Pittendrigh, C.S., *On Temperature Independence in the Clock System Controlling Emergence Time in Drosophila*. Proceedings of the National Academy of Sciences of the United States of America, 1954. **40**(10): p. 1018-1029.
16. Bargiello, T.A. and M.W. Young, *Molecular-Genetics of a Biological Clock in Drosophila*. Proceedings of the National Academy of Sciences of the United States of America-Biological Sciences, 1984. **81**(7): p. 2142-2146.
17. Bargiello, T.A., F.R. Jackson, and M.W. Young, *Restoration of Circadian Behavioral Rhythms by Gene-Transfer in Drosophila*. Nature, 1984. **312**(5996): p. 752-754.
18. Zerr, D.M., et al., *Circadian Fluctuations of Period Protein Immunoreactivity in the Cns and the Visual-System of Drosophila*. Journal of Neuroscience, 1990. **10**(8): p. 2749-2762.
19. Reddy, P., et al., *Molecular Analysis of the Period Locus in Drosophila-Melanogaster and Identification of a Transcript Involved in Biological Rhythms*. Cell, 1984. **38**(3): p. 701-710.
20. Zehring, W.A., et al., *P-Element Transformation with Period Locus DNA Restores Rhythmicity to Mutant, Arrhythmic Drosophila-Melanogaster*. Cell, 1984. **39**(2): p. 369-376.
21. Darlington, T.K., et al., *Closing the circadian loop: CLOCK-induced transcription of its own inhibitors per and tim*. Science, 1998. **280**(5369): p. 1599-1603.
22. Allada, R., et al., *A mutant Drosophila homolog of mammalian Clock disrupts circadian rhythms and transcription of period and timeless*. Cell, 1998. **93**(5): p. 791-804.
23. Rutila, J.E., et al., *CYCLE is a second bHLH-PAS clock protein essential for circadian rhythmicity and transcription of Drosophila period and timeless*. Cell, 1998. **93**(5): p. 805-814.
24. Harmer, S.L., S. Panda, and S.A. Kay, *Molecular bases of circadian rhythms*. Annual Review of Cell and Developmental Biology, 2001. **17**: p. 215-253.
25. Hogenesch, J.B., et al., *The basic-helix-loop-helix-PAS orphan MOP3 forms transcriptionally active complexes with circadian and hypoxia factors*. Proc Natl Acad Sci U S A, 1998. **95**(10): p. 5474-9.

26. Preitner, N., et al., *The orphan nuclear receptor REV-ERB α controls circadian transcription within the positive limb of the mammalian circadian oscillator*. Cell, 2002. **110**(2): p. 251-60.
27. Scully, A.L. and S.A. Kay, *Time flies for Drosophila*. Cell, 2000. **100**(3): p. 297-300.
28. Merrow, M., et al., *Circadian regulation of the light input pathway in Neurospora crassa*. EMBO J, 2001. **20**(3): p. 307-15.
29. Bell-Pedersen, D., *Understanding circadian rhythmicity in Neurospora crassa: from behavior to genes and back again*. Fungal Genet Biol, 2000. **29**(1): p. 1-18.
30. Sweeney, B.M. and F.T. Haxo, *Persistence of a Photosynthetic Rhythm in Enucleated Acetabularia*. Science, 1961. **134**(3487): p. 1361-3.
31. Driessche, T.V., *Circadian Rhythms in Acetabularia - Photosynthetic Capacity and Chloroplast Shape*. Experimental Cell Research, 1966. **42**(1): p. 18-+.
32. Mergenhagen, D. and H.G. Schweiger, *Effect of Different Inhibitors of Transcription and Translation on Expression and Control of Circadian-Rhythm in Individual Cells of Acetabularia*. Experimental Cell Research, 1975. **94**(2): p. 321-326.
33. Nishiwaki, T., et al., *Nucleotide binding and autophosphorylation of the clock protein KaiC as a circadian timing process of cyanobacteria*. Proceedings of the National Academy of Sciences of the United States of America, 2000. **97**(1): p. 495-499.
34. Nakajima, M., et al., *Reconstitution of circadian oscillation of cyanobacterial KaiC phosphorylation in vitro*. Science, 2005. **308**(5720): p. 414-415.
35. Tomita, J., et al., *No transcription-translation feedback in circadian rhythm of KaiC phosphorylation*. Science, 2005. **307**(5707): p. 251-254.
36. Taniguchi, Y., et al., *Three major output pathways from the KaiABC-based oscillator cooperate to generate robust circadian kaiBC expression in cyanobacteria*. Proceedings of the National Academy of Sciences of the United States of America, 2010. **107**(7): p. 3263-3268.
37. O'Neill, J.S., et al., *Circadian rhythms persist without transcription in a eukaryote*. Nature, 2011. **469**(7331): p. 554-558.
38. O'Neill, J.S. and A.B. Reddy, *Circadian clocks in human red blood cells*. Nature, 2011. **469**(7331): p. 498-U70.
39. Edgar, R.S., et al., *Peroxiredoxins are conserved markers of circadian rhythms*. Nature, 2012. **485**(7399): p. 459-U65.
40. Causton, H.C., et al., *Metabolic Cycles in Yeast Share Features Conserved among Circadian Rhythms*. Current Biology, 2015. **25**(8): p. 1056-1062.
41. Cornelius, G. and L. Rensing, *Daily Rhythmic Changes in Mg-2+-Dependent Atpase Activity in Human Red Blood-Cell Membranes Invitro*. Biochemical and Biophysical Research Communications, 1976. **71**(4): p. 1269-1272.
42. Radha, E., et al., *Glutathione Levels in Human-Platelets Display a Circadian-Rhythm Invitro*. Thrombosis Research, 1985. **40**(6): p. 823-831.
43. Goto, K., D.L. Lavalmartin, and L.N. Edmunds, *Biochemical Modeling of an Autonomously Oscillatory Circadian Clock in Euglena*. Science, 1985. **228**(4705): p. 1284-1288.
44. Feeney, K.A., et al., *Daily magnesium fluxes regulate cellular timekeeping and energy balance*. Nature, 2016. **532**(7599): p. 375-+.
45. Finn, R.K. and R.E. Wilson, *Fermentation Process Control - Population Dynamics of a Continuous Propagator for Microorganisms*. Journal of Agricultural and Food Chemistry, 1954. **2**(2): p. 66-69.
46. Kaspar von Meyenburg, H., *Energetics of the budding cycle of Saccharomyces cerevisiae during glucose limited aerobic growth*. Arch Mikrobiol, 1969. **66**(4): p. 289-303.
47. Tu, B.P., et al., *Logic of the yeast metabolic cycle: Temporal compartmentalization of cellular processes*. Science, 2005. **310**(5751): p. 1152-1158.
48. Tu, B.P., *Ultradian Metabolic Cycles in Yeast*. Methods in Enzymology, Vol 470: Guide to Yeast Genetics:, 2010. **470**: p. 857-866.
49. Chen, Z., et al., *Restriction of DNA replication to the reductive phase of the metabolic cycle protects genome integrity*. Science, 2007. **316**(5833): p. 1916-1919.
50. Klevecz, R.R., et al., *A genomewide oscillation in transcription gates DNA replication and cell cycle*. Proc Natl Acad Sci U S A, 2004. **101**(5): p. 1200-5.

51. Kuenzi, M.T. and A. Fiechter, *Changes in Carbohydrate Composition and Trehalase-Activity during Budding Cycle of Saccharomyces Cerevisiae*. Archiv Fur Mikrobiologie, 1969. **64**(4): p. 396-+.
52. Porro, D., et al., *Oscillations in Continuous Cultures of Budding Yeast - a Segregated Parameter Analysis*. Biotechnology and Bioengineering, 1988. **32**(4): p. 411-417.
53. Nagoshi, E., et al., *Circadian gene expression in individual fibroblasts: Cell-autonomous and self-sustained oscillators pass time to daughter cells*. Cell, 2004. **119**(5): p. 693-705.
54. Matsuo, T., et al., *Control mechanism of the circadian clock for timing of cell division in vivo*. Science, 2003. **302**(5643): p. 255-9.
55. Mori, T., B. Binder, and C.H. Johnson, *Circadian gating of cell division in cyanobacteria growing with average doubling times of less than 24 hours*. Proc Natl Acad Sci U S A, 1996. **93**(19): p. 10183-8.
56. Tu, B.P., et al., *Cyclic changes in metabolic state during the life of a yeast cell*. Proc Natl Acad Sci U S A, 2007. **104**(43): p. 16886-91.
57. Futch, B., *Metabolic cycle, cell cycle, and the finishing kick to Start*. Genome Biol, 2006. **7**(4): p. 107.
58. Sohn, H. and H. Kuriyama, *Ultradian metabolic oscillation of Saccharomyces cerevisiae during aerobic continuous culture: hydrogen sulphide, a population synchronizer, is produced by sulphite reductase*. Yeast, 2001. **18**(2): p. 125-35.
59. Wolf, J., et al., *Mathematical analysis of a mechanism for autonomous metabolic oscillations in continuous culture of Saccharomyces cerevisiae*. FEBS Lett, 2001. **499**(3): p. 230-4.
60. Robertson, J.B., et al., *Real-time luminescence monitoring of cell-cycle and respiratory oscillations in yeast*. Proc Natl Acad Sci U S A, 2008. **105**(46): p. 17988-93.
61. Eelderink-Chen, Z., et al., *A circadian clock in Saccharomyces cerevisiae*. Proc Natl Acad Sci U S A, 2010. **107**(5): p. 2043-7.
62. Holmstrom, K.M. and T. Finkel, *Cellular mechanisms and physiological consequences of redox-dependent signalling*. Nat Rev Mol Cell Biol, 2014. **15**(6): p. 411-21.
63. Rhee, S.G., *Cell signaling. H2O2, a necessary evil for cell signaling*. Science, 2006. **312**(5782): p. 1882-3.
64. Stone, J.R. and S. Yang, *Hydrogen peroxide: a signaling messenger*. Antioxid Redox Signal, 2006. **8**(3-4): p. 243-70.
65. Sies, H., *Hydrogen peroxide as a central redox signaling molecule in physiological oxidative stress: Oxidative eustress*. Redox Biol, 2017. **11**: p. 613-619.
66. Marinho, H.S., et al., *Hydrogen peroxide sensing, signaling and regulation of transcription factors*. Redox Biol, 2014. **2**: p. 535-62.
67. Winterbourn, C.C. and A.V. Peskin, *Kinetic Approaches to Measuring Peroxiredoxin Reactivity*. Mol Cells, 2016. **39**(1): p. 26-30.
68. Winterbourn, C.C. and M.B. Hampton, *Thiol chemistry and specificity in redox signaling*. Free Radic Biol Med, 2008. **45**(5): p. 549-61.
69. Lee, S.R., et al., *Reversible inactivation of protein-tyrosine phosphatase 1B in A431 cells stimulated with epidermal growth factor*. J Biol Chem, 1998. **273**(25): p. 15366-72.
70. Woo, H.A., et al., *Inactivation of peroxiredoxin I by phosphorylation allows localized H(2)O(2) accumulation for cell signaling*. Cell, 2010. **140**(4): p. 517-28.
71. Randall, L.M., G. Ferrer-Sueta, and A. Denicola, *Peroxiredoxins as preferential targets in H2O2-induced signaling*. Methods Enzymol, 2013. **527**: p. 41-63.
72. Stocker, S., et al., *A role for 2-Cys peroxiredoxins in facilitating cytosolic protein thiol oxidation*. Nat Chem Biol, 2018. **14**(2): p. 148-155.
73. Sobotta, M.C., et al., *Peroxiredoxin-2 and STAT3 form a redox relay for H2O2 signaling*. Nat Chem Biol, 2015. **11**(1): p. 64-70.
74. Delaunay, A., et al., *A thiol peroxidase is an H2O2 receptor and redox-transducer in gene activation*. Cell, 2002. **111**(4): p. 471-81.
75. Veal, E.A., et al., *A 2-Cys peroxiredoxin regulates peroxide-induced oxidation and activation of a stress-activated MAP kinase*. Mol Cell, 2004. **15**(1): p. 129-39.
76. Rhee, S.G. and H.A. Woo, *Multiple functions of peroxiredoxins: peroxidases, sensors and regulators of the intracellular messenger H(2)O(2), and protein chaperones*. Antioxid Redox Signal, 2011. **15**(3): p. 781-94.

77. Ferrer-Sueta, G., et al., *Factors affecting protein thiol reactivity and specificity in peroxide reduction*. Chem Res Toxicol, 2011. **24**(4): p. 434-50.
78. Forman, H.J., M. Maiorino, and F. Ursini, *Signaling Functions of Reactive Oxygen Species*. Biochemistry, 2010. **49**(5): p. 835-842.
79. Brigelius-Flohe, R. and L. Flohe, *Basic Principles and Emerging Concepts in the Redox Control of Transcription Factors*. Antioxidants & Redox Signaling, 2011. **15**(8): p. 2335-2381.
80. Hall, A., et al., *Structure-based insights into the catalytic power and conformational dexterity of peroxiredoxins*. Antioxid Redox Signal, 2011. **15**(3): p. 795-815.
81. Rhee, S.G., et al., *Peroxiredoxin functions as a peroxidase and a regulator and sensor of local peroxides*. J Biol Chem, 2012. **287**(7): p. 4403-10.
82. Fisher, A.B., *Peroxiredoxin 6: a bifunctional enzyme with glutathione peroxidase and phospholipase A(2) activities*. Antioxid Redox Signal, 2011. **15**(3): p. 831-44.
83. Wood, Z.A., et al., *Structure, mechanism and regulation of peroxiredoxins*. Trends Biochem Sci, 2003. **28**(1): p. 32-40.
84. Chae, H.Z., et al., *Cloning and sequencing of thiol-specific antioxidant from mammalian brain: alkyl hydroperoxide reductase and thiol-specific antioxidant define a large family of antioxidant enzymes*. Proc Natl Acad Sci U S A, 1994. **91**(15): p. 7017-21.
85. Hall, A., et al., *Structural changes common to catalysis in the Tpx peroxiredoxin subfamily*. J Mol Biol, 2009. **393**(4): p. 867-81.
86. Wood, Z.A., et al., *Dimers to doughnuts: redox-sensitive oligomerization of 2-cysteine peroxiredoxins*. Biochemistry, 2002. **41**(17): p. 5493-504.
87. Wood, Z.A., L.B. Poole, and P.A. Karplus, *Peroxiredoxin evolution and the regulation of hydrogen peroxide signaling*. Science, 2003. **300**(5619): p. 650-3.
88. Rhee, S.G., et al., *Sulfiredoxin, the cysteine sulfinic acid reductase specific to 2-Cys peroxiredoxin: its discovery, mechanism of action, and biological significance*. Kidney Int Suppl, 2007(106): p. S3-8.
89. Gutscher, M., et al., *Proximity-based protein thiol oxidation by H₂O₂-scavenging peroxidases*. J Biol Chem, 2009. **284**(46): p. 31532-40.
90. Morgan, B., et al., *Real-time monitoring of basal H₂O₂ levels with peroxiredoxin-based probes*. Nat Chem Biol, 2016. **12**(6): p. 437-43.
91. Schwarzlander, M., et al., *Dissecting Redox Biology Using Fluorescent Protein Sensors*. Antioxid Redox Signal, 2016. **24**(13): p. 680-712.
92. Roma, L.P., et al., *Mechanisms and Applications of Redox-Sensitive Green Fluorescent Protein-Based Hydrogen Peroxide Probes*. Antioxid Redox Signal, 2018. **29**(6): p. 552-568.
93. Morgan, B., M.C. Sobotta, and T.P. Dick, *Measuring E-GSH and H₂O₂ with roGFP2-based redox probes*. Free Radical Biology and Medicine, 2011. **51**(11): p. 1943-1951.
94. Rutter, J., et al., *Regulation of clock and NPAS2 DNA binding by the redox state of NAD cofactors*. Science, 2001. **293**(5529): p. 510-4.
95. Hirayama, J., S. Cho, and P. Sassone-Corsi, *Circadian control by the reduction/oxidation pathway: catalase represses light-dependent clock gene expression in the zebrafish*. Proc Natl Acad Sci U S A, 2007. **104**(40): p. 15747-52.
96. Yoshida, Y., et al., *Cross-talk between the cellular redox state and the circadian system in Neurospora*. PLoS One, 2011. **6**(12): p. e28227.
97. Gyongyosi, N., et al., *Reactive oxygen species can modulate circadian phase and period in Neurospora crassa*. Free Radic Biol Med, 2013. **58**: p. 134-43.
98. Qian, H., et al., *The effects of hydrogen peroxide on the circadian rhythms of Microcystis aeruginosa*. PLoS One, 2012. **7**(3): p. e33347.
99. Ivleva, N.B., et al., *LdpA: a component of the circadian clock senses redox state of the cell*. EMBO J, 2005. **24**(6): p. 1202-10.
100. Ishiura, M., et al., *Expression of a gene cluster kaiABC as a circadian feedback process in cyanobacteria*. Science, 1998. **281**(5382): p. 1519-23.
101. Avitabile, D., et al., *Peroxiredoxin 2 nuclear levels are regulated by circadian clock synchronization in human keratinocytes*. Int J Biochem Cell Biol, 2014. **53**: p. 24-34.
102. Ranieri, D., et al., *Nuclear redox imbalance affects circadian oscillation in HaCaT keratinocytes*. Int J Biochem Cell Biol, 2015. **65**: p. 113-24.

103. Kil, I.S., et al., *Feedback control of adrenal steroidogenesis via H₂O₂-dependent, reversible inactivation of peroxiredoxin III in mitochondria*. Mol Cell, 2012. **46**(5): p. 584-94.
104. Beaver, L.M., et al., *Circadian regulation of glutathione levels and biosynthesis in Drosophila melanogaster*. PLoS One, 2012. **7**(11): p. e50454.
105. Krishnan, N., A.J. Davis, and J.M. Giebultowicz, *Circadian regulation of response to oxidative stress in Drosophila melanogaster*. Biochem Biophys Res Commun, 2008. **374**(2): p. 299-303.
106. Lai, A.G., et al., *CIRCADIAN CLOCK-ASSOCIATED 1 regulates ROS homeostasis and oxidative stress responses*. Proc Natl Acad Sci U S A, 2012. **109**(42): p. 17129-34.
107. Kondratov, R.V., et al., *Early aging and age-related pathologies in mice deficient in BMAL1, the core component of the circadian clock*. Genes Dev, 2006. **20**(14): p. 1868-73.
108. Pardee, A.B., *A restriction point for control of normal animal cell proliferation*. Proc Natl Acad Sci U S A, 1974. **71**(4): p. 1286-90.
109. Hartwell, L.H., et al., *Genetic control of the cell division cycle in yeast*. Science, 1974. **183**(4120): p. 46-51.
110. Johnston, G.C., J.R. Pringle, and L.H. Hartwell, *Coordination of growth with cell division in the yeast Saccharomyces cerevisiae*. Exp Cell Res, 1977. **105**(1): p. 79-98.
111. Johnson, A. and J.M. Skotheim, *Start and the restriction point*. Curr Opin Cell Biol, 2013. **25**(6): p. 717-23.
112. Nyberg, K.A., et al., *Toward maintaining the genome: DNA damage and replication checkpoints*. Annu Rev Genet, 2002. **36**: p. 617-56.
113. Forsburg, S.L. and P. Nurse, *Cell cycle regulation in the yeasts Saccharomyces cerevisiae and Schizosaccharomyces pombe*. Annu Rev Cell Biol, 1991. **7**: p. 227-56.
114. Papagiannakis, A., et al., *Autonomous Metabolic Oscillations Robustly Gate the Early and Late Cell Cycle*. Mol Cell, 2017. **65**(2): p. 285-295.
115. Burnetti, A.J., M. Aydin, and N.E. Buchler, *Cell cycle Start is coupled to entry into the yeast metabolic cycle across diverse strains and growth rates*. Molecular Biology of the Cell, 2016. **27**(1): p. 64-74.
116. Atzori, L., et al., *Growth-associated modifications of low-molecular-weight thiols and protein sulfhydryls in human bronchial fibroblasts*. J Cell Physiol, 1990. **143**(1): p. 165-71.
117. Davies, K.J., *The broad spectrum of responses to oxidants in proliferating cells: a new paradigm for oxidative stress*. IUBMB Life, 1999. **48**(1): p. 41-7.
118. Hirt, H., *Connecting oxidative stress, auxin, and cell cycle regulation through a plant mitogen-activated protein kinase pathway*. Proc Natl Acad Sci U S A, 2000. **97**(6): p. 2405-7.
119. Menon, S.G. and P.C. Goswami, *A redox cycle within the cell cycle: ring in the old with the new*. Oncogene, 2007. **26**(8): p. 1101-1109.
120. Oberley, L.W., T.D. Oberley, and G.R. Buettner, *Cell division in normal and transformed cells: the possible role of superoxide and hydrogen peroxide*. Med Hypotheses, 1981. **7**(1): p. 21-42.
121. Pani, G., et al., *A redox signaling mechanism for density-dependent inhibition of cell growth*. J Biol Chem, 2000. **275**(49): p. 38891-9.
122. Menon, S.G., et al., *Redox regulation of the G1 to S phase transition in the mouse embryo fibroblast cell cycle*. Cancer Res, 2003. **63**(9): p. 2109-17.
123. Burhans, W.C. and N.H. Heintz, *The cell cycle is a redox cycle: linking phase-specific targets to cell fate*. Free Radic Biol Med, 2009. **47**(9): p. 1282-93.
124. Carpenter, G. and S. Cohen, *Epidermal growth factor*. J Biol Chem, 1990. **265**(14): p. 7709-12.
125. Conour, J.E., W.V. Graham, and H.R. Gaskins, *A combined in vitro/bioinformatic investigation of redox regulatory mechanisms governing cell cycle progression*. Physiol Genomics, 2004. **18**(2): p. 196-205.
126. Kerk, N.M. and L.J. Feldman, *A Biochemical-Model for the Initiation and Maintenance of the Quiescent Center - Implications for Organization of Root-Meristems*. Development, 1995. **121**(9): p. 2825-2833.
127. Richard, P., *The rhythm of yeast*. Fems Microbiology Reviews, 2003. **27**(4): p. 547-557.
128. Satroutdinov, A.D., H. Kuriyama, and H. Kobayashi, *Oscillatory metabolism of Saccharomyces cerevisiae in continuous culture*. FEMS Microbiol Lett, 1992. **77**(1-3): p. 261-7.
129. Fomenko, D.E., et al., *Thiol peroxidases mediate specific genome-wide regulation of gene expression in response to hydrogen peroxide*. Proc Natl Acad Sci U S A, 2011. **108**(7): p. 2729-34.

130. Cliften, P., et al., *Finding functional features in Saccharomyces genomes by phylogenetic footprinting*. Science, 2003. **301**(5629): p. 71-6.
131. Ozcan, S. and M. Johnston, *Function and regulation of yeast hexose transporters*. Microbiol Mol Biol Rev, 1999. **63**(3): p. 554-69.
132. Veal, E.A., A.M. Day, and B.A. Morgan, *Hydrogen peroxide sensing and signaling*. Mol Cell, 2007. **26**(1): p. 1-14.
133. Nishimura, K., et al., *An auxin-based degron system for the rapid depletion of proteins in nonplant cells*. Nat Methods, 2009. **6**(12): p. 917-22.
134. Morawska, M. and H.D. Ulrich, *An expanded tool kit for the auxin-inducible degron system in budding yeast*. Yeast, 2013. **30**(9): p. 341-51.
135. Martin, J.L., *Thioredoxin--a fold for all reasons*. Structure, 1995. **3**(3): p. 245-50.
136. Cao, Z., S. Subramaniam, and N.J. Bulleid, *Lack of an efficient endoplasmic reticulum-localized recycling system protects peroxiredoxin IV from hyperoxidation*. J Biol Chem, 2014. **289**(9): p. 5490-8.
137. Johnson, C.H., *Circadian clocks and cell division: what's the pacemaker?* Cell Cycle, 2010. **9**(19): p. 3864-73.
138. Miyagishima, S.Y., et al., *Translation-independent circadian control of the cell cycle in a unicellular photosynthetic eukaryote*. Nat Commun, 2014. **5**: p. 3807.
139. Hong, C.I., et al., *Circadian rhythms synchronize mitosis in Neurospora crassa*. Proc Natl Acad Sci U S A, 2014. **111**(4): p. 1397-402.
140. Zaman, S., et al., *How Saccharomyces responds to nutrients*. Annu Rev Genet, 2008. **42**: p. 27-81.
141. Broach, J.R., *Nutritional control of growth and development in yeast*. Genetics, 2012. **192**(1): p. 73-105.
142. Wang, X. and C.G. Proud, *Nutrient control of TORC1, a cell-cycle regulator*. Trends Cell Biol, 2009. **19**(6): p. 260-7.
143. Mauro, F., A. Grasso, and L.J. Tolmach, *Variations in sulfhydryl, disulfide, and protein content during synchronous and asynchronous growth of HeLa cells*. Biophys J, 1969. **9**(11): p. 1377-97.
144. Kawamura, N., *Cytochemical and quantitative study of protein-bound sulfhydryl and disulfide groups in eggs of Arbacia during the first cleavage*. Exp Cell Res, 1960. **20**: p. 127-38.
145. Williamson, D.H., *The timing of deoxyribonucleic acid synthesis in the cell cycle of Saccharomyces cerevisiae*. J Cell Biol, 1965. **25**(3): p. 517-28.
146. Schwob, E., et al., *The B-type cyclin kinase inhibitor p40SIC1 controls the G1 to S transition in S. cerevisiae*. Cell, 1994. **79**(2): p. 233-44.
147. Schneider, B.L., Q.H. Yang, and A.B. Futcher, *Linkage of replication to start by the Cdk inhibitor Sic1*. Science, 1996. **272**(5261): p. 560-2.
148. Fitch, I., et al., *Characterization of four B-type cyclin genes of the budding yeast Saccharomyces cerevisiae*. Mol Biol Cell, 1992. **3**(7): p. 805-18.
149. Spellman, P.T., et al., *Comprehensive identification of cell cycle-regulated genes of the yeast Saccharomyces cerevisiae by microarray hybridization*. Mol Biol Cell, 1998. **9**(12): p. 3273-97.
150. Robertson, J.B., C.R. Davis, and C.H. Johnson, *Visible light alters yeast metabolic rhythms by inhibiting respiration*. Proc Natl Acad Sci U S A, 2013. **110**(52): p. 21130-5.
151. Hockberger, P.E., et al., *Activation of flavin-containing oxidases underlies light-induced production of H₂O₂ in mammalian cells*. Proc Natl Acad Sci U S A, 1999. **96**(11): p. 6255-60.
152. Bodvard, K., et al., *Light-sensing via hydrogen peroxide and a peroxiredoxin*. Nat Commun, 2017. **8**: p. 14791.
153. Pei, J-F., et al., *Diurnal oscillations of endogenous H₂O₂ sustained by p66^{Shc} regulate circadian clocks*. Nat Cell Biol, 2019. **21**: p. 1553-64
154. Xu, Z. and K. Tsurugi, *A potential mechanism of energy-metabolism oscillation in an aerobic chemostat culture of the yeast Saccharomyces cerevisiae*. FEBS J, 2006. **273**(8): p. 1696-709.
155. Murray, D.B., M. Beckmann, and H. Kitano, *Regulation of yeast oscillatory dynamics*. Proc Natl Acad Sci U S A, 2007. **104**(7): p. 2241-6.
156. Balaban, R.S., S. Nemoto, and T. Finkel, *Mitochondria, oxidants, and aging*. Cell, 2005. **120**(4): p. 483-95.
157. Giorgio, M., et al., *Electron transfer between cytochrome c and p66Shc generates reactive oxygen species that trigger mitochondrial apoptosis*. Cell, 2005. **122**(2): p. 221-33.

158. Kuge, S. and N. Jones, *YAP1 dependent activation of TRX2 is essential for the response of Saccharomyces cerevisiae to oxidative stress by hydroperoxides*. EMBO J, 1994. **13**(3): p. 655-64.
159. Lee, J., et al., *Yap1 and Skn7 control two specialized oxidative stress response regulons in yeast*. J Biol Chem, 1999. **274**(23): p. 16040-6.
160. Mochan, E. and E.K. Pye, *Respiratory oscillations in adapting yeast cultures*. Nat New Biol, 1973. **242**(119): p. 177-9.
161. Slavov, N. and D. Botstein, *Coupling among growth rate response, metabolic cycle, and cell division cycle in yeast*. Mol Biol Cell, 2011. **22**(12): p. 1997-2009.
162. Iwai, K., A. Naganuma, and S. Kuge, *Peroxiredoxin Ahp1 acts as a receptor for alkylhydroperoxides to induce disulfide bond formation in the Cad1 transcription factor*. J Biol Chem, 2010. **285**(14): p. 10597-604.
163. Roger, F., et al., *Peroxiredoxin promotes longevity and H₂O₂-resistance in yeast through redox-modification of protein kinase A*. bioRxiv, 2019: p. 676270.
164. Kuang, Z., et al., *Msn2/4 regulate expression of glycolytic enzymes and control transition from quiescence to growth*. Elife, 2017. **6**.
165. Holmgren, A., *Thioredoxin and glutaredoxin systems*. J Biol Chem, 1989. **264**(24): p. 13963-6.
166. Stocker, S., et al., *The Conundrum of Hydrogen Peroxide Signaling and the Emerging Role of Peroxiredoxins as Redox Relay Hubs*. Antioxid Redox Signal, 2018. **28**(7): p. 558-573.
167. Shao, D., et al., *A redox-dependent mechanism for regulation of AMPK activation by Thioredoxin1 during energy starvation*. Cell Metab, 2014. **19**(2): p. 232-45.
168. Lamia, K.A., et al., *AMPK regulates the circadian clock by cryptochrome phosphorylation and degradation*. Science, 2009. **326**(5951): p. 437-40.
169. Celenza, J.L. and M. Carlson, *A yeast gene that is essential for release from glucose repression encodes a protein kinase*. Science, 1986. **233**(4769): p. 1175-80.
170. Hong, S.P., et al., *Activation of yeast Snf1 and mammalian AMP-activated protein kinase by upstream kinases*. Proc Natl Acad Sci U S A, 2003. **100**(15): p. 8839-43.
171. Sutherland, C.M., et al., *Elm1p is one of three upstream kinases for the Saccharomyces cerevisiae SNF1 complex*. Curr Biol, 2003. **13**(15): p. 1299-305.
172. Nayak, V., et al., *Structure and dimerization of the kinase domain from yeast Snf1, a member of the Snf1/AMPK protein family*. Structure, 2006. **14**(3): p. 477-85.
173. Reddi, A.R. and V.C. Culotta, *SOD1 integrates signals from oxygen and glucose to repress respiration*. Cell, 2013. **152**(1-2): p. 224-35.
174. Demasi, M., G.M. Silva, and L.E.S. Netto, *20 S proteasome from Saccharomyces cerevisiae is responsive to redox modifications and is S-glutathionylated*. Journal of Biological Chemistry, 2003. **278**(1): p. 679-685.
175. Munoz, C.M., et al., *The effect of hydrogen peroxide on the cyclin D expression in fibroblasts*. Cellular and Molecular Life Sciences, 2001. **58**(7): p. 990-996.
176. Diehl, J.A., et al., *Glycogen synthase kinase 3 beta regulates cyclin D1 proteolysis and subcellular localization*. Genes & Development, 1998. **12**(22): p. 3499-3511.
177. Zou, Y.L., et al., *Mirk/dyrk1B kinase destabilizes cyclin D1 by phosphorylation at threonine 288*. Journal of Biological Chemistry, 2004. **279**(26): p. 27790-27798.
178. Sebastian, B., A. Kakizuka, and T. Hunter, *Cdc25m2 Activation of Cyclin-Dependent Kinases by Dephosphorylation of Threonine-14 and Tyrosine-15*. Proceedings of the National Academy of Sciences of the United States of America, 1993. **90**(8): p. 3521-3524.
179. Dunphy, W.G. and A. Kumagai, *The Cdc25 Protein Contains an Intrinsic Phosphatase-Activity*. Cell, 1991. **67**(1): p. 189-196.
180. Savitsky, P.A. and T. Finkel, *Redox regulation of Cdc25C*. Journal of Biological Chemistry, 2002. **277**(23): p. 20535-20540.
181. Ewald, J.C., et al., *The Yeast Cyclin-Dependent Kinase Routes Carbon Fluxes to Fuel Cell Cycle Progression*. Molecular Cell, 2016. **62**(4): p. 532-545.
182. Zhao, G., et al., *Cyclin-Dependent Kinase Co-Ordinates Carbohydrate Metabolism and Cell Cycle in S. cerevisiae*. Molecular Cell, 2016. **62**(4): p. 546-557.
183. Veisova, D., et al., *Role of individual phosphorylation sites for the 14-3-3-protein-dependent activation of yeast neutral trehalase Nth1*. Biochem J, 2012. **443**(3): p. 663-70.

184. Holt, L.J., et al., *Global analysis of Cdk1 substrate phosphorylation sites provides insights into evolution*. Science, 2009. **325**(5948): p. 1682-6.
185. Ubersax, J.A., et al., *Targets of the cyclin-dependent kinase Cdk1*. Nature, 2003. **425**(6960): p. 859-64.
186. Tokiwa, G., et al., *Inhibition of G1 cyclin activity by the Ras/cAMP pathway in yeast*. Nature, 1994. **371**(6495): p. 342-5.
187. Muller, D., et al., *Cyclic AMP mediates the cell cycle dynamics of energy metabolism in Saccharomyces cerevisiae*. Yeast, 2003. **20**(4): p. 351-67.
188. Irokawa, H., et al., *Redox-dependent Regulation of Gluconeogenesis by a Novel Mechanism Mediated by a Peroxidatic Cysteine of Peroxiredoxin*. Sci Rep, 2016. **6**: p. 33536.
189. Laurent, T.C., E.C. Moore, and P. Reichard, *Enzymatic Synthesis of Deoxyribonucleotides. Iv. Isolation and Characterization of Thioredoxin, the Hydrogen Donor from Escherichia Coli B*. J Biol Chem, 1964. **239**: p. 3436-44.
190. Holmgren, A., *Hydrogen donor system for Escherichia coli ribonucleoside-diphosphate reductase dependent upon glutathione*. Proc Natl Acad Sci U S A, 1976. **73**(7): p. 2275-9.
191. Boronat, S., et al., *Lack of a peroxiredoxin suppresses the lethality of cells devoid of electron donors by channelling electrons to oxidized ribonucleotide reductase*. Plos Genetics, 2017. **13**(6).
192. Lindahl, T., *Instability and decay of the primary structure of DNA*. Nature, 1993. **362**(6422): p. 709-15.
193. Gomez-Gonzalez, B. and A. Aguilera, *The need to regulate replication fork speed*. Science, 2017. **358**(6364): p. 722-723.
194. Somyajit, K., et al., *Redox-sensitive alteration of replisome architecture safeguards genome integrity*. Science, 2017. **358**(6364): p. 797-802.
195. Pines, J. and T. Hunter, *Isolation of a human cyclin cDNA: evidence for cyclin mRNA and protein regulation in the cell cycle and for interaction with p34cdc2*. Cell, 1989. **58**(5): p. 833-46.
196. Jackman, M., et al., *Active cyclin B1-Cdk1 first appears on centrosomes in prophase*. Nat Cell Biol, 2003. **5**(2): p. 143-8.
197. Bonnet, J., P. Coopman, and M.C. Morris, *Characterization of centrosomal localization and dynamics of Cdc25C phosphatase in mitosis*. Cell Cycle, 2008. **7**(13): p. 1991-8.
198. Lindqvist, A., V. Rodriguez-Bravo, and R.H. Medema, *The decision to enter mitosis: feedback and redundancy in the mitotic entry network*. J Cell Biol, 2009. **185**(2): p. 193-202.
199. Peters, J.M., *The anaphase promoting complex/cyclosome: a machine designed to destroy*. Nat Rev Mol Cell Biol, 2006. **7**(9): p. 644-56.
200. Pesin, J.A. and T.L. Orr-Weaver, *Regulation of APC/C activators in mitosis and meiosis*. Annu Rev Cell Dev Biol, 2008. **24**: p. 475-99.
201. Bassermann, F., et al., *The Cdc14B-Cdh1-Plk1 axis controls the G2 DNA-damage-response checkpoint*. Cell, 2008. **134**(2): p. 256-67.
202. Mochida, S., et al., *Regulated activity of PP2A-B55 delta is crucial for controlling entry into and exit from mitosis in Xenopus egg extracts*. EMBO J, 2009. **28**(18): p. 2777-85.
203. Domingo-Sananes, M.R., et al., *Switches and latches: a biochemical tug-of-war between the kinases and phosphatases that control mitosis*. Philos Trans R Soc Lond B Biol Sci, 2011. **366**(1584): p. 3584-94.
204. Chang, T.S., et al., *Regulation of peroxiredoxin I activity by Cdc2-mediated phosphorylation*. J Biol Chem, 2002. **277**(28): p. 25370-6.
205. Lim, J.M., et al., *Control of the pericentrosomal H2O2 level by peroxiredoxin I is critical for mitotic progression*. Journal of Cell Biology, 2015. **210**(1): p. 23-33.
206. Kaya, A., et al., *Thiol peroxidase deficiency leads to increased mutational load and decreased fitness in Saccharomyces cerevisiae*. Genetics, 2014. **198**(3): p. 905-17.
207. Iraqui, I., et al., *Human peroxiredoxin Prx1 is an orthologue of yeast Tsa1, capable of suppressing genome instability in Saccharomyces cerevisiae*. Cancer Res, 2008. **68**(4): p. 1055-63.
208. Wong, C.M., K.L. Siu, and D.Y. Jin, *Peroxiredoxin-null yeast cells are hypersensitive to oxidative stress and are genomically unstable*. J Biol Chem, 2004. **279**(22): p. 23207-13.
209. Nystrom, T., J. Yang, and M. Molin, *Peroxiredoxins, gerontogenes linking aging to genome instability and cancer*. Genes Dev, 2012. **26**(18): p. 2001-8.

210. Roux, K.J., et al., *A promiscuous biotin ligase fusion protein identifies proximal and interacting proteins in mammalian cells*. J Cell Biol, 2012. **196**(6): p. 801-10.
211. Choi-Rhee, E., H. Schulman, and J.E. Cronan, *Promiscuous protein biotinylation by Escherichia coli biotin protein ligase*. Protein Sci, 2004. **13**(11): p. 3043-50.
212. Cronan, J.E., *Targeted and proximity-dependent promiscuous protein biotinylation by a mutant Escherichia coli biotin protein ligase*. J Nutr Biochem, 2005. **16**(7): p. 416-8.
213. Leichert, L.I., et al., *Quantifying changes in the thiol redox proteome upon oxidative stress in vivo*. Proc Natl Acad Sci U S A, 2008. **105**(24): p. 8197-202.
214. Sethuraman, M., et al., *Isotope-coded affinity tag (ICAT) approach to redox proteomics: identification and quantitation of oxidant-sensitive cysteine thiols in complex protein mixtures*. J Proteome Res, 2004. **3**(6): p. 1228-33.
215. van der Reest, J., et al., *Proteome-wide analysis of cysteine oxidation reveals metabolic sensitivity to redox stress*. Nat Commun, 2018. **9**(1): p. 1581.
216. Chen, Z. and S.L. McKnight, *A conserved DNA damage response pathway responsible for coupling the cell division cycle to the circadian and metabolic cycles*. Cell Cycle, 2007. **6**(23): p. 2906-12.
217. Janke, C., et al., *A versatile toolbox for PCR-based tagging of yeast genes: new fluorescent proteins, more markers and promoter substitution cassettes*. Yeast, 2004. **21**(11): p. 947-62.
218. Meyer, A.J. and T.P. Dick, *Fluorescent protein-based redox probes*. Antioxid Redox Signal, 2010. **13**(5): p. 621-50.
219. Casadaban, M.J. and S.N. Cohen, *Analysis of gene control signals by DNA fusion and cloning in Escherichia coli*. J Mol Biol, 1980. **138**(2): p. 179-207.
220. Meselson, M. and R. Yuan, *DNA restriction enzyme from E. coli*. Nature, 1968. **217**(5134): p. 1110-4.
221. Wach, A., et al., *New heterologous modules for classical or PCR-based gene disruptions in Saccharomyces cerevisiae*. Yeast, 1994. **10**(13): p. 1793-808.
222. Knop, M., et al., *Epitope tagging of yeast genes using a PCR-based strategy: more tags and improved practical routines*. Yeast, 1999. **15**(10B): p. 963-72.

ABBREVIATIONS

°C	Grade Celsius
µg	Microgram
µl	Microliter
µM	Micromolar
AID	Auxin inducible degron
BSA	Bovine serum albumin
CDC	Cell division cycle
Cdk	Cyclin dependent kinase
CIP	Calf intestinal phosphatase
C _P	Peroxidactic cysteine
C _R	Resolving cysteine
Cry	Cryptochrome
Cyc	Cytochrome
Cys	Cysteine
DAPI	4,6-diamidino-2-phenylindole
Diamide	N,N,N',N'-tetramethylazodicarboxamide
DMSO	Dimethyl sulfoxide
DNA	Deoxyribonucleic acid
dNTP	Deoxyribonucleotide triphosphate
DTT	Dithiothreitol
<i>E. coli</i>	<i>Escherichia coli</i>
ECL	Enhanced chemiluminescence
EDTA	Ethylene diamine tetraacetate
ETC	Electron transport chain
Grx	Glutaredoxin
GSH	Glutathione
h	Hours
H ₂ O ₂	Hydrogen peroxide
HC	Hartwell's Complete
HOC	High oxygen consumption
HEPES	4-(2-hydroxyethyl)-1-piperazine-ethane sulfonic acid
IAA	Indole-3-acetic acid
kb	Kilobase
kDa	Kilodalton
L or l	liter

LB	Lysogeny broth media
LOC	Low oxygen consumption
M	Molarity
mg	Milligram
milliQ-H ₂ O	Double distilled water
min	Minute
ml	Milliliter
mM	Millimolar
NADH	Nicotinamide adenine dinucleotide
NADPH	Nicotinamide adenine dinucleotide phosphate
NEM	N-Ethylmaleimide
nm	Nanometer
OD ₆₀₀	Optical density at 600 nm
OxD	Degree of oxidation
PAGE	Polyacrylamide gel electrophoresis
PBS	Phosphate buffered saline
PCR	Polymerase chain reaction
PEG	Polyethylene glycol
Per	Period
PKA	Protein kinase A
Prx	Peroxiredoxin
RNA	Ribonucleic acid
RNR	Ribonucleotide reductase
roGFP2	Redox sensitive green fluorescent protein 2
ROS	Reactive oxygen species
rpm	Revolutions per minute
RT	Room temperature
s	Seconds
<i>S. cerevisiae</i>	<i>Saccharomyces cerevisiae</i>
<i>S. pombe</i>	<i>Saccharomyces pombe</i>
SDS	Sodium dodecyl sulfate
SOD (or Sod)	Superoxide dismutase
<i>t</i> -BOOH	<i>tert</i> -butyl hydroperoxide
TAE	Tris acetate EDTA
TBS	Tris buffered saline
TEMED	N,N,N',N'-tetramethylethylenediamine
Tim	Timeless

Tpx	Thioredoxin peroxidase
Tris	Tris-(hydroxymethyl)-aminomethane
Trx	Thioredoxin
TrxR	Thioredoxin reductase
Tsa	Thiol specific antioxidant
TTFL	Transcription-translation feedback loop
U	Units
UV	Ultraviolet
w/v	Weight per volume
YMC	Yeast Metabolic Cycle
Yno1	Yeast NADPH oxidase 1

ACKNOWLEDGEMENTS

The journey of a thousand miles, it is said, begins with one step. This is how far the steps have brought me. I am most grateful to God Almighty, without whom it would have been impossible for me to pursue my PhD. I am grateful to my wife, Joyce Amponsah, for the moral support to carry me through the course of this study. Joyce, you understood and cooperated with me during my late-night stays in the lab, considering the strain it would have had on our relationship, for this, I am most grateful. Now to every member of the Morgan and Herrmann labs who have contributed immensely to this feat, I am indebted in gratitude to you. I appreciate all your assistance in diverse ways, and apologize in advance if I am unable to mention here your individual direct contributions.

Dear **Bruce**, you are an amazing supervisor, and I speak plainly, when I say so. I am very grateful for your mentorship and guidance right from our time in Heidelberg to Kaiserslautern and to Saarbrücken. When you asked me to join you in Kaiserslautern for PhD, though I was initially hesitant due to the influence around Heidelberg, I defied the odds to pursue this mission. I am grateful for the opportunity because it paid off. You gave me the flexibility to build my knowledge in the field by attending conferences and presenting my data at any opportunity. The topic was challenging but you helped me through it. The success story is evidenced in the many awards and recognitions I have received over the period. I owe you tones of gratitude. On the other hand, I hope I have fulfilled my part of the bargain, when I promised to join you to form an unbeatable team ☺. I can boldly say your “second place is the first loser” catch phrase is ingrained in my character and propels me to aim higher. Thank you very much Bruce.

Dear **Hannes**, I am very grateful to you for your support throughout my PhD. You challenged me to aim higher. You made me perform experiments that were “near impossible” and I was always ready to rise to the occasion. These acts have made me a better scientist, for which I am very grateful. You were technically my second supervisor ☺ and your inputs into this project are enormous. Thank you for also allowing me stay around to share the oxygen in your lab when the Morgan group moved to Saarbrücken. I am also grateful to you for accepting to be the ‘Vorsitz’ for my thesis examination.

Many thanks to you, Prof. Dr. **Zuzana Storchová**, for the nice collaboration on this project. The intervention of you and **Galal** at the later part of this project wrapped up the story nicely. I am also grateful for accepting to be the second examiner for my thesis examination.

I am grateful to my Bachelor’s student, **Sarah Mergel**, for her assistance to pursue the cell cycle angle of this story. Sarah, your hard work and initial observations made this side of the project worth pursuing. Thank you for the support.

Thank you **Julian Östreicher**, **Gurleen Khandpur**, **Marie Mai** and **Jannik Zimmerman** for providing a congenial atmosphere to work in. You are the best colleagues anyone could wish for. Ours is more than co-workers, but rather, a lab family ☺. I am proud to make you all uncles and aunts in the near future.

Thank you **Vera Nehr** for providing me with technical assistance on this project. Thank you **Andrea Trinkhaus** for being my mum in the lab. I acknowledge your help in getting an apartment to stay in when I was almost stranded. Your efforts helped my wife and I have a home to live in. I am happy to make you an Oma in the near future ☺.

Many thanks to **Simone Adkins**, the best Secretary in the world! You were readily available to solve all my problems ☺. Thank you for help with all my documentations and German translations. When it became difficult for my wife to join me in Kaiserslautern, you made all the calls and wrote all the necessary letters. God bless you!

I am especially grateful to **Felix Boos** for helping to translate the summary of this thesis into the German language. Thank you very much Felix!

To the rest of the Hannes lab, past and present, I am very grateful to you all for your diverse support throughout this project and my stay in Kaiserslautern. Thank you for your criticisms and contributions. Thank you for the cakes ☺ and times we shared together. Thank you **Connie** for making the lab wares ready for experiment and giving me the opportunity to interrupt your work whenever I needed to use the autoclave. Thank you **Sabine** for being an amazing Technician. Thank you **Katja** for learning to be a 'good wife' and showing me what a 'good husband' should do ☺. Thank you **Sree** for being a great friend and colleague. Together with **Gurleen**, you helped prepare my apartment for habitation, for which I owe you two much gratitude. Thank you **Anna** for allowing me to 'de-stress' on you. It was a pleasure to scare you every day, 'Schlagoushi'! Thank you **Sandra** for making me not see you in... 2 years? Thank you **Janina** for being a trustworthy friend and colleague. You will forever remain my 'schatzi' ☺. Thank you **Eva** and **Katharina** for being great colleagues. Thank you **Lena** and **Carina** for being great companions during the final phase of my studies. It was a pleasure to share lab space with you two amazing ladies. You shared my responsibilities in the lab, without me asking, a gesture I really appreciate. Thank you **Vale**, **Michael** and **Ajay** for crossing paths with me in this scientific journey.

To my family and friends in Germany and Ghana, thank you for your kind support. Your prayers and encouragements have made this feat attainable. God bless you all. I also acknowledge financial support from the DFG Priority Program SPP1710, EMBO, TU Nachwuchsring, GlaxoSmithKline and the DAAD for my participation at International conferences.

CURRICULUM VITAE

Prince Saforo Amponsah

Education

01/2016 – 01/2020	Ph.D. , Technische Universität Kaiserslautern Thesis lab: Cellular Biochemistry, Group of Prof. Dr. Bruce Morgan Thesis title: “ <i>PEROXIREDOXINS: Novel mediators of cellular timekeeping</i> ”
10/2013 – 11/2015	Master of Science , Ruprecht-Karls-Universität Heidelberg Course: Molecular Biosciences, Major: Cancer Biology Thesis lab: Molecular OncoSurgery, Universitätsklinikum Heidelberg and German Cancer Research Center (DKFZ) Heidelberg, Group of Prof. Dr. Ingrid Herr Thesis title: “ <i>microRNA regulation of gemcitabine resistance in pancreatic cancer</i> ”
08/2008 – 05/2012	Bachelor of Science , University of Ghana, Legon Specialization: Biochemistry Thesis supervisor: Dr. Kwadwo Asamoah Kusi (Immunology Department, Noguchi Memorial Institute for Medical Research) Thesis title: “ <i>Relationship between avidity and functionality of anti-malarial antibodies from Plasmodium falciparum-exposed individuals</i> ”
2004 – 2007	High School Education/West Africa Senior School Examination , Keta Secondary School

Further Education

09/2011 – 12/2011	CUSAC Semester abroad program at Carleton University, Ottawa (ON), Canada
-------------------	--

Scholarships, Awards and Prizes

15/09/2019	SPP1710 Young Researchers Travel Grant , Thiol-based switches and redox regulation - from microbes to men, St. Feliu de Guixols, Spain
29/05/2019	“ Kongressreisen Stipendien ” of the DAAD, Bonn, Germany
11/04/2019	Best Poster Prize , Nature Conference on Cellular Metabolism, Xiamen, China
27/02/2019	“ Mobilitätsförderung ” (Travel Grant) of the TU Nachwuchsring, TU Kaiserslautern, Germany
28/06/2018	“ Mobilitätsförderung ” (Travel Grant) of the TU Nachwuchsring, TU Kaiserslautern, Germany
22/06/2018	Best Talk Prize , Young Researchers Symposium 2018, Fraunhofer-Center Kaiserslautern, Germany
08/02/2018	Best Poster Prize , Emerging concepts in Mitochondrial Biology Conference, Weizmann Institute of Science, Rehovot, Israel

20/12/2017	Travel Grant , GlaxoSmithKline, München, Germany
21/09/2017	Best Elevator Talk Prize , EMBO Workshop on Thiol oxidation in toxicity and signaling, Sant Feliu de Guixols, Spain
30/06/2017	EMBO Travel Grant (Registration Fee Waiver)
05/07/2016	Best Poster Prize , 3rd Meeting of the study group Redox Biology of the “Gesellschaft für Biochemie und Molekularbiologie” (GBM), Düsseldorf, Germany
08/2015 – 02/2016	Study grant for Master’s thesis, “Gesellschaft der Freunde Universität Heidelberg eV” (GdF), Heidelberg, Germany
28/05/2014	Public Prize for Best Poster Presentation , Young Researchers in Life Sciences Conference, Paris, France
09/2011 – 12/2011	Bursary for Academic Exchange in Canada, Commonwealth Universities Study Abroad Consortium (CUSAC), London, United Kingdom
06/05/2011	Alumni and Shell prizes for Best Level 200 Science Student, University of Ghana, Legon
08/2009 – 05/2011	Academic Sponsorship , Kapadia Education Foundation (for Bachelor’s degree in University of Ghana, Legon)
09/2004 – 06/2007	Government of Ghana Academic Merit Award , Keta Secondary School, Ghana

List of Publications

- Amponsah PS, Metwally G, Mergel S, Storchova Z and Morgan B (2019). Peroxiredoxins couple metabolism and cell division in an ultradian clock. *Nat Chem Biol* (under revision)
- Calabrese G, Peker E, Amponsah PS, Hoehne MN, Riemer T, Mai M, Deponte M, Morgan B, Riemer J (2019). Hyperoxidation of mitochondrial peroxiredoxin limits H₂O₂-induced cell death in yeast. *EMBO J* 38(18):e101552
- Amponsah PS, Fan P, Bauer N, Zhao Z, Gladkich J, Fellenberg J, Herr I (2017). microRNA-210 overexpression inhibits tumor growth and potentially reverses gemcitabine resistance in pancreatic cancer. *Cancer Lett* 388: 107-117
- Amponsah PS (2016). Cellular redox – living chemistry. *Science in School* 36: 15-17
- Morgan B, Van Laer K, Owusu TN, Ezeriņa D, Pastor-Flores D, Amponsah PS, Tursch A, Dick TP (2016). Real-time monitoring of basal H₂O₂ levels with peroxiredoxin-based probes. *Nat Chem Biol* 12(6): 437-43
- Fan P, Liu L, Yin Y, Zhao Z, Zhang Y, Amponsah PS, Xiao X, Bauer N, Abukiwan A, Nwaeburu CC, Gladkich J, Gao C, Schemmer P, Gross W, Herr I (2016). MicroRNA-101-3p reverses gemcitabine resistance by inhibition of ribonucleotide reductase M1 in pancreatic cancer. *Cancer Lett* 373(1):130-7

DECLARATION

I hereby declare that this thesis is a record of bonafide work carried out by me, under the supervision of Prof. Dr. Bruce Morgan, for the award of a Doctorate degree at the Technische Universität Kaiserslautern. No other sources or aids for assistance, other than those specified, were used in the writing of this thesis.

I further declare that the work reported in this thesis has not been submitted and will not be submitted, either in part or full, for the award of any other degree or diploma in this institute or any other institute or University.

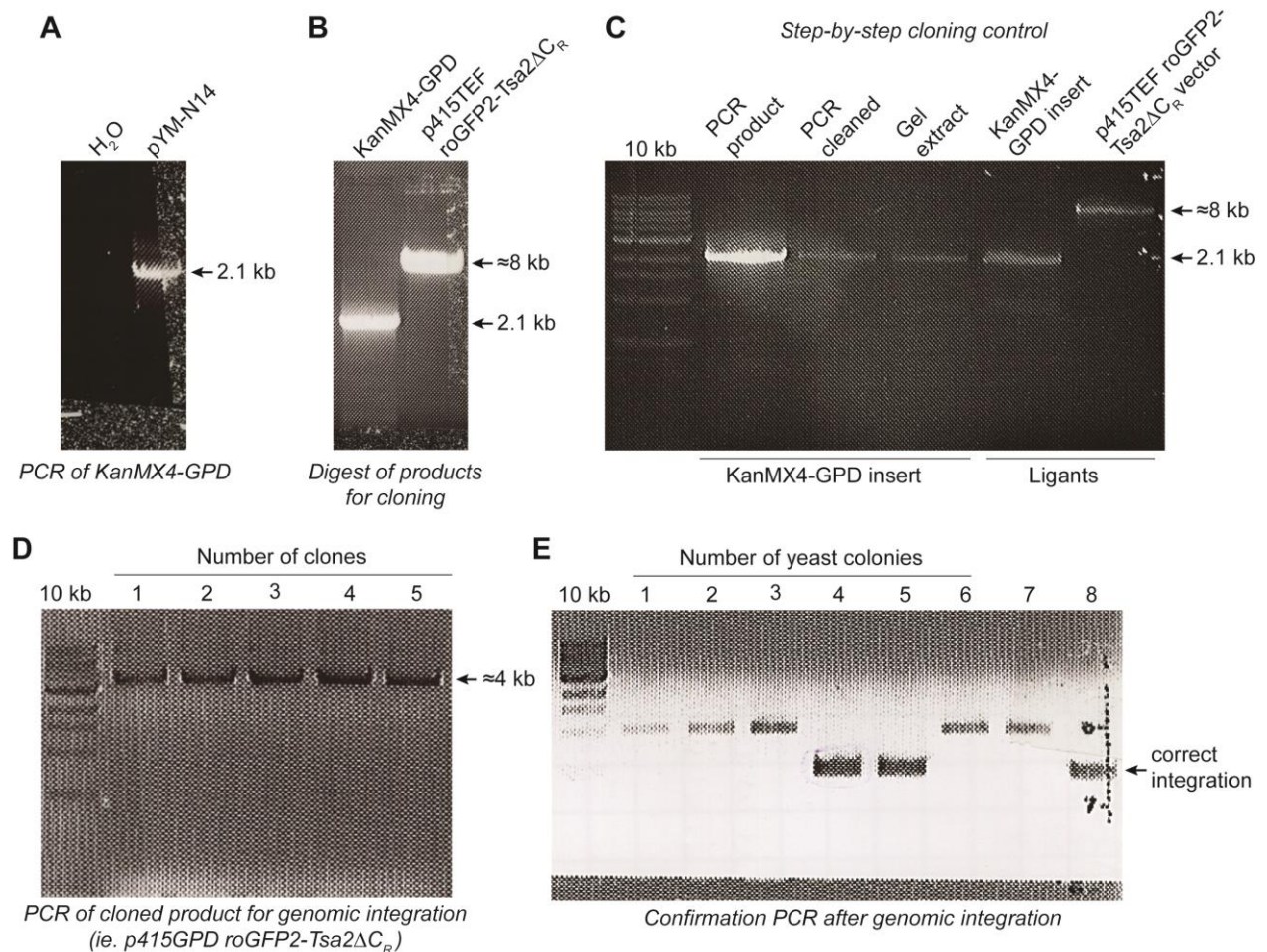
Prince Saforo Amponsah

Kaiserslautern, 28.11.2019

APPENDIX

A1: Construction of a genomically integrated roGFP2-Tsa2 Δ C_R expressing yeast strain

A1.1: PCR amplifications, cloning and confirmation of engineered yeast



Agarose gel showing:

- KanMX4-GPD PCR product amplified from the pYMN-14 plasmid.
- Digest of KanMX4-GPD PCR product and p415TEF roGFP2-Tsa2 Δ C_R plasmid with appropriate restriction enzymes, for subsequent ligation.
- Step-by-step control of KanMX4-GPD roGFP2-Tsa2 Δ C_R plasmid construction process.
- Confirmation of constructed KanMX4-GPD roGFP2-Tsa2 Δ C_R plasmid by PCR.
- Confirmation by PCR, of yeast cells showing successful genomic integration of the KanMX4-GPD roGFP2-Tsa2 Δ C_R biosensor construct.

A1.2: Sequence map of re-constituted p415 roGFP2-Tsa2ΔCr plasmid for PCR and genomic integration (5' → 3')

GACGAAAGGGCCTCGTGATACGCCTATTTTTATAGGTTAATGTCATGATAATAATGGTTTCTT
AGGACGGATCGCTTGCCTGTAACCTACACGCGCCTCGTATCTTTAATGATGGAATAATTTG
GGAATTTACTCTGTGTTTATTTATTTTTATGTTTTGTATTTGGATTTTAGAAAGTAAATAAAG
AAGGTAGAAGAGTTACGGAATGAAGAAAAAAAAATAAACAAAGGTTTAAAAAATTTCAAC
AAAAAGCGTACTTTACATATATATTTATTAGACAAGAAAAGCAGATTAATAGATATACATT
CGATTAACGATAAGTAAAATGTAAAATCACAGGATTTTCGTGTGTGGTCTTCTACACAGACA
AGATGAAACAATTCGGCATTAAACCTGAGAGCAGGAAGAGCAAGATAAAAGGTAGTATTT
GTTGGCGATCCCCCTAGAGTCTTTTACATCTTCGGAAAACAAAACTATTTTTTCTTTAATTT
CTTTTTTACTTTCTATTTTTAATTTATATATTTATATTAATAAAATTTAAATTATAATTTT
ATAGCACGTGATGAAAAGGACCCAGGTGGCACTTTTCGGGGAAATGTGCGCGGAACCCCTA
TTTGTTTATTTTTCTAAATACATTCAAATATGTATCCGCTCATGAGACAATAACCCTGATAAA
TGCTTCAATAATATTGAAAAGGAAGAGTATGAGTATTCAACATTTCCGTGTGCGCCCTTATT
CCCTTTTTTGCGGCATTTCCTTTCCTGTTTTTGTCTACCCAGAAACGCTGGTGAAAGTAAAA
GATGCTGAAGATCAGTTGGGTGCACGAGTGGGTTACATCGAACTGGATCTCAACAGCGGTA
AGATCCTTGAGAGTTTTCGCCCCGAAGAACGTTTTCCAATGATGAGCACTTTTAAAGTTCTGC
TATGTGGCGCGGTATTATCCCGTATTGACGCCGGGCAAGAGCAACTCGGTGCGCCGCATACAC
TATTCTCAGAATGACTTGGTTGAGTACTACCAGTCACAGAAAAGCATCTTACGGATGGCAT
GACAGTAAGAGAATTATGCAGTGCTGCCATAACCATGAGTGATAACACTGCGGCCAACTTA
CTTCTGACAACGATCGGAGGACCGAAGGAGCTAACCCTTTTTTGCACAACATGGGGGATCA
TGTAACTCGCCTTGATCGTTGGGAACCGGAGCTGAATGAAGCCATACCAAACGACGAGCGT
GACACCACGATGCCTGTAGCAATGGCAACAACGTTGCGCAAATTAACTGGCGAACTACT
TACTCTAGCTTCCCGGCAACAATTAATAGACTGGATGGAGGCGGATAAAGTTGCAGGACCA
CTTCTGCGCTCGGCCCTTCCGGCTGGCTGGTTTATTGCTGATAAATCTGGAGCCGGTGAGCGT
GGGTCTCGCGGTATCATTGCAGCACTGGGGCCAGATGGTAAGCCCTCCCGTATCGTAGTTAT
CTACACGACGGGAGTCAGGCAACTATGGATGAACGAAATAGACAGATCGCTGAGATAGGT
GCCTCACTGATTAAGCATTGGTAACTGTCAGACCAAGTTTACTCATATATACTTTAGATTGAT
TTAAACTTCATTTTTAATTTAAAAGGATCTAGGTGAAGATCCTTTTTGATAATCTCATGACC
AAAATCCCTTAACGTGAGTTTTTCGTTCCACTGAGCGTCAGACCCCGTAGAAAAGATCAAAGG
ATCTTCTTGAGATCCTTTTTTCTGCGCGTAATCTGCTGCTTGCAAACAAAAAAACCACCGCT
ACCAGCGGTGGTTTGTGTTGCCGGATCAAGAGCTACCAACTCTTTTTCCGAAGGTAACCTGGCT
TCAGCAGAGCGCAGATACCAAATACTGTCCTTCTAGTGTAGCCGTAGTTAGGCCACCACTTC
AAGAACTCTGTAGCACCGCCTACATACTCGCTCTGCTAATCCTGTTACCAGTGGCTGCTGCC
AGTGGCGATAAGTCGTGTCTTACCGGGTTGGACTCAAGACGATAGTTACCGGATAAGGCGC
AGCGGTGCGGGCTGAACGGGGGGTTCGTGCACACAGCCCAGCTTGGAGCGAACGACCTACAC







CGAACTGAGATACCTACAGCGTGAGCTATGAGAAAGCGCCACGCTTCCCGAAGGGAGAAAG
GCGGACAGGTATCCGGTAAGCGGCAGGGTCGGAACAGGAGAGCGCACGAGGGAGCTTCCA
GGGGGAAACGCCTGGTATCTTTATAGTCCTGTCTGGGTTTCGCCACCTCTGACTTGAGCGTCG
ATTTTTGTGATGCTCGTCAGGGGGGCGGAGCCTATGGAAAAACGCCAGCAACGCGGCCTTTT
TACGGTTCCTGGCCTTTTGTGGCCTTTTGTCTACATGTTCTTTCCTGCGTTATCCCCTGATTC
TGTGGATAACCGTATTACCGCCTTTGAGTGAGCTGATACCGCTCGCCGACGCCGAACGACCG
AGCGCAGCGAGTCAGTGAGCGAGGAAGCGGAAGAGCGCCCAATACGCAAACCGCCTCTCCC
CGCGCGTTGGCCGATTCAATTAATGCAGCTGGCACGACAGGTTTCCCGACTGGAAAGCGGGCA
GTGAGCGCAACGCAATTAATGTGAGTTACCTCACTCATTAGGCACCCCAGGCTTTACACTTT
ATGCTTCGGCTCCTATGTTGTGTGGAATTGTGAGCGGATAACAATTTACACAGGAAACAG
CTATGACCATGATTACGCCAAGCGCGCAATTAACCCTCACTAAAGGGAACAAAAGCTG**GAG**
CTCATAGCTTCAAATGTTTCTACTCCTTTTTTACTCTTCCAGATTTTCTCGGACTCCGCGCAT
CGCCGTACCACTTCAAACACCCAAGCACAGCATACTAAATTTCCCCTCTTCTTCTCTAGG
GTGTCGTTAATTACCGTACTAAAGGTTTGGAAAAGAAAAAAGAGACCGCCTCGTTTCTTTT
TCTTCGTCGAAAAAGGCAATAAAAATTTTTATCACGTTTCTTTTTTCTTGAAAATTTTTTTTTG
ATTTTTTCTCTTTCGATGACCTCCCATTGATATTTAAGTTAATAAACGGTCTTCAATTTCTCA
AGTTTCAGTTTCATTTTTCTTGTCTATTACAACTTTTTTTACTTCTTGCTCATTAGAAAGAAA
GCATAGCAATCTAATCTAAGTTT**TCTAGAGGATCC**ACC**ATGGCTAGCCGTACGCTGCAGGTC**
GACGGATCCCCGGGTTAATTAAGGCGCGCCAGATCTGTTTAGCTTGCCCTCGTCCCCGCCGGG
TCACCCGGCCAGCGACATGGAGGCCAGAATACCCTCCTTGACAGTCTTGACGTGCGCAGCT
CAGGGGCATGATGTGACTGTCGCCGTACATTTAGCCATAACATCCCATGTATAATCATT
GCATCCATACATTTTGATGGCCGCACGGCGCGAAGCAAAAATTACGGTCTCTCGCTGCAGAC
CTGCGAGCAGGGAAACGCTCCCCTCACAGACGCGTTGAATTGTCCCCACGCCGCGCCCCTGT
AGAGAAATATAAAAGGTTAGGATTTGCCACTGAGGTTCTTCTTTCATATACTTCTTTTAAAA
TCTTGCTAGGATACAGTTCTCACATCACATCCGAACATAAACAACCATGGGTAAGGAAAAG
ACTCACGTTTCGAGGCCGCGATTAAATTCCAACATGGATGCTGATTTATATGGGTATAAATG
GGCTCGCGATAATGTCGGGCAATCAGGTGCGACAATCTATCGATTGTATGGGAAGCCCGATG
CGCCAGAGTTGTTTCTGAAACATGGCAAAGGTAGCGTTGCCAATGATGTTACAGATGAGATG
GTCAGACTAAACTGGCTGACGGAATTTATGCCTCTTCCGACCATCAAGCATTATCCGACT
CCTGATGATGCATGGTTACTCACCCTGCGATCCCCGGCAAAAACAGCATTCCAGGTATTAGA
AGAATATCCTGATTCAGGTGAAAATATTGTTGATGCGCTGGCAGTGTTCTGCGCCGGTTGC
ATTCGATTCCTGTTTGAATTGTCTTTAACAGCGATCGCGTATTCGTCTCGCTCAGGCCG
AATCACGAATGAATAACGGTTTGGTTGATGCGAGTGATTTTGTGACGAGCGTAATGGCTGG
CCTGTTGAACAAGTCTGGAAAGAAATGCATAAGCTTTTGCCATTCTACCGGATTCAGTCGT
CACTCATGGTGATTTCTCACTTGATAACCTTATTTTTGACGAGGGGAAATTAATAGGTTGTAT
TGATGTTGGACGAGTCGGAATCGCAGACCGATAACCAGGATCTTGCCATCCTATGGAACCTGCC
TCGGTGAGTTTTCTCCTTCATTACAGAAACGGCTTTTTCAAATAATGGTATTGATAATCCTG

ATATGAATAAATTGCAGTTTCATTTGATGCTCGATGAGTTTTTCTAATCAGTACTGACAATAA
AAAGATTCTTGTTTTCAAGAACTTGTCAATTTGTATAGTTTTTTTATATTGTAGTTGTTCTATTT
TAATCAAATGTTAGCGTGATTTATATTTTTTTTTTCGCCTCGACATCATCTGCCAGATGCGAAG
TTAAGTGCGCAGAAAGTAATATCATGCGTCAATCGTATGTGAATGCTGGTTCGCTATACTGCT
GTCGATTTCGATACTAA CGCCGCCATCCAGTGTGAAAAC GAGCTCAGTTTATCATTATCAAT
ACTCGCCATTTCAAAGAATACGTAAATAATTAATAGTAGTGATTTTCCTAACTTTATTTAGTC
AAAAAATTAGCCTTTTAATTCTGCTGTAACCCGTACATGCCAAAATAGGGGGCGGGTTACA
CAGAATATATAACATCGTAGGTGTCTGGGTGAACAGTTTATTCCTGGCATCCACTAAATATA
ATGGAGCCCGCTTTTTAAGCTGGCATCCAGAAAAAAAAAAGAATCCCAGCACCAAAATATTG
TTTTCTTACCAACCATCAGTTCATAGGTCCATTCTCTTAGCGCAACTACAGAGAACAGGGG
CACAAACAGGCAAAAAACGGGCACAACCTCAATGGAGTGATGCAACCTGCCTGGAGTAAAT
GATGACACAAGGCAATTGACCCACGCATGTATCTATCTCATTCTTACACCTTCTATTACCT
TCTGCTCTCTGATTTGAAAAAGCTGAAAAAAAAGGTTGAAACCAGTCCCTGAAATTAT
TCCCCTACTTGACTAATAAGTATATAAAGACGGTAGGTATTGATTGTAATTCTGTAAATCTAT
TTCTTAAACTTCTTAAATTCTACTTTTATAGTTAGTCTTTTTTTTAGTTTTAAAACACCAGAAC
TTAGTTTCGACGGATTCTAGAACTAGTGGATCCCCCGGACGACAGAGAATTCATCGATGG
CTAGCGAATTCTCAAAGGGTGAAGAATTGTTTACAGGTGTTGTTCCATTTTTAGTCGAATTGG
ACGGTGACGTTAATGGTCATAAGTTTAGTGTAGTGGTGAAGGTGAAGGTGACGCAACATAC
GGTAAATTGACCTTGAAGTTTATTTCAACTACTGGTAAATTGCCAGTTCCTTGGCCAACCTTG
GTAACCCTTTAACATATGGTGTACAATGTTTCAGTAGATACCCTGATCATATGAAACAACA
CGACTTTTTCAAGTCTGCTATGCCAGAAGGTTACGTTCAAGAAAGAACTATTTTCTTTAAGG
ATGACGGTAACTACAAGACCAGAGCAGAAGTCAAATTTGAAGGTGACACTTTGGTTAACAG
AATCGAATTGAAGGGTATCGATTTCAAGGAAGACGGTAAACATCTTGGGTCATAAATTGGAAT
ACAACACTACAACCTGTCACAATGTATACATAATGGCCGATAAGCAAAAAGAATGGTATCAAAGT
CAACTTCAAGATCAGACATAACATCGAAGATGGTCTGTTCAATTAGCTGACCACTATCAAC
AAAATACACCTATTGGTGACGGTCTGTTTTGTTACCAGACAACCATTACTTGTCTACCTGCT
CAGCTTTATCCAAAGATCCAAATGAAAAGAGAGACCATATGGTATTGTTAGAATTTGTCACC
GCAGCAGGTATCACATTGGGTATGGATGAATTGTATAAAACTAGTGGTGGTTCAGGTGGTGG
TGGTTCAGGTGGTGGTGGTTCAGGTGGAGGAGGATCAGGAGGAGGAGGATCAGGAGGAGG
AGGATCAGGAGGAGAATTCGTAGCAGAAGTTCAAAAACAAGCCCCACCATTTAAGAAAACC
GCCGTAGTCGACGGTATCTTCGAGGAAATTTCACTGGAAAAGTATAAAGGTAAGTACGTTGT
TCTAGCTTTTGTCCATTGGCTTTTTCATTTGTCTGTCCAACCTGAGATTGTTGCGTTTTCCGAT
GCCGCCAAGAAATTCGAAGATCAGGGCGCCAAGTTTTATTTGCCTCCACCGACTCTGAATA
TTCCTTACTGGCATGGACCAACCTTCCCAGAAAAGACGGTGGATTAGGTCCAGTTAAAGTTC
CTTTGCTTGCTGATAAGAATCATTCCTTATCCAGAGACTATGGCGTTTTGATTGAAAAAGAA
GGTATAGCTTTAAGAGGTTTGTTCATAATCGACCCGAAGGGAATCATTAGACATATCACTAT
CAATGATTTATCTGTTGGCAGAAACGTCAATGAAGCTTTGAGATTAGTCGAAGGTTTCCAGT

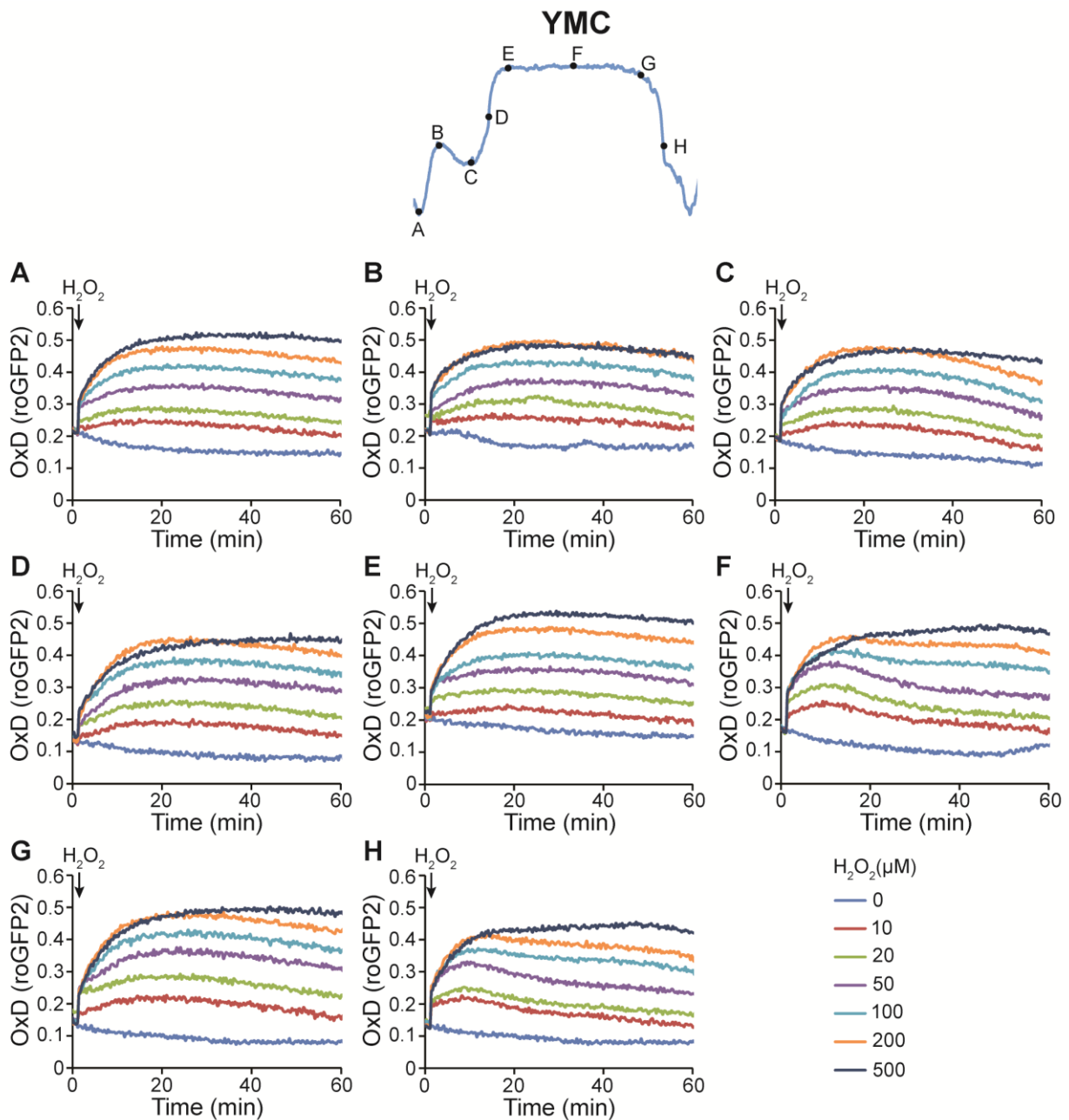
GGACTGACAAAAATGGTACAGTTTTGCCATGCAACTGGACCCAGGAGCCGCCACCATCAA
ACCTGACGTTAAAGATTCCAAGGAGTATTTCAAAAATGCCAATAATTAACCTCGAGTCATGTA
ATTAGTTATGTCACGCTTACATTCACGCCCTCCCCCACATCCGCTCTAACCGAAAAGGAAG
GAGTTAGACAACCTGAAGTCTAGGTCCTATTTATTTTTTATAGTTATGTTAGTATTAAGAA
CGTTATTTATATTTCAAATTTTTCTTTTTTTCTGTACAGACGCGTGTACGCATGTAACATTAT
ACTGAAAACCTTGCTTGAGAAGGTTTTGGGACGCTCGAAGGCTTTAATTTGCGGCCGGTACC
CAATTCGCCCTATAGTGAGTCGTATTACGCGCGCTCACTGGCCGTCGTTTTACAACGTCGTGA
CTGGGAAAACCTGGCGTTACCCAACCTAATCGCCTTGCAGCACATCCCCCTTTCGCCAGCT
GGCGTAATAGCGAAGAGGCCCGCACCGATCGCCCTTCCAACAGTTGCGCAGCCTGAATGG
CGAATGGCGCGACGCGCCCTGTAGCGGCGCATTAAAGCGCGGGGTGTGGTGGTTACGCGC
AGCGTGACCGCTACACTTGCCAGCGCCCTAGCGCCCGCTCCTTTCGCTTTCTTCCCTTCCTTT
CTCGCCACGTTTCGCCGGCTTTCCCCGTCAAGCTCTAAATCGGGGGCTCCCTTTAGGGTTCCGA
TTTAGTGCTTTACGGCACCTCGACCCCAAAAACCTTGATTAGGGTGATGGTTCACGTAGTGG
GCCATCGCCCTGATAGACGGTTTTTCGCCCTTTGACGTTGGAGTCCACGTTCTTTAATAGTGG
ACTCTTGTCCAAACTGGAACAACACTCAACCCTATCTCGGTCTATTCTTTTGATTTATAAGG
GATTTTGCCGATTTTCGGCCTATTGGTTAAAAAATGAGCTGATTTAACAAAAATTTAACGCGA
ATTTTAACAAAATATTAACGTTTACAATTTCTGATGCGGTATTTTCTCCTTACGCATCTGTG
CGGTATTTACACCGCATATCGACGGTCGAGGAGAACTTCTAGTATATCCACATACCTAATA
TTATTGCCTTATTA AAAATGGAATCCCAACAATTACATCAAAATCCACATTCTTTCAAATC
AATTGTCCTGTACTTCCTTGTTTCATGTGTGTTCAAAAACGTTATATTTATAGGATAATTATAC
TCTATTTCTCAACAAGTAATTGGTTGTTTGGCCGAGCGGTCTAAGGCGCCTGATTCAAGAAA
TATCTTGACCGCAGTTAACTGTGGGAATACTCAGGTATCGTAAGATGCAAGAGTTTCAATCT
CTTAGCAACCATTATTTTTTCTCAACATAACGAGAACACACAGGGGCGCTATCGCACAGA
ATCAAATTCGATGACTGGAAATTTTTGTTAATTTTCAAGAGTTCGCCTGACGCATATACCTTTT
TCAACTGAAAAATTGGGAGAAAAAGGAAAGGTGAGAGGCCGGAACCGGCTTTTCATATAGA
ATAGAGAAGCGTTCATGACTAAATGCTTGCATCACAATACTTGAAGTTGACAATATTATTTA
AGGACCTATTGTTTTTTCCAATAGGTGGTTAGCAATCGTCTTACTTTCTAACTTTTCTTACCTT
TTACATTTTCAAGCAATATATATATATATTTTCAAGGATATACCATTCTAATGTCTGCCCTATGT
CTGCCCTAAGAAGATCGTCGTTTTTGGCAGGTGACCACGTTGGTCAAGAAATCACAGCCGAA
GCCATTAAGGTTCTTAAAGCTATTTCTGATGTTTCGTTCCAATGTCAAGTTTCGATTTTCGAAAAT
CATTTAATTGGTGGTGCTGCTATCGATGCTACAGGTGTCCCACTTCCAGATGAGGCGCTGGA
AGCCTCCAAGAAGGTTGATGCCGTTTTGTTAGGTGCTGTGGGTGGTCCATAATGGGGTACCG
GTAGTGTTAGACCTGAACAAGGTTTACTAAAAATCCGTAAAGAACTTCAATTGTACGCCAAC
TTAAGACCATGTAACCTTTCATCCGACTCTCTTTTAGACTTATCTCCAATCAAGCCACAATTT
GCTAAAGGTAAGTACTGACTTCGTTGTTGTCAGAGAATTAGTGGGAGGTATTTACTTTGGTAAGAG
AAAGGAAGACGATGGTGTGTTGTCGCTTGGGATAGTGAACAATACACCGTTCCAGAAGTG
CAAAGAATCACAAGAATGGCCGCTTTCATGGCCCTACAACATGAGCCACCATTGCCTATTTG

GTCCTTGGATAAAGCTAATGTTTTGGCCTCTTCAAGATTATGGAGAAAACTGTGGAGGAAA
CCATCAAGAACGAATTCCCTACATTGAAGGTTCAACATCAATTGATTGATTCTGCCGCCATG
ATCCTAGTTAAGAACCCAACCCACCTAAATGGTATTATAATCACCAGCAACATGTTTGGTGA
TATCATCTCCGATGAAGCCTCCGTTATCCCAGGTTCCCTGGGTTTGTGTCATCTGCGTCCTT
GGCCTCTTTGCCAGACAAGAACACCGCATTTGGTTTGTACGAACCATGCCACGGTTCTGCTC
CAGATTTGCCAAAGAATAAGGTTGACCCTATCGCCACTATCTTGTCTGCTGCAATGATGTTG
AAATTGTCATTGAACTTGCCTGAAGAAGGTAAGGCCATTGAAGATGCAGTTAAAAAGGTTTT
GGATGCAGGTATCAGAACTGGTGATTTAGGTGGTTCCAACAGTACCACCGAAGTCGGTGATG
CTGTCGCCGAAGAAGTTAAGAAAATCCTTGCTTAAAAAGATTCTCTTTTTTTATGATATTTGT
ACATAAACTTTATAAATGAAATTCATAATAGAAACGACACGAAATTACAAAATGGAATATG
TTCATAGGGTAGACGAAACTATATACGCAATCTACATACATTTATCAAGAAGGAGAAAAAG
GAGGATAGTAAAGGAATACAGGTAAGCAAATTGATACTAATGGCTCAACGTGATAAGGAAA
AGAATTGCACTTTAACATTAATATTGACAAGGAGGAGGGCACCACACAAAAAGTTAGGTG
TAACAGAAAATCATGAAACTACGATTCTAATTTGATATTGGAGGATTTTCTCTAAAAAAA
AAAAATACAACAAATAAAAAACACTCAATGACCTGACCATTTGATGGAGTTTAAGTCAATA
CCTTCTTGAACCATTTCCATAATGGTGAAAGTTCCCTCAAGAATTTTACTCTGTCAGAAACG
GCCTTACGACGTAGTCGATATGGTGCCTCTCAGTACAATCTGCTCTGATGCCGCATAGTTA
AGCCAGCCCCGACACCCGCCAACACCCGCTGACGCGCCCTGACGGGCTTGTCTGCTCCCGGC
ATCCGCTTACAGACAAGCTGTGACCGTCTCCGGGAGCTGCATGTGTCAGAGGTTTTACCCGT
CATCACCGAAACGCGCGA

Colour codes:

-  KanMX4 marker
-  GPD promoter
-  roGFP2 domain
-  Linker domain
-  Ts2ΔC_R domain
- Binding sites for primers P3 and P4
-  Restriction sites

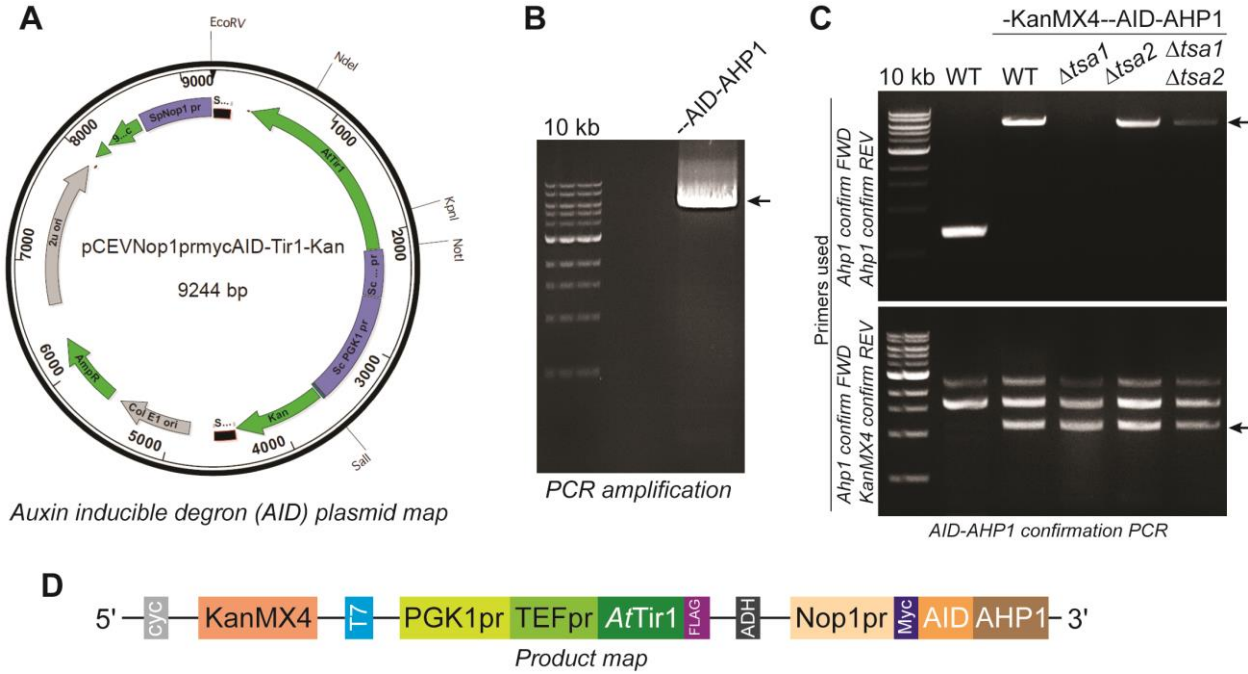
A2: Confirmation of functional roGFP2-Tsa2ΔC_R biosensor under continuous culture conditions in the fermenter



RoGFP2-Tsa2ΔC_R biosensor expressing cells sampled from various phases of the YMC respond to H₂O₂ in a concentration dependent manner.

A3: Construction of yeast strains capable of conditional genomic Ahp1 depletion via an auxin-inducible degron (AID) system

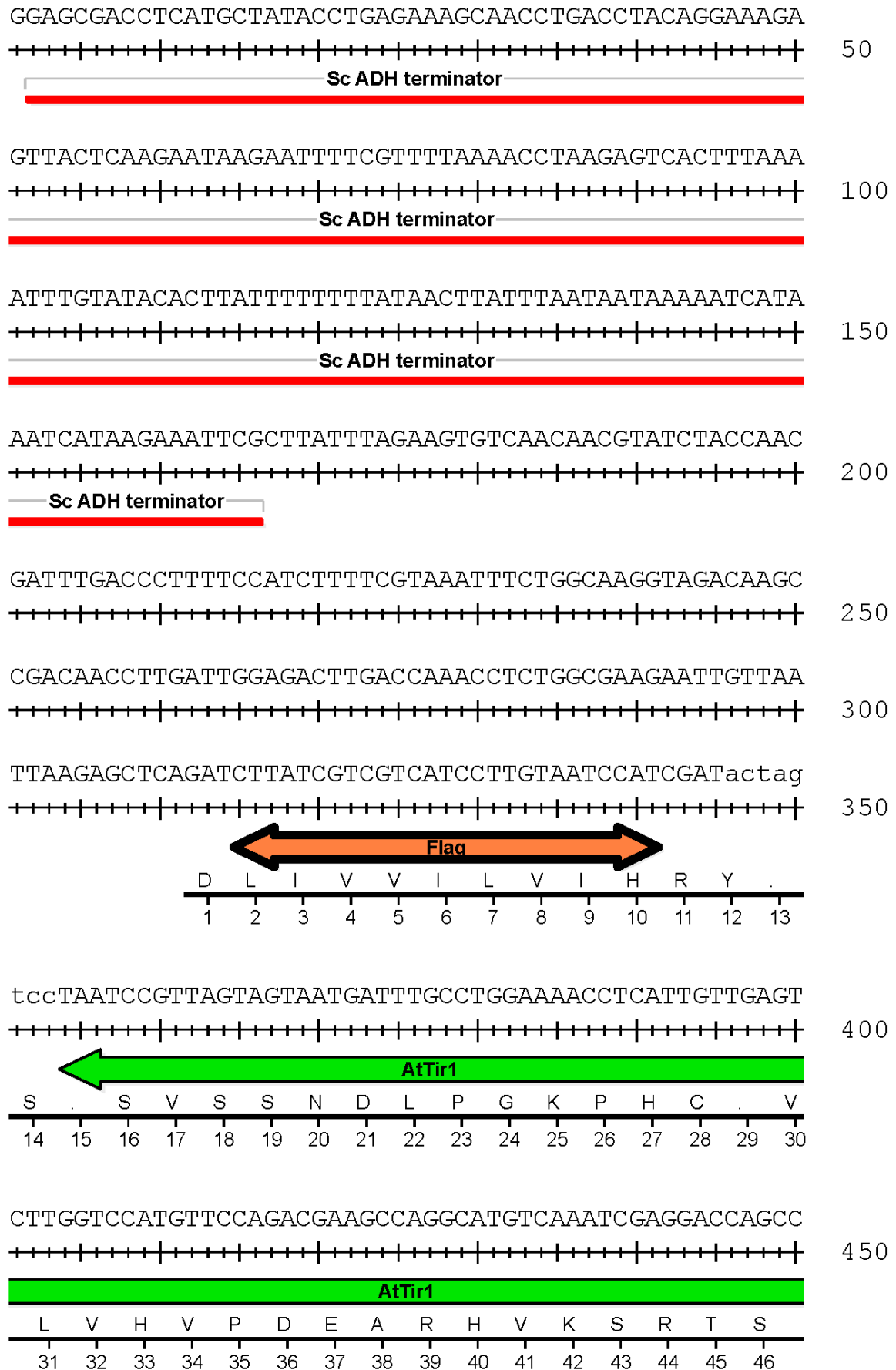
A3.1: PCR amplifications, cloning and confirmation of engineered yeast



- A. Map of AID/A/TIR1 plasmid.
- B. Agarose gel showing PCR product from amplification of the AID/A/TIR1 plasmid for genomic integration.
- C. Agarose gel showing confirmation by PCR, of various yeast strains showing successful genomic integration of the Ahp1-AID/A/TIR1 construct.
- D. Product map of the genomically integrated construct

A3.2: Sequence map of AP2099 (pCEVNop1prmycAID-Tir1-Kan) as provided by Prof. Dr.

Blanche Schwappach (5' → 3')



TCAAGCTCTTTCAGATTCTGCAAGTGGCAGCGATAGCAGCGAGACCATC 1700

AtTir1

V K L F Q I P A S G S D S S E T I
447 448 449 450 451 452 453 454 455 456 457 458 459 460 461 462 463

GGTGGAGAAGCCTTCGCAGGAAGAAAGCACAGAACCTTAAAATTCTTAA 1750

AtTir1

G G E A F A G R K H K N L K I L K
464 465 466 467 468 469 470 471 472 473 474 475 476 477 478 479 480

AAGACTTGGCTATGAGCTCCAAGCAATCGTCGGTGACCACCATCCTCTTC 1800

AtTir1

R L G Y E L Q A I V G D H H P L
481 482 483 484 485 486 487 488 489 490 491 492 493 494 495 496

AGCCTTATCTCTTCAAGCCACGTGTAAGACGAAGACATGGCCTCAATCCA 1850

AtTir1

Q P Y L F K P R V R R R H G L N P
497 498 499 500 501 502 503 504 505 506 507 508 509 510 511 512 513

KpnI

TGGATACACGTAACCTCCCCATCCGTCAGGTACCAAATTAAAGTCAGCAA 1900

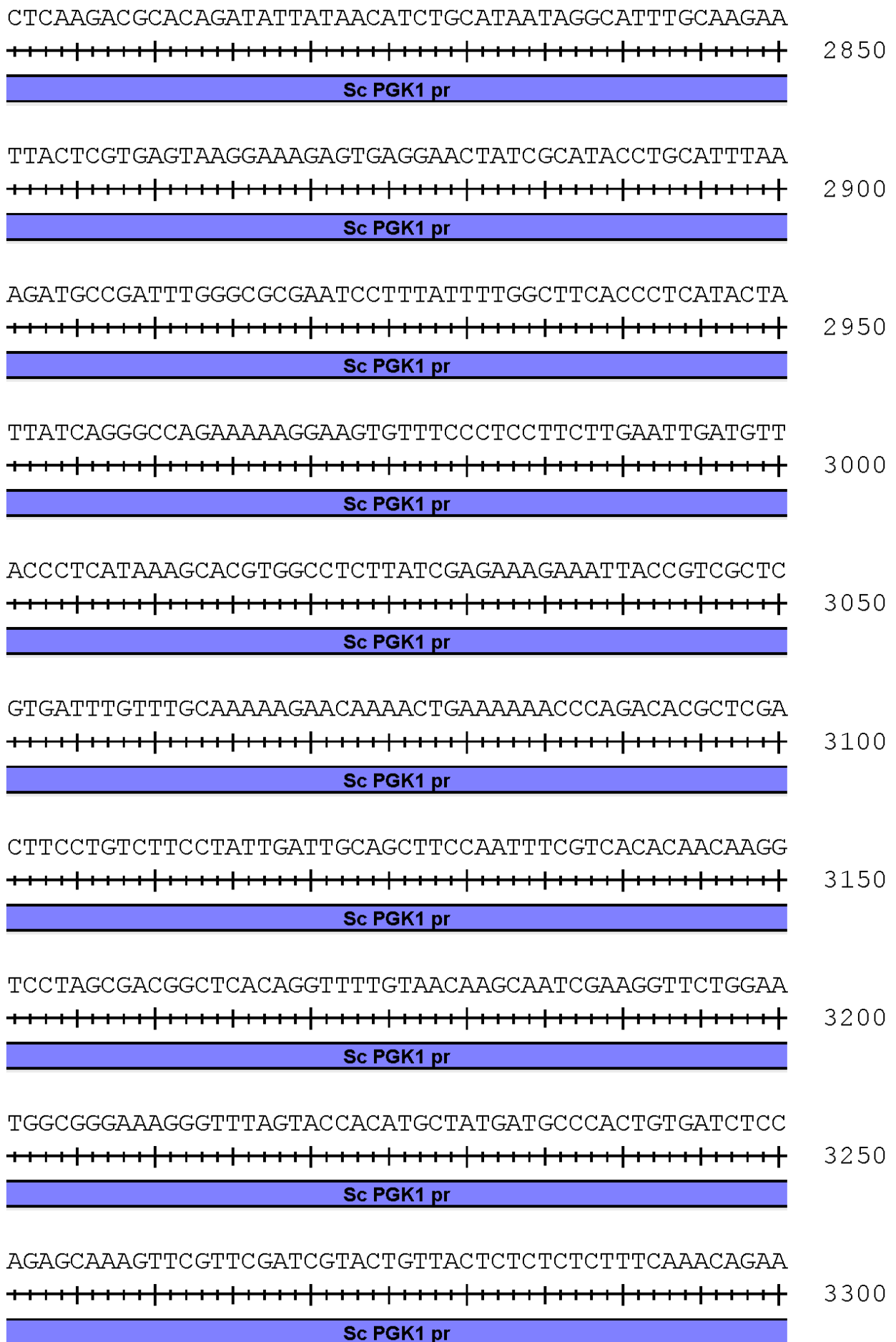
AtTir1

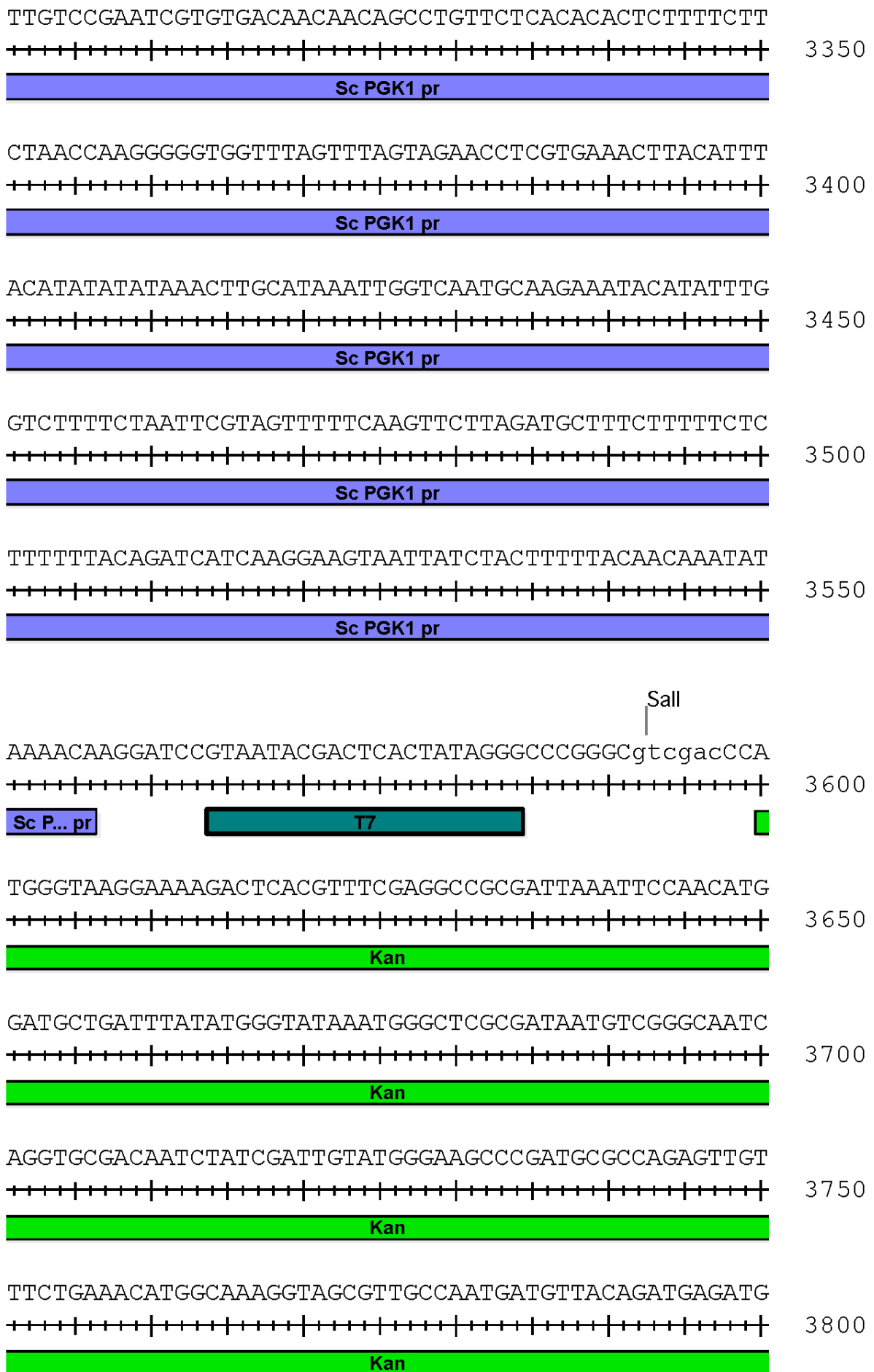
W I H V T S P S V R Y Q I K V S K
514 515 516 517 518 519 520 521 522 523 524 525 526 527 528 529 530

AGTGAGGTTTTCTTTAAGCTCCACGGATCTCACTTTCGGGAACCTCCTA 1950

AtTir1

V R F S F K L H G S H F R E P P
531 532 533 534 535 536 537 538 539 540 541 542 543 544 545 546





CGGTGAGTTTTCTCCTTCATTACAGAAACGGCTTTTTCAAAAATATGGTA 4350

Kan

TTGATAATCCTGATATGAATAAATTGCAGTTTCATTTGATGCTCGATGAG 4400

Kan

TTTTTCTAAcgGCTAGCTAAGATCCGCTCTAACCgAAAAGGAAGGAGTTA 4450

Kan →

Sc Cyc terminator

GACAACCTGAAGTCTAGGTCCCTATTTATTTTTTTATAGTTATGTTAGTA 4500

Sc Cyc terminator

TTAAGAACGTTATTTATATTTCAAATTTTTCTTTTTTTCTGTACAGACG 4550

Sc Cyc terminator

CGTGTACGCATGTAACATTATACTGAAAACCTTGCTTGAGAA**GGTTTTGG** 4600

Sc Cyc terminator

GACGCTCGAAGATCCAGCTGCATTAATGAATCGGCCAACGCGCGGGGAGA 4650

Sc Cyc ...inator

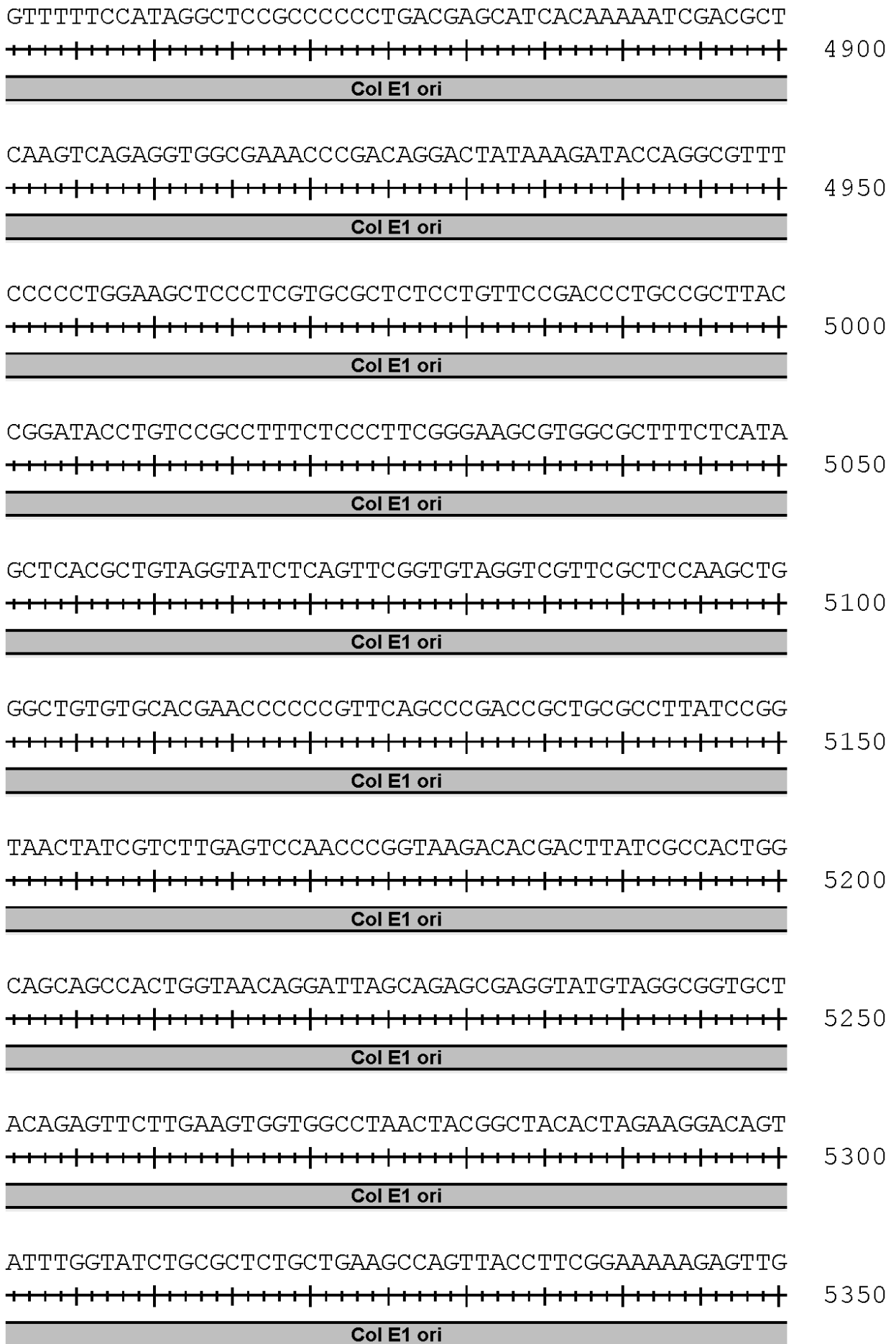
GGCGGTTTGCGTATTGGGCGCTCTTCCGCTTCCTCGCTCACTGACTCGCT 4700

GCGCTCGGTCGTTCGGCTGCGGCGAGCGGTATCAGCTCACTCAAAGGCGG 4750

TAATACGGTTATCCACAGAATCAGGGGATAACGCAGGAAAGAACATGTGA 4800

GCAAAGGCCAGCAAAGGCCAGGAACCGTAAAAAGGCCGCGTTGCTGGC 4850

Col E1 ori



TGCGCTCTATAATGCAGTCTCTTGATAACTTTTTGCACTGTAGGTCCGTT 7000

2u ori

AAGGTTAGAAGAAGGCTACTTTGGTGTCTATTTTCTCTTCCATAAAAAAA 7050

2u ori

GCCTGACTCCACTTCCCGCGTTTACTGATTACTAGCGAAGCTGCGGGTGC 7100

2u ori

ATTTTTTCAAGATAAAGGCATCCCCGATTATATTCTATACCGATGTGGAT 7150

2u ori

TGCGCATACTTTGTGAACAGAAAGTGATAGCGTTGATGATTCTTCATTGG 7200

2u ori

TCAGAAAATTATGAACGGTTTCTTCTATTTTGTCTCTATATACTACGTAT 7250

2u ori

AGGAAATGTTTACATTTTTCGTATTGTTTTTCGATTCACTCTATGAATAGTT 7300

2u ori

CTTACTACAATTTTTTTGTCTAAAGAGTAATACTAGAGATAAACATAAAA 7350

2u ori

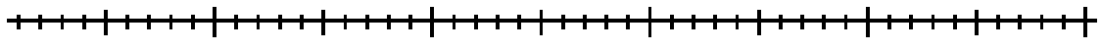
AATGTAGAGGTCGAGTTTAGATGCAAGTTCAAGGAGCGAAAGGTGGATGG 7400

2u ori

GTAGGTTATATAGGGATATAGCACAGAGATATATAGCAAAGAGATACTTT 7450

2u ori

TGAGCAATGTTTGTGGAAGCGGTATTCGCAATATTTTAGTAGCTCGTTAC

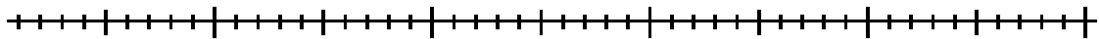


7500



2u ori

AGTCCGGTGCGTTTTTGGTTTTTTGAAAGTGCGTCTTCAGAGCGCTTTTG

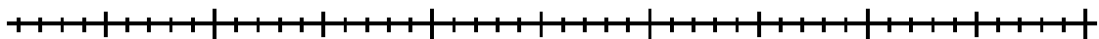


7550

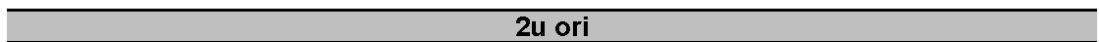


2u ori

GTTTTCAAAGCGCTCTGAAGTTCCTATACTTTCTAGAGAATAGGAACTT

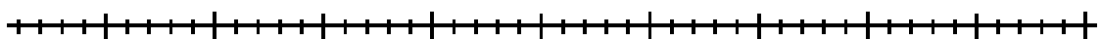


7600



2u ori

CGGAATAGGAACTTCAAAGCGTTTCCGAAAACGAGCGCTTCCGAAAATGC

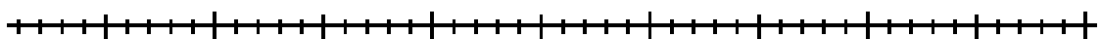


7650



2u ori

AACGCGAGCTGCGCACATACAGCTCACTGTTTCACGTCGCACCTATATCTG

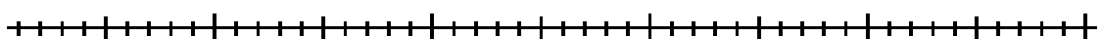


7700



2u ori

CGTGTTGCCTGTATATATATATACATGAGAAGAACGGCATAGTGCGTGTT

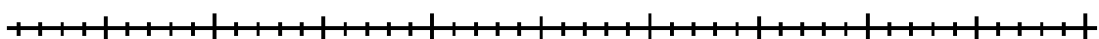


7750



2u ori

TATGCTTAAATGCGTACTTATATGCGTCTATTTATGTAGGATGAAAGGTA

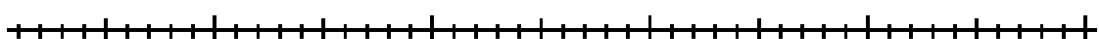


7800



2u ori

GTCTAGTACCTCCTGTGATATTATCCCATTCCATGCGGGGTATCGTATGC

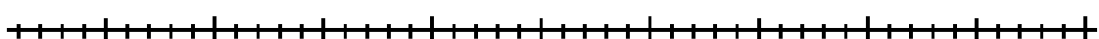


7850



2u ori

TTCTTCAGCACTACCCCTTAGCTGTTCTATATGCTGCCACTCCTCAATT

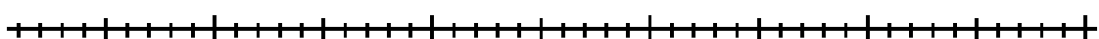


7900

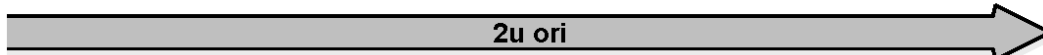


2u ori

GGATTAGTCTCATCCTTCAATGCTATCATTTCTTTGATATTGGATCATG

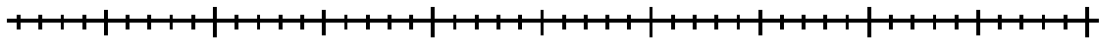


7950



2u ori

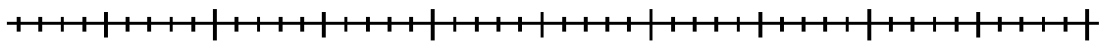
GTAGACAACCCTTAATATAACTTCGTATAATGTATGCTATACGAAGTTAT



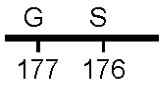
8000



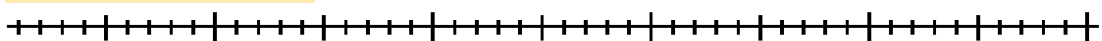
TAGGTCTAGAGATCTGTTTAGCTTGCCTCGTCCCCGCCGGGtACctgat



8050



accttcacgaacgcgcCGCCTCCGGGCCACCGCTTGATTTTTGGCAGGA

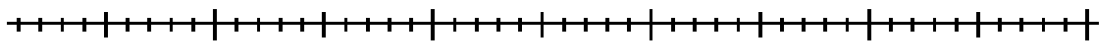


8100



V K V F A A A E P G G S S K Q C S
175 174 173 172 171 170 169 168 167 166 165 164 163 162 161 160 159

AACCATCACGTTCTTCCGGTATGATCTCACCGGTGGCCATCCCACAACTT

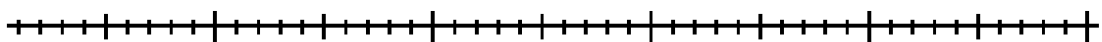


8150



V M V N K R Y S R V P P W G V V Q
158 157 156 155 154 153 152 151 150 149 148 147 146 145 144 143 142

GTGCCTTGGCCGAGGTTTGGCTGGATCTTAGGcatgaattctctaGTG

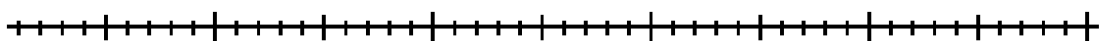


8200

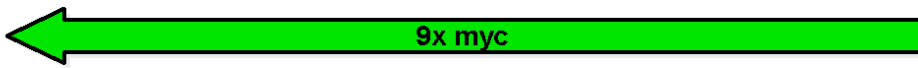


A K A P P K A P D K P M F E R T
141 140 139 138 137 136 135 134 133 132 131 130 129 128 127 126

GATCCGTTCAAGTCTTCTTCTGAGATTAATTTTTGTTTCACCGTTCAAGTC

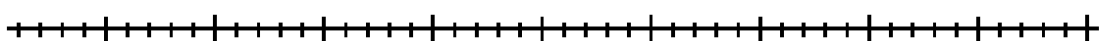


8250



S G N L D E E S I L K Q E G N L D
125 124 123 122 121 120 119 118 117 116 115 114 113 112 111 110 109

TTCTCGGAGATTAGCTTTTGTTCACCGTTCAAATCTTCTTCAGAAATCA

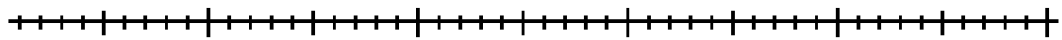


8300



E E S I L K Q E G N L D E E S I L
108 107 106 105 104 103 102 101 100 99 98 97 96 95 94 93 92

ACTTTTGTTCACCTCTAGAGGATCCGTTCAAGTCTTCTTCTGAGATTAAT

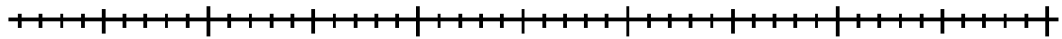


8350



K Q E G R S S G N L D E E S I L
91 90 89 88 87 86 85 84 83 82 81 80 79 78 77 76

TTTGTTCACCGTTCAAGTCTTCCTCGGAGATTAGCTTTTGTTCACCGTT

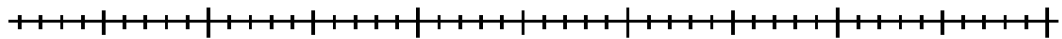


8400

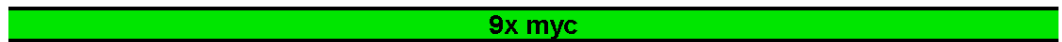


K Q E G N L D E E S I L K Q E G N
75 74 73 72 71 70 69 68 67 66 65 64 63 62 61 60 59

CAAATCTTCTCAGAAATCAACTTTTGTTCACCTCTAGAGGATCCGTTCA

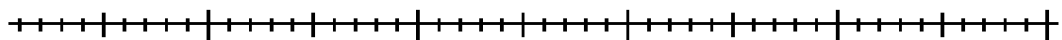


8450



L D E E S I L K Q E G R S S G N L
58 57 56 55 54 53 52 51 50 49 48 47 46 45 44 43 42

AGTCTTCTTCTGAGATTAATTTTGTTCACCGTTCAAGTCTTCCTCGGAG

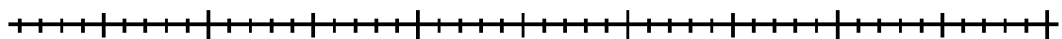


8500



D E E S I L K Q E G N L D E E S
41 40 39 38 37 36 35 34 33 32 31 30 29 28 27 26

ATTAGCTTTTGTTCACCGTTCAAGTCTTCTCAGAAATCAACTTTTGTTC

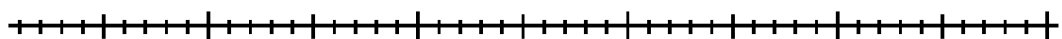


8550

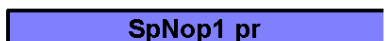


I L K Q E G N L D E E S I L K Q E
25 24 23 22 21 20 19 18 17 16 15 14 13 12 11 10 9

ACCACTAGCAGCAGAACCGGACATGAcacgtgtactgttttagttgattt

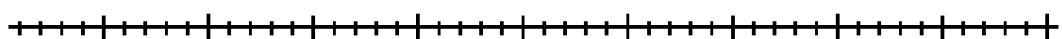


8600



G S A A S G S M
8 7 6 5 4 3 2 1

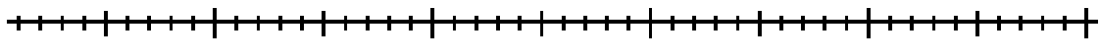
aagttaattttatcgaagttattgtaagtaatgggcaacttagatataatc



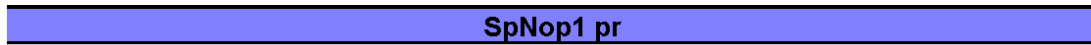
8650



attaacctacaagaaggaaactaaacaagttccagttatctgaatcgt

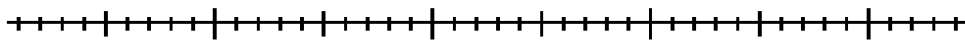


9200



EcoRV


ttttccgagaagaggctgatgactcaatGATATCAGATCCACTA



9244



Colour code:

 Binding sites for primers P7 and P8

„Nature gave men two ends – one to sit on and one to think with. Ever since then man’s success or failure has been dependent on the one he used most.“

George R. Kirkpatrick